Development of Environmental Tracers for Sediments and Phosphorus

Owen Pryce[1]

Bachelor of Science (Honours)

Lancaster Environment Centre, Lancaster University

Submitted for the Degree of Doctor of Philosophy

May 2011

[1]NERC Funded, project code NER/SA/2006/14021

ProQuest LLC.
789 East Eisenhower Parkway
P.O. Box 1346
Ann Arbor, MI 48106 – 1346

Owen Pryce, Bachelor of Science (Honours)

Development of Environmental Tracers for Sediments and Phosphorus

Submitted for the Degree of Doctor of Philosophy

May 2011

Abstract

Tracing eroded sediments can aid in minimising the impacts of soil erosion by improving the understanding of transport processes. A large range of sediment tracers exists; however, to date there has been no combined use of tracers which represent the full particle size range of sediments transported in overland flow. This is relevant because particles of different sizes show differing transport behaviour, but are all capable of transporting sediment bound contaminants such as phosphorus. The aim of this project was to develop a dual tracing method for both sediments and colloids in order to better represent the transport of phosphorus.

The link between soil erosion and eutrophication resulting from phosphorus transport was demonstrated. A range of sediment and colloid tracers were reviewed to select the two most appropriate tracers for this project (rare earth oxides (REOs) and fluorescent microspheres). Published methodologies relating to these tracers were investigated. The tracers were then applied to soil boxes receiving simulated rainfall, as well as a field plot, to compare their transport to the relevant phase of phosphorus.

The results showed comparable behaviour between REOs and particulate phosphorus. Fluorescent microspheres had low recoveries in surface runoff due to infiltration into the soil profile which limited their ability to trace colloid bound phosphorus. However, REOs were shown to be a useful tracer due to their ability to identify the sources and transport pathways of particulate phosphorus. Furthermore, the results gained from methodological development are useful for the future development of both tracing methods. Therefore, the results of this thesis provide significant steps towards improved understanding of phosphorus transport from arable land which can lead to reductions in nutrient loss and eutrophication.

Statement of Authorship

I declare that the work contained within this thesis is my own, and has not been submitted elsewhere for the award of a higher degree.

Acknowledgements

My thanks and gratitude goes out to everyone who has helped me during my time at Lancaster University. The support of my friends, family, and the staff at Lancaster University has been invaluable. Particular thanks go to Dr. Alona Armstrong and Dr. Nick Kettridge for their advice and guidance. However, the project would have been a far more difficult task if it were not for the continued and unwavering support of my supervisor, Prof. John Quinton, and my partner Miss Lucia Hoffart. I cannot describe how important your support has been.

Contents

List of Figures

List of Tables

Chapter 1

Introduction

Food security is as important to this country's future wellbeing - and that of the world's - as energy security ... We need to do three things. First, we need to produce more food. Second, we need to do it sustainably. And third we need to make sure that the food we eat safeguards our health ... How are we going to do it? ... By using science and technological advance to assist us ... One of the reasons we're doing this is because we are less clear about the difference climate change will make to our land in 20 or 30 years time. So prioritising the protection of our soil, our water, our plants and our biodiversity is something that makes sense today.' (Benn, 2010)

1.1 Intensive Agriculture and Diffuse Pollution

This thesis aims to develop a methodology for tracing different size fractions of sediments and associated phosphorus. Sediment and phosphorus loss from arable land is a by-product of intensive agricultural land use which impacts upon the environment (Haygarth and Jarvis, 1997; Toy et al., 2002). Development of tracing methodologies allows more efficient monitoring of transport patterns, greater understanding of transport behaviour and improved land management (Owens and Collins, 2006); therefore, tracing sediment and associated phosphorus contributes to the science to which Hilary Benn is referring in the opening quote. One of the problems highlighted by Benn is sustainable agriculture. The global population has increased from 2.5 to 6.9 billion people in the last 60 years (United Nations Statistics Division, 2010). It has been necessary to increase arable and livestock production in order to sustain this population and the increasing consumption of western countries (availability per capita of red meat and wheat in the United States of America has risen 19% and 21% respectively in the last 40 years (United States Department of Agriculture, 2007)). However, in many cases this has resulted in detrimental effects upon the soil, resident biodiversity and neighbouring water quality (Baker, 1985; Ball et al., 1997; Robinson and Sutherland, 2002).

As well as increases through the use of pest control and development of new crop varieties (Wild, 2003), arable productivity has been increased through the intensive chemical fertilisation of soils (Follett et al., 1981). Phosphorus is one of the most commonly applied fertilisers because it is one of the three macronutrients essential for crop growth (Russel, 1973). Food production is estimated to have doubled in the second half of the twentieth century as a result of this intensive fertilisation (Montgomery, 2007z'). Inorganic phosphate (the most common form of applied fertiliser) is hydrophobic, and therefore binds to soils and forms poorly insoluble complexes (Russel, 1973). The need to balance storage of phosphorus by soils with crop production results in high application rates of fertilisers; Bennett et al. (2001) calculated an annual phosphorus input to soils of approximately 18.5 $Tg.y^{-1}$. However, this redistribution of global phosphorus has led to soils be-

coming enriched; the average phosphorus surplus of European soils is 19 $kg.ha^{-1}$, while 31% of UK soil phosphorus surplus is concentrated in arable land (Edwards and Withers, 1998). Bennett et al. (2001) estimated phosphorus storage in terrestrial and freshwater ecosystem to be at least 75% greater than pre-industrial levels, rising from an accumulation rate of approximately 3.5 $TgP.y^{-1}$ (1960) to approximately 10 $TgP.y^{-1}$ (1995).

Soil erosion causes the loss of soils from arable lands to surface water systems, with mean loss rates for European arable land having recently been estimated at 3.6 $t.ha^{-1}.y^{-1}$ (Cerdan et al., 2010). Although erosion can be minimised with effective management (Quinton and Catt, 2004), increased concentrations of nutrients (phosphorus) are being transported to surface water as a result of the intensive fertilisation described (Ulen et al., 2007). The consequential eutrophication causes increased flora production resulting in the loss of the native flora, declining fauna due to water deoxygenation, and the production of neurotoxins from various algal species (Mainstone et al., 2008). This results in surface water being unfit for consumption or recreation without costly treatment or remediation.

Phosphorus use will not be curtailed to avoid the impacts of eutrophication because food production is reliant upon soil fertility (Edmeads, 2003) (recent evidence suggests organic farming without the routine use of phosphorus fertilisers results in phosphorus depletion (Gosling and Shepherd, 2005)). However, inorganic phosphate fertilisers have to be formed from mined deposits of rock phosphate, a non-renewable source which will eventually become depleted (Brink, 1978). Therefore, minimising the loss of phosphate from agricultural soils is not only important today for protecting neighbouring aquatic ecosystems, it will also be vital in the future to minimise loss of a essential resource.

Gaining a greater understanding of the causes and actions of soil erosion allows development of mitigation methods which help to protect and improve the environment (Deasy et al., 2009). This occurs in two ways: firstly, the impacts of soil erosion are curtailed; secondly, the productivity of agricultural land is improved so that chemical fertilisation can be minimised, which also reduces the need for

land use change to feed the expanding global population. Improved understanding can be gained through successful tracing.

1.2 Sediment Tracing

Tracing the transport of sediments allows improved understanding of erosion processes (Zhang et al., 1994) and validation of erosion models (Quine, 1999). The use of tracing techniques simplifies the identification of erosion and deposition locations, visualisation of transport pathways and calculations of erosion rates (Quine et al., 1997; Walling, 2005). This information can be used to investigate phosphorus behaviour because of the propensity of phosphorus to bind to soils.

Sediment tracers can be used to show a range of soil processes. At a basic level, the detection of the tracers at different locations from their original position of application indicates the transport of soil particles. This process can be used to show the sources and sinks of sediments (Polyakov et al., 2004). Tracers can be applied to a known depth down the soil profile to allow measurement of erosion rates at set locations. Taking cores at the tracer locations following a known period of time shows the erosion rate by the decreased depth of the tracer in the soil profile following erosion of the soil surface (Yang, Song, Sui and Ding, 2008). Equally, this method can be used to show deposition rates by the accumulation of material above the tagged position (Knaus and Gent, 1989). The placing of tracers to known depths in the soil profile has also been used to show the depth of rilling and gullying. Placing layers of different tracers at known depths in the soil profile allows determination of the depth of concentrated erosion by detection of the tracers in eroded sediments (Wei et al., 2003).

Tracers can also be used on larger scales, for example to determine sediment sources in a catchment or watershed; different locations inside a large area can be distinguished by quantifying different combinations of elements, different magnetic properties, different particle size distributions or other similar variable soil properties (Caitcheon, 1998; Collins et al., 1998). These 'fingerprints' of each source location can be used to determine the contribution of each source to a sed-

iment sink (Fox and Papanicolaou, 2008). If the concentration of the tracer at the point of application is known then tracing data can also be used for mass balance calculations. Mass balance requires that the inputs and outputs from a system are known in order to calculate accumulation or loss rates for the given analyte. Tracers can be used to show the mass of sediments entering or leaving a location and can therefore be used to calculate accumulation rates (Albrecht, 1999; Zhang et al., 2001).

However, tracing eroded sediments is complex. The broad spectrum of particle sizes that constitute soil generates an equally broad spectrum of behaviours. Large particle sizes ($\geq$ 1 μm) respond in a broadly similar way depending upon their size and mass (Kinnell, 2002; Rose, 2004). Colloid material ($\leq$ 1 μm) exhibits very different behaviour as a result of being able to move through pores and macropores, allowing more rapid transport than larger particles (Cey et al., 2009). Furthermore, the presence of surface charge leads to colloid transport being governed by pore water chemistry as well as physical hydrology (Tyan and Gschwend, 1994).

The behaviour of phosphorus is equally complex because it exists in multiple forms. Both organic and inorganic phosphorus can exist bound to particulates or dissolved into solution (McDowell, Sharpley, Condron, Haygarth and Brookes, 2001; McDowell, Sharpley and Folmar, 2001). The equilibrium between phosphorus in solution and the solid phase is governed by the soil chemistry; changes in soil hydrology and phosphorus inputs can rapidly shift its position, although the equilibrium leans heavily towards the solid phase (McDowell and Sharpley, 2001; McGechan and Lewis, 2002). As phosphorus is bound to colloids it can be transported rapidly even when the bulk soil is not eroded (Heathwaite, Haygarth, Matthews, Preedy and Butler, 2005). Transport behaviour in particulates is complicated by the non-uniform distribution of phosphorus in sediment size classes, where it preferentially binds in high concentrations to the fine (clay and fine silt) fractions of soil (Syres and Walker, 1969; Quinton et al., 2001).

This complex behaviour makes the tracing of sediment and associated phos-

phorus difficult. Tracers exist for sediments (defined from here onwards as material > 1 μm), colloids (defined from here onwards as material < 1 μm) and the dissolved phase (see Chapter 3). However, many of these tracers only represent one particle size of a system which spans many orders of magnitude in range. Furthermore, a good sediment tracer may not perform as effectively for tracing phosphorus due to the differences in sediment and phosphorus chemistry. A methodology that traces multiple phases simultaneously is required to gain more reliable phosphorus transport data. This project attempts to develop such a tracing methodology by combining a sediment tracer and a colloid tracer, and comparing their transport to the different phases of phosphorus. The combination of tracers to represent such a wide range of particle sizes in surface runoff is believed to be novel. Investigations into the methodologies used with the selected tracers will increase the understanding of their behaviour. Furthermore, this will be the first study where the selected tracers are compared directly to the transport of phosphorus.

1.3 Aims and Objectives

The aims of this thesis are to:

1. Provide compelling evidence of the need for, and a lack of, a multi-phase sediment tracer.

2. Develop a combination of tracers which will allow tracing of particles larger and smaller than the arbitrary 0.45 μm threshold used to define particulate and dissolved material in surface runoff.

3. Identify the usefulness of the developed methodology for tracing sediment associated diffuse pollutants (inorganic soil phosphorus).

These aims will be achieved by completing the following objectives:

1. Highlighting the impacts and extent of diffuse pollution, summarising the legislative requirements for its control, and identifying how tracing can help to meet these requirements (Chapter 2).

2. Reviewing the present tracing methodologies (Chapter 3).

3. Selecting a sediment tracer and a colloid tracer using a developed set of selection criteria (Chapter 3).

4. Identifying any methodological weaknesses (or lack of development) in the use of the selected tracers (Chapter 3), and develop solutions to these weaknesses (Chapters 4 and 5).

5. Applying the selected tracers to a controlled soil system in a manner that allows the transport of each tracer to be compared to the relevant phase of phosphorus (particulate and colloidal) (Chapter 6).

6. Performing an experiment with the same aims as objective 5 but at a larger scale and under field conditions, with methodological modifications based upon the results of controlled simulations (Chapter 7).

1.4 Thesis Outline

The objectives outlined in Section 1.3 will be addressed in the following chapters. Chapter 2 discusses the importance and impacts of diffuse pollution (specifically sediment and phosphorus transport caused by water erosion), describes the relevant legislation and outlines how sediment tracing can aid in controlling and reducing this pollution. This meets Objective 1. Chapter 3 goes on to review candidate sediment tracers and highlights the short-comings of present techniques, meeting Objectives 2 and 3.

Chapters 4 and 5 report the development of rare earth oxide and fluorescent microsphere techniques (the tracers selected for this project), addressing Objective 4. Chapter 6 details the application of both tracers to soil boxes receiving simulated rainfall, while Chapter 7 describes the application of the tracers to a field plot, addressing Objectives 5 and 6 respectively.

Chapter 8 reviews the work that has been performed, assesses its originality and success in meeting the project aims and objectives, describes conclusions

and implications based upon the results and highlights its contribution towards improving tracing methods. Further work that can be performed, to build on the work that has been achieved, is described at the end of Chapter 8.

Chapter 2

Background

2.1 Chapter Outline

This chapter provides the rationale for the project. Diffuse pollution is described in more detail and the legislation that requires its control is outlined. This thesis focuses upon diffuse pollution caused by soil erosion, therefore sediment transport and its impacts are reviewed. The consequential transport of particulate bound phosphorus, and the impacts this causes, are described. Details of particle transport mechanisms are outlined. The chapter is concluded by a summary of how the development of tracing methods can aid in mitigating the diffuse pollution described.

2.2 Definition of Diffuse Pollution

Water pollution occurs in two forms – point source pollution and diffuse pollution. Point source pollution is defined as originating from *'identifiable and recognizable pipes, sewer outfalls, underwater diffusers and discharge channels'* (Campbell et al., 2004). Its visibility makes it easy to identify, therefore legislation has been effective in monitoring, controlling and reducing point sources (Carpenter et al., 1998). However, water pollution is still a concern as a result of diffuse sources (Ripa et al., 2006). In contrast to point source pollution, diffuse pollution is defined as originating from *'land-use activities (urban and rural) that are dispersed across a catchment, or sub-catchment, and do not arise as a process effluent, municipal sewage effluent, or farm effluent discharge'* (D'Arcy et al., 2000). Its dispersed nature makes it difficult to monitor and control because:

- '*Discharge enters the receiving surface waters in a diffuse manner at intermittent intervals that are related mostly to the occurrence of meteorological events*';
- '*Waste generation arises over an extensive area of land and is in transit overland before it reaches surface waters, or infiltrates into shallow aquifers*';
- '*Diffuse sources are difficult or impossible to be monitored at the point of origin*';
- '*Unlike traditional point sources where treatment is the most effective method of pollution control, abatement of diffuse load is focused on land and run off management practices*';
- '*The extent of diffuse waste emissions (pollution) is related to certain uncontrollable climate events, as well as geographic conditions and may differ greatly from place to place and from year to year*' (Campbell et al., 2004).

Arable fields receiving precipitation are an example of a diffuse source. Sediment and bound contaminants (phosphorus) are detached and transported by raindrop splash and overland flow (Section 2.4). Dissolved pollutants are transported in the

direction of flow, both laterally and vertically. Diffuse pollution occurs when transported material reaches a location where its presence modifies chemical, physical or biological properties, i.e. surface water or an aquifer.

The complexity caused by unpredictable rainfall inputs is highlighted by numerous studies in published literature, e.g. (Haygarth, Wood, Heathwaite and Butler, 2005; Edwards and Withers, 2008; Deasy et al., 2008). For example, Preedy et al. (2001) reported that during 169 hours of intermittent rainfall, 46% of the total phosphorus loss occurred in a single four hour period, while Heathwaite and Dils (2000) reported a six fold increase of phosphorus concentrations in drainflow during stormflow conditions.

The two diffuse pollutants that this project will focus upon are sediments (specifically sediments originating from arable farmland) and phosphorus. Phosphorus is routinely applied to arable farmland to increase soil fertility and is subsequently transported with sediments by soil erosion. Diffuse transport of sediments and phosphorus has widespread and serious impacts in the UK because arable land covers 22.4% of the UK landmass (Office for National Statistics, 2001) and the application of phosphate fertilisers to this area of land is routine. The two pollutants are inter-linked because inorganic ortho-phosphate is hydrophobic and when applied to soils as soluble phosphate it will bind to soil surfaces and form inorganic precipitates (Russel, 1973). Therefore, there is a high correlation between total eroded sediment and total eroded phosphorus, although this relationship can vary with storm size due to the particle size selectivity of events of differing intensity or energy combined with the increasing pollutant carrying capacity of sediments as particle size decreases (Quinton et al., 2001).

2.3 Description and Impacts of Diffuse Pollutants

2.3.1 Sediments

Sediment transport into surface water bodies reduces flow capacity and increases the likelihood of flooding (Yin and Li, 2001). Its presence also increases turbidity which limits light penetration and impacts primary production and the biotic community (Wood and Armitage, 1997). The loss of soil from arable land can result in land abandonment in severe cases (Keay-Bright and Boardman, 2002; Bakker et al., 2005). As well as being a pollutant in their own right, sediments transport other contaminants bound to their surfaces such as metals (Quinton and Catt, 2007) and pathogens (Tyrrel and Quinton, 2003). Soil erosion contributes to the transport of phosphorus into water bodies and is therefore associated with the causes of eutrophication (Catt et al., 1998; Haygarth, Condron, Heathwaite, Turner and Harris, 2005; Withers et al., 2007). The specific impacts of eutrophication are described in Section 2.3.3. Soil erosion also results in the transport of colloids which is described in more detail in Section 2.5.

Soil erosion affects the environment on local, regional and global scales. Global soil erosion rates are estimated at 0.38 $mm.y^{-1}$, 60% of which is induced by human activity, with Southeast Asia being the most seriously affected area (Yang et al., 2003). The total area affected by water induced soil erosion is 1.1 billion ha, of which 0.8 billion ha are severely affected (Lal, 2003). It is expected that global climate change combined with land use change will result in increased erosion rates (Yang et al., 2003). Soil erosion on a global scale may also be directly influencing climate change by impacting upon the global carbon cycle. Low density (< 1.8 $Mg.m^{-3}$) soil organic carbon (SOC) is preferentially transported by soil erosion and could result in emissions of carbon (C) up to 0.8-1.2 $Pg.y^{-1}$ (Lal, 2003). However, these processes are not well understood, and whether soil erosion acts as a source or a sink of C is debated (Oost et al., 2007).

Croplands which are affected by soil erosion also received inputs of phospho-

rus for fertilisation. The global transport of phosphorus away from agricultural land used for crop production, as a result of soil erosion, has been estimated at 19.3 million metric tonnes $P.y^{-1}$ (Liu et al., 2008). When phosphorus eroded from agricultural land reaches surface water it causes the impacts described in Section 2.3.3.

The effects of soil erosion at a local or regional level are more visible than global impacts. Rompaey et al. (2001) studied an 850 km^2 area (Brabant Plateaux, central Belgium, continental temperate climate) of generally high silt content luvisols (> 750 $g.kg^{-1}$) with an average field size of 2.5 ha. Mean annual erosion rates greater than 10 $Mg.ha^{-1}$ (stated as a threshold considered a threat for land sustainability) occurred in one third of the arable land. Average erosion rates were 6.0 $Mg.ha^{-1}$, with maximum rates up to 50 $Mg.ha^{-1}$ in erosion hot-spots. Summer crops such as sugar beet, maize and potatoes provided high soil cover, but high intensity convective showers caused muddy floods in villages on the edge of the plateaux and resulted in pesticides and nutrients being transported into local surface waters which impacted local flora and fauna. This is a good example of how soil erosion is both a threat to arable sustainability and impacts upon the receiving water systems.

Lopez-Bermudez et al. (1998) performed work in Murcia, Spain (semi-arid Mediterranean climate) on approximately 250 ha of experiment plots comprised of a mixture of arable (perennial shrubs) and abandoned arable land. Erosion rates up to 10 $Mg.ha^{-1}.y^{-1}$ were reported. Eroded sediments were responsible for the pollution of local water systems with pesticides and nutrients. This demonstrates how the impacts of soil erosion are similar in two very different climates with different arable land-use.

Eggermont and Verschuren (2003) studied the impact of sedimentation upon lake bed species of Lake Tanganyika in East Africa (tropical climate). Two locations were examined: i) locations adjacent to pristine tributary drainage areas, and: ii) locations adjacent to areas where forests had been converted to crop land of both high and low population density. The land use change and subsequent

sediment transport to the lake resulted in faunal migration away from shore line in the lake bottom ecosystems in response to inputs of coarse, low organic sediments. This may endanger much of the fauna in this ecosystem as it is limited to a narrow depth range above an oxycline. This is a good example of how the presence of sediment can cause severe ecological impacts regardless of whether associated contaminants are also transported (as described in the two previous examples). This example also further demonstrates how the impacts of soil erosion are felt in a range of different climates.

2.3.2 Colloids

Environmental colloids are described as small discrete material in the size range of 1 nm and 1 μm (Gimbert et al., 2008). Examples in the vadose zone and soil surface include inorganic mineral oxides, organic macromolecules (Haygarth et al., 2006), and bacteria and viruses (DeJonge et al., 2004; Gimbert et al., 2008). Inorganic colloids have amphoteric surfaces of metal oxides and carbonates, but can also have charged surfaces (phyllosilicate faces) or organic coatings. Examples and size ranges of common colloids are summarized in Figure 2.1. The majority of colloid transport studies have concentrated on subsurface colloid transport because this pathway represents a significant transport route of hydrophobic contaminants to groundwater (Grolimund et al., 1996; Goppert and Goldscheider, 2008).

Colloids are an important vehicle for pollutant transport as they bind contaminants to their surface, have very high surface area to volume ratios and experience high transport rates (McCarthy and McKay, 2004). Contaminant bonding occurs via ion exchange and hydrophobic partitioning. Colloids, such as bacteria and viruses, are pollutants in their own right. However, this project is more concerned with the actions of mineral colloids (clay) which transport contaminants (phosphorus) that would normally be bound to sediments (McGechan, 2002). Diffuse pollution is heavily influenced by the action of colloids which have been shown to be a key transporter of phosphorus (Siemens et al., 2004; Heathwaite, Haygarth, Matthews, Preedy and Butler, 2005). The impacts of colloid facilitated transport

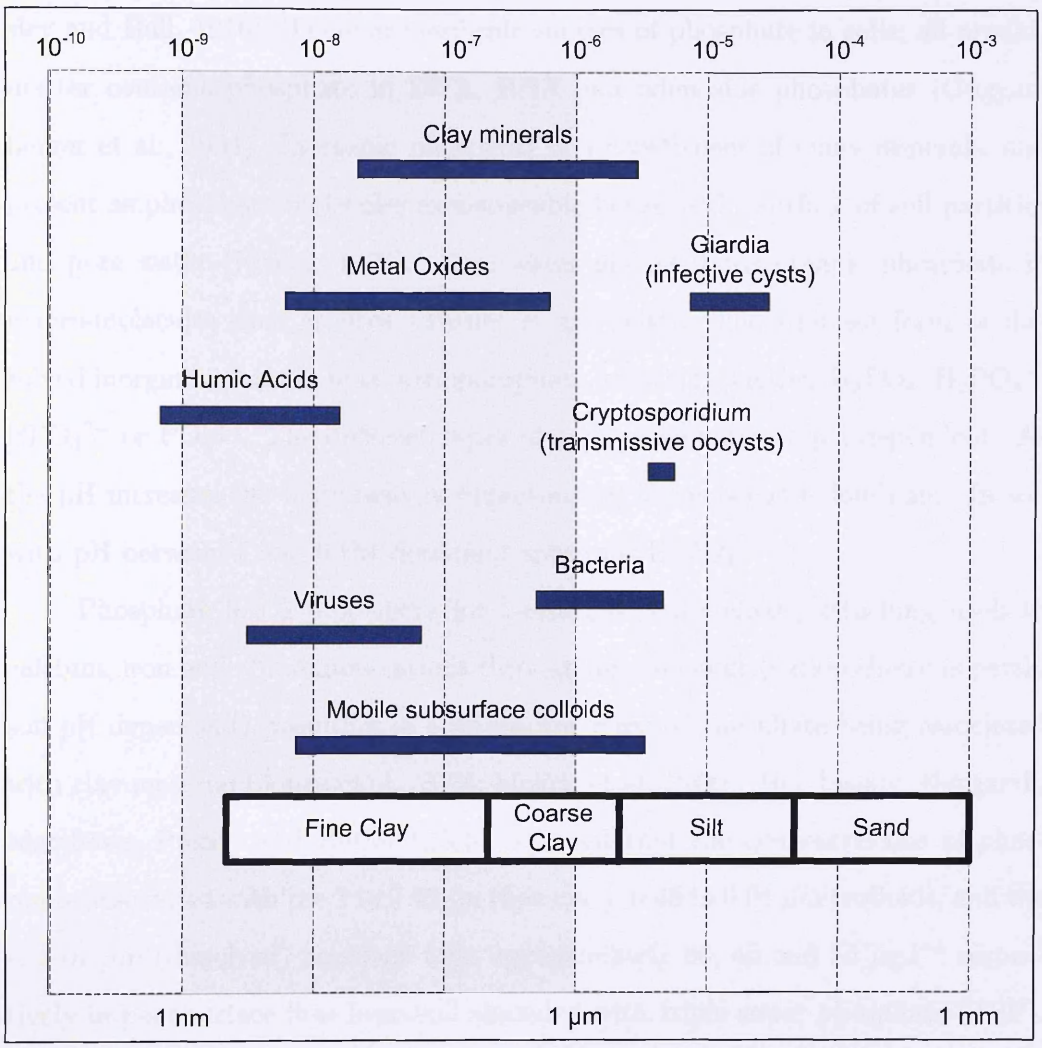

Figure 2.1: Size range of common colloids and microorganisms found in the vadose and saturated zone, reproduced from Kretzschmar et al. (1999). The region which represents colloids is indicated by colouration between 1 nm and 1 μm.

of phosphorus are described in Section 2.3.3. The physical impacts of mineral colloids contribute to the effects of soil erosion described in Section 2.3.1.

2.3.3 Phosphorus

Phosphorus is the eleventh most abundant element in the Earth's crust. It is present as phosphate (phosphorus bound tetrahedrally to four oxygen atoms) due to its high reactivity (Goldwhite, 1981). Bonding of phosphorus atoms via oxygen atoms allows long chain polyphosphates and organophosphates to be formed (Em-

sley and Hall, 1976). There are multiple sources of phosphate in soils; all organic matter contains phosphate in DNA, RNA and adenosine phosphates (Guggenberger et al., 1994). Inorganic phosphate is a constituent of many minerals, and present as phosphate molecules exchangeable between the surface of soil particles and pore water (Russel, 1973). Pore water also contains organic phosphate in macro-molecules such as urea (Turner et al., 2003). The simplest form of dissolved inorganic phosphate is orthophosphate, existing as either H_3PO_4, $H_2PO_4^-$, HPO_4^{2-} or PO_4^{3-}. The different types of orthophosphate are pH dependent. As the pH increases the more heavily deprotonated forms become dominant. In soil with pH between 4 and 6 the dominant species is $H_2PO_4^-$.

Phosphate has a propensity for binding to soil colloids, attaching itself to calcium, iron and aluminium cations through ion exchange (cation choice is partly soil pH dependent), resulting in a significant mass of phosphate being associated with clay material (Jonge et al., 2004; Makris et al., 2006). Heathwaite, Haygarth, Matthews, Preedy and Butler (2005) reported that the concentrations of phosphate associated with the 2 to 0.45μm (fine clay), 0.45 to 0.01 μm (colloid), and the < 0.01 μm (dissolved) fractions were approximately 60, 40 and 35 $\mu g.l^{-1}$ respectively in near-surface flow from soil amended with triple super phosphate (TSP). This highlights the ability of inorganic phosphate to bind to colloids. Furthermore, saturation of soils with phosphate may induce increased colloid mobilisation (Ilg et al., 2008).

Dissolved inorganic phosphate exists in equilibrium between sorption onto the soil surface and in solution (Russel, 1973). Sorption has been extensively investigated, modelled and reviewed, and can be separated into initial rapid sorption to surfaces, followed by a series of slower absorption processes at and below the surface (McGechan and Lewis, 2002) (Figure 2.2). Orthophosphate can absorb to surface metal ions by ligand exchange, commonly with an aquo group but also with hydroxyl, alcohol and carbonate groups. Jonge et al. (2004) reported that 75% of phosphorus leaching from soils was particulate associated. Transport can either be via sediment transport (Section 2.4), colloid transport (Section 2.5) or as

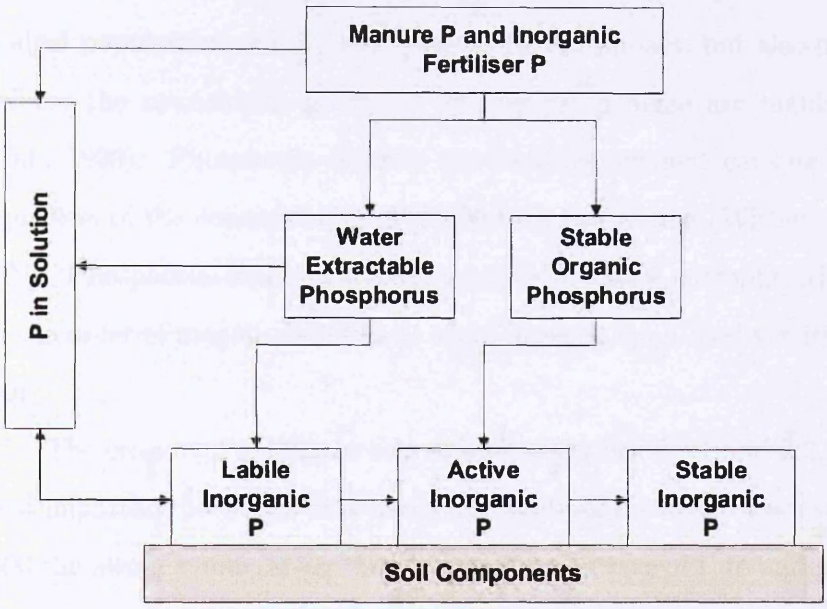

Figure 2.2: Simplified schematic representation of the main inorganic soil phosphorus pools reproduced from Vadas et al. (2007).

truly dissolved phosphate. This results in a three phase transport system where the sources and pathways that dominate are dependent upon the scale (Dougherty et al., 2004; Haygarth, Wood, Heathwaite and Butler, 2005; Doody et al., 2006), land use and hydrology of the system (Dougherty et al., 2004; Fortune et al., 2005; Deasy et al., 2008).

The most publicized effect of phosphorus transport to surface waters (previously mentioned in Sections 2.3.1 and 2.3.2) is eutrophication. The process can be defined by its causes and impacts: *'the enrichment of water by nutrients, stimulating an array of symptomatic changes including increased production of algae and/or higher plants, which can adversely affect the diversity of the biological system, the quality of the water and the uses to which the water may be put'* (Environment Agency, 1998).

Similarly to soil erosion, eutrophication is a global issue (Bennett et al., 2001); examples of eutrophication occur at multiple scales with varying degrees of impact. Kosenius (2010) summarised the main impacts of eutrophication, stating that both marine and freshwater eutrophication increases turbidity, accelerates algal bloom

growth, impacts upon fish populations and decreases oxygen levels. The increase in algal populations is the most easily observed impact, but also one of the most serious; the neurotoxins produced by blue-green algae are highly toxic (Smith et al., 1999). Phosphorus is often the limiting nutrient causing eutrophication regardless of the concentration of nitrogen in the system (Withers and Haygarth, 2007). Phosphorus inputs above 0.1 $mg.l^{-1}$ can cause eutrophication, and should be one order of magnitude lower to avoid impacts upon biodiversity (Deasy et al., 2009).

The erosion of sediments and colloids (Sections 2.3.1 and 2.3.2) is one of the most important pathways that transports phosphorus to surface water. In the year 2000 the average mineral and manure application rate of P to agricultural land for Western Europe has been reported as 19 $kg.ha^{-1}$ (Csatho et al., 2007). Loss of P from agricultural soil is reported as being highly variable, ranging between values of 0.1 to 6 $kg.ha^{-1}$ (Withers and Haygarth, 2007). Based on these figures the average loss of P from agricultural land is approximately 16%, the remainder either being utilised by crops for growth or adding to the soil's stores of P. It is estimated that agricultural sources contribute up to 75% of phosphorus in European waters if point sources are well controlled (Withers and Haygarth, 2007). Heathwaite, Dils, Liu, Carvalho, Brazier, Pope, Hughes, Phillips and May (2005) calculated that, in rural locations, 70% of total phosphorus loads in lakes originate from agricultural practices, 33% of which resulted from arable land use. Arable land contributes 40% of the phosphorus load to the Baltic Sea despite occupying only 6% of land area in Sweden (Ulen et al., 2007). Croplands are the most significant source of diffuse phosphorus load (31%) in the USA (Carpenter et al., 1998).

2.4 Sediment Transport

Eroded sediment can be classed as a diffuse pollutant because soil erosion often occurs over dispersed areas and transports sediments in a diffuse manner (unless rilling/gullying occurs), as defined in Section 2.2. Soil erosion is defined as *'a two phase process consisting of the detachment of individual soil particles from*

the soil mass and their transport' (Morgan, 2005). Ignoring wind and mechanical processes (detachment resulting from tillage), detachment and transport of soil particles are caused by the transfer of energy from both rainfall (Pimentel et al., 1995) (Section 2.4.1) and overland flow (Wan et al., 1996) (Section 2.4.2). Erosion rates by both rainsplash and overland flow are influenced by soil classification; as physical properties such as aggregation strength and shear strength increase between soil classes, so does the energy requirement to detach and transport a set mass of soil (Bryan, 2000). The particle size of sediments also affects erosion due to the increasing energy requirements of mobilisation and transportation as particle size increases (Kinnell, 2002). Colloids are transported by the same mechanisms as sediments, but also have some unique transport behaviour which is described separately in Section 2.5.

2.4.1 Transport by Rainsplash

When a raindrop hits a surface its kinetic energy causes a series of processes to occur: i) a proportion of the energy is transferred normal to the surface causing compaction, while the majority is reflected back from the surface; ii) the water then rapidly disperses from the point of impact and returns creating a series of waves, the energy of which is sufficient to detach soil particles from the surface and launch them into the air (Morgan, 2005). Rainsplash has been shown to contribute heavily to erosion rates (Sutherland et al., 1996), especially at slopes greater than 9% (Wan et al., 1996; Mermut et al., 1997) and with coarse soils, where surface flow may not possess sufficient energy to detach sediments (Issa et al., 2006). Splash transport is exacerbated by wind driven rain (Erpul et al., 2002). Raindrop diameter and momentum are also important in determining the severity of splash erosion (Salles and Poesen, 2000). As a result, rainfall has a twofold effect, providing compaction and sealing of the surface (Mamedov et al., 2006) as well as detachment and transport of particulates (Kinnell, 2002). However, the influence of splash detachment and transport is known to decrease as the depth of surface water increases due to the absorption of impact energy. This results in the

proportion of material transported by splash decreasing relative to the amount of material transported in surface flow as erosion events proceed through time (Kinnell, 2002).

2.4.2 Transport by Overland Flow

Once water ponds onto a surface (see Morgan (2005) or Rose (2004) for a description of infiltration processes) it will begin to flow in the direction of the steepest slope. Cohesion between soil particles prevents detachment unless the flow velocity provides sufficient kinetic energy. The higher the adhesion of the soil, the higher the kinetic energy of the flow must be for erosion to occur. Erosion caused by movement of surface water can be divided into two processes: i) concentrated flow (Slattery and Bryan, 1992), and ii) unconcentrated flow (Issa et al., 2006). Concentrated flows are directed into a single channel resulting in higher erosion rates than surrounding areas and the formation of deep cut rills (Nearing et al., 1997). Unconcentrated flow is the non-uniform sheet flow that occurs between these rills which is broken up into multiple interconnected courses absent of a single channelized flow pathway due to surface roughness (Dunkerly, 2004). These two types of flow transport sediments until their kinetic energy becomes insufficient at which point deposition occurs.

Kinnell (2002) outlined four different transport mechanisms for different sizes of sediments in rain impacted flows. This provides a useful description of sediment transport mechanisms which are likely to occur during this experimental work. The four mechanisms are:

- Raindrop detachment with transport by raindrop splash (RD-ST);
- Raindrop detachment with transport by raindrop-induced flow transport (RD-RIFT);
- Raindrop detachment with transport by flow (RD-FT);
- Flow detachment with transport by flow (FD-FT).

RD-ST occurs when an impacting raindrop detaches and transports a soil particle away from its original location (Section 2.4.1). RD-RIFT occurs when there is water flowing over the soil surface. Raindrops penetrate through the surface flow to detach soil particles. The detached particles are transported through the flow as they settle back to the soil surface where they remain until they are transported by further raindrop impacts. Transport is through a combination of raindrop impact and surface flow. This may only induce rolling of coarser particles, rather than saltation. RD-FT occurs when the flow has sufficient force to transport bedload material, but insufficient force to detach it; therefore detachment is still caused by raindrop impact but transport is caused by the action of surface flow. FD-FT occurs when the flow has sufficient kinetic energy to detach and transport material.

A combination of all four mechanisms will occur during both unconcentrated and concentrated flows. The mechanisms transporting a particle will depend upon its size and also the kinetic energy of the surface flow and rainfall. The main processes governing sediment transport are shown in Figure 2.3.

2.5 Colloid Transport

A significant distinction can be made between colloid sized particles (< 1 μm) and larger sediment (sand, silt and coarse clay > 1 μm). Colloids can be transported through pores that larger sediments cannot, and can be mobilised and transported by flow with lower kinetic energy (see Section 2.4.2). This results in distinctly different transport behaviour, where colloids can be transported vertically through the soil profile (Gimbert et al., 2008). Furthermore, colloids will remain suspended even when larger sediments have settled out of suspension due to insufficient kinetic energy of surface flow. This generates comparatively higher transport rates of colloids. Colloid transport can occur on the soil surface, in the vadose zone and in the saturated zone, therefore colloid behaviour is dependent upon the location being described. This project focuses on surface colloids, therefore the transport of colloids is largely described in Sections 2.4.1 and 2.4.2. However, there is some unique transport behaviour of colloids which is described separately in this section.

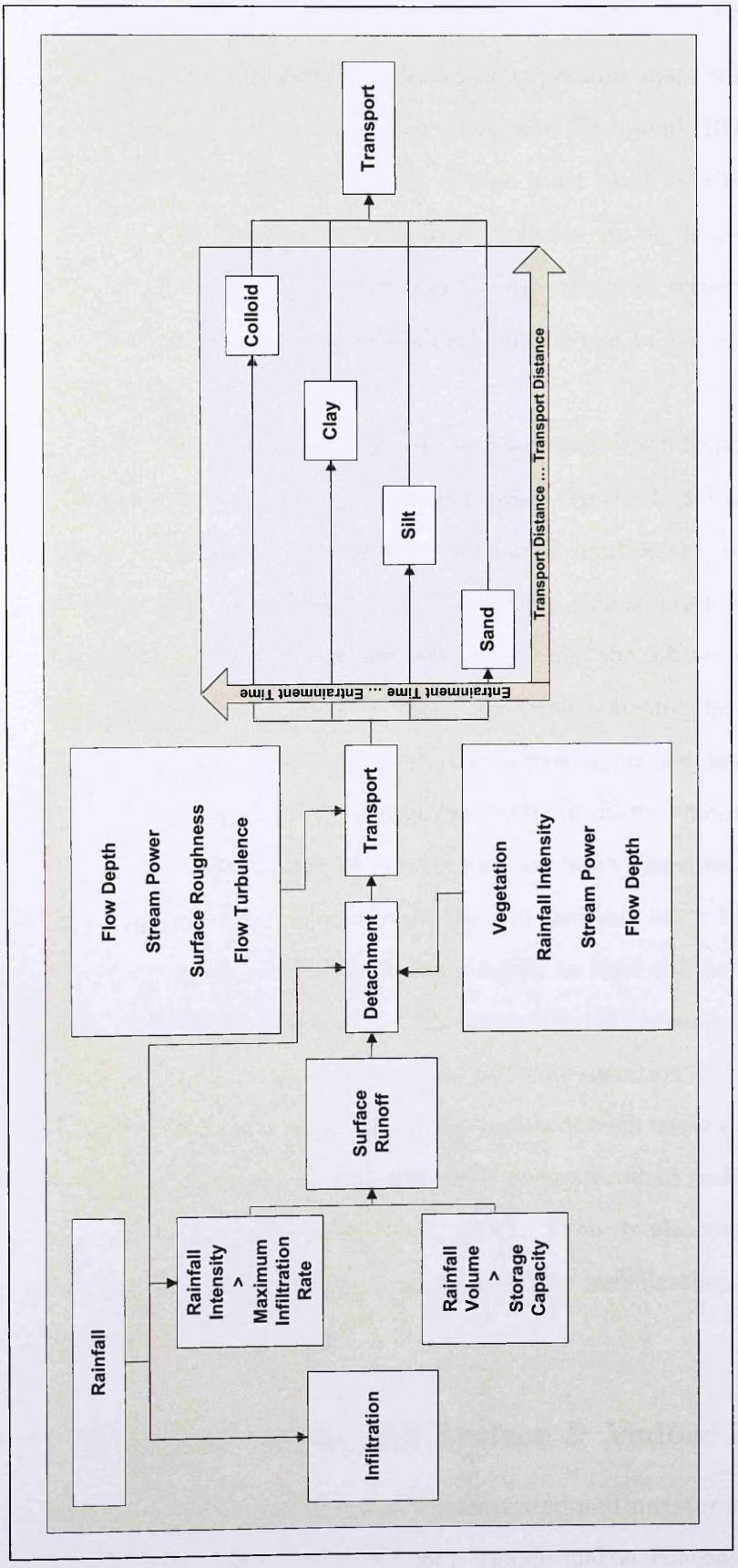

Figure 2.3: Conceptual model of soil erosion processes highlighting the influences upon detachment and transport and the size selective transport distances of sediment.

2.5.1 Mobilisation

Similarly to sediments, hydrodynamic forces exert pressure upon colloids removing them from the surface of the solid phase (Tyan and Gschwend, 1994; Massoudieh and Ginn, 2007; Sen and Khilar, 2009). Forces must reach a critical magnitude before they will cause mobilization. However, colloids can be detached and transported when surface runoff has insufficient kinetic energy to transport larger (silt and sand) particles. Furthermore, mobilized colloids can be transported with infiltrating water into the soil profile.

Changes in pore water chemistry can lead to sudden mobilization. This effect can be explained by the Derjaguin-Verwey-Landau-Overbeek (DVLO) theory and the behaviour of two like-charged surfaces in an ionic solution (Everett, 1992; Tyan and Gschwend, 1994). Both surfaces will develop a diffuse layer of counter ions. An attraction then exists between the first surface and the diffuse layer of counter ions surrounding the second surface (and visa versa) causing the surfaces to be attracted towards one another (force A). The diffuse layers are naturally repelled from each other due to their like-charge (force B). In dilute ionic solutions (such as rain water) the diffuse layers of counter ions are more dispersed. Therefore, in dilute ionic solutions, force B acts upon the two surfaces when they are further apart which in turn prevents force A from acting to bind the surfaces together. As a result, the surfaces move apart. The same process occurs when pore water salt concentrations drop below the critical salt concentration (CSC) (Ryan and Elimelech, 1996; DeJonge et al., 2004). Large inputs of fresh water through rainfall, irrigation or other discharge can therefore result in rapid colloid mobilization (Tyan and Gschwend, 1994; Laedgsmand et al., 2007). There is also some evidence to suggest that excessive fertilization can lead to the mobilization of phosphorus carrying colloids (Ilg et al., 2008).

2.5.2 Behaviour on the Soil Surface & Vadose Zone

There are obvious differences between the saturated and unsaturated zones (McCarthy and Zachara, 1989). High O_2 and organic matter concentrations on the

soil surface and in the vadose zone result in a high sorption potential of the solid phase. Chemical properties are far less stable than in the saturated zone because the water content is variable. The chemical conditions of the zone differ between geographical and temporal locations due to changes in rainwater frequency and intensity. The presence of the gas – liquid interface presents an extra complexity, which results in higher colloid retention and mobilization due to trapping and repulsion of colloids by the interface (Sharma et al., 2008). This can dominate over ionic concentration effects (Lazouskaya et al., 2006). The lack of saturation results in hydrodynamic forces capable of mobilizing colloids occurring less frequently than in the saturated zone (Denovio et al., 2004). Colloid movement is primarily vertical.

2.6 Extent of Diffuse Pollution

Of the United Kingdom's land area, 67.8% is agricultural, 33.1% (54,200 km^2) of which is arable land (Office for National Statistics, 2001) and potentially susceptible to soil erosion. Although the contribution from a single diffuse source may be minimal, the combined effect of all sources is serious. Diffuse pollution affects 5,339 km of rivers, 286 km^2 of lochs and 16,646 km^2 of groundwater in Scotland, while point source pollution affects only 3,844 km, 196 km^2 and 9697 km^2 of the same waterbodies respectively (Scottish Environment Protection Agency, n.d.). A UK based risk assessment for phosphorus has shown that 37% of lakes and 50% of rivers are at risk, or probably at risk, from diffuse sources (Mainstone et al., 2008). Between 1994 and 1998 the number of surface water bodies sensitive to eutrophication in the UK increased from 33% to 61% (Withers et al., 2000). The extent of diffuse pollution has been driven by land use change. In the UK, the ratio between arable and pasture land has changed from 1:1.6 to 1.8:1 between 1930 and 1990.

2.7 Control of Diffuse Pollution

There is now extensive legislation that requires diffuse pollution to be abated. Soil erosion and the resultant nutrient loss must be minimized for compliance to be achieved. Tracing can therefore aid in meeting the targets of European and domestic legislation because it can help in identifying diffuse pollution (Section 2.8).

2.7.1 European Water Framework Directive

The Water Framework Directive (WFD) became law in December 2003 (Kaika, 2003). Among the aims of the directive is *'Achieving and/or maintaining 'good' status, in terms of ecological quality, for all waters within a set time frame (2015)'*, (Barth and Fawell, 2001). A water body is classified as 'good' when: i) there are no, or only very minor, anthropogenic alterations; and ii) the value of the biological quality elements for the surface water body reflect those normally associated with that type under undisturbed conditions. This takes into account natural background levels of potential pollutants and benthos (Muxika et al., 2007). At present many areas of the UK are failing to achieve compliance; therefore improved mitigation is required (Hutchins et al., 2009), although this is possibly a result of the time lag between management changes and improvement in indicators (Collins and McGonigle, 2008). The presence of sediment and associated contaminants (transported to surface waters by the mechanisms described in Section 2.4) will be monitored by the WFD (Crane, 2003), therefore the directive will require reductions in soil erosion and associated nutrient transport (Jonge et al., 2004; Deasy et al., 2008).

2.7.2 Bathing Water Directive

The European Bathing Water Directive became law in March 2008. The directive is concerned with the quality of *'any element of surface water where the competent authority expects a large number of people to bathe'* (Commission of the European

Communities, 2006a). Samples must be taken during the bathing season. The directive classifies bathing water quality as excellent, good, sufficient or poor. Quality is identified by quantification of intestinal enterococci and escherichia coli concentrations. Sufficient is the minimum quality that must be reached by all European member states, for all bathing water, by the end of 2015 (Commission of the European Communities, 2006a).

The bacteria used for quality classification are a constituent of the manure that is routinely applied to agricultural land and transported to surface water bodies after rainfall events (Tyrrel and Quinton, 2003; Kay et al., 2007). This material has also been shown to increase erodibility of soils (McDowell and Sharpley, 2002). Bacteria are associated with ≤ 60 μm sediment and can survive for up to six weeks in river bed sediment while being transported to recreational surface waters (Jamieson et al., 2005). Mitigation of diffuse agricultural pollutants, specifically soil erosion, will aid in meeting the standards outlined in the directive.

2.7.3 Draft European Soils Framework Directive

At the date of writing this thesis, a new European Soil Framework Directive has not been put into force despite the European Commission stating that *'a comprehensive EU strategy for soil protection is required'* (Commission of the European Communities, 2006c,d). The economic, social and environmental impacts of various options have been assessed. It is estimated that 115 million hectares, or 12% of Europe's total land area, is subject to water erosion and 42 million hectares to wind erosion. The estimated cost of this erosion is between 0.7 and 14 billion Euros annually (Commission of the European Communities, 2006b,e). It is stated that the anthropogenic causes of soil erosion appear to be increasing and the occurrence of extreme weather events and rising temperatures as a result of climate change is exacerbating the situation (Commission of the European Communities, 2006d). Any implemented strategy will require improved land use and management strategies to protect soils from diffuse pollution caused by sediment and phosphorus transport.

2.7.4 DEFRA Soil Strategy

The DEFRA soil strategy outlines how DEFRA will address the long term environmental issues facing English soils. The strategy aims that by 2030 *'all England's soils will be managed sustainably and degradation threats tackled successfully'* (Department of the Environment, Food and Rural Affairs, 2009a). The strategy highlights soil erosion as the *'most significant threat facing our soils'*, estimating that approximately 2.2 million tonnes of topsoil is eroded annually in the UK. The stated cost of this erosion is 45 million pounds sterling per annum, including nine million pounds sterling in lost production (Department of the Environment, Food and Rural Affairs, 2009b). The objectives of the strategy are to be partly met by *'improving our evidence base; filling the gaps in our knowledge ... and ensuring that policy development is based on the latest scientific information'* (Department of the Environment, Food and Rural Affairs, 2009a). Tracing sediment and associated phosphorus transport will help to meet these criteria and therefore help to meet the objectives of the strategy.

2.8 The Argument for Tracing

This chapter has described three diffuse pollutants. It has shown that these diffuse pollutants have severe impacts upon receiving surface waters (Sections 2.3.1, 2.3.2, and 2.3.3), described the mechanisms of their transport to surface water via soil erosion (Section 2.4), shown that this occurs upon a high percentage of the UK's landmass (Section 2.6) and shown that there is UK and European policy and legislation that requires this diffuse pollution to be minimised or abated (Section 2.7). One method that can be used to help minimise soil erosion is sediment tracing.

Soil erosion has been described as *'easy to observe, but hard to measure'*, (Polyakov and Nearing, 2004). Soil scientists have continually developed more effective methods to trace eroding sediments (see Chapter 3) because it simplifies the measurement of erosion. Making sediment traceable by adding an identifi-

able component allows measurement of transport distances and rates, visualisation of transport pathways, and the ranking of contributions from different sediment sources. Furthermore, the use of sediment tracers in field studies helps to ensure that erosion events are not un-monitored because of the unpredictable timing of diffuse pollution (Section 2.2). This improves our understanding of soil erosion, which in turn aids in development of mitigation methods. Tracing of sediments also improves the understanding of phosphorus transport because of the related behaviour described in Section 2.3.3; therefore, development of tracing methodologies can reduce the impacts of sediment and phosphorus transport to surface waters and help the UK comply with environmental standards required by UK and European legislation and policy.

However, the transport of sediments and associated phosphorus varies dramatically with particle size (Section 2.4). Therefore there is a need to develop methods of simultaneously using multiple tracers which represent multiple size fractions of sediments. The most obvious size distinction is between colloids and sediments because these are the two size fractions between which the largest change in transport behaviour occurs (Sections 2.4 and 2.5); the following chapter reviews tracers presently used for colloids and sediments.

Chapter 3

Related Work

3.1 Chapter Outline

This chapter reviews a range of sediment tracing methodologies. A distinction is made between tracers for sediments ($\geq$ 1 μm) and tracers for colloids and solutes ($\leq$ 1 μm). A set of selection criteria is formed based upon different levels of tracer performance and the requirements of tracers in published literature. A brief summary of candidate tracers (for both sizes of material) is presented before rare earth oxides and fluorescent microspheres (the selected tracers) are reviewed in more detail. Any methodological issues associated with using the selected tracers, highlighted in published literature, are also described.

3.2 Tracing

Tracing sediment improves the understanding of soil erosion processes and sediment transport patterns, while resultant data can be used to validate erosion models (Quine, 1999). Specific uses of tracers were described in Section 1.2. Good examples of tracers improving knowledge of soil erosion include the use of rare earth oxides (REOs) to investigate deposition of sediments following breaks of slope (Michaelides et al., 2010) or the use of ^{137}Cs to give estimates of erosion rates from arable land in Turkey (Sac et al., 2008). Tracing also allows more efficient testing of erosion mitigation methods and therefore aids in reducing the diffuse pollution described in Chapter 2.

It is possible in extreme cases to visually distinguish topographical positions experiencing erosion and deposition, and to measure average erosion rates from plots using sediment traps. However, without tracers it is not possible to identify sediment sources or quantify their contribution to a sediment sink when erosion rates are low. Stevens and Quinton (2008) identified and described the distance over which sediment is transported into tramline features; this would not have been possible without the use of a tracer. Similarly when larger scales are investigated, for example whole catchments, it is not possible to quantify different sediment sources without a tracing method such as fingerprinting (Carter et al., 2003)

A distinction can be made between tracers which occur in soils with no additional inputs (native) and tracers applied to soils (applied). Native tracers are components of the soil which aid in identifying locations of erosion and deposition, for example ^{137}Cs or any of the elements used in fingerprinting methodologies (Motha et al., 2002; Huh and Su, 2004). Their initial input into the soil profile is assumed to have been spatially uniform, so that redistribution is related to erosional processes. However, redistribution due to non-erosional processes must be taken into consideration when using these types of tracers, for example the redistribution of ^{137}Cs in the plough layer of arable land (Lindstrom et al., 1992), which can add experimental difficulties. Unlike applied tracers, they require no application to the investigated site.

The use of applied tracers allows greater selectivity of physical and chemical properties appropriate to the experimental objectives. However, the application of applied tracers results in an additional methodological step which can result in increased experimental error (Polyakov et al., 2004). Furthermore, despite having the ability to modify the properties of the tracer, creating a tracer which accurately mimics soil and does not modify soil properties when being used can be difficult (Duke et al., 2000; Ventura et al., 2002), for example, the magnetic tracer used by Ventura et al. (2002) resulted in an armouring effect changing soil erodability.

The choice between native and applied tracers is typically dependent upon the scale of the experiment and the data required. Native tracers are preferable for large field or watershed scale experiments where processes occurring at large scales are being examined (Collins et al., 1998). Applied tracers are more applicable to smaller scale experiments where their improved versatility is not hindered by the demands of application (Lei et al., 2006).

The information gathered through sediment tracing techniques can be improved by using a tracer which exists in multiple, distinguishable forms (MD-tracer). An MD-tracer is comprised of several different tracers, each of which has the same physical and chemical properties. Tagging topographical positions, each with a different component of the MD-tracer, allows the mass of eroded sediment from each position to be quantified from the concentration of each MD-tracer component in surface runoff. Relating to a previous example; Stevens and Quinton (2008) divided the area on both sides of a tramline in multiple sections, each running parallel to the tramline at increasing distances away from it, and applied a different REO to each section. This allowed the mass of sediment transported into the tramline from each section to be quantified from the concentration of each REO in eroded sediment collected at the bottom of the tramline. The use of MD-tracers in this fashion allows spatially precise data to be collected, allowing connectivity between sources and sinks of sediments to be shown (Polyakov et al., 2004).

There is a large range of different sediment tracers available which will be

described in Section 3.4.1. Each sediment tracer has unique properties which make them suitable for a specific type of sediment tracing experiment. A set of selection criteria was developed in order to successfully select the two most appropriate methods which could be used for tracing both sediments and colloids in surface runoff.

3.3 Tracer Selection Criteria

Two MD-tracers were required, one for sediments and one for colloids. Both tracers had to possess the ability to show sediment loss and redistribution after single erosion events. The aim of this thesis was not to develop completely new tracing methods. Many tracers already exist for these size fractions, therefore a series of selection criteria was required to assess the strengths and weaknesses of the candidate tracers to allow two suitable tracers to be selected.

Tracers are used in all disciplines of science in order to obtain quantitative and qualitative references for the transport rates or pathways of a specific analyte (i.e. radio transmitters on migrating birds in ecology (Harmata, 2002) or ICMP pings to test network speeds in computer science (G. Hoffart, IT42, Germany, personal communication)), and can be divided into two categories:

- Tracers which have similar or identical properties to the analyte so that external influences upon the tracers result in comparable behaviour to the analyte, and:
- Tracers which follow comparable pathways to the analyte, but which have differing physical properties so that transport behaviour is different.

These two classifications of tracers will be referred to as A-grade and B-grade. Examples are conservative dyes for ground water tracing (A-grade) (Gouzie et al., 2010), and applied magnetic particles for sediment tracing (B-grade) (Ventura et al., 2001, 2002). The difference between the two grades is in response to stimuli; an A-grade tracer will show near identical transport rates to its analyte because it possesses similar chemical and physical properties. A B-grade tracer will only

reflect the magnitude of the stimuli because its chemical and physical properties differ from the analyte.

B-grade sediment tracers will indicate the total mass of sediment transported from an area during a single rainfall event and will allow comparison of eroded masses from areas of differing erodibility. It is assumed that, as long as B-grade tracing is occurring, the tracers and analyte will follow comparable transport pathways i.e. movement into gullies, or deposition in areas of low slope. This allows transport pathways to be visualised from surface sampling regardless of the tracer grade.

These two tracer grades will be used to select the tracers in this project from a series of candidate tracers. The grades will also be used in subsequent chapters to assess the selected tracers' performance. The grades will be used in combination with perceived difficulties or drawbacks with any of the candidate tracers, as well as with the selection criteria published by Zhang et al. (2003).

Zhang et al. (2003) stated that tracers must: i) be strongly bound with soil particles, or easily incorporated into soil aggregates; ii) have great sensitivity in analysis; iii) be easy and inexpensive to measure; iv) possess low background concentration in soils; v) not interfere with sediment transport; vi) have low plant uptake; vii) be environmentally benign, and; viii) have the availability of multiple tracers that are similar in physiochemical properties but are distinct in signature (what is being referred to in this thesis as MD tracers). It is important that any selected candidate tracers meet these criteria. The majority of the criteria are already met by the candidate tracers because all candidate tracers have been used in previous publications. Furthermore, some of these criteria only apply to applied MD-tracers and are therefore non-applicable. However, any failure to meet these criteria will be noted during the assessment of the candidate tracers.

3.4 Candidate Tracers

3.4.1 Sediment Tracers

Native Tracers

Radionuclides:

There are two major sources of ^{137}Cs ($t_{\frac{1}{2}}$ = 30.07 years) in the environment: i) nuclear weapons testing, and; ii) the Chernobyl nuclear incident, from which ^{137}Cs is subsequently deposited during precipitation (Sac et al., 2008). It binds strongly with fine soil particles and undergoes little diffusive movement. This results in decreasing ^{137}Cs concentration through the soil profile (Matisoff et al., 2002). The extent of erosion or deposition at a chosen location can be gauged from comparison to an undisturbed reference sample (Zhang et al., 1994; Owens et al., 1996; He and Walling, 1997). Activity in sediment sources will be lower than undisturbed areas due to removal of the radionuclide, with the converse relationship existing for sediment sinks, allowing visualisation of sediment redistribution. Models which describe the relationship between changes in activity and erosion rates can be used to provide quantitative erosion data (Poreba, 2006). Tillage processes result in re-distribution of the concentration profile, however, this can be corrected for using mathematical models (Quine, 1999; Poreba, 2006). However, there is growing evidence suggesting spatial variation in ^{137}Cs results from processes other than soil erosion, e.g. non uniform inputs (Perk et al., 2002; Huh and Su, 2004).

The radionuclide ^{210}Pb has a similar length half-life to ^{137}Cs ($t_{\frac{1}{2}}$ = 22.3 years) and can be used in a similar way. Walling and He (1999) described the methods for measuring soil erosion using ^{210}Pb and highlighted its minimal use compared to ^{137}Cs at the time of publication; ^{210}Pb is a product of decaying ^{222}Rn ($t_{\frac{1}{2}}$ = 3.8 days) produced from ^{226}Ra ($t_{\frac{1}{2}}$ = 1622 years) as part of the ^{238}U decay sequence. ^{210}Pb is produced from soil and rock which contains ^{226}Ra and is termed 'supported' ^{210}Pb; it also deposited onto the surface of soils when ^{222}Rn defuses through the soil profile into the atmosphere and decays. This provides a source of ^{210}Pb which is not in equilibrium with its parent ^{226}Ra and is termed

'unsupported' ^{210}Pb. The amount of unsupported ^{210}Pb can be determine by measuring both ^{210}Pb and ^{226}Ra to determine the production rate of supported ^{210}Pb. Unsupported ^{210}Pb has a strong affinity for sediment particles, therefore its redistribution at the soil surface is related to sediment transport. As it is a natural radionuclide it can be used to determine soil erosion rates in locations where deposition of ^{137}Cs has been minimal.

These methodologies are useful for providing retrospective, medium term (circa. 40 year) erosion rates; however, neither ^{137}Cs or ^{210}Pb can be used to accurately measure short term, event based erosion (Blake et al., 2002). Although both tracers meet all of the applicable criteria set out by Zhang et al. (1994) (dependent upon radiation counter availability) they are not used to show sediment transport and redistribution from a single erosion event. Furthermore, the two radionuclides cannot be used as an MD-tracer because the locations of tracer deposition cannot be influenced.

^{7}Be is a natural fallout radionuclide with a short half-life ($t_{\frac{1}{2}}$ = 53.3 days), formed in the atmosphere by cosmic ray spallation of oxygen and nitrogen, deposited from the atmosphere during precipitation and originally used in fluvial sediment tracing (Fitzgerald, 2001). The radionuclide can be used in the same fashion as ^{137}Cs or ^{210}Pb, by measuring activity in an area experiencing erosion and comparing to an undisturbed area (Blake et al., 2002). When used as a soil tracer it is assumed that ^{7}Be inventories are depleted after protracted periods without precipitation and further diminished by dilution during tillage. Distribution of ^{7}Be inventories after intensive precipitation can therefore be used to identify sediment sources and sinks from erosion events (Blake et al., 2002; Matisoff et al., 2002). Newer models allow a longer use of ^{7}Be for tracing during the wet season (Walling et al., 2009). ^{7}Be is the most appropriate radionuclide for this project as it can be used to show sediment transport from single events. However, ^{7}Be cannot be used as an MD tracer as it does not exist in multiple forms.

The analysis of soil samples for radionuclide concentrations can be time consuming and very expensive. Sample throughput times can be slow, and are depen-

dent upon the number of analysers available. This can be a major hindrance for gaining good spatial resolution of transport patterns, especially at larger scales.

Magnetics:

Soils have their own unique magnetic signature derived from variations in the concentrations of magnetic minerals such as hematite, goethite, and magnetite. The concentrations of these minerals are dependent upon the concentrations in the parent rock from which the soil was formed causing a variable magnetic susceptibility in the soil profile. The redistribution of soil at the plot/field scale can be determined by comparison of surface measurements of magnetic susceptibility to the magnetic susceptibility profile in an undisturbed soil core (Royall, 2001). The technique has methodological similarities to the ^{137}Cs technique, and therefore also lacks sufficient temporal resolution for this project.

Fingerprinting:

Fingerprinting is a source ascription method used to determine the provenance of sediment in larger (> 500 km^2) catchments (Collins et al., 1998). Fingerprinting allows the contribution from two or more distinct soils to a single deposition location to be determined (Walling, 2005). The method has two fundamental steps: i) chemical and physical properties of different sediment sources are investigated to find indicators which are unequivocally different; ii) comparison of the fingerprint properties of sediment sources with collected suspended sediment samples to determine the relative importance of the different sources.

Samples from the source locations undergo a large range of analysis including measurements of trace metals (Fe, Mn, Al), heavy metals (Cu, Zn, Pb, Cr, Ni, Co), base cations (Na, Mg, Ca, K), radionuclides (^{137}Cs, ^{210}Pb, ^{7}Be), organic matter content, particle size analysis and magnetic susceptibilities (Motha et al., 2002). Use of a single indicator is likely to result in incorrect source to sediment matches, therefore multiple indicators are used to develop a more distinguishable fingerprint for each source. The concentration of the analytes in the mixed sediment is used to determine the contribution from each source with the aid of un-mixing models

(Fox and Papanicolaou, 2008).

The collection of samples requires no specific methods other than those normally used for representative soil sub-sampling, while indicator analysis is performed via standard methods, e.g. mass spectroscopy, atomic absorption spectroscopy or similar for trace elemental analysis, gamma spectrometry for radionuclide activity quantification; however, soil samples are typically screened to remove sediments > 100 μm to ensure that suspended fluvial sediments are properly represented (Walling et al., 2008). The application of statistical testing to discriminate different sediment sources (e.g. Kruskal-Wallis H test (Collins and Walling, 2002)) and un-mixing models is required as the indicators for source ascription are typically present in all source fingerprints (Walling et al., 1999). The specific details of these statistical methods are beyond the scope of this thesis.

The technique has typically been deployed to determine the contribution from different source types, e.g. comparing land use or land management techniques (Collins et al., 1998). This makes the technique useful for policy and management driven investigation, but far less applicable for determining sediment sources and sinks inside an area of homogeneous land use. Furthermore, the technique is only applicable for watershed scale experiments (> 500 km^2) and determination of sediment sources from fluvial samples (Collins et al., 1997, 1998; Carter et al., 2003).

Applied Tracers

There are many examples of particles and materials that are applied to soils to act as soil tracers. These tracers are selected to have a characteristic that makes them easily detectable so that their redistribution can be visualised. Tracers that are applied to soils must either bind strongly without modifying soil properties or replicate the transport behaviour of the particle size of interest. The use of applied tracers is recent in comparison to native tracers which have been used for over 30 years (Poreba, 2006), therefore the number of studies using applied tracers is significantly lower than for native tracers.

Magnetic Particles:

Polystyrene plastic beads containing magnetite (3.2 mm diameter and 1.2 $g.cm^{-3}$) were developed and used by Ventura et al. (2001, 2002) to study detachment and deposition processes at the plot scale. Plots of a fine loam soil were tilled by hand to a depth of 20 cm and the tracers were incorporated into the soil profile to a depth of 3 cm at a concentration of 5% by weight at the top of the plot. Simulated rainfall (35 and 70 $mm.hr^{-1}$) and surface inflow (4 and 10 $l.min^{-1}$) were applied to the top of the plot until steady state conditions were achieved. Magnetic susceptibility readings were taken by hand, and in-situ, using an MS2D magnetic susceptibility meter. Multiple measurements were taken so that spatial plots of magnetic susceptibility could be plotted showing source and sink locations via the intensity of the magnetic signal. Measurements could be used to calculate masses of deposited tracer at different slope positions.

This allowed event based processes to be easily monitored giving improved temporal resolution compared to many native tracers. However, the beads had to be applied at concentrations below 10% by weight to prevent armouring effects modifying detachment processes. Furthermore, the concentration of the tracer in eroded sediments was 20% by weight indicating that the tracers were acting in a non-conservative manner.

Similar work was performed previously by Govers et al. (1994) using larger 15 mm plastic beads, and by Lindstrom et al. (1992) using 11 mm steel hexagonal nuts. However, the beads and nuts are likely to show only B-grade tracing ability due to their single, large size. Although the tracers could potentially be used in multiple forms, their size may limit their incorporation into soil aggregates and they have been shown to modify soil properties. Furthermore, all magnetic tracers must be considered as gravel tracers as they have diameters $\geq$ 2 mm.

Recent investigations by A. Armstrong (Lancaster University, UK, personal communication) have identified the possibility of modifying the magnetic properties of soil through heating. Heating soils to different temperatures creates different levels of magnetic susceptibility allowing the creation of an MD-tracer. Back-

ground interference is likely to be low because the magnetic susceptibilities of the modified soil are distinctly different to unmodified soil. This is possible due to the range of different types of magnetic susceptibility which allow the sediment to be uniquely modified and identified, similar to the fingerprinting technique which has been described previously. A further advantage is that the tracer material has very similar properties to the parent soil, minimising issues of tracer suitability. However, this technique is still under development and was not ready for application at the start of this project. As a result, the use of soil with modified magnetic properties was not an option for this project.

Work by G. Guzman (Instituto de Agricultura Sostenible, Spain, personal communication) has also applied magnetic particles as a sediment tracer, but using fine sand sized iron oxides. The size of these particles should allow either incorporation into soil aggregates, or more representative transport rates than the gravel sized soil tracers used by Govers et al. (1994) and Lindstrom et al. (1992). The oxides are mixed with soil and distributed over the experimental plot and so should be transported in a conservative manner. The tracers are an MD-tracer, as various different distinguishable oxides exist. However, the methodologies are still under development and to date there have been no publications detailing experiment methods or results. As a result, the use of this methodology was not a possibility for this project.

Ceramic Prills:

Ceramic prills were manufactured by Plante et al. (1999) and Duke et al. (2000), containing 10-15% Dy for use as an inert tracer for soil studies. The spheres were manufactured by Kinetico Inc. (Nashwauk, MN, USA), under the trade name Macrolite, in three different sizes ranging from $\approx$ 0.25 mm to $\approx$ 0.75 mm. The prills were manufactured by combining ceramics with Dy_2O_3, although the exact manufacture method was not published. The prills possessed a porous mineral surface structure which was seen as crucial to their ability to mimic the transport behaviour of microaggregates.

The ceramic prills were successfully detected in soil samples and sediments

via induced neutron activation analysis (INAA). Limits of detection were reported as less than 7.6 $\mu g.g^{-1}$. The Dy label showed minimal leaching from the prills suggesting that the tracers have suitable structural integrity for long term use as sediment tracers. However, there were no subsequent publications reporting the use of the prills in tracer tests, therefore there are no studies suggesting that the prills can exhibit A-grade behaviour. Obtaining the prills may prove difficult as they were manufactured by a third party company and the method of manufacture is unknown. A new set of prills would therefore have to be prepared which would require the characterisation work of Plante et al. (1999) and Duke et al. (2000) to be repeated. Furthermore, INAA is an expensive analytical technique with limited availability. Dissolution of the prills to allow analysis by a spectrometric technique may prove difficult.

Radionuclides:

Radioactive tracers have previously been applied to soils as sediment tracers by Syversen et al. (2001). A 5 m $\times$ 50 m plot (14% slope, tilled silty clay) was artificially contaminated with ^{134}CsCl (specific activity 37 $\times$ 10^3 $kBq.mg^{-1}$) using manure spreading equipment. A 5 m $\times$ 5 m planted buffer strip was created at the base of the plot to investigate the ability of such strips to attenuate sediment transport. Detection of the tracer was performed in situ using a 76 mm NaI detector equipped with a Canberra multichannel analyzer. Measurement time at each measurement point was 30 s. Measurements were recorded at the intersections of a 1 m $\times$ 1 m grid system in the plot, at the intersections of a 0.5 m $\times$ 1 m grid system in the buffer strip and also from sediments in surface runoff collected from downslope of the buffer strip. Measurements were taken on eight occasions during a three year period. Measurements were also taken of soil cores collected from each measurement point. ^{134}Cs activity was measured above and below the top 1 cm layer to determine vertical and horizontal tracer distribution. Activity was measured using the same detector as in-situ measurements but with a counting time of 30 min to 1 h.

As tracer distributions are uniform (compared to fallout radionuclides) prior

to experimentation it is easier to identify event based redistribution patterns than with natural fallout radionuclide. Although the tracers will show A-grade tracing behaviour, there are many associated risks and controls with the use of radionuclides, as was highlighted by Syversen et al. (2001): i) ^{134}Cs strongly associates with clay particles, therefore soil texture will influence tracer transport; ii) inaccurate manual spreading can result in inhomogeneous tracer distribution; iii) applications of the tracer in the field requires permission from authorities and special security procedures to be followed; iv) the experimental plot must remain undisturbed unless the mixing associated with tillage is to be compensated for.

Rare Earth Oxides:

Rare earth oxides (REOs) are the oxides of the lanthanoid elements, available as inert silt sized powders which have been used as sediment tracers (Zhang et al., 2003; Polyakov and Nearing, 2004). They are readily available for purchase from chemical suppliers and therefore require no specific manufacture. Due to their inert nature, specifically their insolubility in water, they are suitable soil tracers (Topp, 1965). Typically, they are mixed with parent soil and the tagged mixture is applied to the experimental plot (Zhang et al., 2003; Stevens and Quinton, 2008). They have been shown to bind uniformly into different sized aggregates and are assumed to not affect sediment behaviour (Zhang et al., 2001; Kimoto, Nearing, Zhang and Powell, 2006).

Detection of the REOs is non-problematic. Only comparatively small quantities of REOs need to be applied to experiment sites to give a detectable tracer signal because the background concentrations of the lanthanoid elements in soils are low ($\approx$ 5 - 50 $mg.Mg^{-1}$) (Topp, 1965). Quantification of the lanthanoid component of the REOs via ICP-MS or ICP-OES provides part per billion (PPB) detection limits (Zhang et al., 2001). REOs have to be removed from soils into a solution to allow detection via ICP methods; however, this is achievable by heating in concentrated acid solutions which is a common feature of many soil digestion methods (Zhang et al., 2001; Stevens and Quinton, 2008; Michaelides et al., 2010).

The availability of different oxides allows MD-tracing (Michaelides et al.,

2010). REOs meet all of the criteria set out by Zhang et al. (2001) and have the potential to provide A-grade tracing for sediments.

Tagging with REOs may result in some modification of the soil particle size distribution through the mechanical mixing processes and wetting of the soil used to incorporate the REOs (Zhang et al., 2003).

As with all applied tracers, the use of REOs at large scales requires the distribution of tagged soils which can present a technical challenge to be overcome (Polyakov et al., 2004; Stevens and Quinton, 2008). Imprecise results can be generated when the sub-samples collected for analysis (typical acid digestion methods require soil masses of $\approx$ 1 g (Zhang et al., 2001)) have small masses compared to total eroded sediment masses due to uneven distribution of the tracers in the eroded sediment (Liu et al., 2004). This leads to the requirement to analyse a higher number of samples to provide a reliable average. However, analysis via ICP-MS can be expensive (up to £10 per sample (C. Stevens, Lancaster Environment Center, UK, personal communication)), especially when performed by a third party research group. This may place limits on the number of samples available for analysis which can limit the amount of information gathered from an experiment.

Tracer enrichment ratios reported in studies examining sheet erosion (Zhang et al., 2003; Polyakov and Nearing, 2004) suggest that REOs bound to aggregates may experience independent transport upon aggregate breakdown. The strength of binding between soil aggregates and REO particles during erosion has not been investigated, therefore there is limited knowledge regarding the extent to which REO particles are removed from aggregates and transported as primary particles. Although these data are lacking, it is important for the interpretation of results from REO tracing experiments.

Sediment Tracer Summary

The grading of all sediment tracers is presented in Table 3.1 (following the description of colloid sediment tracers). Native tracers are generally inappropriate for plot

scale, event based erosion studies. Certain native tracers (radionuclides, surface magnetic susceptibility) can be used to show sediment redistribution patterns at the plot scale. However, all native tracers lack sufficient temporal resolution for this project, apart from ^{7}Be which lacks the ability to act as an MD-tracer. ^{7}Be is short lived and requires constant atmospheric inputs, therefore indoor use (simulated rainfall) would require ^{7}Be applications. This would then be considered an applied tracer.

Applied tracers allow redistribution of sediments to be more easily visualised on an event-by-event time scale. However, tracing ability is reduced as they typically possess differing physical properties to the soil. Tagging soil aggregates with a component to make them detectable removes this issue by creating a tracer with the same properties as the soil. There is now a growing body of literature that uses REOs in this manner. As a result, REOs present the most suitable MD-tracer for this project.

3.4.2 Colloid Tracers

Surface runoff has always been traditionally separated into particulate (≥ 0.45 μm) and dissolved (≤ 0.45 μm) fractions, effectively ignoring the role of colloids. This issue has been commented upon (Haygarth et al., 2006) and a growing interest is being taken in surface colloid transport. Colloids play an important role in contaminant transport because of their rapid transport by surface runoff of very low stream power and their large relative surface area allowing high concentrations of contaminants are transported (Chapter 2). Despite this, there have been no publications which apply a colloid tracer (≤ 0.45 μm) to surface runoff from uncovered soils. This makes the selection of a suitable colloid tracer more difficult as there is limited information on the use of candidate tracers in surface runoff.

It is believed that all tracing studies published to date have either examined sub-surface tracer transport, or infiltration of tracers from the soil surface (Mortensen et al., 2004; Burkhardt et al., 2008). Colloid investigations typically use packed columns of clean quartz or silica particles to replicate sub-surface porous

systems (saturated and unsaturated). Field experiments are less common because of the need for large numbers of tracers and are typically used to investigate the behaviour of in-situ colloids (El-Farhan et al., 2000). All tracers described in this section are applied to the system being studied and are therefore classed as applied tracers.

Mineral Colloids:

Clay minerals are a common colloid tracer as they have identical densities and surface properties to clay colloids in soils (Compere et al., 2001) and should therefore exhibit A-grade tracing behaviour. Detection of mineral particles can be done in a number of ways, typically by turbidity measurement, or examining diffraction at 300/350 nm using spectrophotometry (Zhuang et al., 2004; Chen and Flury, 2005). In order for clay minerals to be used as a colloid tracer there can be no other clay particles present in the test matrix, unless the tracers have a distinguishing feature. As a result, clay minerals are commonly used in saturated column experiments with clean sand matrices and sediments that have been screened to remove natural colloids (Tang and Weisbrod, 2009). This prevents the use of clay minerals in field studies.

Organic Colloids:

Organic colloids have been used as tracers as they can be cultivated and can perfectly replicate colloid transport (therefore demonstrating A-grade tracing behaviour). Flagellates ($\approx$ 2 - 5 μm) (Harvey et al., 1995), humic acids ($\leq$ 110 nm) (Mibus et al., 2007) and bacteriophages (0.025 μm) (McKay et al., 2002; Keller and Sirivithayapakorn, 2004) have been used, representing a wide range of colloid sizes. Bacteriophages present a considerable advantage for pathogen studies due to diminished health risks compared to many viruses and bacteria and are typically enumerated by the plaque method (Bales et al., 1991; Blanford et al., 2005). Fluorescent dyes (fluorescine, rhodamine, hydroethidine) can be bound to both flagellates and bacteriophages giving a greater range of enumeration techniques and easier use in field tracer tests (Harvey et al., 1995; Gitis et al., 2002). How-

ever, the size and transport behaviour of bacteriophages is distinctly different to that of larger colloids. Furthermore, the tracers require cultivation and tagging prior to use. The tagging of bacteriophages requires a time consuming dialysis technique. These tracers are typically used when their exact characteristics are required.

Deoxyribonucleic Acid:

Deoxyribonucleic acid (DNA) labelled clay was developed by Mahler et al. (1998) for use as a colloid tracer. The most significant advantage is the almost limitless number of distinct tracers that can be created by using different DNA sequencing. However, the creation and detection of DNA tracers will be considerably more complex than for more simple tracers, requiring complex organic synthesis and the use of specialised synthetic equipment.

Applied Particles:

Manufactured particles such as silica microspheres (0.30 μm, 2.2 g.cm^{-3}) and silica coated zirconia colloids (0.11 μm) have been used to trace colloids (Vilks et al., 1997; Elimelech et al., 2000; Loveland et al., 2003). These can be detected by turbidity measurement or ICP-MS if the particles are manufactured from an element not present in the flow matrix (Loveland et al., 2003). This allows more realistic matrices to be used, but requires extra preparation of the tracers.

Fluorescent Microspheres:

Fluorescent microspheres are formed by polymerisation of a polymer in the presence of a fluorescent dye. Microspheres are available as suspensions of single particle sizes. This allows easy investigation of the influence of particle size upon transport behaviour. They can be used as an MD-tracer because multiple dye colours are available. Charged functional groups can be placed on the surface of microspheres resulting in development of surface charge similar to natural colloids (Chapter 2). Microspheres are readily available and require no manufacturing by the user. Detection of microspheres can be performed by epi-fluorescent mi-

croscopy, flow cytometry or fluorescent spectroscopy.

However, the density of microspheres is significantly lower than natural clay minerals which may result in faster transport due to lower settling velocities compared to clays. Furthermore, microspheres are perfectly spherical which is unrepresentative of clay particles that are typically platelets. A further drawback of microspheres is the cost; microspheres have to be purchased from a third party unless manufacturing equipment is available. Prices for 10 ml of 2.5% microsphere solution range up between 140 pounds sterling to over 1000 pounds sterling depending upon particle size. This can dramatically limit the scale and reproducibility of experiments.

Colloid Tracer Summary

The use of mineral clays would be inappropriate for this study as the tracers have to be applied in a location where natural clay colloids are ubiquitous. Flagellates and bacteriophages make suitable colloid tracers but require extensive manufacture. The use of colloids manufactured from silica presents the same issues as using clay minerals, unless they contain a distinct element. This makes the availability of multiple tracers difficult. Fluorescent microspheres are the most common tracer for colloids and have none of the previously mentioned issues. The availability of multiple dye colours, tracer sizes and surface properties will allow more detailed information to be gathered than if a single tracer was used. As the tracers are readily available there are no manufacturing requirements. This selection process is summarised in Table 3.1.

3.5 Rare Earth Tracers

3.5.1 Chemistry

The rare earth elements (REEs) are the first of the f-block metals (Table 3.2). The name rare earth element is unjustified, as apart from promethium which has no stable isotopes, they are all ubiquitous in the environment and found in various

Table 3.1: Summary of the reviewed tracers, their tracing grade and potential shortcomings.

Rank	Tracer	B-Grade	A-Grade	Comparison to Zhang et al. (2001) Criteria & Other Issues
		Sediment Tracers		
1	Rare Earth Oxides	✓	✓	Possible modification of the soil's physical properties during tagging. Enrichment ratios greater than one have been reported.
2	Applied Radionuclides	✓	✓	Issues surrounding use in the environment.
3	Ceramic Prills	✓	✖	Poorly incorporated into aggregates.
4	Magnetic Particles	✓	✖	Poorly incorporated into aggregates, may cause surface armouring.
5	Fingerprinting	✓	✓	Not an MD-tracer at small scale. Potentially expensive analysis.
6	Surface Magnetics	✓	✓	Cannot be used to show sediment transport from single events. Analysis can be expensive, not an MD-tracer.
7	^{137}Cs, ^{210}Pb, ^{7}Be	✓	✓	Cannot all be used to show sediment transport from single events. Analysis can be expensive, not an MD-tracer.
		Colloid Tracers		
1	Fluorescent Microspheres	✓	✓	Potentially high background interference. Expensive to purchase the tracers in large quantities.
2	Artificial Particles	✓	✓	Require potentially expensive manufacture.
3	DNA	✓	✓	Expensive and complicated to synthesise and analyse.
4	Organic Colloids	✓	✓	Often require synthesis or modification.
5	Mineral Colloids	✓	✓	Non-applicable for systems containing clay.

minerals. They are electropositive resulting in the common +3 oxidation state. Higher oxidation states than this are uncommon (Topp, 1965). The lanthanoids undergo a contraction in atomic radius across the period (lanthanoid contraction) as a result of increasing nuclear charge (Shriver and Atkins, 2002).

The REEs' common oxidation state of +3 and large atomic radius make them excellent acceptors of ligands, therefore rare earth oxides (REOs) are common (Table 3.3). The most common oxide is the M_2O_3 sesquioxide form. Other forms are M_6O_{11}, $M(OH)_3$, MO_2 and MO. The sesquioxides are all strongly basic and will absorb water and CO_2 from the atmosphere. Their colours generally tend to be pale, and they exhibit properties similar to the alkaline earth oxides. Of the three types of the sesquioxide, the lighter of the lanthanoides usually form type A and the middle lanthanoides type B. As a single molecule it takes the form of a MO_7 capped octahedron (Topp, 1965).

Table 3.2: Chemical data of the rare earth elements (Shriver and Atkins, 2002).

Atomic N^o	Name	Symbol	Mass N^o	Radius (M^{3+}) (Å)	Configuration of M^{3+}
57	Lanthanum	La	138.9	1.16	[Xe]
58	Cerium	Ce	140.1	1.14	[Xe] 4f1
59	Praseodymium	Pr	140.9	1.13	[Xe] 4f2
60	Neodymium	Nd	144.2	1.11	[Xe] 4f3
61	Promethium	Pm	146.9	1.09	[Xe] 4f4
62	Samarium	Sm	150.4	1.08	[Xe] 4f5
63	Europium	Eu	152.0	1.07	[Xe] 4f6
64	Gadolinium	Gd	157.2	1.05	[Xe] 4f7
65	Terbium	Tb	158.9	1.04	[Xe] 4f8
66	Dysprosium	Dy	162.5	1.03	[Xe] 4f9
67	Holmium	Ho	164.9	1.02	[Xe] 4f10
68	Erbium	Er	167.3	1.00	[Xe] 4f11
69	Thulium	Tb	168.9	0.99	[Xe] 4f12
70	Ytterbium	Tm	173.0	0.99	[Xe] 4f13

Table 3.3: Chemical data of the rare earth oxides (Topp, 1965).

Formula	Mass ($g.mol^{-1}$)	Structure	Colour
La_2O_3	325.80	Sesquioxide A	White
CeO_2	172.10	Fluorite	White
Pr_6O_{11}	1021.39	Fluorite/Sesquioxide C	Black
Nd_2O_3	336.40	Sesquioxide B	Pale Pink
Sm_2O_3	348.80	Sesquioxide B	Pale Yellow
Gd_2O_3	362.40	Sesquioxide B	Pale Blue

3.5.2 Prior Publications

The first use of REE tracers for environmental studies was by Knaus and Gent (1989) as a marker for marsh accretion. Tian et al. (1994) performed the first study using rare earth compounds as sediment tracers. Zhang et al. (2001, 2003) further explored the potential of the REOs for sediment tracing (binding and extraction) and applied them at the plot scale, as did Wei et al. (2003), Liu et al. (2004) and Polyakov and Nearing (2004). These publications demonstrated that REOs make suitable tracers for sediment transport studies under controlled conditions with high erosion rates.

REOs were then applied to more varied plot studies and larger scale field studies. Polyakov et al. (2004) and Kimoto, Nearing, Shipitalo and Polyakov (2006) applied REOs to a small agricultural watershed over a period of four years to test their longevity in the environment. Liu et al. (2004), Lei et al. (2006) and Zhang et al. (2008) used REOs to study concentrated flow processes. Further studies of tracer suitability in coarse material by Kimoto, Nearing, Zhang and Powell (2006) reinforced the REOs potential as a sediment tracer. REOs were used by Stevens and Quinton (2008) to study the effects of tramlines on sediment transport in UK arable fields. Yang, Song, Sui and Ding (2008); Yang, Wang, Sui and Ding (2008) used REOs to study erosion in Chinese red soils and Loess slopelands. Polyakov et al. (2009) used REOs in a semi-arid rangeland catchment to identify sediment redistribution patterns. The most recent published use of REOs was by Michaelides et al. (2010) to examine the deposition patterns of

eroded sediments across a break of slope using a 2.5 m × 6 m soil plot receiving simulated rainfall.

3.5.3 Methodologies

Methodologies used with REO tracers can be divided into: i) tagging; ii) application; iii) sample collection, and; iv) extraction. REOs are mechanically mixed with the soil to achieve tagging. Zhang et al. (2001) achieved this with soil that had been wetted to 10% moisture content to aid with REO incorporation. This practice was continued in the majority of papers that followed. An exception was Stevens and Quinton (2008) who mixed REOs with dry sand. In the majority of publications which originate from China the tagging method is not detailed.

For small scale experiments (typically indoors with simulated rainfall), application is usually achieved by filling an excavated area with tagged soil. This can either be the whole plot (Polyakov and Nearing, 2004), bands of tracer (Zhang et al., 2003) or square sections of tracer (Michaelides et al., 2010). Tagged soil is distributed using agricultural spreading equipment (Polyakov et al., 2004) or by hand (Polyakov et al., 2009) during larger field experiments where excavation and repacking is impractical. Distributed tagged material can be incorporated by tillage where possible (Kimoto, Nearing, Shipitalo and Polyakov, 2006). Alternatively, a single location that represents the surrounding area can be tagged to minimise the area of the field plot to which tracers are applied (Yang, Wang, Sui and Ding, 2008).

Samples are collected as surface runoff and as shallow surface cores or scrapes. Zhang et al. (2001) extracted REOs from samples by heating in a solution of nitric acid, hydrogen peroxide and hydrochloric acid, as did the majority of publications which followed. However, Stevens and Quinton (2008) used aqua regia. The quantification of REOs in extracted solutions is performed by ICP-MS. INAA is used in the majority of publications which originate from China as it does not require REO extraction from sediments, but it is a far less available technique.

3.5.4 Transport Behaviour

Enrichment ratios (the ratio of tracer concentration in eroded sediment compared to undisturbed soil) are used to show the accuracy of tracing methods. A value greater than one indicates either the preferential transport of tagged sediments or the removal of the tracer from tagged sediments. They are therefore a useful indicator of tracer behaviour. However, enrichment ratios are less useful when less than 100% of the plot area is tagged. In these cases, enrichment ratios greater than one can occur due to preferential erosion around tagged areas (Zhang et al., 2003).

Initially, enrichment ratios in runoff can be high due to poorly incorporated powders (Polyakov and Nearing, 2004). Zhang et al. (2003) reported decreasing sediment ratios (1.97 - 1.20) during the first out of six simulated rainfall events. Stevens and Quinton (2008) reported enrichment ratios between 3.99 and 6.62 from tagged soils rained upon for 10 minutes. Polyakov and Nearing (2004) reported an enrichment ratio falling from 3.0 and stabilising at 1.7 during the first out of eight simulated rainfall events.

However, high tracer concentrations are also reported following the initial loss of poorly incorporated powders. Polyakov and Nearing (2004) reported enrichment ratio fluctuations between 1.4 and 1.8 over eight rainfall events (eight hours total). Zhang et al. (2003) reported average estimated sediment ratios above 1.17 for the first three out of six rainfall events (three hours total). Kimoto, Nearing, Shipitalo and Polyakov (2006) reported enrichment ratios ranging between 0.4 and 2.3 over a four year period in a 0.68 ha watershed. REOs are known to bind into a range of aggregates between 0.01 mm and 4.75 mm (Zhang et al., 2001); however, the reported enrichment ratios show either removal of REOs from tagged sediments or the breakdown of aggregates which results in REOs binding predominantly to the finer fractions of soil. However, tracer enrichment is known for other tracers; Polyakov and Nearing (2004) stated that enrichment ratios for ^{137}Cs vary from 1.1 to 3.0.

Enrichment ratios are predominantly close to parity in publications where

concentrated flow is studied and sediment concentrations are high ($\approx$ 1000 g.l^{-1}). Li et al. (2002) and Lei et al. (2006) reported average sediment ratios of 1.04 and 0.87 respectively for concentrated flow studies. This demonstrates how the particle size selective nature of unconcentrated flow results in greater enrichment due to preferential transport of fine material (Morgan, 2005).

Kimoto, Nearing, Zhang and Powell (2006) reported that background REE concentrations increase with decreasing sediment size, reporting that this may explain the perceived increased REO concentrations in eroded sediments. However, in the case of Polyakov and Nearing (2004), the 2-3% increase in clay and fine and medium silt fractions in eroded sediments could not account for a fivefold increase in the background REE concentration. However, higher extraction of background REEs from eroded sediments may explain some tracer enrichment values greater than one.

The evidence suggests a number of different factors lead to REO enrichment. Poorly incorporated tracers are removed during the initial stages of an erosion event giving an initially high, but falling, enrichment ratio. Aggregate breakdown leads to transport of unbound REOs and also REOs bound to finer material. This will only lead to tracer enrichment if finer material is selectively transported. Furthermore, the increased background REE concentrations in fine particles and severe erosion near tracer bands will also result in enrichment, but cannot account for all enrichment reported.

3.5.5 Methodological Issues

Mixing

Mixing rare earth compounds with soil should avoid modification of the soil's chemical and physical properties. The tagging procedure of Matisoff et al. (2001) formed slurries of soil and soluble REE-nitrates which were dried by filtration. This would have caused aggregate breakdown. Furthermore, removal of organic matter and fine sediments during filtration would hinder the reformation of the aggregates present in the parent soil which was to be replicated. Mixing insoluble

REO powders with soils does not require such aggressive treatment. This will limit the negative effects of mixing. However, the effect of published REO tagging methods on the particle size distributions of tagged soils has not been investigated.

Mixing of REO powders with soil has been performed with both moistened (Zhang et al., 2001) and dry soils (Stevens and Quinton, 2008). Obtaining a uniform distribution of REOs in the tagged material is important. Tagged material with poor REO distribution may result in untagged sediments being transported or variations in the REO concentrations vertically through the soil profile. Different methods of tagging soils with REOs have not been compared for either uniformity of distribution or the effect upon particle size distribution.

Application

Scale is the main influence upon methodological inaccuracies because issues are exacerbated at larger scales. At the field scale, tracer application can either be at a discrete point or a whole area application. Point applications reduce workload (Yang, Song, Sui and Ding, 2008), but *'test precision may be low'* if the point selected is unrepresentative of the surrounding area (Liu et al., 2004). However, Kimoto, Nearing, Shipitalo and Polyakov (2006) reported co-efficients of variation up to 43% for tracer concentrations inside tagged areas after blanket applications using a seed spreader.

Tillage can be used to mix tracers into the soil profile following blanket applications in order to prevent erosion of underlying untagged material. However, tillage results in redistribution of tracers so that there is *'no measureable way to differentiate the relative contributions of tillage or water erosion to the diffusive, or short distance, movement ... observed'* (Polyakov et al., 2004). Furthermore, tillage is not possible on un-cultivated land which could result in incidental transport of poorly incorporated tagged soil (Polyakov et al., 2009). This would be dependent upon the volume and intensity of rainfall prior to an erosion inducing rainfall event.

Sampling

REO methods are only able to determine the original location of REO tracers once the tracers are redistributed by multiple erosion events. This is because the original source of sediment reaching an outlet after multiple erosion events can be identified but the location of the sediment prior to the final erosion event is unknown (Polyakov et al., 2009). There is no way to identify event-based redistribution unless the plot surface is sampled between every event.

Representative sub-sampling of large sediment masses can be difficult, therefore large scale studies producing large masses of eroded sediments present difficulties. Lei et al. (2006) reported using 50 mg samples for INAA analysis, sub-sampled from 6.7 - 28.5 kg of well mixed sediment. Sub-sampling was reported as a potential reason for errors in erosion estimates. Increasing sample numbers will reduce error but will increase time and expense.

Extractions

Different methods of extracting REOs from tagged soils have been used by Zhang et al. (2001) and Stevens and Quinton (2008). Neither of these methods has been compared on a single soil. Furthermore, there has been no reported extraction of a certified reference material on any of the REO tracing publications to date. Lanthanoid elements are known to suffer from interferences during ICP-MS analysis (J. Gomez, Instituto de Agricultura Sostenible, Spain, personal communication), therefore extraction of a reference material should be performed.

3.6 Fluorescent Polystyrene Microspheres

3.6.1 Chemistry

Fluorescent microspheres are formed by a dispersion polymerisation technique; a solution of styrene containing a fluorescent dye is mechanically mixed with an immiscible solvent causing polymerisation as discrete particles. The process only requires a single step and is easy to control, allowing a broad range of particle

sizes to be formed. The use of different polymer solutions allows a very specific choice of dyes and surface properties. Particle sizes typically range from 10 nm to 10 μm, with size variation for a stated size $\leq$ 1%. Many different dyes can be used covering the entire visible spectrum (blue to red) which are incorporated throughout the sphere. Functional groups (for example carboxylate groups) can easily be added to the sphere surface. The majority of microspheres have a density of approximately 1.05 g.cm^{-3} which is lower than silica particles. Microspheres can either be purchased as dilute solutions (1 - 2.5% by mass) in a dispersing agent, or as dried powders. The stated shelf lives of microsphere solutions are approximately one year.

3.6.2 Prior Publications

The use of microspheres as groundwater tracers began in the late 1980s and early 1990s when the importance of colloid facilitated contaminant transport was being realised (Harvey et al., 1995). Since that time microspheres have been used to examine:

- Colloid mobilisation by, and attachment to, the air water interface (Bradford et al., 2004; Lazouskaya et al., 2006; Sharma et al., 2008);
- The effects of flow velocity and ionic strength of pore water on colloid transport (Huber et al., 2000; Zhang and Wang, 2006; Close et al., 2006);
- The effects of flow velocity on transport pathways (Baumann and Werth, 2004);
- Particle size effects (Becker et al., 1998; Weisbrod et al., 2003; Bradford et al., 2007);
- Conditions affecting colloid deposition (Li et al., 2006; Lauth et al., 2007; Bridge et al., 2007);
- Effects of porosity on colloid transport (Baumann and Werth, 2005) and,

- Investigation of aquifer transport properties (Goldscheider et al., 2003).

There have been no publications detailing microsphere manufacturing or application methods because microspheres are available as ready prepared solutions. However, there have been a number of publications detailing specific enumeration tools for colloid studies using microspheres.

3.6.3 Methodologies

The three most common techniques for enumeration are epi-fluorescent microscopy, flow cytometry and fluorescent or UV/Vis spectroscopy. Epi-fluorescent microscopy allows detection of microspheres in a range of sample matrices and to very low detection limits because of the ability to visualise single microspheres. The technique is typically applied where either fluorescent spectroscopy or flow cytometry has difficulties to quantify microspheres because of matrix interference from other fluorescent compounds, for example, the work by Burkhardt et al. (2008) on field infiltration patterns of microspheres. Flow cytometry and spectroscopic techniques are more rapid and have excellent limits of detection in clean samples. Detectors can be used in-line with column experiments. However, samples must be free of particulate material; furthermore, the techniques have an inability to distinguish between dyes contained in microspheres and natural dissolved material with similar wavelengths.

Effluent from column experiments or ground water studies is best analysed by either fluorescent spectroscopy or flow cytometry due to rapid sample throughput. However, *'colloid transport in porous media has been typically studied in column experiments from which data analysis was limited to the evaluation of effluent breakthrough curves'* (Weisbrod et al., 2003). Publications have begun to focus on investigating transport of colloids by visualising their three-dimensional locations inside plastic or glass chambers. At the pore scale this requires the use of microscopic techniques (Sirivithapakorn and Keller, 2003; Zhang and Wang, 2006) or x-ray microtomography (Li et al., 2006). Images of colloid transport through columns or chambers can be taken using macrophotography (Bridge et al., 2007;

Lauth et al., 2007) or magnetic resonance imaging (MRI) (Rosen et al., 2005; Baumann and Werth, 2005).

However, all of the studies described have investigated microsphere transport through porous media. As far as the author is aware there have been no publications to date where fluorescent microspheres have been used as a tracer for colloids in overland flow. Work by Burkhardt et al. (2008) examined microsphere infiltration on level 1.4 m x 1.4 m field plots, with no interest in surface runoff. Mortensen et al. (2004) performed a similar study on a 3 m x 3 m isolated block of clay till, while Cey et al. (2009) performed field infiltration experiments to establish the effect of macroporosity on colloid transport. Epi-fluorescent microscopy was used for microsphere enumeration in all three studies. As a result there is a large body of literature on microsphere use in clean artificial systems, and some limited data from infiltration studies, but the use of microspheres as a surface colloid tracer for natural soils appears to be novel. Furthermore, fluorescent spectroscopy has not been used to enumerate fluorescent microspheres from soil samples. This will require a significant amount of method development to be performed.

3.6.4 Methodological Issues

Fluorescent spectroscopy was chosen as the enumeration method prior to the commencement of the project. It was selected in preference to epi-fluorescent microscopy as it provides a more rapid method of enumeration. However, no published data were found on the use of fluorescent spectroscopy to enumerate fluorescent microspheres in surface runoff samples from bare soil plots. Particulate material will have to be removed from samples prior to enumeration. However, unlike the majority of microsphere studies using 'clean' systems, surface runoff samples will also contain dissolved organic matter (DOM) which is comprised partly of fluorescent macromolecules such as tryptophan and tyrosine.

3.7 Chapter Summary

Rare earth oxides and fluorescent microspheres have been selected for the sediment and colloid tracers respectively. These tracers provide advantages over the other candidate tracers and are the most suitable tracers for the needs of this project. Using both tracers simultaneously will allow the contribution from different soil particle sizes to be determined under different hydrological conditions and with different soil properties.

Certain methodological issues have been highlighted for both tracers. There is a lack of comparison of different tagging and extraction methods used for REO tracers. There has also been no extraction of lanthanoids from a certified reference material to check for instrumental interference. Fluorescent microspheres are to be enumerated by fluorescent spectroscopy. This will require the complete separation of the microspheres from all particulate and dissolved material in surface runoff samples. These issues will be investigated in the following chapters.

Chapter 4

Rare Earth Oxide Method Development

4.1 Chapter Outline

Rare earth oxides (REOs) are an effective and well developed set of sediment tracers, as has been discussed in Chapter 3 (Section 3.5). However, the chapter also highlighted methodological issues such as ICP-MS interferences. Furthermore, the increasing range of publications using REOs has resulted in a choice of application and extraction methods, none of which have been compared on the same soil.

This chapter compares potential REO tagging and extraction methods on a range of REO and rare earth elements (REEs) containing materials, quantifies the impact of different tagging methods upon soil particle size and examines the change in tagging and extraction efficiency when applied REO concentration is varied. This has been done to improve the effectiveness of REO tracers when tracing particulate phosphorus in subsequent chapters, and to improve REO usability for practitioners of sediment tracing.

4.2 Introduction

As was outlined in Chapter 3, not all publications which utilise rare earth oxides (REOs) have used identical methods for applying and extracting REOs. Different extraction methods were used by Zhang et al. (2003) and Stevens and Quinton (2008); both methods were selected due to their previous use in the dissolution of metals from soils. The concentration of background rare earth elements (REEs) extracted from soils is irrelevant provided that this concentration has low variability and all applied REOs are dissolved. Therefore, a method of shorter duration and lower corrosive strength may be more appropriate. Other methodological differences include the concentration of REOs used to tag soils (measured as integer values higher than the background REE concentration) and the water content of soils during tagging.

Users of REO tracers need to make a series of decisions in order to improve comparability between tracing studies. These include:

- What is the most appropriate REO concentration (as an integer value multiplied by the background REE concentration) to achieve uniform distributions of REOs in tagged soils and to allow effective recovery;
- What method of tagging soils is most appropriate to achieve a uniform distribution of REOs in tagged soils;
- What method of tagging soils is most appropriate for different experimental styles (distribution over field plots, repacking into soil boxes) when the effect of different tagging methods upon particle size distribution of the parent soil is considered;
- What is the duration and corrosive strength that is required for an extraction method to recover applied REO powders whilst providing uniform background REE concentrations from soils.

Added to these difficulties, a recent meeting of sediment tracing practitioners (Tag and Trace 2009, Bristol University, UK) revealed a common issue of ICP-MS

interferences when certain REOs are analysed. Interferences which cause overestimation of REO recoveries cannot be fully quantified, and in some cases are not even identified, unless a reference material of known REE/REO concentration is examined. Analysis of REO powders cannot be used to determine interferences due to the unknown purities of powders, and to date there have been no reported extractions of background REEs from a certified reference soil. Furthermore, analysis of samples is generally not performed by the research group conducting the tracing experiment due to the complex nature of ICP-MS analysis. This inhibits the adoption of standard analytical practice for all REO tracing studies and slows the interpretation of anomalous or counter-intuitive results.

This chapter will provide a comparison of common REO methodologies in order to distinguish positive and negative attributes of published methods, and to help ensure the successful use of REOs in the subsequent chapters of this thesis. These aims will be met by investigating: i) the uniformity of REO distribution in tagged soils following different tagging methods; ii) the impact of different tagging methods upon the particle size distribution of tagged soils; iii) the influence of applied REO concentration on tagging and extraction methods; iv) the ability of different extractants to provide reliable REO quantifications, and; v) the overestimation of REEs extracted from a certified reference soil and REO powders.

4.3 Materials

The soils used were two silty clay loams (Loddington and Rosemaund, UK), a clay loam (Hattons, UK) and an untreated silt loam topsoil purchased from Broughton Aggregates, all of which had been air dried and sieved to < 1 mm (Table 4.1). A reference soil certified by the Chinese National Analysis Centre for Iron and Steel (ref NCS DC 73383), which was supplied ground to a fine powder was also used. Heating during extractions was performed on a Seal Analytical BD50 heating block (50 tube capacity, 450°C max) in 100 ml volumetric glass boiling tubes. All acids used were analytical reagent grade. Samples were analysed on a Thermo Elemental X7 ICP-MS. REOs were the same REO powders used by Zhang et al.

Table 4.1: Percentages of sand, silt and clay (primary particle size) of Loddington, Rosemaund, Hattons and Broughton soils.

Soil	Clay	Silt	Sand	Classification
	Percentage - %			
Loddington	38%	60%	2%	Silty clay loam
Rosemaund	30%	67%	3%	Silty clay loam
Hattons	32%	46%	22%	Clay loam
Broughton	5%	50%	45%	Silt loam

(2001) and Zhang et al. (2003). Common REO properties are summarised in Table 4.2. The particle size analysis of REO powders showed coarser particle size distributions than those reported by Zhang et al. (2001), but agreed on the size order of powders. The discrepancy is likely due to the difference in the method of size distribution determination (laser diffraction versus sedimentation).

Particle size analysis was performed on a Malvern S2000 particle size analyser. Samples are dispersed into water and flowed in front of a laser; the resultant diffraction pattern of the beam is recorded and a particle size distribution is calculated using Mie theory (Mie, 1908). Particle size distributions (PSDs) were recorded three times for each sample, with a 10 second interval between each measurement, from which mean PSDs were calculated.

4.4 Methods

4.4.1 Tagging Methods

Four different tagging methods were used to investigate the effect of tagging upon the particle size distribution of tagged soils and the uniformity of REO distribution in tagged soils.

Dry Tagging

The method of Stevens and Quinton (2008) was followed. Air dried soil (10 g) was placed in a 1 L container. REOs were added and mixed with an electric

Table 4.2: Selected REO characteristics. Particle size data was collected via laser diffraction. Density values are taken from Zhang et al. (2003). Abundances are taken from Topp (1965).

Formula	Percentage Silt (2 - 63 μm)	Modal Particle Size	Size Range (d^{10} - d^{90})	Density	Natural Elemental Abundance (Topp, 1965)	Crystal Structure
	%	μm	μm	g.cm^{-3}	REE mg.Mg^{-1}	
La_2O_3	91.21	4.37	1.87 - 19.96	6.51	19	Sesquioxide
CeO_2	73.79	39.80	5.79 - 110.21	7.65	44	Fluorite
Pr_6O_{11}	97.77	10.00	4.12 - 33.35	6.83	6	Sesquioxide
Nd_2O_3	91.71	6.61	2.40 - 37.60	7.24	24	Sesquioxide
Sm_2O_3	97.25	5.75	2.38 - 10.77	7.86	7	Sesquioxide

mixer. Following this, nine aliquots of untagged blank soil (10 g each) were added sequentially, with mixing between each addition.

Wet Tagging

The method of Zhang et al. (2001) was followed. Soil (10 g) was placed in a 1 L container. REOs were added and mixed with an electric mixer. Following this, nine aliquots of untagged blank soil (10 g each) were added sequentially with mixing between each addition. All soil was pre-wetted to 15% moisture content.

Saturated Tagging

The method of Matisoff et al. (2001) was followed, substituting reagents for REO powders. Air dried soil (100 g) was dispersed in 600 ml of de-ionised water and mechanically stirred so all sediment was entrained. The necessary masses of REOs were combined with the slurry. The mixture was stirred for 25 minutes followed by a settling period of 24 hours. The supernatant was removed by filtration (2.4 μm) and the collected sediment dried at 105°C. Dried soil was lightly ground with a pestle and mortar so that all soil passed a 1 mm sieve (the original upper particle size limit).

Spray Tagging

A freely draining plastic container was filled with fine sand to a depth of 15 cm. Air dried soil (100 g) was placed on top of the sand and spread evenly to a depth of 5 cm. A filter paper with a pore size of 30 μm was placed between the sand and soil layers to allow easy excavation of the soil. The necessary masses of REOs were dispersed in 300 ml of de-ionised water and placed in a sprayer. The mixture was sprayed onto the surface of the soil at a rate that did not allow ponding to occur. REOs were held in suspension by agitation of the sprayer. Spray tagging can either be used as a tagging method of soil that is subsequently applied to an experimental plot (as was the case in this study), or as a direct REO application method (investigated in Chapter 7).

The Broughton soil was used for the investigation of effects of tagging upon particle size. Soil samples (100 g) were tagged at 0, 50 and 500 times background Nd concentration using Nd_2O_3. Three replicates were made of each concentration for each tagging method (i.e. nine samples per tagging method). Samples were homogenised following tagging (without affecting the particle size) and three sub-samples taken from each tagged sample using a splitting apparatus. In total 27 sub-samples were measured for each tagging method at different REO concentrations (each measured three times). All samples were compared to untagged samples of the Broughton soil (the method blanks).

The Rosemaund soil was selected for uniformity investigations. The REOs La_2O_3, Pr_2O_3, Nd_2O_3 and Sm_2O_3 were used to tag 100 g of soil at 0, 50 and 500 times background REO concentrations, with three replicates of each concentration for each tagging method. Following tagging, the soils were dried at 105 °C to allow accurate weighing and the REOs extracted using the USEPA 6350 method (Section 4.4.2). Only the USEPA 6350 method was used to extract REOs from tagged soil. Tagged soil cannot be used to compare extraction methods because variations in results may be caused by non-uniformity of the REO distribution resulting from poor tagging. The mass of soil used (100 g) was selected because a smaller mass of soil would have made the mixing process unrealistic, whereas a larger mass would have been more difficult to sub-sample representatively (sub-samples were 0.5 g).

4.4.2 Extraction Methods

Extraction methods were performed upon REO powders, untagged soils (Hattons, Loddington and Rosemaund were used to give a range of soil types), the certified reference soil and tagged Rosemaund soil. A method based upon the USEPA 6350 extraction method was used, as well as the published methods of Stevens and Quinton (2008) and Zhang et al. (2003). The USEPA method was chosen as it does not require the samples to be left for 24 hours following extraction or the use of hydrochloric acid (unlike the method of Zhang et al. (2003)), and is therefore milder than both the published methods being examined. A shortened version of

the USEPA method was also used to establish the efficiency of REE/REO extraction over very short extraction durations. The comparison of the four methods did not allow independent examination of all variables (duration, presence of individual reagents and their volumes, ratios of reagent volumes, temperatures). The number of samples required to test all variable independently, upon all extractable materials, was beyond the scope of this investigation.

Stevens and Quinton (2008)

Soil samples (0.5 g) or REO powders (20 g) were placed in boiling tubes. HCl (10 ml, 37%) and HNO_3 (3.33 ml, 69%) were added and left at room temperature for one hour. Samples were heated to 110°C (3°C.min^{-1}). Additional HCl (3 ml, 37%) and HNO_3 (1 ml, 69%) were added. The samples were left at 110°C for one hour then warmed to 140°C for four hours (or until near dryness).

Zhang et al. (2003)

Soil samples (0.5 g) or REO powders (20 mg) were placed in boiling tubes. HNO_3 (10 ml, 69%) was added and the samples heated at 85°C for two hours. H_2O_2 (2.5 ml, 30%) was added after cooling to less than 70°C. The samples were heated for 2-3 minutes after effervescence had subsided. HCl (5 ml, 36%) was added and the samples heated at 85°C for a further 2 hours. The boiling tubes were then removed from the heating block and left for 24 hours.

USEPA 6350

Soil samples (0.5 g) or REO powders (20 mg) were placed in boiling tubes. HNO_3 (10 ml, 69%) was added and the solutions warmed to 95°C for 15 minutes. Further aliquots of HNO_3 (5 ml each, 69%) were added until no evolution of brown gas was observed. The samples were heated at 95°C for a further two hours. The boiling tubes were allowed to cool and de-ionised water (2 ml) and H_2O_2 (2 ml, 30%) were added. The boiling tubes were then re-heated to 95°C until effervescence ceased, at which point a further two aliquots of H_2O_2 (2 ml, 30%) were added.

The samples were then heated at 95°C for a further two hours.

USEPA 6350 (shortened)

Soil samples (0.5 g) or REO powders (20 mg) were placed in boiling tubes. HNO_3 (20 ml, 69%) was added and the solutions warmed at 95°C for one hour. The boiling tubes were allowed to cool, and de-ionised water (2 ml) and H_2O_2 (6ml, 30%) was added. The samples were then heated at 95°C for a further hour.

Following all extraction methods samples were: i) made to 100 ml volume with de-ionised water; ii) pre-filtered at 2.7 μm through Whatman GF/D glass microfiber pre-filters; iii) diluted to REE concentrations inside the ICP-MS calibration range (1-50 PPB) using 1% nitric acid (ICP-MS standards were REEs in 1% nitric acid); and iv) filtered at 0.45 μm using Whatman disposable syringe filters.

4.5 Results

4.5.1 Tagging Methods

Particle Size Effects

The PSD data (Figure 4.1) shows that the particle size distribution of tagged soil was influenced by the tagging method. Spray tagging had no significant effect upon PSD (Table 4.3). However, all other methods significantly altered the percentage volume of at least one of the common size fractions ($p > 0.05$). The presence of water during wet tagging, and the dispersion of soils in water during saturated tagging resulted in a breakdown/weakening of aggregates in the sand fractions, and an increase in the very fine sand and silt fractions. This was especially prominent for saturated tagging. Soils which had been tagged with REOs at 50 and 500 times background concentration via dry and spray tagging showed no difference in PSD to soils which had undergone the tagging methods, but with no applied REOs. Soil tagged by the wet method showed significant increases in the fine and very fine sand fractions when tagged at 50 and 500 times background concentration when

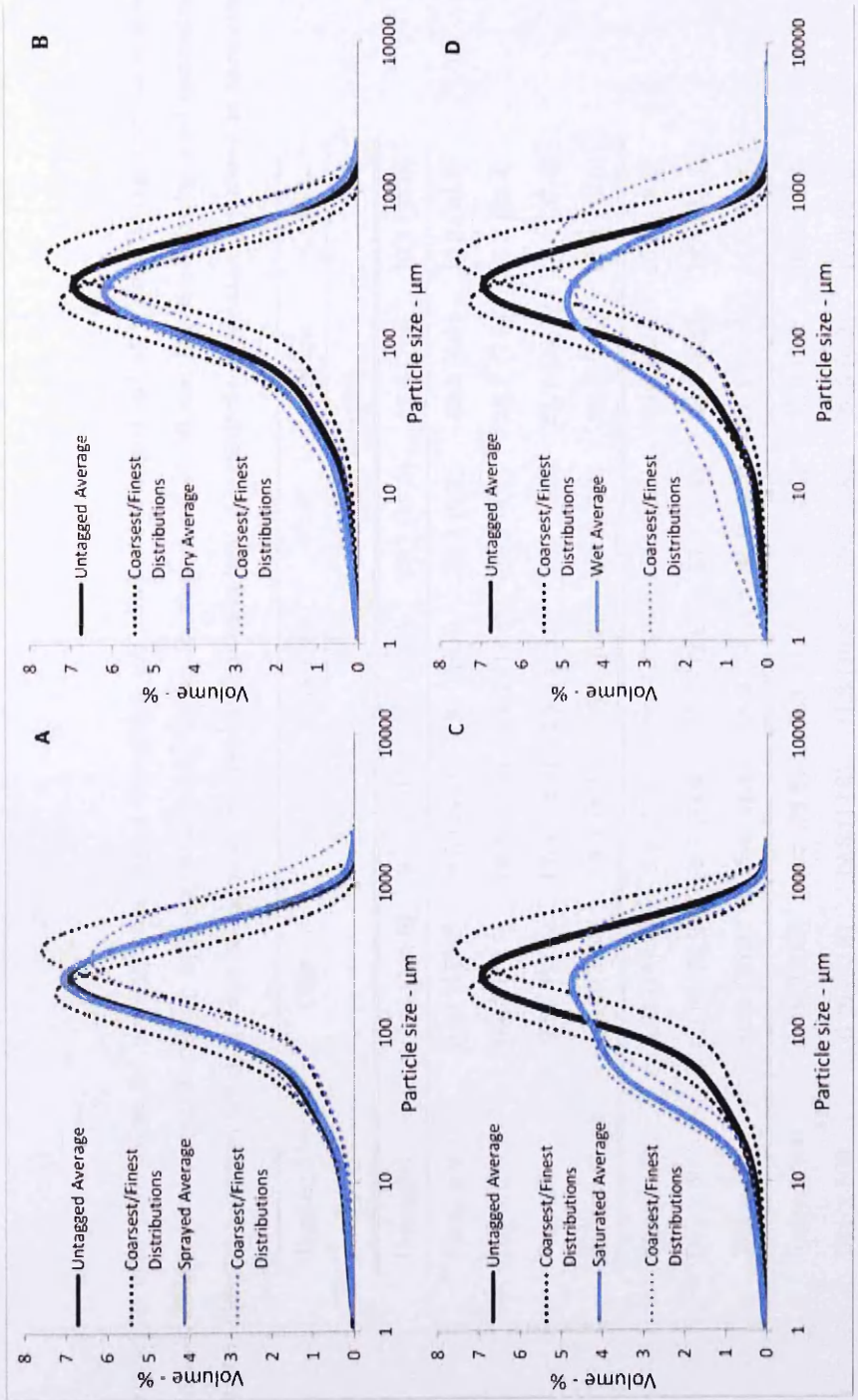

Figure 4.1: Particle size distributions of Broughton soil after tagging at zero times background REE concentration (A - spray tagging, B - dry tagging, C - saturated tagging, D - wet tagging) compared to untagged Broughton soil. Measurements were made via laser diffraction. Average distributions are formed from nine replicated samples.

Table 4.3: Particle size class percentages for untagged and tagged Broughton soil. Values for tagged soil at 0 times background concentration which are significantly (p <0.05) different to untagged soil are highlighted in bold. Values for tagged soil at 50 and 500 times background concentration which are significantly (p <0.05) different to tagged soil at 0 times background are also highlighted in bold. Co-efficients of variation are shown in parentheses.

Tagging Method	Clay	Silt	Very Fine	Fine	Medium	Coarse
			Sand Fraction			
Untagged	0.043 (118.8)	9.7 (27.0)	9.6 (18.9)	28.7 (12.0)	32.9 (7.8)	19.2 (27.0)
Spray x 0	0.02 (155.2)	8.5 (25.1)	9.1 (16.9)	29.3 (6.3)	33.3 (6.6)	19.9 (20.4)
Dry x 0	**0.09** (70.7)	**12.6** (18.2)	**11.4** (11.8)	28.9 (5.4)	**28.7** (7.8)	18.3 (22.4)
Wet x 0	**0.21** (97.4)	**17.4** (34.9)	**15.4** (26.6)	27.9 (15.5)	**22.7** (11.1)	16.4 (37.4)
Saturated x 0	**0.19** (30.4)	**19.1** (8.9)	**18.5** (6.4)	**26.5** (6.1)	**22.4** (6.8)	**13.4** (19.3)
Spray x 50	0.02 (150.5)	8.4 (27.9)	8.4 (18.7)	28.5 (6.6)	33.8 (8.4)	20.9 (18.2)
Dry x 50	0.11 (172.1)	13.7 (14.9)	11.1 (12.8)	27.9 (5.7)	28.8 (8.4)	18.4 (21.3)
Wet x 50	0.12 (76.0)	15.4 (21.4)	**18.3** (14.1)	**31.0** (9.9)	**21.1** (14.5)	14.2 (23.3)
Spray x 500	0.03 (150.5)	8.5 (28.8)	9.3 (21.0)	29.9 (5.6)	33.0 (9.3)	19.2 (17.8)
Dry x 500	0.10 (53.8)	12.5 (14.0)	11.3 (10.8)	29.6 (5.8)	29.5 (6.2)	17.0 (21.0)
Wet x 500	0.14 (156.4)	15.8 (49.3)	**17.8** (22.5)	**30.6** (14.3)	21.8 (18.5)	13.9 (21.8)

compared to soil tagged at 0 times background concentration. Percentages of all other size classes (coarser and finer) declined. This may indicate a slight ability of REO powders to form aggregates in this size range. However, the loss of coarser fractions may also indicate disaggregation processes. No data were available for soil tagged via saturated tagging at 50 and 500 times background concentration.

Uniformity

The uniformity of REO tagging cannot be shown by either: i) the percentage of recovered REOs from tagged soils, or; ii) the variability of REO concentration between sub-samples of tagged soils. When examined in isolation, the mean recovery of applied REOs from tagged soils can be be 100%, but variable. Similarly, the variation in REO concentration between sub-samples of tagged soils may be low, but the percentage of recovered REOs may also be low. Previously the uniformity of REO distribution amongst different particle size classes has been investigated (Zhang et al., 2001; Kimoto, Nearing, Zhang and Powell, 2006). However, a non-uniform distribution of REOs amongst different size classes may not result in a non-uniform distribution of REOs in bulk tagged soil provided that the tagged soil is well mixed. Equation 4.1 was used in order to combine both total REOs recovered and the variation across replicates to give

$$U = \frac{M/100}{1 + CV/100} \tag{4.1}$$

where U is uniformity, M is the mean extracted percentage of REOs from all replicates and CV is the co-efficient of variation of the replicates. Values of uniformity vary between one and zero for the perfect and worst possible tags respectively. Table 4.4 reports the uniformities of Rosemaund soil, tagged by the four tagging methods

Saturated tagging provided the most uniform distribution of REOs, averaged from the two REO concentrations. Dispersion of both the soil and REOs increases the surface area of both components so that REOs are more uniformly distributed once dry. Dry tagging provided the next best uniformity at both REO concentrations, presumably due to the lack of moisture which allowed aggregates to remain

Table 4.4: Uniformity of REO distribution in tagged soils, tagged by the four different tagging methods (Section 4.4.1), extracted using USEPA 6350 (Section 4.4.2)(n = 5 for each value) and calculated using Equation 4.1. A uniformity of one indicates a perfectly uniform REO distribution.

Method	Dry	Wet	Saturated	Spraying
50 × Background	0.77	0.65	0.78	0.68
500 × Background	0.80	0.80	0.81	0.73

separated, again increasing the area of soil available for REO contact. The low uniformity shown by wet tagging at fifty times the background REE concentration suggests that the presence of moisture hinders mixing due to the formation of larger aggregates and clods which was observed during the mixing process. Increasing the mass of REOs applied improved the uniformity of the tag for all mixing methods. The difference in uniformity between dry, wet or saturated tagging was minimised when REOs were applied at 500 times background concentration.

4.5.2 Extraction Methods

REO Powders

The dissolution of the REO powders (Table 4.5) highlighted the insolubility of cerium (IV) oxide, which was observed during all ICP-MS sample preparation methods. Low recoveries of Ce were also found by X. Zhang (Grazinglands Research Lab, USA, personal communication). The other four REOs showed excellent solubility, dissolving rapidly upon contact with nitric acid leaving no visible particulate material. Excluding CeO_2, there was an increase in solubility across the period from lanthanum to samarium. The four extraction methods showed very little variation in the ability to dissolve the REO powders. The only statistically significant results ($p < 0.05$) was a higher dissolution of Sm_2O_3 by the method of Stevens and Quinton (2008) compared to USEPA 6350 (shortened) and lower dissolution of Pr_6O_{11} by USEPA 6350 (shortened) compared to the other three methods.

Table 4.5: Solubility and purities (in parentheses) of REO powders dissolved by four ICP-MS sample preparation methods. Solubility is calculated as the percentage of REO powder smaller than 0.45 μm which was recovered. Coefficients of variation are shown in bold and in parentheses (n = 3 for each data point).

Powder	Stevens and Quinton (2008)	Zhang et al. (2003)	USEPA 6350	USEPA 6350(shortened)
	% Solubility (**CV**)			
La_2O_3	82.4 (**2.5**)	83.2 (**3.8**)	86.1 (**2.6**)	82.3 (**3.8**)
CeO_2	2.9 (**5.5**)	0.4 (**16.3**)	0.4 (**52.7**)	0.5 (**80.1**)
Pr_6O_{11}	94.0 (**6.2**)	89.5 (**3.7**)	89.6 (**1.8**)	76.2 (**3.8**)
Nd_2O_3	98.4 (**2.3**)	94.8 (**11.4**)	94.9 (**4.8**)	77.9 (**33.6**)
Sm_2O_3	107.1 (**1.5**)	106.0 (**3.2**)	103.6 (**3.0**)	101.1 (**1.2**)

Recoveries of Sm_2O_3 were greater than 100%. This is possibly due to interferences during ICP-MS analysis, the presence of other Sm compounds, or imperfections in the structure of the REO used. It should also be noted that recoveries under 100% are not an indication that interference did not occur, but that the percentage of powder as pure soluble REO plus any interference summed to less than 100%.

Untagged Soils

The method of Stevens and Quinton (2008) yielded the highest concentrations of REEs from all UK soils (Figure 4.2). This was expected because the combination of nitric and hydrochloric acids at a ratio of 1:3 (aqua regia) is well established as an aggressive soil digestion method. Comparison of the USEPA methods shows that increasing extraction time from two to four hours increased the mass of background REEs extracted. The method of Zhang et al. (2003) extracted higher concentrations of background REEs than the longer of the USEPA methods, although it is unknown if this was solely the result of increased extraction time, or other differences between the methods. However, Zhang et al. (2003) reported increased extraction efficiency when the extraction time was increased to 24 hours, suggesting that extraction time is the most important factor.

The method of Zhang et al. (2003) gave the lowest co-efficient of variations (CVs) for replicated samples (Figure 4.2). Co-efficients of variation which show statistical differences ($p < 0.05$) are indicated in Figure 4.2. Aqua regia and USEPA 6350 (shortened) consistently provided the highest CVs. This appears to be due to a combination of increased strength and lower extraction time respectively. The additional REEs dissolved by aqua regia appear to be variable in either their concentration or the ease of their dissolution, causing higher variations between samples.

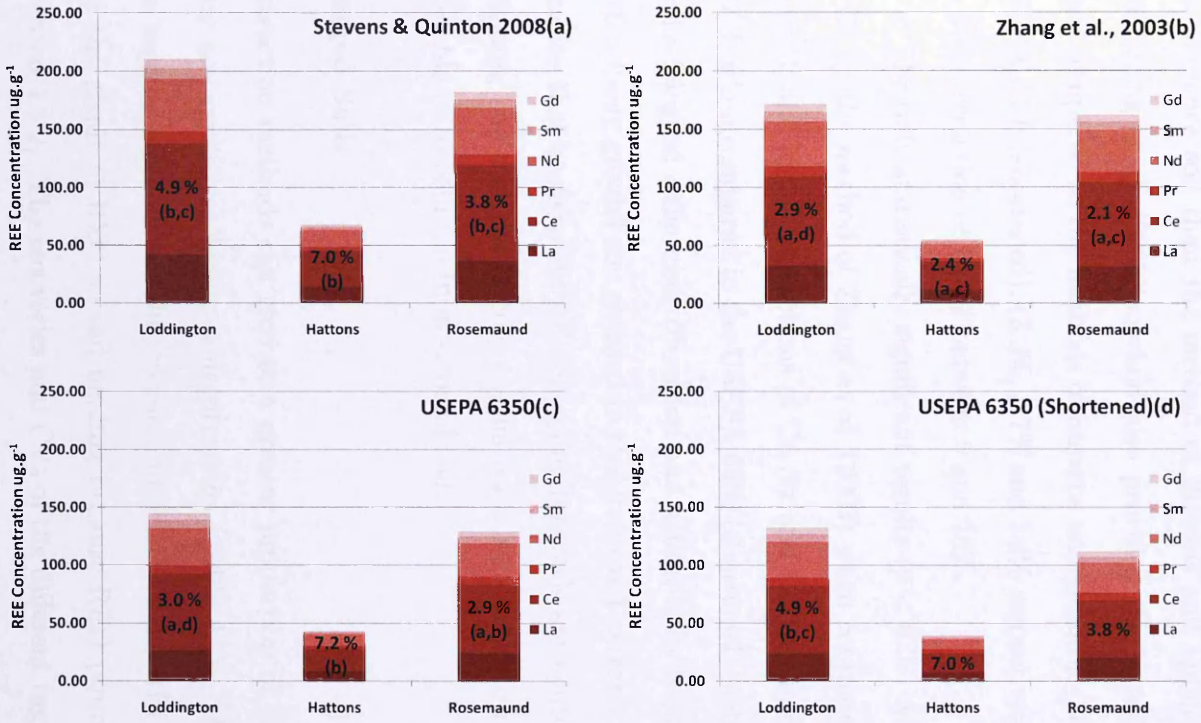

Figure 4.2: Concentrations of selected REEs ($\mu g.g^{-1}$) extracted from Rosemaund, Hattons and Loddington soils by the methods of Stevens and Quinton (2008), Zhang et al. (2003), USEPA 6350 and USEPA 6350 (shortened) (n = 3 for all values). Co-efficients of variation are shown inside result bars. Co-efficients of variation which are statistically different ($p < 0.05$) to other values are indicated. The letter adjacent to the co-efficient value indicates the method to which that value is statistically different.

Certified Reference Soil

The performance of the extraction methods upon the certified reference soil was reflective of the performance upon untagged UK soils, with the exception that the method of Zhang et al. (2003) extracted a higher concentration of REEs from the reference soil than the method of Stevens and Quinton (2008) (Table 4.6). The Zhang et al. (2003) method also provided the lowest average CVs (2.2%), when compared to the methods of Stevens and Quinton (2008), USEPA 6350 and USEPA 6350 (shortened), (3.3%, 4.7% and 5.4% respectively). The results showed an over-extraction of Gd of between 5 and 16%.

The only statistically significant results ($p < 0.05$) were a higher extraction of Ce by the method of Zhang et al. (2003) when compared to the USEPA 6350 method, and higher extractions of Ce, Pr and Gd by the method of Zhang et al. (2003) when compared to the USEPA 6350 (shortened) method. The predominant methodological differences (duration and action of hydrogen peroxide) combined with a finely ground soil resulted in this improved extraction. This may be an indication that background REE compounds of soils are soluble in the less aggressive reagents, but that the action of aqua regia is required to make these compounds available to dissolution in un-ground soil.

Tagged Soils

Extraction methods can recover a greater proportion of the tagged REOs when they are applied at higher concentrations (Table 4.7). The differences between the tagging methods are due to the uniformity of the REO distribution, and are not the result of REO to soil binding because REO powders are highly soluble (Section 4.5.2). The recoveries and CVs of the different tagging methods are used to calculate the uniformities described in Section 4.5.1, and therefore do not need to be commented upon again. Recoveries which differed significantly ($p < 0.05$) are indicated in Table 4.7.

Table 4.6: Extracted values of REEs from the certified reference soil (NCS DC 73383) using the four REO extraction methods described in Section 4.4.2. Co-efficients of variation are shown in bold and in parentheses. Percentage recoveries are shown in parentheses (n = 3 for all values).

Element	Quoted Value	Stevens & Quinton (2008)	Zhang et al. (2003)	USEPA 6350	USEPA 6350(shortened)
			$\mu g.g^{-1}$ **(CV)** (%)		
La	164.0	140.2 **(3.3)** (85.5)	145.8 **(4.5)** (88.9)	138.7 **(4.0)** (84.6)	136.0 **(5.9)** (82.9)
Ce	402.0	362.3 **(3.5)** (90.3)	385.1 **(1.9)** (95.9)	358.7 **(3.8)** (89.2)	348.5 **(4.6)** (86.7)
Pr	57.0	47.3 **(3.7)** (83.0)	49.4 **(1.8)** (86.7)	46.3 **(4.4)** (81.3)	45.3 **(4.4)** (79.4)
Nd	210.0	190.6 **(3.7)** (90.8)	202.9 **(1.7)** (96.6)	189.3 **(4.5)** (90.1)	187.3 **(6.4)** (89.2)
Sm	18.0	16.4 **(3.3)** (91.2)	17.3 **(1.6)** (95.9)	16.5 **(5.8)** (91.6)	16.3 **(7.8)** (90.4)
Gd	7.8	8.6 **(3.3)** (110.6)	9.1 **(1.5)** (116.1)	8.4 **(6.0)** (107.2)	8.2 **(2.9)** (104.7)

Table 4.7: Recovery of REOs from tagged soils extracted via the USEPA 6350 method. Recovery is calculated as the percentage of the applied REOs which were dissolved into the extractant (n = 5 for each value). Average recoveries which are statistically different ($p < 0.05$) to recoveries from other methods are indicated. The letter adjacent to the recovery value indicates the method to which that value is statistically different.

	REE	Dry(a)	Wet(b)	Saturated(c)	Spraying(d)
		% Recovery (CV)			
50 × Background	La	75.2 (3.5)	62.8 (1.8)	75.1 (8.4)	61.1 (2.6)
	Pr	78.8 (4.2)	66.4 (5.4)	82.7 (3.8)	68.8 (3.0)
	Nd	82.2 (3.4)	71.6 (5.2)	85.3 (5.7)	74.0 (2.9)
	Sm	82.5 (3.4)	71.4 (5.3)	82.9 (6.3)	72.8 (2.5)
	Average	79.7(b,d)(3.6)	68.0(a,c)(4.4)	81.5(b,d)(6.0)	69.2(a,c)(2.7)
500 × Background	La	75.9 (1.8)	76.0 (2.7)	78.6 (5.3)	70.8 (5.0)
	Pr	79.4 (1.8)	80.9 (2.4)	81.3 (2.0)	75.4 (4.5)
	Nd	85.7 (1.7)	87.2 (3.6)	86.0 (2.7)	79.7 (4.7)
	Sm	83.6 (1.9)	86.7 (6.7)	85.6 (3.3)	78.1 (4.2)
	Average	81.1(d)(1.8)	82.7(d)(3.8)	82.9(d)(3.3)	76.0(a,b,c)(4.6)

4.6 Discussion

4.6.1 Tagging Method

Uniformity

Tagged uniformity was improved when cohesion between aggregates was minimised, either by using dry soil or soil dispersed in water (Section 4.5.1). In all situations there was an improvement in uniformity when the applied REO concentration was increased from 50 to 500 times background REE concentration. Therefore, tagging with a high concentration of REOs should be used to provide improved uniformity, especially if sub-sampling masses will be small compared to the mass of tagged soil. The flushing of unincorporated REO powders at the start of erosion experiments has been reported (Polyakov and Nearing, 2004) which may be exacerbated by high REO concentrations. This was not investigated. This effect has only been reported in the initial stages of rainfall simulation and does not appear to have subsequent impacts. At higher REO concentrations there was no difference in uniformity between dry, wet or saturated tagging methods, therefore

the choice of tagging method is dependent upon the effect on particle size.

Particle Size Effect

All tagging methods, apart from spray tagging, resulted in modifications of the soil's particle size distribution, compared to untagged soil, when dispersed in water (Section 4.5.1). More aggressive tagging methods resulted in greater shifts in particle size distribution towards the silt and clay classes. Whether or not this effect will impact experimental results is dependent upon the exact use of the tagged material and the objectives of the experiment. When tagged material is distributed over a large plot and incorporated via ploughing (Polyakov et al., 2004), or when a soil box containing only tagged material is used (Polyakov and Nearing, 2004) the soil will retain a high degree of homogeneity. However, a large difference in soil composition across a plot will be created if material tagged via saturated tagging is packed into an excavated area surrounded by untagged soil (Zhang et al., 2003).

Spraying

Spray tagging provided the lowest uniformity of REO distribution. Although the method is not as suitable for forming tagged soil (to be distributed or repacked) when compared to dry or saturated tagging, it does provide a fast and simple method of applying REOs to a soil surface in a uniform manner. Therefore, it is a suitable method for applying REOs to large scale experiments (i.e. field scale) because the formation and distribution of tagged soil is then no longer required. Furthermore, the uniformity of REO distribution when tagged via dry or wet methods is likely to decrease with increasing soil mass (due to the logistical difficulty of mixing large quantities of soil) and is dependent upon a uniform method to apply REOs to the plot; therefore, spray tagging may be the most uniform method of creating large masses of tagged soil (e.g. > 25 kg). Furthermore, the precision in application rate and application area achieved by modern agricultural spraying equipment lends itself to effective REO distribution via spraying.

Selection

The dry tagging method of Stevens and Quinton (2008) should be used when soil is to be repacked next to untagged soil because particle size modification is minimal, and uniformity of REO distribution is good when compared to wet tagging at lower REO concentrations. The saturated tagging method of Matisoff et al. (2001) is preferable if the tagged soil is to be mixed with untagged soil and distributed as it provides the most uniform REO tag over a range of REO concentrations. Spray tagging is a suitable method of applying REOs to large experimental plots if either: i) the plot is ploughed after application, or; ii) sediment sources and not estimates of erosion rates are of interest. All tagging methods should be used at high REO concentration to ensure uniform REO distributions. Again, it should be noted that the potential loss of weakly bound REO tracers has been observed at the start rainfall simulation experiments (Polyakov and Nearing, 2004) and that the tagging concentration of REOs may affect the extent of this process, although this was not investigated in this study.

4.6.2 Extraction Method

All REO powders (excluding CeO_2) were highly soluble in all extractants, therefore the selection of an extraction method is solely based upon the CV of blank soil extractions. As was stated in the introduction, the concentration of background rare earth elements (REEs) extracted from soils is irrelevant provided that this concentration has low variability and all applied REOs are dissolved. It was shown that aqua regia's strength is a hindrance to precise background REE determination, and therefore is less appropriate than other methods. Of the other three methods, an improvement in CV was seen when the USEPA 6350 method was run for four hours instead of two. More marginal improvements were seen when the method of Zhang et al. (2003) was used.

The influence of HCl upon REO dissolution is unknown. However, the ratios of acid in the method of Zhang et al. (2003) are not those used to form aqua regia. Furthermore, HCl is added two hours after nitric acid has begun its oxidizing

reaction with the soil which will remove nitrate ions from the solution. This is important as the strength of aqua regia occurs due to presence of both fresh nitric and hydrochloric acid. Therefore, it is likely that improvements between the methods of Zhang et al. (2003) and USEPA 6350 originated from the additional extraction time and not the presence of HCl, because improvements have been seen in this study by increasing duration from two to four hours, and also reported by Zhang et al. (2003) when increasing extraction time from 4 hours to 24 hours.

As was stated in Section 4.4.2, independently testing each variable (duration, presence of individual reagents and their volumes, ratios of reagent volumes, temperatures) upon all four soils would have generated a number of samples larger than could be analysed. Therefore, based on the results of this study, the extraction method of Zhang et al. (2003) is the most suitable for REO determination. However, extending the duration of the USEPA method to 24 hours may give comparable extractions without the use of chlorinated reagents, and therefore should be investigated further.

Over-extraction was observed for both Gd (from the reference material) and Sm (from Sm_2O_3 and tagged soil). Over-extractions of Gd from REO powder has also been reported by J. Gomez (Instituto de Agricultura Sostenible, Spain, personal communication). A probable explanation is polyatomic interference during ICP-MS analysis, such as that caused by combination of ^{18}O and ^{139}La giving a false measurement of ^{157}Gd. It was for this reason that Gd was omitted from tagging experiments and from the dissolution of REO powders.

4.7 Conclusions

This chapter has shown that tagging uniformity can be improved, at the expense of modification of the parent soil's particle size distribution. When REOs were applied at higher concentrations all tagging methods showed more uniform REO distributions and all extraction methods showed increased REO recovery. Extractions improve with increasing time, while the strength of aqua regia has shown to be counter-productive to REO analysis.

Analytical interference is an issue that is difficult to control because the persons conducting tracing experiments often have limited influence upon analytical procedures. However, ICP-MS issues appear to exist for only a few of the REOs and do not threaten the future use of REOs for sediment tracing. The uniformity of different tagging methods has been shown. However, the strength of binding and the position of REOs in tagged aggregates following different tagging methods has not been shown in this study and may influence the choice of tagging method.

Chapter 5

Microsphere Method Development

5.1 Chapter Outline

Fluorescent microspheres (FMs) are a common environmental colloid tracer (Goldscheider et al., 2003; Baumann and Werth, 2004; Burkhardt et al., 2008). The majority of studies using microspheres apply them to 'clean' systems, typically either columns of sand/silica or artificial porous matrices. Fluorescent spectroscopy can be used for microsphere enumeration from these systems because the lack of dissolved organic matter (tryptophan, tyrosine, etc.) provides low background fluorescent noise. It is used preferentially to epi-fluorescent microscopy due to its shorter analysis times. However, samples cannot be analysed via fluorescent spectroscopy unless they are free from particulates and dissolved organic matter (DOM). As a result, epi-fluorescent microscopy has been used for enumeration in the few studies where microspheres are applied to 'real' soil systems. This chapter investigates the potential of using fluorescent spectroscopy to enumerate microspheres from surface runoff samples. This would provide a more rapid method of enumerating microspheres from soil and water samples.

5.2 Introduction

Fluorescent spectroscopy (FS) is the most commonly used technique for microsphere enumeration during tracer studies. Fluorophores contained in samples are made to fluoresce and the wavelength and intensity of the emitted photons is recorded. Identification of different fluorophores is made by measuring the wavelengths of the photons which cause the fluorophores to fluoresce and the wavelengths of the photons emitted by the fluorophore. Counts of photons emitted from the fluorophores increase with fluorophore concentration. Quantification of fluorophores is performed by comparing the photon count from the measured sample to the photon counts from a range of calibration standards containing known quantities of that fluorophore. FS allows rapid detection of microspheres of any size or dye colour (200-800 nm wavelength emission). The photon counting range available on modern spectrometers allows analysis over many orders of magnitude of concentration. Distinction between microspheres of different colours is simple due to the wide wavelength range of excitation source (200 - 800 nm) and wavelength resolution of the detectors ($<$ 1 nm). However, FS is sensitive to sample matrix effects, requiring that samples must be free of particulate material. Furthermore, FS cannot distinguish between microspheres and dissolved compounds that fluoresce at the same wavelengths.

The majority of colloid tracer studies are performed in columns of quartz sand, silica, or sieved and rinsed sediments, designed to replicate the soil subsurface. These systems contain no dissolved fluorescent compounds (humic acids, tryptophan, tyrosine, etc.), and samples contain little or no particulate material that cannot be easily removed (Zvikelsky et al., 2008). FS is therefore the ideal enumeration method because samples can be analysed more rapidly than if microscopic techniques were used; furthermore, there are no limits on microsphere size.

Colloid transport in surface runoff is linked to agricultural nutrient loss (Heathwaite, Haygarth, Matthews, Preedy and Butler, 2005) resulting in diffuse pollution that causes eutrophication of surface waters (Withers and Haygarth,

2007). Surface runoff and infiltrated surface water samples contain dissolved organic matter (DOM), particulate organic matter and sediments. Therefore, fluorescent spectroscopy cannot be used to directly analyse these samples. In publications where microspheres are used in the vadose zone (unsaturated soil samples) microscopic methods are used for enumeration, with the associated time and size restrictions.

It will be necessary to remove sediments and minimize DOM interference if fluorescent spectroscopy is to be used to enumerate microspheres in surface runoff. It will be possible to detect microspheres in surface runoff samples without the complete removal of background fluorescence by using concentrations of microspheres which give a signal that is detectable above background noise. However, it is desirable to minimise DOM because there is likely to be a loss of microspheres through infiltration, and also because of the expense of fluorescent microspheres.

Ward et al. (1997) developed a method to remove particulates from groundwater samples so that microspheres could be enumerated via FS. Microspheres are retained by filtration at a pore size smaller than their diameter and are subsequently dissolved into acetone. Dissolved material in the original filtrate is discarded prior to dissolution and insoluble particulates are retained on the membrane. This technique could be used to prepare surface runoff samples. However, samples with high sediment concentrations will be difficult to filter through membranes of low porosity, and the contact of acetone with organic matter on the membrane will form DOM in the sample. Removal of sediments from microsphere solutions, prior to dissolution, should allow the method of Ward et al. (1997) to be followed.

This chapter compares centrifugation and filtration as methods to remove sediments from soil surface water samples, assesses the success of the Ward et al. (1997) method of sample preparation of surface water samples, demonstrates the ability of fluorescent spectroscopy to enumerate small ($\leq$ 50 nm) microspheres, and discusses the suitability of fluorescent spectroscopy for analysis of microspheres in surface water samples.

5.3 Materials

Four mono-dispersed fluorescent microsphere (FM) solutions were used. Microspheres had uniformly incorporated dyes and mean diameters of 0.022 μm (red, 1.7×10^{15} ms.ml^{-1}), 0.25 μm (green, 1.2×10^{12} ms.ml^{-1}), 0.89 μm (red, 2.8×10^{10} ms.ml^{-1}) and 2.2 μm (blue, 2.0×10^{9} ms.ml^{-1}), containing 1% solids with densities of 1.05 g.cm^{-3}, suspended with an unspecified dispersing agent. The microspheres were manufactured by Duke Scientific Ltd. Microsphere concentrations are reported as the volume of concentrated microsphere solution per liter of sample (μl.l^{-1}). All acetone used was analytical reagent grade. Filter membranes were nylon to allow use with acetone. All acetone samples were stored in glass sample vials.

A fluoroSENS fluorescent spectrometer (Gilden Photonics) with a xenon arc lamp excitation source (200 - 800 nm) was used for sample analysis. A sealed cuvette of ultra pure de-ionised water (18.2 MΩ.cm^{-1}) was used to scan the water Raman line for quality control. The water Raman line has a constant intensity and can therefore be used to monitor the light intensity of the arc lamp through time. Samples were analyzed in a synthetic quartz cuvette, optically transparent between 200-2500 nm. Microsphere concentrations were quantified by emission scanning (applying light of a fixed wavelength and measuring the intensity of emitted photons over a range of different wavelengths). Solvents of higher polarity will red shift emission spectra to longer wavelengths (Lakowicz, 1983), therefore emission scanning of microspheres in water and acetone was performed using settings optimised for the specific solvent.

5.4 Methods

5.4.1 Centrifugation

Samples containing eroded sediments in surface runoff, infiltrated surface water samples and soil samples may all require analysis if microspheres are used as trac-

ers in soil systems (soil samples require dispersion in water for analysis via FS). Soil erosion is particle size selective, with fine sediment being transported faster than coarse sediment so that the particle size distribution of eroded sediments is finer than the parent soil (unless high erosion rates occur). Samples containing eroded sediments in surface runoff will therefore be the most difficult to prepare if centrifugation is used to remove sediment from microsphere solutions. Samples were therefore formed using eroded sediments contained in surface runoff.

A soil box with a size of 25 cm $\times$ 50 cm was packed with soil from the Hattons Field Site, UK (clay loam, see Chapter 4) at a density of 1.4 g.cm^{-3}. After pre-wetting, the box was set at an angle of nine degrees and rained upon at an intensity of 45 mm.hr^{-1} using a gravity fed rainfall simulator and de-ionised water. Eroded sediment becomes depleted in coarse particles as slope decreases, therefore a slope of nine degrees was used to provide samples with a broad particle size distribution (slopes steeper than nine degrees are generally unrepresentative of UK arable land) Armstrong et al. (2010).

Sediment concentration in the run-off was approximately 8 g.l^{-1}. This high concentration is most likely the result of the small size of the soil box. The short distance of transport between locations of detachment and the end of the soil box would result in less opportunity for sediment deposition causing elevated sediment concentrations in the surface runoff. Although this concentration is less representative of sediment concentrations generated from field experiments, it does provide a more rigorous test of separation methods.

Homogenised subsamples of eroded sediments in surface runoff were taken, and aliquots of dilute red 0.89 μm microsphere solution were added so that the total sample volume was 50 ml. Samples were then centrifuged at 2400 rpm for 5 minutes and the top 25 ml of supernatant was removed. Blue (2.2 μm) and green (0.25 μm) microspheres were not used because the low density of microspheres will result in almost identical transport distances during centrifugation and therefore there will be minimal difference in recovery.

5.4.2 Filtration

Soil samples (dispersed in water) will be more difficult to prepare than surface runoff samples if filtration is used to remove sediment from microsphere solutions. Sediment masses will be high ($\geq$ 1 g) unless a small un-representative sample is taken, or unless the experimental scale is very small. This will lead to greater sediment loading of filters, regardless of the volume of water used to disperse the water. Furthermore, the removal of coarse sediment using sieve screening is unlikely to reduce the level of filter blocking as very fine sediments, larger than the filter pore size, will still be present. Samples were therefore formed by dispersing 2 ± 0.005 g of Hattons soil ($\leq$ 1 mm) into 50 ml of de-ionised water containing aliquots of dilute microsphere solution. Samples were mixed by hand and left to settle for five minutes prior to filtration. Three different filter papers were tested for their ability to remove particulate material and transmit the microspheres: i) a glass microfiber pre-filter with a 2.7 μm pore size, high loading capacity and flow rate, and a Herzberg speed of 41 seconds, ii) a qualitative cellulose filter paper with a 10 μm pore size, medium particle retention and flow rate, with a Herzberg speed of 150 seconds, and iii) a qualitative cellulose filter paper with 30 μm pore size, a high loading capacity and flow rate, with a Herzberg speed of 28 seconds. These filters were selected to identify whether pore size or porosity is the most influential factor for microsphere transfer. All filtration was performed under vacuum and with washing using de-ionised water so that the total filtrate volume was 150 ml.

5.4.3 Dissolution

The method of Ward et al. (1997) for the dissolution of microspheres was followed. Microsphere samples prepared by filtration and centrifugation (Sections 5.4.1 & 5.4.2) were filtered through either 0.45 μm or 0.2 μm nylon membranes (depending upon microsphere size). The original filtrate (containing DOM) was discarded and acetone was filtered through the membrane to facilitate dissolution. The acetone filtrate was then analysed for microsphere concentration via fluorescent spectroscopy. Filtration and centrifugation reduces DOM formation in

the acetone filtrate by minimising contact of sediment with acetone. Therefore, samples containing sediment were analysed to quantify the reductions in DOM resulting from the centrifugation and filtration of samples.

Recovery checks were performed prior to sample analysis to determine optimum contact time between microspheres and acetone. Aliquots (0.5 ml) of 0.89 μm red microsphere solution (1000 $\mu l.l^{-1}$) were pipetted onto 0.45 μm nylon membranes under vacuum. The vacuum was removed and 25 ml of acetone was applied to the membrane with contact times of 1, 2, 5 and 10 minutes. The acetone was collected under vacuum and re-made to 25 ml. A further two washings with the same contact times were made to check for residual microspheres that had not dissolved. Three replicates were made of each contact time. A reference sample was made by adding a 0.5 ml aliquots of 0.89 μm microsphere solution (1000 $\mu l.l^{-1}$) into 24.5 ml of acetone.

Samples free from sediment were analysed so that microsphere recoveries after filtration and centrifugation could be calculated. Dissolved standards were formed using the Ward et al. (1997) method. Four concentrations were analysed (25, 5, 1 and 0.2 $\mu l.l^{-1}$) for each size of microsphere. Aqueous standards were formed by dilution of the purchased microsphere solutions. Six concentrations were analysed (25, 5, 1, 0.25, 0.05 and 0.01 $\mu l.l^{-1}$) for each size of microsphere.

5.4.4 22 nm Microspheres

The smaller size of the 22 nm microspheres allows alternative sample preparation. Microspheres were separated from particulates by filtration at 0.45 μm, and also by centrifugation at 2400 rpm for 60 minutes. Microspheres could not be dissolved into acetone following particulate removal as microspheres could not be retained. However, filtration at small pore sizes, and longer centrifugation times, will have been more effective at removing finer sediments and particulate organic material. Following preparation, samples were directly analysed by fluorescent spectroscopy as aqueous solutions.

5.5 Results

5.5.1 Dissolution

Recoveries of microspheres following the Ward et al. (1997) method increased with contact time due to more effective dissolution (Table 5.1). All four contact times showed good recovery with greater than 90% of microspheres dissolved during the first washing, and co-efficients of variation below ten percent. All standard microsphere samples (no sediment) showed good linear correlation between microsphere concentration and recorded photon count (Table 5.2). Blank water samples gave significantly lower photon counts than microsphere solutions, possibly as a result of light scattering by microspheres, resulting in the calculation of negative limits of detection (LODs). In these situations the LODs are reported as the lowest concentration of microspheres measured, which is higher than the true LODs. The photon count of blue microspheres becomes constant at 180,000 photons.s^{-1} at microsphere concentrations below 0.05 μl.l^{-1} because the excitation/emission peak occurs on the water Raman line. Therefore blue microspheres cannot be detected below this concentration. The photon count of red microspheres was low when compared to blue and green microspheres due to the photomultiplier tubes' insensitivity to red light. However, this effect is consistent at all microsphere concentrations and consequently has no effect upon microsphere detection.

Table 5.1: Recovery data for 0.89 μm red microspheres dissolved in acetone. Stated percentages are comparisons to the reference sample, co-efficients of variation are shown in parentheses (n = 3 for all values).

	1	2	5	10
	Contact time (minutes)			
1st Washing	91.6% (9.2%)	95.0% (6.4%)	99.1% (2.8%)	107.6% (7.1%)
2nd Washing	3.6% (6.6%)	3.6% (23.8%)	3.4% (86.8%)	4.6% (8.0%)
3rd Washing	1.6% (23.2%)	0.9% (21.7%)	0.6% (92.2%)	1.0% (27.2%)
Total	96.8%	99.5%	103.1%	113.2%

Table 5.2: Data from the linear equation describing un-dissolved and dissolved microsphere concentration (x) plotted against photon count (y), where M is gradient and C is intercept on the y-axis, for microsphere concentrations between 25 - 0.01 $\mu l.l^{-1}$ (un-dissolved), and 25 - 0.2 $\mu l.l^{-1}$ (dissolved) (n = 5 for each concentration). Co-efficients of variation (CV) are averaged from all concentrations.

Microspheres	M	C	r^2	Average CV	LOD ($\mu l.l^{-1}$ ($ms.ml^{-1}$))
Undissolved					
Green(0.25 μm)	74760	12356	0.99	2.0%	0.01 (1.2×10^4)
Red (0.89 μm)	3200	876	0.99	5.9%	0.01 (2.8×10^2)
Blue (2.2 μm)	61715	179750	0.99	1.9%	0.05 (1.0×10^2)
Dissolved					
Green (0.25 μm)	31956	12165	0.99	6.0%	0.04 (4.8×10^4)
Red (0.89 μm)	222	166	0.99	5.3%	1.02 (2.3×10^4)
Blue (2.2 μm)	10040	24908	0.99	6.7%	0.48 (9.6×10^2)

5.5.2 Filtration

As stated, contact of acetone with sediment during the dissolution of microspheres releases fluorescent DOM into the acetone filtrate, preventing detection of microspheres. Filtration prior to dissolution decreased the intensity of the fluorescent interference by over 95% regardless of which filter was used (Table 5.3). The largest fluorescent microspheres (blue 2.2 μm) had the lowest recovery. However, a higher percentage of red microspheres (0.89 μm) than green microspheres (0.25 μm) were recovered, possibly due to drag effects related to microsphere diameter. The 2.7 μm glass microfiber filter gave the highest recovery for all microsphere sizes despite having the smallest pore size. The ability to cope with high sediment loading therefore had a greater influence upon recovery than pore size. The percentage of microspheres retained was highly variable even though sediment mass was constant, shown by the variation between replicates. Recoveries of microspheres following filtration at 10 μm were significantly ($p < 0.05$) lower than following filtration at either 2.7 μm or 30 μm. There was no significant difference in recovery when comparing the 2.7 μm or 30 μm filters. Samples were only analysed at a single concentration because recovery was so variable.

Table 5.3: DOM reduction and microsphere recoveries for filtered microsphere samples. Reductions in background fluorescence (BGF) are calculated as the decrease in fluorescence of a filtered blank sample compared to a non-filtered blank sample. Recoveries of microspheres are calculated from comparison of the photon count recorded from the filtered samples (minus background) to the photon count estimated from Table 5.2.

Microspheres		Filter pore-size		
		2.7 μm	10 μm	30 μm
Green (0.25 μm)	Reduction in BGF	97.8%	98.0%	97.7%
	Recovery	54.2%	28.0%	45.4%
	CV	29.7%	33.7%	28.5%
Red (0.89 μm)	Reduction in BGF	96.3%	97.7%	95.9%
	Recovery	89.9%	22.8%	58.1%
	CV	24.3%	15.8%	14.7%
Blue (2.2 μm)	Reduction in BGF	98.4%	98.5%	97.9%
	Recovery	21.9%	5.5%	17.0%
	CV	17.8%	3.9%	31.5%

5.5.3 Centrifugation

Centrifugation prior to dissolution proved more successful than filtration. The correlation of microsphere concentration (x) plotted against photon count (y) was excellent (r = 0.99) (Figure 5.1). This suggests that microspheres experience very little gravitational effect during centrifugation, even when present in highly turbid samples. Average coefficients of variation (3.9%) were significantly lower than samples that had been filtered (Table 5.3), indicating that microsphere loss during centrifugation was consistent, and that variation between replicates was minimal. The limit of detection for red 0.89 μm microspheres was 1.7×10^5 ms.ml^{-1} (4.3×10^6 ms.sample^{-1}).

5.5.4 22 nm Microspheres

The small size of the 22 nm microspheres made separation from particulates simple. Limits of detection for samples containing sediment filtered at 0.45 μm or centrifuged were of the same order of magnitude as the clean reference samples

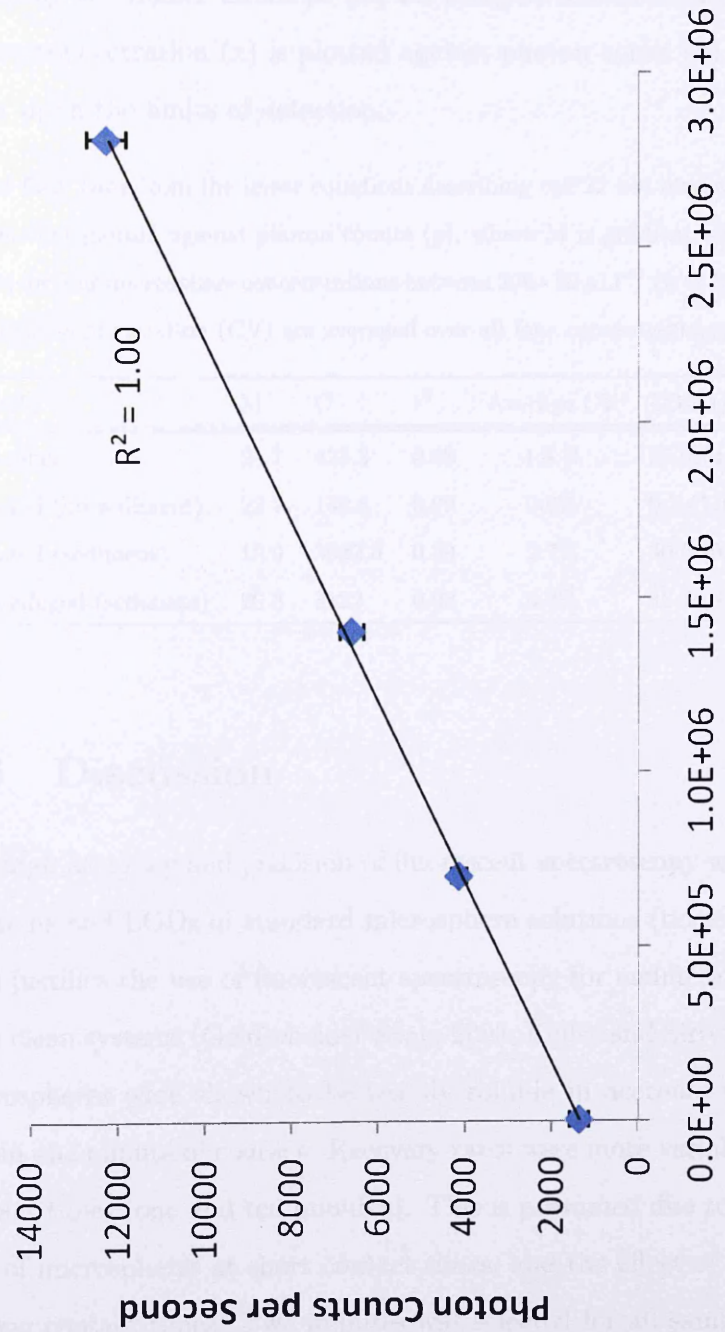

Figure 5.1: Graphical plot of microsphere concentration against photon count for centrifuged microsphere samples.

(Table 5.4). Filtration of samples resulted in a loss of 15.7% of microspheres for samples with no sediment and 43.1% when sediment was present. Centrifugation resulted in an average loss of 38.4% of microspheres. Background fluorescence is shown by the higher intercept (C) for samples containing sediment when microsphere concentration (x) is plotted against photon count (y). This had a limited effect upon the limits of detection.

Table 5.4: Data from the linear equations describing red 22 *nm* diameter microsphere concentrations (x) plotted against photon counts (y), where M is gradient and C is intercept on the y-axis, for four microsphere concentrations between 200 - 50 $\mu l.l^{-1}$ (n = 5 for each concentration). Co-efficients of variation (CV) are averaged over all four concentrations.

Sample	M	C	r^2	Average CV	LOD ($\mu l.l^{-1}$ ($ms.ml^{-1}$))
Reference	24.7	423.3	0.98	4.6 %	25.0 (4.3×10^{10})
Filtered (no sediment)	22.7	140.8	0.99	2.6%	0.7 (1.1×10^{9})
Filtered (sediment)	18.9	3632.0	0.99	2.7%	30.6 (5.2×10^{10})
Centrifuged (sediment)	20.3	3122	0.98	6.2%	48.7 (8.3×10^{10})

5.6 Discussion

The high accuracy and precision of fluorescent spectroscopy was shown by the calibrations and LODs of standard microsphere solutions (no sediment - Table 5.2). This justifies the use of fluorescent spectroscopy for enumeration of microspheres from clean systems (Goldscheider et al., 2003; Keller and Sirivithayapakorn, 2004). Microspheres were shown to be readily soluble in acetone, with 90% dissolving within one minute of contact. Recovery rates were more variable at long and short contact times (one and ten minutes). This is presumed due to incomplete dissolution of microspheres at short contact times, and the effect of acetone evaporation at long contact times. Two minutes was selected for all sample preparation as it provided the most repeatable results. Furthermore, the difference in microsphere recovery was minimal when compared to five minutes, while shorter contact periods save time and minimise acetone loss through evaporation.

Microspheres in acetone showed lower fluorescent intensity compared to aqueous solutions (Table 5.2). However, Ward et al. (1997) suggested that dissolution of microspheres increases photon count due to releases of dye molecules. It is possible that different dyes or polymers do not react in the same way to contact with acetone.

Centrifugation proved to be more successful than filtration for the separation of microspheres from particulates. Filtration resulted in variable numbers of microspheres passing the filter, generating imprecise results. The mass of sediment in real surface runoff samples will not be consistent, which would result in further variations in microsphere retention following filtration. Conversely, centrifugation resulted in consistent microsphere recoveries with an average co-efficient of variation of 3.9% for all replicates. Furthermore, centrifugation is more efficient as multiple samples can be prepared simultaneously. Slow sample preparation would negate the use of fluorescent spectroscopy as an analytical tool, as its primary advantage over microscopic methods is its speed of sample analysis.

Detection limits of epi-fluorescent microscopy reported by Burkhardt et al. (2008) for soil samples collected from the surface of an experimental plot were 4 $\times$ 10^5 ms.g^{-1} (automated counting, the LOD was lower for manual counting). The size of the microspheres used was 1 μm, approximately the same as the 0.89 μm red microspheres used in this research. If the microspheres from 1 g of soil were extracted by centrifugation and dissolution and enumerated by fluorescent spectroscopy the limit of detection would be one order of magnitude higher (4.3×10^6 ms.g^{-1}). This could be decreased if a larger mass of soil was used, but increased sediment masses result in increased analytical issues (blocking of filters etc.).

However, there are limitations if centrifugation and dissolution are used. As centrifugation is density dependent it will only remove material more dense than the microspheres. This will result in organic particulates and macromolecules being present in the supernatant. Any material larger than the 0.45 μm filter pore size will be retained, and may dissolve into solution upon contact with ace-

tone (material retention on filter membranes was observed after centrifugation). Therefore, no method reported in this paper achieves complete separation of microspheres from dissolved fluorescent compounds. Although centrifugation and dissolution offers the ability to increase the concentration of microspheres in samples (if original sample volumes are > 25 ml), the filtration of large sample volumes at 0.45 μm is slow unless very little particulate material is present in the supernatant after centrifugation. This negates one of the advantages of using fluorescent spectroscopy for enumeration - that it provides rapid analysis times. Dissolution into acetone results in variations in the number of microspheres dissolved (Table 5.1), and also results in a lower signal from a given microsphere concentration compared to un-dissolved microspheres in aqueous solutions (Table 5.2). This will affect both the signal to noise ratio during analysis and the precision of results. Finally, the use of acetone raises certain analytical issues. Some evaporation of acetone between microsphere dissolution and analysis is inevitable, even if this is only during sample transfer into cuvettes. The use of sealable cuvettes becomes essential as evaporation of acetone in the sample chamber will lead to over estimation of microsphere concentrations, and more seriously, the risk of combustion of highly flammable acetone vapour (the flashpoint of acetone is $-17.8°C$). Only quartz cuvettes formed by direct fusion can be used as acetone is an excellent solvent for synthetic fibres, disposable plastic cuvettes or glued quartz cuvettes cannot be used. It is recommended that concentrations of microsphere are used which allow detection above background noise as a result of the issues of dissolving microspheres into acetone. This can be achieved by using centrifugation to remove particulate material but without dissolution into acetone.

Small (22 nm) microspheres proved to be easier to analyse than larger microspheres as they were more easily separated from particulate material. Both filtration and centrifugation proved effective in separation, although neither method can remove DOM from samples. Filtration provided lower limits of detection, which is believed to result from the removal of organic material ≥ 0.45 μm. Detection limit concentrations were approximately 10,000 times lower than purchased micro-

sphere solutions. Enumeration of such small microspheres by other methods would prove difficult. Flow cytometry typically has lower size limits of approximately 1 - 0.5 μm, with Becker et al. (1998) reporting the use of flow cytometry to enumerate 0.2 μm diameter microspheres. Enumeration by epi-fluorescent microscopy would require filtration at the lowest pore size typically available (approximately 15 nm), and a very high magnification. Epi-fluorescent microscopy has been reportedly used to enumerate microspheres as small as 50 nm, but only when used in conjunction with UV-Vis spectroscopy (Keller and Sirivithayapakorn, 2004). Detection limits were not stated and the analysis time required for counting such high numbers of microspheres would be high.

5.7 Conclusions

There are advantages to using fluorescent spectroscopy for enumeration of fluorescent microspheres. Sample analysis is rapid and unlike other methods it allows detection of very small fluorescent microspheres (as well as fluorescent dyes and natural fluorescent compounds). For samples containing limited DOM it is the most suitable enumeration method. However, its full potential as a tool for colloid tracing in soil surface waters has not yet emerged. Separation from DOM and particulate material is time consuming and cannot be achieved by the methods investigated, resulting in decreased signal to noise ratios. Furthermore, improved enumeration requires the complexity of sample preparation to be increased. This diminishes the rapid analysis advantage of fluorescent spectroscopy. However, it has been demonstrated that fluorescent spectroscopy can enumerate microspheres from surface runoff samples if samples are suitably prepared. Furthermore, fluorescent spectroscopy is the only analytical method that can enumerate microspheres in the nanometre size range. This provides an alternative to bacteriophage use in pathogen transport studies.

Chapter 6

Indoor Simulations

6.1 Chapter Outline

The mobilisation and transport behaviour of one rare earth oxide (REO) powder and one size of fluorescent microspheres were compared to that of particulate and dissolved fractions of phosphorus. Packed soil boxes set at angles of 3%, 6% and 9% were rained upon using a gravity fed rainfall simulator. The tracers were applied to a strip across the box where the phosphorus concentration was increased through the addition of monoammonium phosphate (MAP) solution. Each gradient was repeated in triplicate, and identical simulations were made of untagged soil boxes (18 simulations in total). Relationships between the concentrations of the tracers and phosphorus fractions were then used to assess the performance of the tracers against the selection criteria developed in Chapter 3.

6.2 Introduction

The fifth objective of this project was to apply the selected tracers to a controlled soil system in a manner that allowed the transport of each tracer to be compared to the relevant phase of phosphorus (sediment and colloid bound) (Section 1.3). Reviewing present tracing technologies (Chapter 3) led to the selection of rare earth oxides (REOs) for sediment tracing and fluorescent microspheres for colloid tracing. Development of experimental methodologies of both tracers had been performed (Chapters 4 and 5), therefore the success of the tracers in tracing a multi-phase diffuse pollutant had to be quantified.

Phosphorus (P) was identified as the diffuse pollutant of interest (Chapter 2). Bioavailable phosphorus loss from both arable soils (Catt et al., 1998; Fortune et al., 2005; Withers et al., 2007) and grasslands (Haygarth, Condron, Heathwaite, Turner and Harris, 2005; Preedy et al., 2001; Haygarth et al., 2006) causes severe impacts upon receiving water systems (Carpenter et al., 1998; Withers and Haygarth, 2007; Mainstone et al., 2008). REOs have been identified as a successful tracer of sediments (Polyakov and Nearing, 2004)(Chapter 3). Therefore, it can be assumed that hydrophobic diffuse pollutants, for example, persistent organic pollutants (POPs) are also being traced. Tracing phosphorus using REOs is therefore aided by the fact that *'only a small proportion of the total soil phosphate is accessible for exchange in soils low in phosphate, or that have not received phosphate fertiliser for a long time'* (Russel, 1973).

However, particulate inorganic phosphate (PP) exists in equilibrium with dissolved inorganic phosphate (DP) because inorganic amorphous phosphate precipitates and inorganic surface bound phosphates are labile (Foth, 1990). The desorption of labile phosphorus from metal binding sites increases as the surface water or pore water becomes diluted (McGechan and Lewis, 2002), the extent of which is dependent upon soil texture (Maguire et al., 2002). The lability of these phosphorus fractions is also dependent upon the time since their introduction into the soil system (due to the slow mineralisation of surface bound labile ortho-phosphate and crystallisation of amorphous phosphate precipitates). This

causes the proportion of available phosphorus from agricultural amendments to decrease through time (Morgan, 1997; Yang et al., 2002). Furthermore, inorganic phosphate is known to bind preferentially to finer fractions of soils (clays), while REO powders have a lower size range of 2 μm which limits the size of particles to which they can bind. Zhang et al. (2001) showed almost uniform binding of REO particles into different aggregates size classes (silt loam) in the range 0.01 mm to $>$ 4.75 mm with a marginal preference for the finer classes (silts). However, Kimoto, Nearing, Zhang and Powell (2006) showed higher concentrations of REOs in the aggregate range of 0.09 mm to 4.75 mm than in the finer range $<$ 0.01 mm to 0.09 mm of a gravelly, sandy loam soil. Therefore, the tracing of PP using REOs may be complex, because:

1. Residence time on the plot will affect the PP concentration of sediments (this may well affect long term field experiments commencing after fertiliser application);

2. PP concentration in runoff from a given mass of sediment will vary if runoff becomes diluted;

3. PP may be transported at a higher rate compared to REOs due to the strong preference of phosphorus to bind to clay sized sediments.

It is therefore important to assess similarities between REO and PP transport while assuming that their behaviour cannot be identical.

Colloids $<$ 0.45 μm have transport speeds comparable to (or faster than) dissolved material (McGechan and Lewis, 2002; Jonge et al., 2004; Sen and Khilar, 2009). Therefore, the $<$ 0.45 μm fraction of runoff is a combination of phosphorus bound to a large range of differently sized colloids and truly dissolved phosphate. Microspheres have proven to be an excellent tracer of colloids in ground water (Goldscheider et al., 2003; Close et al., 2006) and the soil subsurface (Mortensen et al., 2004; Burkhardt et al., 2008), and therefore constitute an excellent tracer for the $<$ 0.45 μm phosphorus fraction. However, microspheres cannot replicate the behaviour of colloid bound phosphorus because, unlike colloid bound phosphorus,

they have a fixed size and are not in equilibrium with a dissolved phase. Therefore, they may also experience difficulty in replicating identical behaviour to the < 0.45 μm phosphorus fraction.

Phosphorus can be considered a three phase contaminant. The complex chemistry of phosphorus (McGechan and Lewis, 2002; Dougherty et al., 2004) which results in phosphate ions moving in and out of solution (McDowell, Sharpley, Condron, Haygarth and Brookes, 2001; Vadas et al., 2005; Kleinman et al., 2006) makes it a challenging but beneficial comparator for the selected tracers. Therefore, the aims of this experiment are:

1. To investigate whether the selected tracers can be used for basic tracing (B-grade) of different phases of phosphorus;

2. To identify whether higher grade tracing (A-grade) is prevented by the complex chemistry of phosphorus and the differences in the particle sizes of phosphorus and tracers.

6.3 Experimental Design

In Chapter 3, tracer performance was divided into two grades, A and B (Section 3.3). The primary difference between the two grades is in response to a stimulus; an A-grade tracer will show near identical transport rates and concentrations to its analyte due to comparable chemical and physical properties, while a B-grade tracer will only reflect the magnitude of the stimulus as its chemical and physical properties differ.

An experiment was required to identify the grade of REOs and microspheres as tracers for phosphorus. Assessment is simplified when there is a non-uniform concentration distribution of phosphorus on the experimental plot. This causes variations in the concentration of phosphorus in runoff through time. This behaviour can be compared to that of the tracers. Therefore, the inorganic phosphorus concentration had to be increased in the area of the plot to which the tracers were applied. Alternatively, an organic form of phosphate could have been applied

and quantified using nuclear magnetic resonance (NMR); however, organic and inorganic phosphates have different behaviours and are of less interest to this project. Organic matter provides a highly bio-available source of phosphorus and is therefore important for environmental quality (Haygarth et al., 2006). However, organic phosphate exhibits more complex behaviour than inorganic ortho-phopshate due to many different forms existing (e.g. swine or poultry manure, bovine excreta etc. (Vadas et al., 2007)) which would have complicated this investigation, therefore this work is focused on inorganic phosphate.

Two designs were possible where either:

1. Phosphate is applied to multiple sections of the plot, each of which contains a different REO and microspheres colour. Phosphorus concentrations increase in sections higher up the plot. Contributions from each upslope section are identifiable by a stepped increase of phosphorus concentration in runoff;

2. Phosphate is applied to a single section which is tagged with one REO and one size of microspheres. Contributions from the tagged section are identifiable by phosphorus concentrations above background concentrations.

Both experiments would generate data showing breakthrough times and concentration trends in runoff. However, design two was seen as the most suitable for a number of reasons. Applications of very concentrated phosphate solution will affect the phosphorus chemistry on the plot, and the more this is modified the more the system moves away from a realistic system. Furthermore, the required increases in phosphorus concentration needed to distinguish multiple sources may not be possible due to soils having a limit upon phosphate absorption. Variations of phosphorus concentration in runoff from different sections may become indistinct when multiple sections are used due to the small size of the plot (25 cm $\times$ 50 cm). Increasing the complexity of the experiment may have resulted in less information being gathered. Finally, current publications have shown that the behaviour of different REOs is similar (Zhang et al., 2001; Kimoto, Nearing, Zhang and Powell, 2006), so that there was no need to test multiple REOs. Similarly,

microspheres of identical size, made of the same material, are assumed to have identical transport behaviour.

A factor that affected the erodibility of the soil (soil class, structure, density, porosity or antecedent moisture condition) or the power of eroding forces (rainfall intensity, rainfall energy, plot gradient, macrotopography or surface cover) had to be varied to ensure that similarities or differences between the tracers and the related phosphorus fractions did not result from the specific experimental conditions. This variation should have had a similar effect on both the tracer and phosphorus fraction, and would therefore allow an improved assessment of the tracers.

The plot gradient was varied as this was one of the simplest influences to modify accurately in a reproducible manner. Rainfall intensity had to represent short duration, intense, UK storms i.e. $\leq$ 60 mm.hr^{-1} (highest UK one hour storm total was 92 mm, Maidenhead (Berks), 12.07.1901 (Met Office, 2008)). An increase in rainfall intensity to significantly increase erosion rates would represent an unrealistic rainfall intensity for the present UK climate. Dropping the rainfall intensity would have lowered sample volumes which were already required to provide sub-samples for analysis of total phosphorus (TP), dissolved phosphorus (DP), REO and microsphere concentrations as well as particle size. This may have resulted in an inability to perform all the analysis effectively, especially on initial runoff samples where discharge is low and sampling frequency is high.

The experimental design and choice of a small soil box size had advantages and disadvantages. The small soil box size would lead to soil transport behaviour which is modified compared to what eroded soil particles experience under field conditions due to the effects of slope length and the lack of surface run-on (see Section 6.4.5 for greater detail on the effects of soil box size on sediment transport processes). However, the small size of the soil boxes resulted in far shorter preparation time prior to rainfall simulation, especially compared to larger setups where only one soil flume is available and which takes considerable time to prepare for experimentation. This allowed replication of the experiments at different slopes to give a larger data set. The scale of the experiments also resulted in smaller

total masses of eroded sediments compared to larger experiments which made representative sub-sampling for analysis easier to perform. Furthermore, the expense of microspheres precluded the use of larger scale experiments where recovery may have been lower due to a longer pathlength and where application rates would have to be higher.

Similarly to the majority of indoor rainfall simulation experiments using REOs (Zhang et al., 2003; Polyakov and Nearing, 2004; Michaelides et al., 2010), the selected rainfall intensity (50 $mm.hr^{-1}$) and slope (3% - 9%) were selected to provide volumes of surface runoff easily sufficient for REO and P analysis. The steady state runoff rates (approx. 100 $ml.min^{-1}$) allowed sampling at higher temporal resolution than if lower slopes or rainfall intensities were used. However, these conditions are more severe than typically experienced during field experiments (e.g. a 24 hour period with a total of 9.2 mm of rainfall was the largest rainfall event recorded by Stevens and Quinton (2008) when performing a UK based REO tracing field experiment). Therefore, these harsh conditions provided a good comparison of REO and P transport in high volumes of surface runoff, but provided a poorer comparison of transport when erosion is predominantly by splash transport or in very shallow rain impacted flows (Kinnell, 2002).

Only the slope of the plots was varied during the experiment. Working with a second variable (soil texture, rainfall intensity) would have provided greater data to compare REO and P transport, which will be affected by these variables; for example, inorganic ortho-phosphate preferentially binds to clay and silts (Quinton et al., 2001), therefore when a higher percentage of clay sized particles are transported the relationship between REO/microspheres and P transport will change. There was insufficient time to fully investigate further variables. This limits the applicability of the results of this experiment to erosion events with comparable characteristics.

Multiple surface runoff samples were collected during each rainfall event (see Section 6.5 for greater details) and analysed for REO, microsphere and P concentrations. This allowed changes in concentration over time to be shown, allowing

comparison of transport behaviour during erosion events. However, collecting multiple samples during each event prevented determination of REO and P concentrations in different size fractions of eroded sediments due to the limited number of samples which could be analysed. This data may have provided greater information on how REOs and P were being transported from the soil, but would have limited the investigation of how REO, microsphere and P concentrations changed temporally during an erosion event.

6.4 Materials

6.4.1 Soil

The soil selected was a silt loam top soil (A horizon), comprising 4.6% clay, 49.9% silt and 45.5% sand, (primary particle size distribution) (Armstrong et al., 2010) screened to 10 mm and untreated. Background Nd concentration (10.99 $\mu g.g^{-1}$) was determined by USEPA extraction and analysis via ICP-MS (Chapter 4). Background total phosphorus concentration (649 $mg.kg^{-1}$) was determined by standard acid soil digestion for phosphorus determination and analysis via the molybdate blue colorimetric method using a Seal AQ2 discrete analyser. Soil pH (7.2) was determined by mixing a 1:1 soil to water mixture on an end over end shaker for 15 minutes and measuring the pH of the resultant slurry after a 30 minute settling period. Soil colour (10 YR 4/3 - dull yellowish brown) was determined manually using a standard soil colour chart. The soil was further sieved to 2 mm prior to use. The mass of soil required for all simulations (205 kg) was homogenised by hand so that no variation in physical or chemical properties existed between simulations.

6.4.2 Rare Earth Oxide

Only one rare earth oxide (REO) was required for the experiment. Work performed in Chapter 3 aided in REO selection; CeO_2 was known to be insoluble in acidic solution, while Gd_2O_3 and Sm_2O_3 had both shown over-extraction from reference soils (Tables 4.5 and 4.6). Nd_2O_3 was the most soluble in acidic solution of the

remaining available REOs (La_2O_3, Nd_2O_3 and Pr_6O_{11}) and so would give the most precise results (Table 4.5). Nd_2O_3 was taken from the same supply of REOs as used in Chapter 3 and comprised of 89.1% silt with a modal particle size of 6.61 μm, a size range of 2.4 - 37.6 μm (d^{10} - d^{90}) and a density of 7.24 g.cm^{-3}.

6.4.3 Fluorescent Microspheres

Only one size and colour of fluorescent microspheres was required. The microspheres selected had a diameter of 0.3 μm, contained a uniformly incorporated yellow-green dye and possessed carboxylate functional groups on their surface. This size was selected as it allowed effective separation of microspheres from particulates by centrifugation, but also allowed dissolution into acetone as they could be trapped by filter membranes suitable for use with solvents (> 0.2 μm). Carboxylate surface functional groups should aid in replication of the negative charge of clay particles; however, neither the charge density nor the zeta potential of the purchased microspheres was detailed in supporting literature. The yellow-green dye was chosen as fluorescent spectrometers are insensitive to red light wavelengths and previously used blue microspheres possessed excitation-emission peaks close to the water Raman line. The microspheres were manufactured by Polysciences INC and came supplied as a 2.5% aqueous suspension (1.69×10^{13} microsphere.ml^{-1}).

6.4.4 Phosphorus

The source of phosphate used to increase the phosphorus concentration of the tagged area had to result in a spatially uniform distribution of inorganic phosphate absorbed onto the surface of soil aggregates. An organic form of phosphate could not achieve this due to the need to mineralise organic material to form inorganic phosphate. Soluble granular inorganic fertiliser requires wetting of soils to release phosphate into solution. This would make a uniform phosphate distribution harder to achieve and replicate than if a solution of phosphate was used.

There were many options for the soluble inorganic phosphate source, including: monocalcium phosphate ($Ca(H_2PO_4)_2$); monoammonium phosphate (NH_4-

H_2PO_4); diammonium phosphate ($(NH_4)_2HPO_4$); ammonium polyphosphate (various forms e.g. ($(NH_4)_3HP_2O_7$), and phosphoric acid (H_3PO_4) (Follett et al., 1981).

Phosphoric acid was not selected due to the low pH of concentrated solutions (1M H_3PO_4 has a pH of 1.08). Polyphosphates are known for their ability to remain in solution through sequestration of metal ions and so were also not selected. Monocalcium phosphate (triple super phosphate) has a far lower solubility (20 $g.l^{-1}$) than ammonium phosphates and was disregarded.

Monoammonium phosphate (MAP) was selected in preference to diammonium phosphate as it forms solutions of lower pH (4 and 8 respectively). This would result in the orthophosphate form $H_2PO_4^-$ dominating the applied solution. Furthermore, improved binding of phosphate to soil aggregates may occur due to the lower pH of the solution. Purchased MAP (molecular weight 115.03, density 1.8 $g.cm^{-3}$) was manufactured by Acros organics as a 99%+ pure crystalline powder.

6.4.5 Soil Box

Steel soil boxes with dimensions of 0.25 m width, 0.5 m length and 0.3 m depth were used. The soil boxes had covered exit channels set 0.03 m below the height of the side walls and similar drainage pipes at the base of the box (Figure 6.1). Although this is a relatively small plot size, there are a number of publications that examine phosphorus behaviour at similar scales, for examples McDowell and Sharpley (2002) (1 m $\times$ 0.15 m), Kleinman et al. (2004) (1 m $\times$ 0.2 m) and Wright et al. (2006) (0.95 m $\times$ 0.5 m).

The soil boxes have the shortest path length of those referenced, and flow pathlength is known to modify the characteristic of eroded sediments (Kinnell, 2000). As a detached particle travels through surface flow it settles downwards through the flow towards the soil surface. Once at the soil surface the particle will either be deposited until it becomes re-detached, or it will travel at a slower rate by saltation or rolling. A short path length such as the one used in this experiment will cause some particles, which would settle to the soil surface on a longer slope, to be

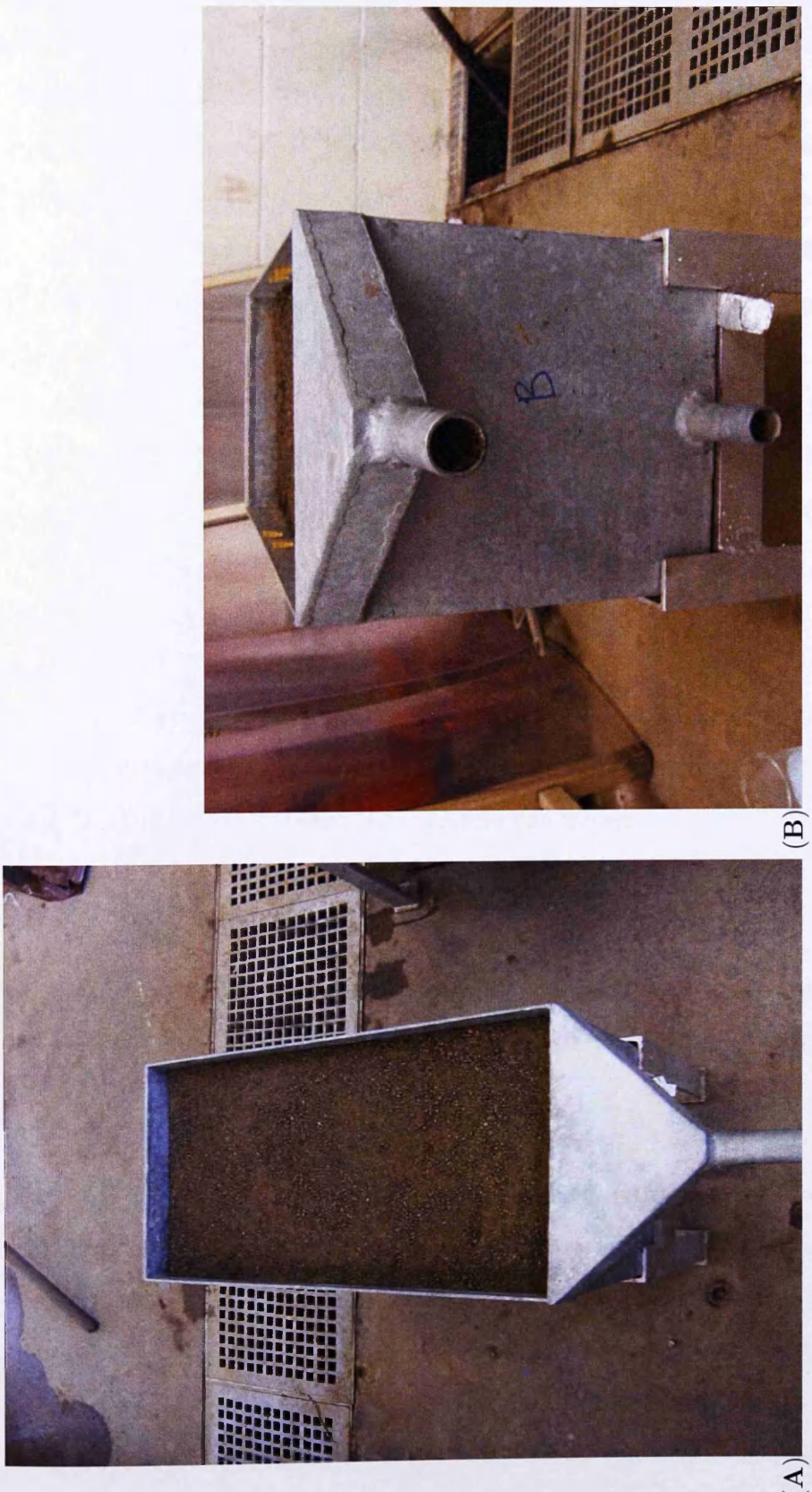

(B)

(A)

Figure 6.1: Images of one of the soil boxes showing top view (A), and front view(B).

transported into sample bottles without reaching the soil surface. This may cause masking of differences in transport behaviour of REO and P when transported by particles of different size. Conversely, the lack of surface run-on to the top soil box will result in runoff rates which are lower than those experienced by a section of soil on a larger plot (unless this section is at the top of a slope and does not experience run-on). This will cause the kinetic energy of overland flow to be reduced which in turn will cause lower detachment rates, slower transport rates and higher deposition due to faster particle settling rates.

A further difference between the soil box used and a larger plot is splash-in/splash-out processes. Material will be splashed out of the soil box by the impact of raindrops, although this will be limited to some extent by the lip surrounding the box. However, unlike a section of soil on a larger plot, there is no source of sediment to be splashed into the soil box. This will cause a net loss of sediment which would not be experienced on a larger plot.

Despite these differences, the aim of this experiment is not to replicate field scale phosphorus chemistry/soil erosion processes. Furthermore, any variations in phosphorus behaviour should be identified by the tracers.

6.4.6 Rainfall Simulator

A gravity fed rainfall simulator was used. It comprised of an open topped steel tank with dimensions of 50 cm width, 78 cm length, and 20 cm depth suspended 308 cm from the floor (Figure 6.2).

The base of the tank formed a needle bed of 972 (36 $\times$ 27) hypodermic needles (25 gauge - 0.5 mm outer thickness, 25 mm length) placed through holes in the base of the tank. An internal wall 3 cm from the back of the tank and 5 cm lower than the exterior walls acted as an overflow to the drain. This allowed a constant head of water to be applied to the needles. A removable gate in the centre of the internal wall allowed the head to be changed from 15 cm (gate in place) to 5 cm (gate removed). The rainfall rate could be further varied by blocking the hypodermic needles with rubber bungs. A nylon mesh screen (hole size 2.25 mm^2)

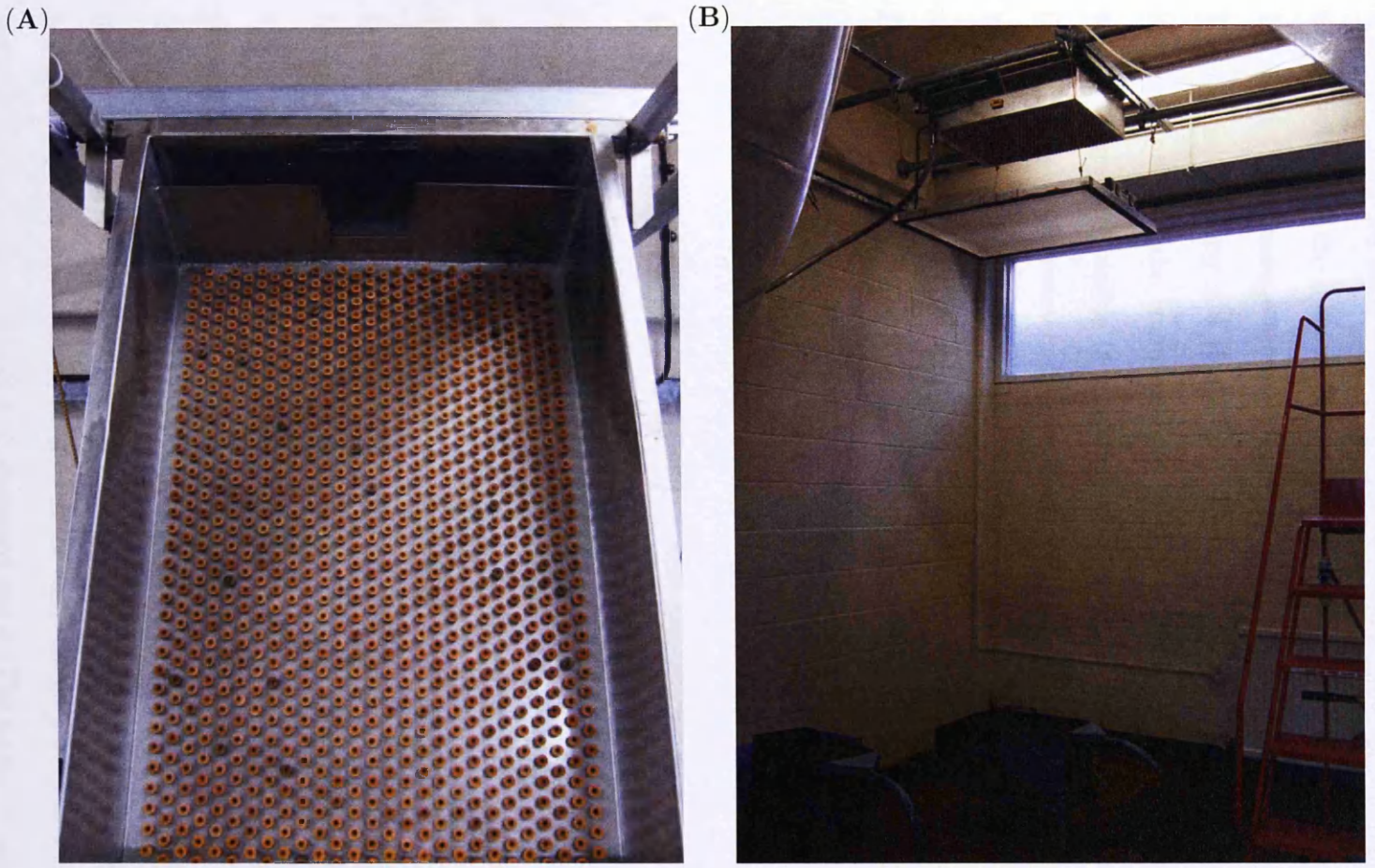

Figure 6.2: Images of the gravity rainfall simulator showing the inside view of the simulator with removable overflow gate and back of the hypodermic needles (A), and side view of the rainfall simulator with mesh screen and steel soil box (B).

was suspended 45 cm below the base of the tank to break up rain drops and give a less uniform drop size distribution. Water was supplied to the simulator using a RIOS 100 millipore water de-ioniser through a 6 mm gauge plastic pipe attached to the bottom of the front of the tank. The water had a mean conductivity of 1.3 μS.cm^{-1} and average temperature of 18.9 °C (averaged from all simulations). The rainfall intensity and spatial and temporal variability was investigated and improved prior to the commencement of the experiments to provide the most consistent results possible (see Appendix A for full details). The final selected intensity was approximately 50 mm.hr^{-1}. The uniformity of rainfall, calculated using the Christiansen Uniformity Co-efficient was greater than 90%. No data on these factors was available prior to the commencement of this experiment. Improvements in the simulator required replacement of all needles and standard operational procedures to be developed. Rainfall intensity declined after periods of one hour which limited the duration of experiments.

6.5 Methods

6.5.1 Soil Preparation

Three soil boxes were used to triplicate each gradient (3%, 6%, and 9%, tagged and untagged, 18 runs in total). The soil boxes were prepared with a bed of pea gravel (depth $\approx$ 12 cm) under a layer of coarse sand (depth $\approx$ 9 cm) separated by layers of highly permeable weed control fabric. Soil was packed upon the sand to a density of 1.4 g.cm^{-3} and a depth of approximately 6.5 cm so that the top of the soil layer was 0.5 cm proud of the exit lip to ensure effective flow off the plot. The soil was packed as 4 $\times$ 1.5 cm and 1 $\times$ 0.5 cm layers to ensure the density profile was as uniform as possible. Surfaces were checked with spirit levels following packing. The soil was removed at the end of each simulation. The exposed side walls of the boxes were cleaned with deionised water. The sand and gravel layers were flushed with deionised water to remove any microspheres or phosphate which may have been transported vertically from the overlying soil layer.

6.5.2 Soil Moisture Analysis

Soil moisture was measured using a Delta-T ML2-x theta probe inserted into the surface soil at the rear of the soil box. Voltages were converted into moisture contents using the manufacture's published voltage/moisture calibrations for mineral soils. Measurements were taken at one minute intervals during wetting prior to simulations and at the start of all sample collections during simulations.

6.5.3 Tracer and Phosphorus Addition

The tracers and MAP were applied to a 2.5 cm long strip which ran the width of the soil box 10 cm downslope from its top. The distance between the tagged section and the exit point, and also the width of the strip, had been calculated based upon previous calibration simulations applying only MAP. The position of the strip was chosen to ensure at least one low phosphorus concentration sample was collected prior to breakthrough of applied phosphate. The length of the strip was adjusted to allow accurate MAP application. The calibration simulations were also used to examine the most suitable method of REO application and to ensure experimental methods were as effective and reproducible as possible.

Nd_2O_3 Addition

Application of Nd_2O_3 had to result in minimal modification of the tagged soil because only one area of the plot was being tagged (see Section 3.5.5 for discussion of plot homogeneity). Spraying of REOs was shown to cause the least modification of parent soil particle size distribution (Chapter 4). However, spraying of Nd_2O_3 suspensions was considered to be inaccurate at such a small scale. An alternative was to isolate the tagged area by insertion of aluminium sheets into the soil profile. This allowed a suspension of Nd_2O_3 to be ponded over the tagged area resulting in transfer of the Nd_2O_3 to the soil surface as the suspension infiltrated. However, removal of the sheets without disturbing the soil surface was difficult due to the high moisture content of the tagged soil. Furthermore, the depth of erosion from the box would certainly exceed the depth of Nd_2O_3 application by either spraying

or infiltration unless the soil in the tagged section was 'tilled' following addition. As a result, the dry tagging method described in Chapter 4 was used.

Soil was excavated to a depth of approximately 2.5 cm and mixed with Nd_2O_3 to 500 times background Nd concentrations (6.4 mg of Nd_2O_3 per gram of soil). The required mass of Nd_2O_3 powder was mixed with one tenth of the excavated soil, the remainder being added in a stepwise fashion. No additional water was added due to the evidence from Chapter 4 of aggregate breakdown during wet tagging.

Care was taken not to disturb the surface of the tagged area once the soil had been repacked. Blank runs could have been conducted with excavation and mixing of the tagged section (without Nd_2O_3), but it was decided to leave the tagged area undisturbed. This would allow analysis of the effect of the tagging procedure upon sediment transport dynamics if simulations were seen to produce drastically differing results.

The soil boxes had to be wetted after Nd_2O_3 addition to aid re-incorporation of the tagged section back into the surrounding soil (Zhang et al., 2003; Polyakov and Nearing, 2004). The soil boxes were rained upon for 15 minutes at zero gradient with an intensity of 50 $mm.hr^{-1}$, and with a plastic mesh placed 3 cm above the soil surface to prevent splash erosion causing Nd_2O_3 transport. A fast wetting was selected over wetting via capillary action to cause some aggregate instability via the action of slaking, to result in a more homogeneous soil surface. Surface sealing was not expected to occur from this wetting due to the low clay content of the soil (Lado et al., 2004; Lado and Ben-Hur, 2004) and a lack of splash impact.

Phosphate Addition

There was a risk of ortho-phosphate ions moving into solution and being transported if MAP had been added prior to the wetting that followed REO addition; therefore MAP had to be applied after Nd_2O_3 addition. The soil was left to dry until it reached a moisture content of $\approx 30\%$, at which point the solution of MAP

was added. Soil suction (pF) is reported as being almost constant between 20-40% ($\approx 10^{-1}$ bar) (Russel, 1973) allowing MAP infiltration rates to be comparable between replicates regardless of small variations in moisture content.

The mass of MAP required to increase the phosphorus content of the tagged area (2.5 cm depth) to five times the background concentration (2635 mg of MAP) was dissolved into 35 ml water. The high phosphate concentration of the solution (62.9 $mg.ml^{-1}$) would help drive phosphate to soil binding and improve the precision of MAP application.

This would ensure that phosphate concentrations in runoff do not vary with the depth of erosion. Achievement of saturation was important to help ensure that applied phosphate was detected above background phosphate.

The MAP solution was slowly syringed (drop-wise) onto the soil surface at a rate that avoided the solution flowing off the tagged area. The soil boxes were left for 36 hours following MAP addition to allow phosphate ions to bind to aggregate surfaces and excess MAP solution to drain.

Phosphate to soil binding is reported as occurring in two stages; a rapid (minutes to hours) binding to the soil surface, followed by a far slower (weeks to months) but stronger binding (Morgan, 1997; Yang et al., 2002). The phosphate was given sufficient time to bind to aggregate surfaces but there was not sufficient time to leave soil boxes for weeks or months prior to simulations.

Fluorescent Microspheres

Sanderson (2002) reported a microsphere recovery rate of 3% in runoff using a comparably sized soil box, rainfall rate, a gradient of 5 degrees and microspheres of diameter of 6 μm (enumerated using a haematocytometer). An estimate of 1% microsphere recovery in runoff was made taking into account variations in gradients, distance to the exit point and microsphere size. Measurement of the background fluorescence and total runoff volumes of calibration simulations were used to calculate the number of microspheres that would have to be applied to the tagged area so that the average microsphere concentration in the runoff would be

detectable over the variability of background fluorescence.

The microspheres were added to the tagged section immediately prior to the start of the simulation in order to mitigate the risk that a sequence of wetting and draining would transport microspheres vertically into the soil profile. The volume of microsphere solution required was pipetted into DI water so that the total volume was 10 ml and was applied to the tagged area via syringing (drop wise). Simulations were conducted with increasing gradient (3%, 6%, 9%) so that the recovery of microspheres in runoff should increase. This could be combined with applying increased concentrations of microspheres if they were not detected in initial simulations. The volume of microsphere solution used was 0.5 ml, 2 ml and 4 ml for 3%, 6% and 9% slopes respectively.

6.5.4 Simulations

Simulations were conducted consecutively with the soil boxes being pre-wetted immediately prior to simulations to ensure antecedent moisture conditions were uniform. Fast runoff generation was desired so that tracers and applied phosphate were not transported down slope by splash erosion or vertically into the soil profile prior to runoff commencing. Furthermore, the intensity of the rainfall simulation was known to drop after approximately two hours (Appendix A).

Wetting could not be performed by applying water to the soil surface because applied phosphate may have been transported laterally if ponding occurred. Water was introduced into the base of the soil box via connection of the drain outlet with a second soil box which was filled with deionised water over a 15 minute period.

There was the possibility of sub-surface dissolved and colloid bound phosphate being transported upwards by the wetting front, therefore the water table was maintained below the soil surface. The soil boxes were subsequently left to drain for a further 15 minutes. This allowed the soil moisture content to stabilise while weakly held gravitational water drained, leaving adhesive and cohesive water and gravitational water that could not drain freely.

A rapid wetting was chosen as there was the possibility of dissolved phosphate

diffusing through pore water by Brownian motion if the soil had been left to saturate slowly over a period of multiple hours. This procedure ensured that soil moisture was as constant as possible prior to simulations, minimising impacts upon the simulations.

Runoff was collected continuously into 1 l acid washed sample bottles which were swapped at the time points indicated in Figure 6.3. Samples were collected at higher frequency at the beginning of the simulations in order to precisely identify tracer and phosphate breakthrough times.

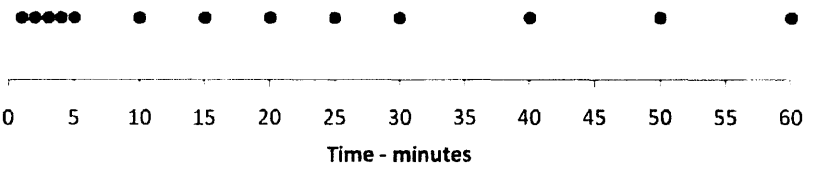

Figure 6.3: Visual representation of the points in time when sample bottles were exchanged.

6.5.5 Sample Analysis

Phosphorus Analysis

Subsamples of surface runoff were taken as close to the time of sample collection as was practically possible (between 1-5 minutes) and with minimal disturbance of the samples due to the ability of phosphate to rapidly change phase. Filtration of samples after the simulations had ceased may have resulted in incorrect phosphate behaviour being observed. Sub-samples (5 ml) were filtered at 0.45 μm using pre-rinsed whatman syringe filters. A 1 ml aliquot of the filtrate was added to 19 ml of Dde-ionised (DI) water for total dissolved phosphorus analysis. Unfiltered sub-samples (1 ml) were added to 19 ml of DI water for total phosphorus analysis. Dilutions were performed to bring samples inside analytical concentration ranges (calculated from trial simulations) and because sufficient sample volume for undiluted analysis (16.2 ml) could not be collected from the first five samples without compromising REO and microsphere analysis. Samples were digested via

an acid/persulfate digestion at high temperature and pressure and analysed using a Seal AQ2+ discrete analyser via the molybdate blue method (full details of quality control can be found in Appendix C). All sample analysis was performed by the author. Triplicate measurements were taken from the penultimate sample for quality control.

Rare Earth Analysis

After eroded sediments in surface runoff and surface samples had been dried they were sieved to $\leq$ 2 mm and homogenised by hand mixing. Representative sub-samples were taken using a splitting apparatus. Samples were split until their mass was between 0.5 and 1 g. Samples were reduced to 0.5 g by cone and quartering ensuring no visible particle size selectivity. Sub-samples as large as possible were taken (to the nearest 0.05 g) when total eroded sediment mass from runoff was $<$ 0.5 g. Samples were digested using the USEPA method (Chapter 3). Each set of samples was digested with a sample of reference soil to check for analytical interference, and a reference blank to check for contaminations. Triplicate digestions of the penultimate runoff sample were made for quality control. Once digested, the samples were made up to 100 ml, homogenised, and a 50 ml sub-sample was centrifuged. The top 10 ml of the supernatant was removed and sent to the University of Plymouth (Devon, UK) for analysis via ICP-OES.

Fluorescent Microsphere Analysis

The work performed in Chapter 4 suggested that dissolution of microspheres into acetone may not be successful due to an inability to completely remove background interference, and because of analytical issues resulting from the use of acetone. The alternative was centrifugation of samples without the removal of dissolved organic matter (DOM). Sub-samples (5 ml) of surface runoff were diluted with DI water to 25 ml and centrifuged at 2500 rpm for 20 minutes. The top 10 ml of the supernatant was removed. The same fluorescent spectrometer and equipment used in Chapter 4 was used to analyse samples via emission scanning.

Background fluorescent noise occurs at the emission location of the chosen microspheres (this was unavoidable regardless of microsphere colour). It was expected that the presence of microspheres in samples from tagged simulations would result in significantly higher photon counts than samples from blank simulations. However, background fluorescent noise is variable depending on the concentration of fluorescent material in the samples; therefore, a method to calculate the contribution of microspheres to the recorded photon count was devised to allow better calculation of microsphere concentrations in samples with photon counts close to background levels. This involved taking a measurement of background fluorescent noise in samples from blank simulations at: i) a location away from microsphere fluorescence, and; ii) the microsphere emission location. This relationship was then used to calculate the contribution of microspheres to total fluorescence in samples from tagged simulations (a fuller description of this method is found in Appendix D).

Particle Size Analysis

Particle size analysis of eroded sediments in surface runoff samples was recorded prior to drying using a Malvern Hydro 2000 particle size analyser (Chapter 4). There was insufficient sample volume to analyse any of the first five samples. Analysis was performed on samples collected between 10 to 15 minutes, 25 to 30 minutes and 40 to 50 minutes. Samples were inverted five times (after subsampling for phosphorus) and 10 ml of runoff was removed.

6.6 Results & Discussion

6.6.1 Soil Box Behaviour

As this thesis is focused on the evaluation of the tracers it is not proposed to discuss the sediment and discharge behaviour of the soil boxes in detail. However, a full description and interpretation of soil box behaviour (discharge, sediment

concentration, particle size of runoff and soil moisture content) is presented in Appendix E. In summary, the main observations of behaviour were that:

- Discharge increased to steady state after approximately 20 minutes. Steady state discharge from 6% slopes (100 $ml.min^{-1}$) was significantly higher than from 3% and 9% slopes (90 $ml.min^{-1}$) at all sampling intervals ($p < 0.05$).

- Sediment concentrations increased through time to reach near steady state conditions after 20 minutes. Steady state concentrations increased with slope (7 $g.l^{-1}$, 4 $g.l^{-1}$ and 3 $g.l^{-1}$ (mean) from slopes of 9%, 6% and 3% respectively).

- Sediment concentrations from tagged simulations at 3% slope were significantly lower than untagged simulations ($p < 0.05$) between 2 and 10 minutes.

- Particle size distributions (PSDs) showed a coarsening of sediment through time, with the majority of eroded sediment in the silt fraction (77% - 88%). Distributions were finest from 6% slopes (possibly due to higher discharge) and coarsest from 9% slopes.

- Significantly higher percentages of silt and lower percentages of very fine sand, fine sand and medium sand were collected from 6% than from 9% slope at all sampling intervals ($p < 0.05$).

- Sub-surface soil moisture (0-6 cm depth) showed some decline (between two steady state conditions) at slopes of 6% and 9%. A possible explanation is the effect of surface sealing observed in rainfall simulations using the same soil (Armstrong et al., 2010).

- Soil boxes produced the behaviour expected, with increased erosion rates from higher slopes.

- The aims of the experimental design were achieved as simulations showed reproducible behaviour which was distinct at each slope gradient.

6.6.2 Applied Particulate Phosphorus (PP_{map}) Behaviour

The behaviour of the phosphate applied to the tagged section (mono–ammonium phosphate - P_{map}) was calculated by subtraction of the mean phosphate concentrations of blank runs from the mean phosphate concentration of tagged runs (Figure 6.4). This allowed correct comparison of the behaviour of phosphate applied to the tagged section with the behaviour of the tracers. All particulate phosphorus (PP) values were calculated from total phosphorus (TP, total particulate and total dissolved phosphorus) minus total dissolved phosphorus (TDP), both of which were determined analytically (see Section 6.5.5). Particulate and dissolved phosphorus are defined as the phosphorus concentration above and below the 0.45 μm size boundary at which samples were filtered prior to total dissolved phosphorus analysis.

Applied particulate phosphorus (PP_{map}) concentrations rose at the start of the simulations followed by almost steady state conditions (Figure 6.5). The rise of PP_{map} concentrations occurred because values were low or negative at the start of simulations when eroded sediment originated from close to the exit point where there was no tagged sediment. The PP_{map} concentrations rose when eroded sediment from the tagged section arrived at the exit point (breakthrough of PP_{map}).

Replicated simulations showed more variability of PP_{map} concentrations at the start of simulations than at the end. The average co-efficient of variation (CV) of replicated samples collected during the same sampling interval was 93.2% for the first five samples collected from simulations at 9% slope (1-5 minutes), but 43.8% for the final five samples collected (25-60 minutes). This shows how initial variations between soil boxes were minimised through time as steady state conditions, which were reproducible, were reached. Subtle differences in soil surface topography, which would magnify variations in the volume of surface runoff when overland flow volumes were initially low could have caused this initial variation of PP_{map} concentration from replicated simulations. Early variability of PP_{map} concentrations could have also been caused by differences in starting soil moisture

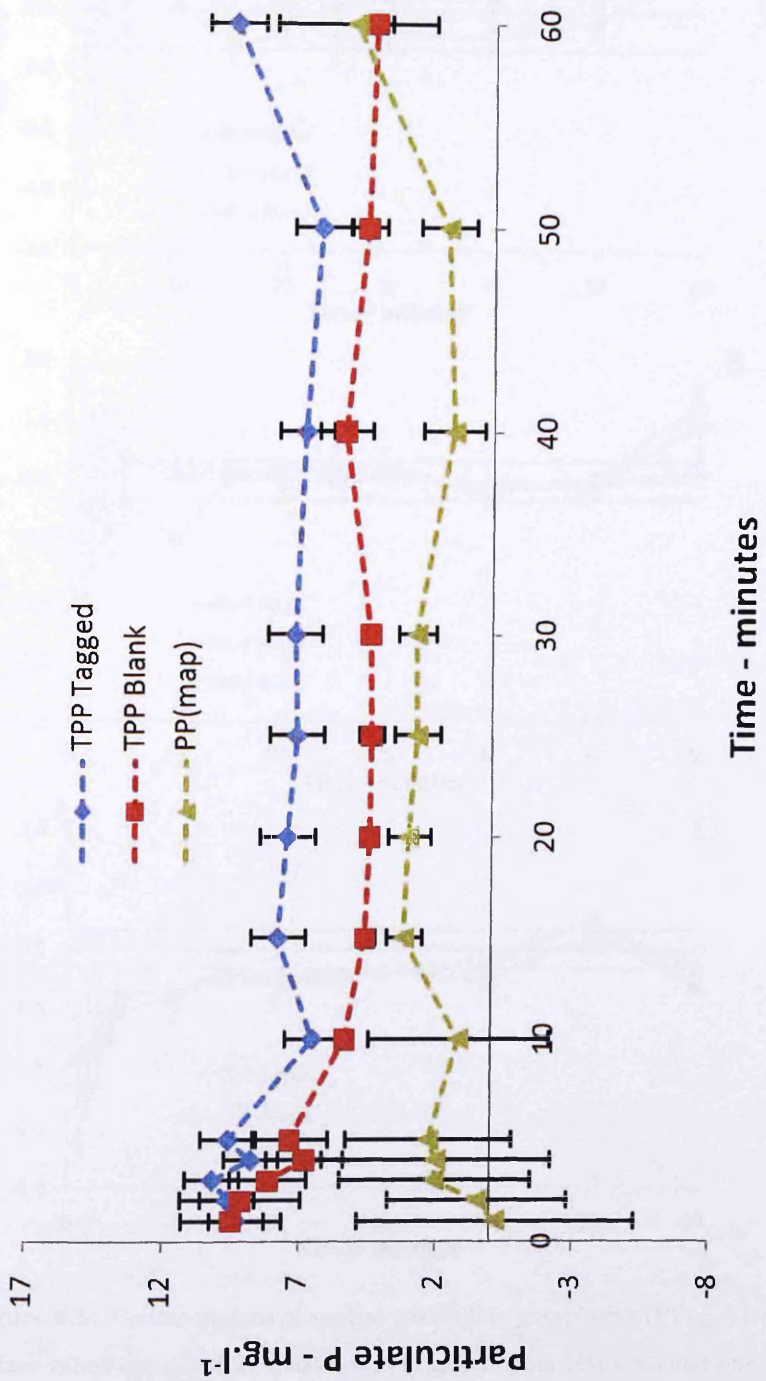

Figure 6.4: Graphical representation of applied particulate phosphorus (PP_{map}) determination for simulations at 6% slope using the mean concentration of particulate phosphorus (PP) from blank simulations subtracted from the mean concentration of PP from tagged simulations.

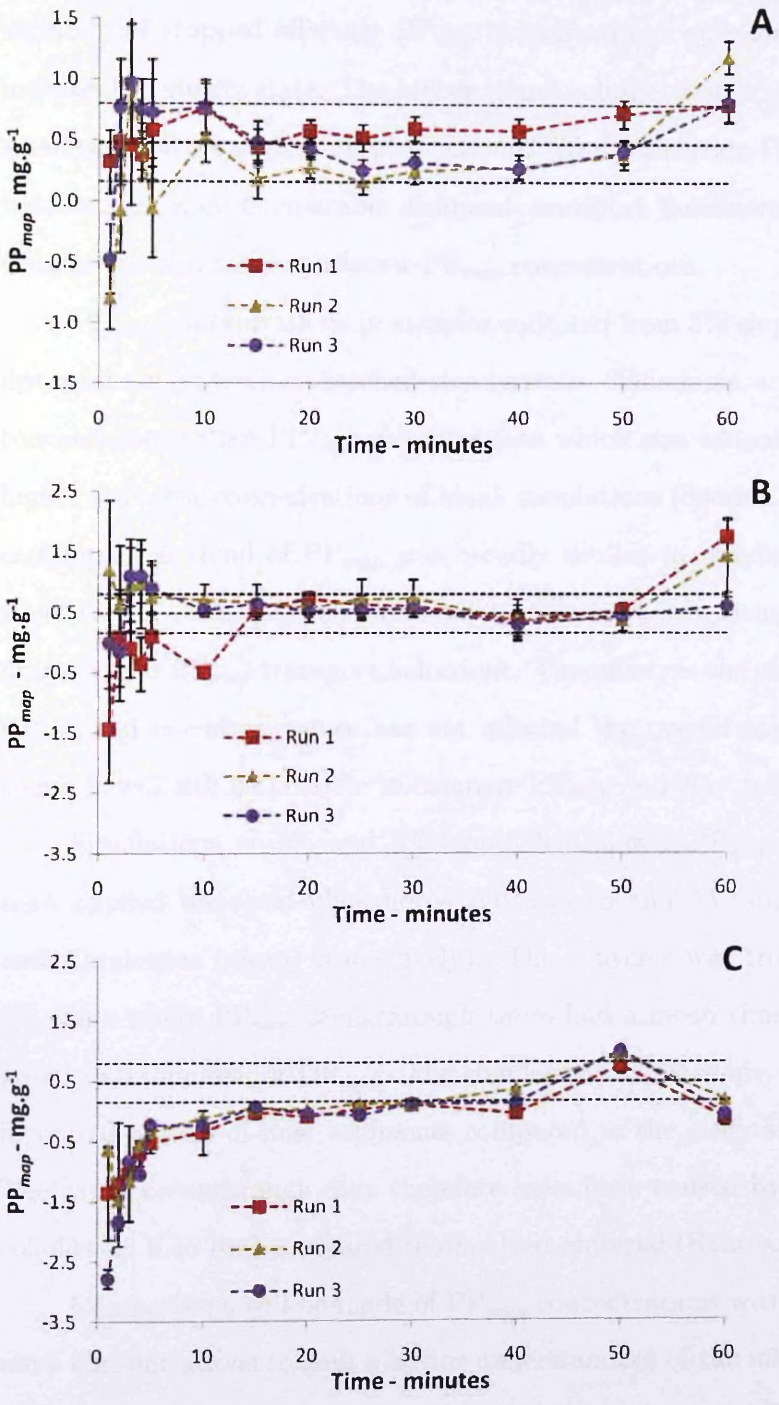

Figure 6.5: Concentrations of applied particulate phosphorus (PP_{map}) from eroded sediment in surface runoff samples (phosphate concentrations from blank simulations are subtracted). Horizontal lines indicate PP_{map} enrichment ratios of 1, 3 and 5 respectively. Figures A-C represent simulations at 9-3% slope respectively. Error bars are calculated from error associated with blank simulation subtraction and the variation from triplicate analysis of the penultimate samples.

content, which would have affected the early sediment transport behaviour. These variabilities stopped affecting PP_{map} concentrations once surface runoff volumes increased to steady state. The higher runoff volume at steady state would prevent small variabilities such as those mentioned from influencing PP_{map} concentrations, resulting in more comparable sediment transport behaviour between replicated simulations and more consistent PP_{map} concentrations.

PP_{map} concentrations in samples collected from 3% slopes had negative values until concentrations reached steady state. This is an artefact of higher PP_b concentrations than PP_{map} concentrations which was caused by the significantly higher sediment concentrations of blank simulations (Section 6.6.1). However, the concentration trend of PP_{map} was broadly similar to simulations at 9% and 6% slope (rising concentrations followed by steady state), demonstrating the same fundamental PP_{map} transport behaviour. Therefore, as the calculation of negative PP_{map} concentration values has not affected the overall observed concentration trend, it will still be possible to compare PP_{map} and Nd_2O_3 behaviour.

Simulations at 9% and 3% slopes had slower PP_{map} breakthrough times than applied dissolved phosphorus (DP_{map}) (3 and 15 minutes compared to 2 and 10 minutes (mean) respectively). The converse was true for simulations at 6% slope where PP_{map} breakthrough times had a mean time of 4 minutes, compared to 5 minutes for DP_{map}. The simulations at 6% slope were shown to erode increased masses of finer sediments compared to the other slopes (Appendix E). The rapid breakthrough may therefore have been caused by preferential flow of colloids (< 0.45 μm) compared to dissolved material (Ryan and Elimelech, 1996).

Comparisons will be made of PP_{map} concentrations with discharge and sediment concentrations to gain a better understanding of the influences upon PP_{map} transport. This will also be done for Nd_2O_3 in Section 6.6.3, and will help in the comparison of PP_{map} and REO transport. However, the observable behaviour of PP_{map} and Nd_2O_3 is influenced by concentration breakthrough at the start of simulations because they were applied to a single strip of the soil box. This makes comparisons to measurements less useful because breakthrough at the start of sim-

ulations will influence correlation plots and hide the influence of factors such as discharge once breakthrough has occurred.

PP_{map} and discharge correlated poorly at 6% and 9% slopes when compared to the simulations 3% slope (Figure 6.6), which showed more consistent correlation. There is an expectation that PP_{map} concentration will rise with discharge at the start of the simulations due to increased transfer of PP_{map} tagged sediments from the tagged section. Correlation between discharge and PP_{map} was poor because PP_{map} and discharge reached steady state at different times. PP_{map} showed high initial concentrations at 6% and 9% slope which then dropped to steady state after 10 minutes (Figure 6.5). This contrasts to discharge which rose through time to reach steady state after twenty minutes, and which also did not show an early discharge spike (see Appendix E).

This difference in behaviour at the start of the simulations could be caused by a number of factors: i) it could indicate increased transport of sediment by splash erosion relative to the mass of sediment transport in overland flow; ii) it may also be the result of PP_{map} being transported in fine fractions of sediments (fine silts and clays) which reach steady state concentrations in surface runoff while discharge is still increasing and causing erosion of coarser sediments which contain less PP_{map}; iii) increased transfer of phosphate from the particulate phase into the dissolved phase will occur as discharge increases affecting the relationship between PP_{map} and discharge. These factors appear to cause PP_{map} to correlate poorly to discharge; on a soil box with uniform concentrations of non-labile P it would be expected that PP concentration and discharge would show improved correlation.

However, correlations between PP_{map} and discharge from simulations at 3% slope gave higher r^2 values. This is due to the lack of a concentration spike at the start of the simulations and steady state being reached after 15 minutes due to slower sediment transport. This may indicate a decline in the importance of splash erosion as a transport mechanism. Furthermore, at lower slope, the changing equilibrium between phosphate in the particulate phase and dissolved phase caused by increasing discharge has more time to adjust prior to sediment

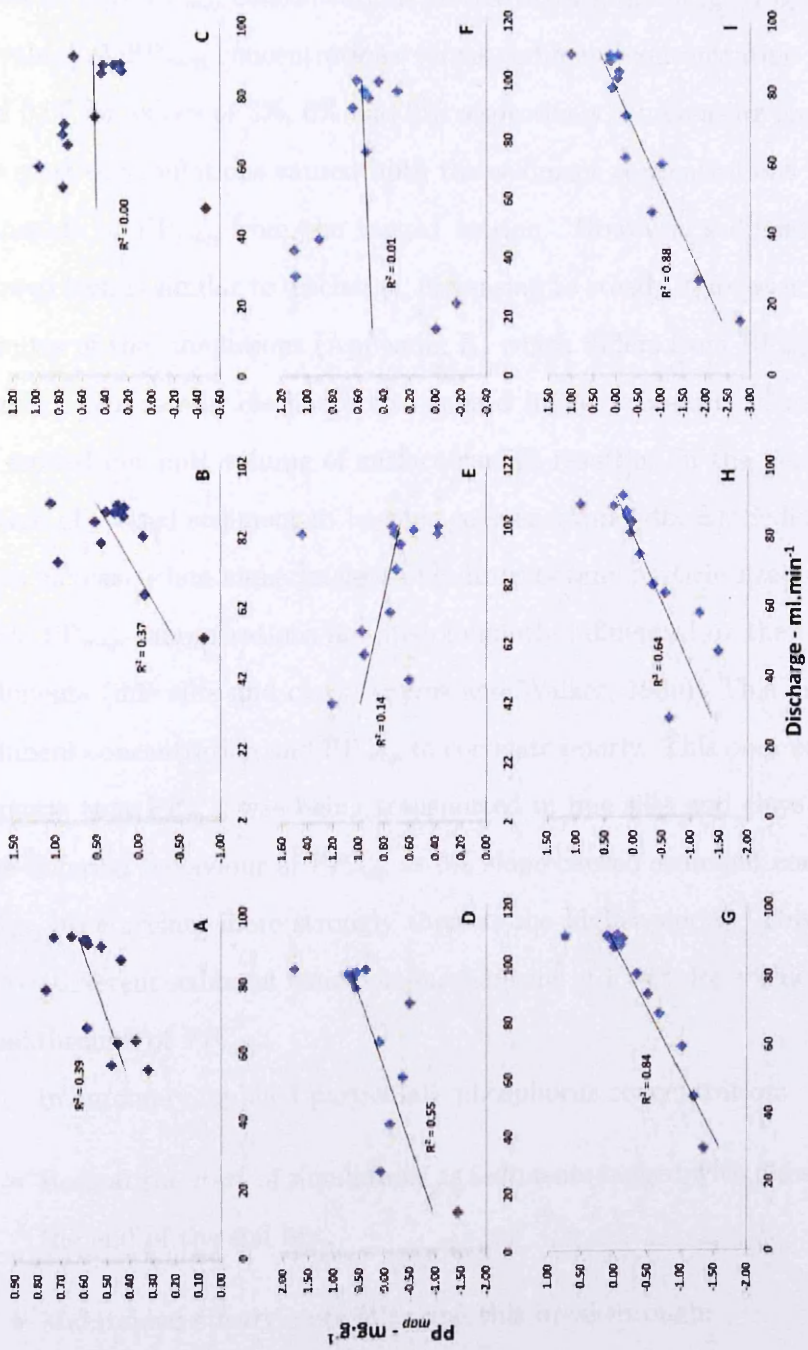

Figure 6.6: Scatter plot of applied particulate phosphorus (PP_{map}) from eroded sediment in surface runoff samples plotted against discharge. Figures A-C, D-F and G-I represent triplicate simulations at slopes of 9%, 6% and 3% respectively.

being removed from the soil box. This may cause changes in the ratio of particulate to dissolved phosphorus to coincide more closely with changes in discharge.

PP_{map} concentrations plotted against sediment concentration produced lower r^2 values than PP_{map} concentrations plotted against discharge (Figure 6.7) (average r^2 values of PP_{map} concentrations versus sediment concentration were 0.68, 0.10 and 0.06 for slopes of 3%, 6% and 9% respectively). Increasing erosion rates from the start of simulations caused both the sediment concentrations to rise and also transport of PP_{map} from the tagged section. However, sediment concentration showed trends similar to discharge, increasing to steady state over the first twenty minutes of the simulations (Appendix E) which differs from PP_{map} concentration trends. Increases in discharge also caused higher masses of coarser sediment to be eroded per unit volume of surface runoff, resulting in the particle size distribution of eroded sediment to become coarser (Appendix E). Sediment concentrations increase when higher masses of sediments (any particle size) are transported, while PP_{map} concentrations are predominantly influenced by the transport of fine sediments (fine silts and clays) (Syres and Walker, 1969). This difference caused sediment concentration and PP_{map} to correlate poorly. This poor correlation again suggests that PP_{map} was being transported in fine silts and clays as is expected. The differing behaviour of PP_{map} at 3% slope caused sediment concentration and PP_{map} to correlate more strongly than at the higher slopes. This again is likely due to different sediment transport mechanisms at lower slope which caused slower breakthrough of PP_{map}.

In summary, applied particulate phosphorus concentration:

- Rose at the start of simulations as sediments tagged with phosphorus reached the end of the soil box;
- Maintained steady state following this breakthrough;
- Correlated poorly to discharge and sediment concentration at 6% and 9% slope due to PP_{map} being associated with the finer fractions of eroded sediments (fine silts and clays), with improved correlation at 3% slope;

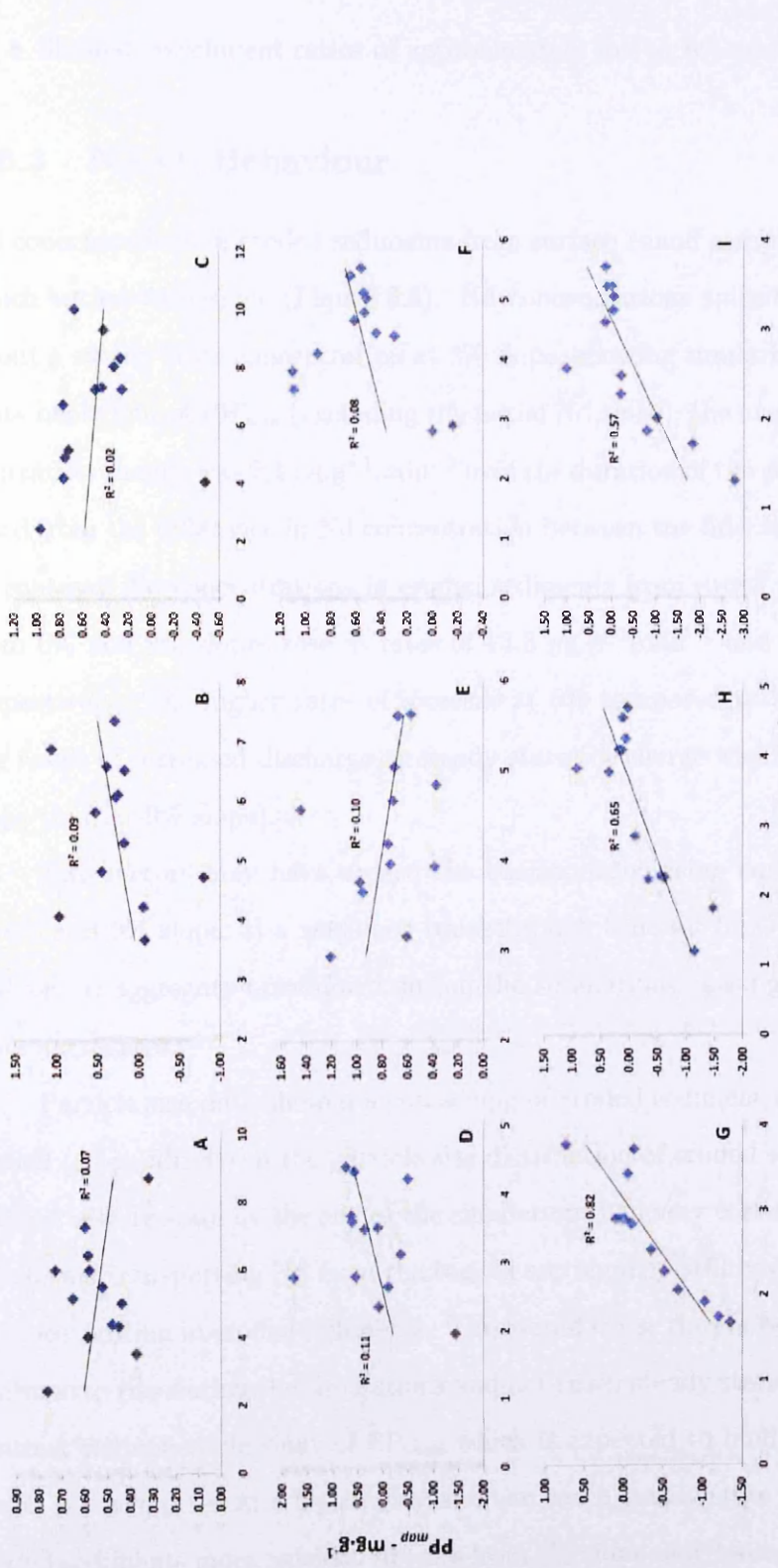

Figure 6.7: Scatter plot of applied particulate phosphorus (PP_{map}) from eroded sediment in surface runoff samples plotted against sediment concentration. Figures A-C, D-F and G-I represent triplicate simulations at slopes of 9%, 6% and 3% respectively.

- Showed enrichment ratios of approximately five at 6% and 9% slope.

6.6.3 Nd_2O_3 Behaviour

Nd concentrations in eroded sediments from surface runoff samples showed trends which varied with slope (Figure 6.8). Nd concentrations spiked, then fluctuated about a steady state concentration at 3% slope, showing similarities to the steady state behaviour of PP_{map} (excluding the initial Nd spike); the average rate Nd concentration change was 2.4 $\mu g.g^{-1}.min^{-1}$ over the duration of the simulations (calculated from the difference in Nd concentration between the first and final samples). In contrast, Nd concentrations in eroded sediments from runoff samples collected from 6% and 9% slopes rose at rates of 13.3 $\mu g.g^{-1}.min^{-1}$ and 8.9 $\mu g.g^{-1}.min^{-1}$ respectively. The higher rates of increase at 6% compared to 9% slope is likely the result of increased discharge at steady state (discharge was 11% higher at 6% slope than at 9% slope).

Two factors may have caused the continuously rising concentration of Nd at 6% and 9% slope: i) a very long breakthrough time for REO tagged particles, and/or; ii) aggregate breakdown during the simulations causing release of REOs from aggregates.

Particle size data showed a coarsening of eroded sediment as the events proceeded (Appendix E). If the particle size distribution of eroded sediments had not reached steady state by the end of the simulation then very coarse tagged material which was transporting Nd from the tagged section may still have been increasing in concentration in eroded sediments. This would cause the concentration of Nd to continue to rise during the simulations and not reach steady state. This would also contrast with the behaviour of PP_{map} which is expected to bind to finer material which is transported at a higher rate and can reach steady state concentrations in eroded sediments more quickly. Results from 3% slope may have differed from this behavioural pattern due to the lower slope causing poor transport of larger REO tagged particles (see Appendix E for a discussion of low slope behaviour). It is also possible that disaggregation caused the release of Nd from tagged aggregates,

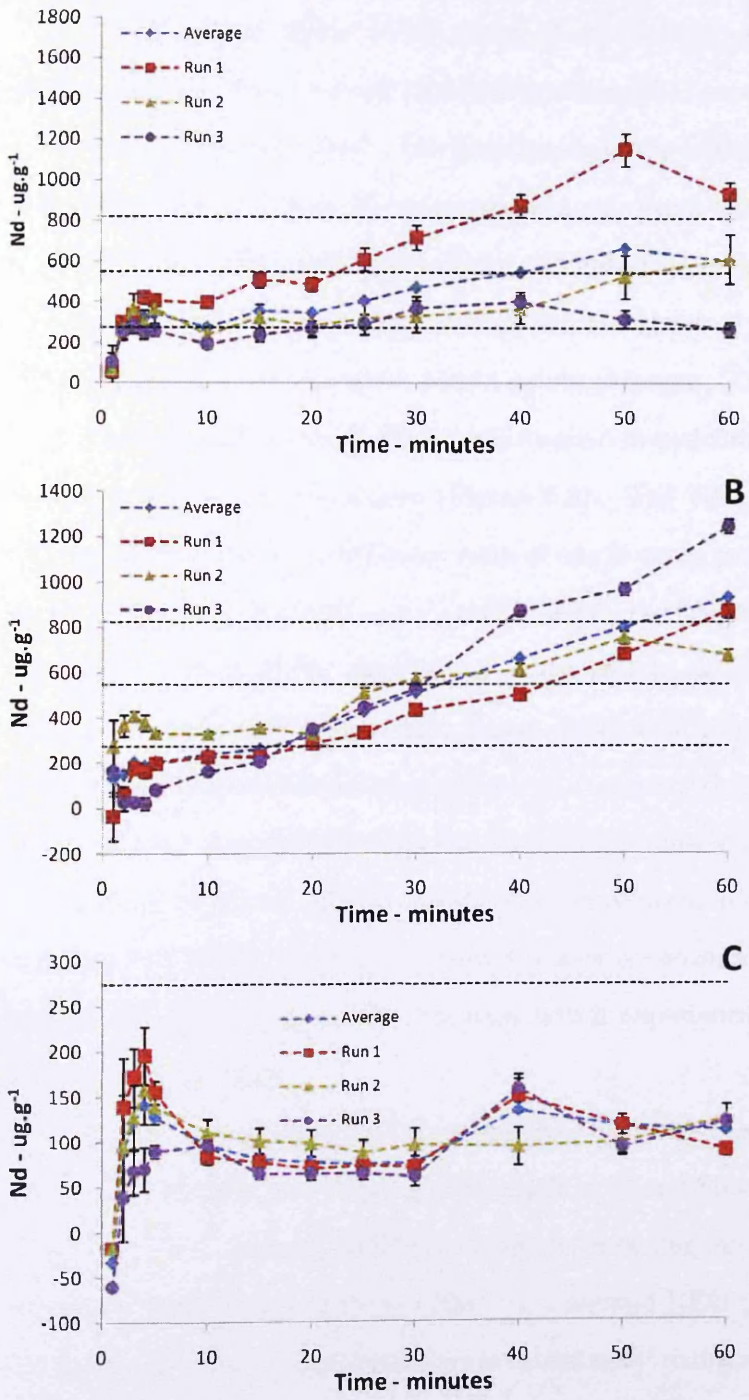

Figure 6.8: Concentrations of Nd in eroded sediments from surface runoff samples from tagged simulations. Horizontal lines indicate increasing Nd enrichment ratios of 1, 2 and 3 respectively. Figures A-C represent simulations at 9-3% slope respectively. Error bars are calculated from error associated with blank simulation subtraction and the variation from triplicated analysis of the penultimate samples.

and that this process was functioning during the entirety of the simulation.

Concentration spikes at the start of simulations suggested loss of poorly bound Nd_2O_3 which has been reported in other REO studies (Zhang et al., 2003; Polyakov and Nearing, 2004). The prominence of the initial Nd concentration spike in samples collected from 3% slope resulted only from the low Nd concentrations which followed. The peak height of the concentration spikes increased with slope. This is expected because at higher slope the transport of unbound REO particles will be higher due to increased stream power (Morgan, 2005).

The rising Nd concentration trend resulted in enrichment ratios (ERs) greater than one at 6% and 9% slopes (Figure 6.8). The Nd concentration in eroded sediment that gives an enrichment ratio of one is equal to the concentration of Nd in the tagged section (5495 $\mu g.g^{-1}$) multiplied by the fraction of the plot covered by the tagged section (0.05). Enrichment ratios rose to one through time because of Nd_2O_3 experiencing breakthrough. Tracer enrichment greater than one may occur if tracers are removed from aggregates and transported independently. However, an enrichment ratio greater than one does not conclusively indicate loss of tracers from tagged material; higher erosion rates may occur around a tagged location resulting in a higher contribution than the average erosion rate, or the tracer may be preferentially bound to fine fractions which experience higher transport rates than coarser fractions.

Enrichment ratios greater than one have been reported by Zhang et al. (2003) (ER = 2), Polyakov and Nearing (2004) (ER = 3) and Stevens and Quinton (2008) (ER = 6) when applying REOs to soils experiencing unconcentrated flow from simulated rainfall. Zhang et al. (2003) also showed REO predicted sediment concentrations (a form of enrichment ratio) constantly rising at a faster rate than the measured sediment concentration. This occurred because the tracer was located in the mid-slope where erosion rates were higher than the average for the plot. Therefore, the rising concentrations of Nd and high enrichments shown in Figure 6.8 are not unexpected.

Enrichment of Nd was below one in samples collected from 3% slope. This

was not the result of Nd_2O_3 placement at a location of low erosion (shown by enrichment of Nd at 6% and 9% slopes), therefore slopes lower than 6% appear to affect the transport of REO particles. Low slope effects may result from higher settling velocities of REO particles (compared to equivalently sized silica particles), as discussed in Section 6.6.5. Slopes with gradients close to 3% are known to produce differing behaviour to higher slopes (Cochrane and Flanagan, 2006) due to the effects of higher ponding depths and the increased connectivity of surface water (Armstrong et al., 2010); this is discussed in more detail in the review of soil box behaviour in Appendix E.

Comparisons to discharge and sediment concentration will now be made, as has been done for PP_{map}. As was previously stated, the behaviour of Nd_2O_3 is influenced by its transport from the tagged section which causes low concentrations at the start of simulations and complicates comparisons. However, there is an expectation that Nd concentrations should correlate to discharge because the rise in discharge as the simulations proceed should result in greater transport of Nd from the tagged location until both reach steady state.

Positive correlation values indicate that this was partly the case (Figure 6.9). However, relationships were non-linear because Nd concentrations continued to rise after discharge reached steady state (6% and 9% slopes only), and because early concentration spikes of Nd were not replicated by discharge. The possible reasons for the increase in Nd concentration through time, which were not shown by discharge, have been discussed. In summary, it is possible that coarse sediment which was transporting Nd was still increasing in concentration once discharge had reached steady state due to slow transport rates, and that disaggregation caused release of unbound Nd.

Nd concentrations and sediment concentrations may correlate if rising erosion rates causing increased sediment concentrations also caused increased transport of Nd from the tagged section. Correlations to sediment concentration were lower than to discharge for samples collected from all slopes (Figure 6.10); average r^2 values for correlations between Nd concentration and sediment concentration were

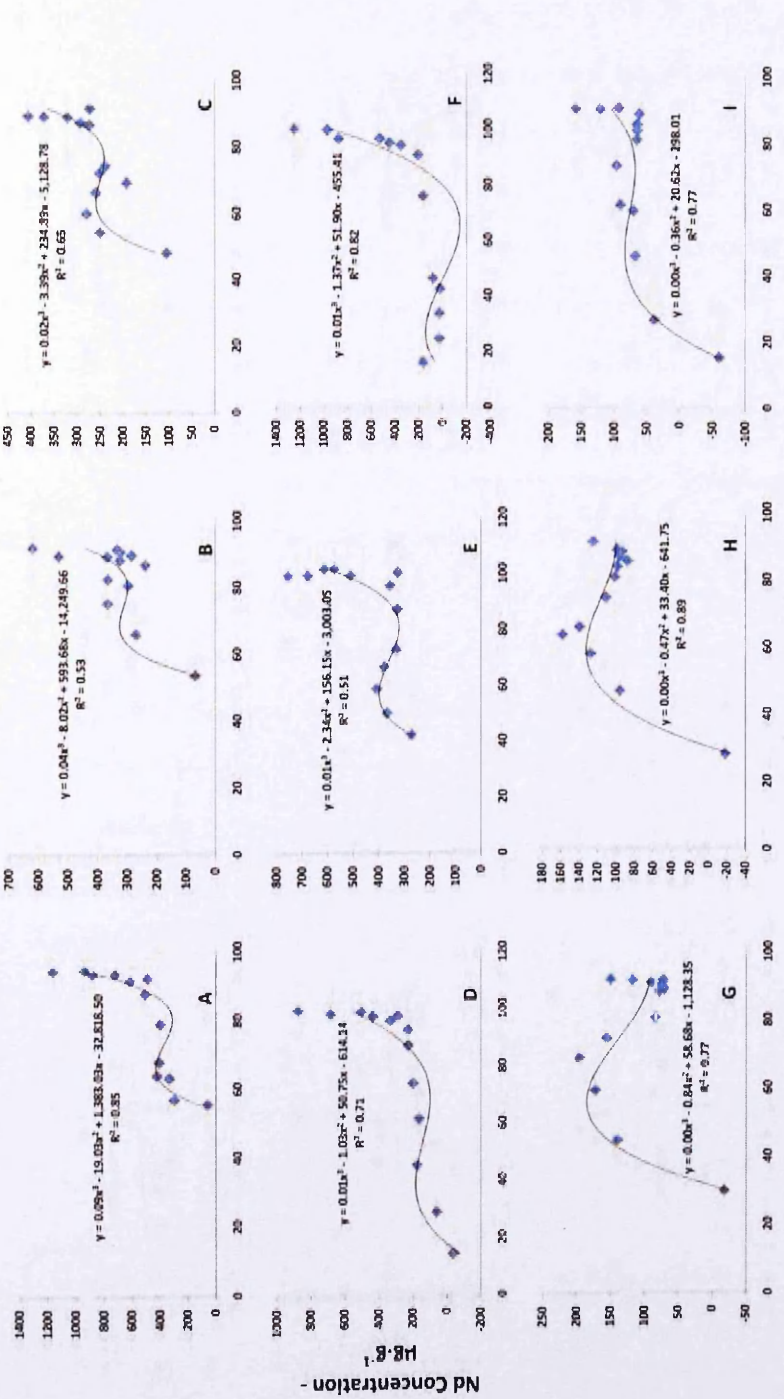

Figure 6.9: Scatter plots of Nd concentrations from eroded sediment in surface runoff samples plotted against discharge. Figures A-C, D-F and G-I represent triplicated simulations at slopes of 9%, 6% and 3% respectively. Lines of best fit are plotted as third order polynomials

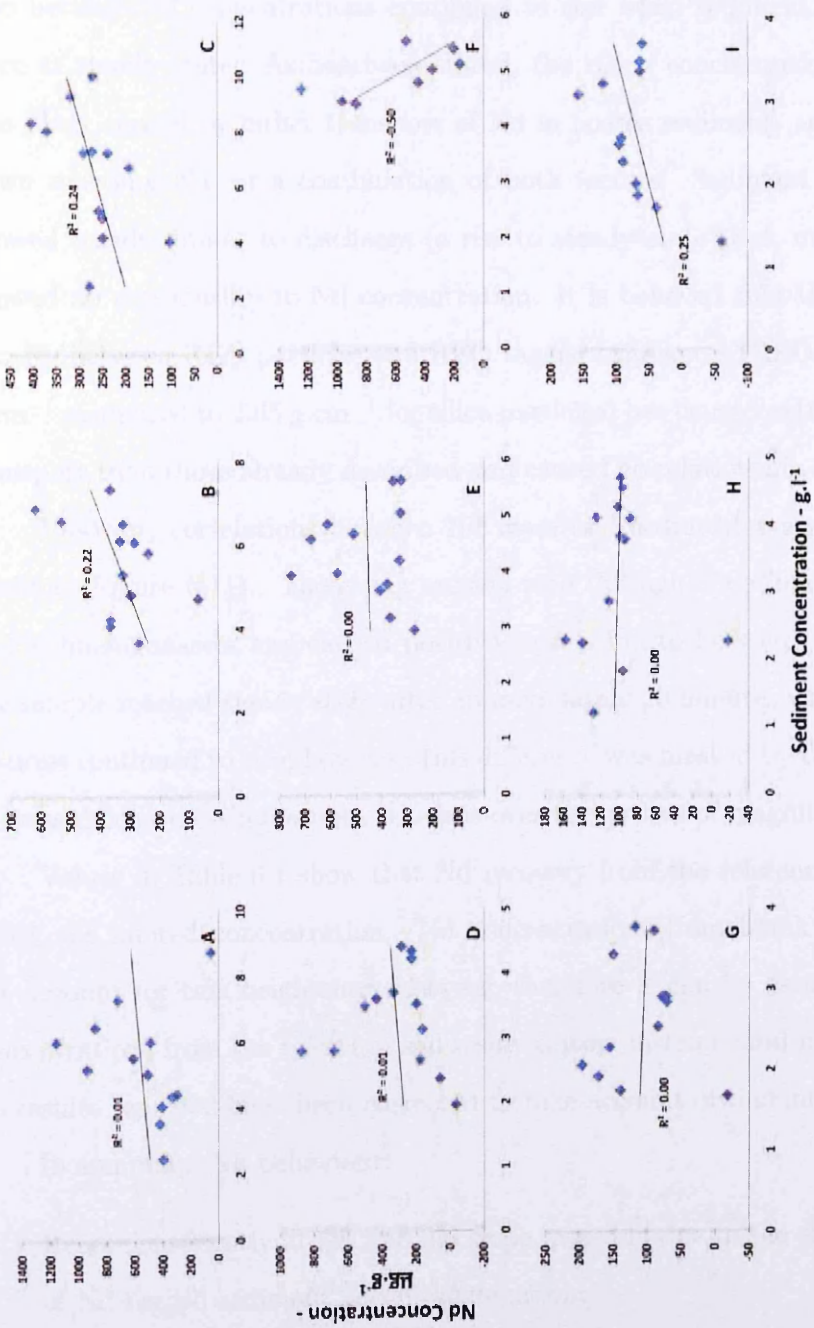

Figure 6.10: Scatter plots of Nd concentrations from eroded sediment in surface runoff samples plotted against sediment concentration. Figures A-C, D-F and G-I represent triplicated simulations at slopes of 9%, 6% and 3% respectively.

0.16, 0.17 and 0.08 for slopes of 9%, 6% and 3% respectively (linear correlation) and showed no second or third order polynomial relationships. The poor correlation was caused by high Nd values at the start of simulations when unbound Nd_2O_3 was being transported from the plot, coinciding with low sediment concentrations, and also because Nd concentrations continued to rise when sediment concentrations were at steady state. As has been stated, the rising concentration trend of Nd was likely caused by either transport of Nd in coarse sediment, aggregate breakdown releasing Nd, or a combination of both factors. Sediment concentrations showed trends similar to discharge (a rise to steady state) but, unlike discharge, showed no relationship to Nd concentration. It is believed that the difference in density between REO particles and REO tagged aggregates (REO density is 7.42 $g.cm^{-1}$ compared to 2.65 $g.cm^{-1}$ for silica particles) has caused extra differences in transport than those already described and caused no relationship to be observed.

However, correlations between Nd mass and sediment mass were strongly positive (Figure 6.11). The rising erosion rate through time increased both Nd and sediment masses and caused positive correlation to be seen. Sediment mass per sample reached steady state after approximately 20 minutes while Nd concentrations continued to rise; however, this difference was masked by the large change in mass during the simulations, which is over two orders of magnitude in size.

Values in Table 6.1 show that Nd recovery from the reference soil was 19% above the quoted concentration. Nd concentrations from blank samples could not account for this heightened recovery, therefore it can be assumed that high concentrations from the reference soil resulted from instrumental interference. All Nd results reported have been corrected to take account of this interference.

In summary, Nd behaviour:

- Roses consistently at 6% and 9% slope, possibly due to the slower transport of Nd tagged sediment and disaggregation;
- Showed steady state behaviour and lower concentrations at 3% slope, possibly due to surface sealing and higher ponding, which is known to occur at lower slopes (see Appendix E), inhibiting transport of larger REO tagged

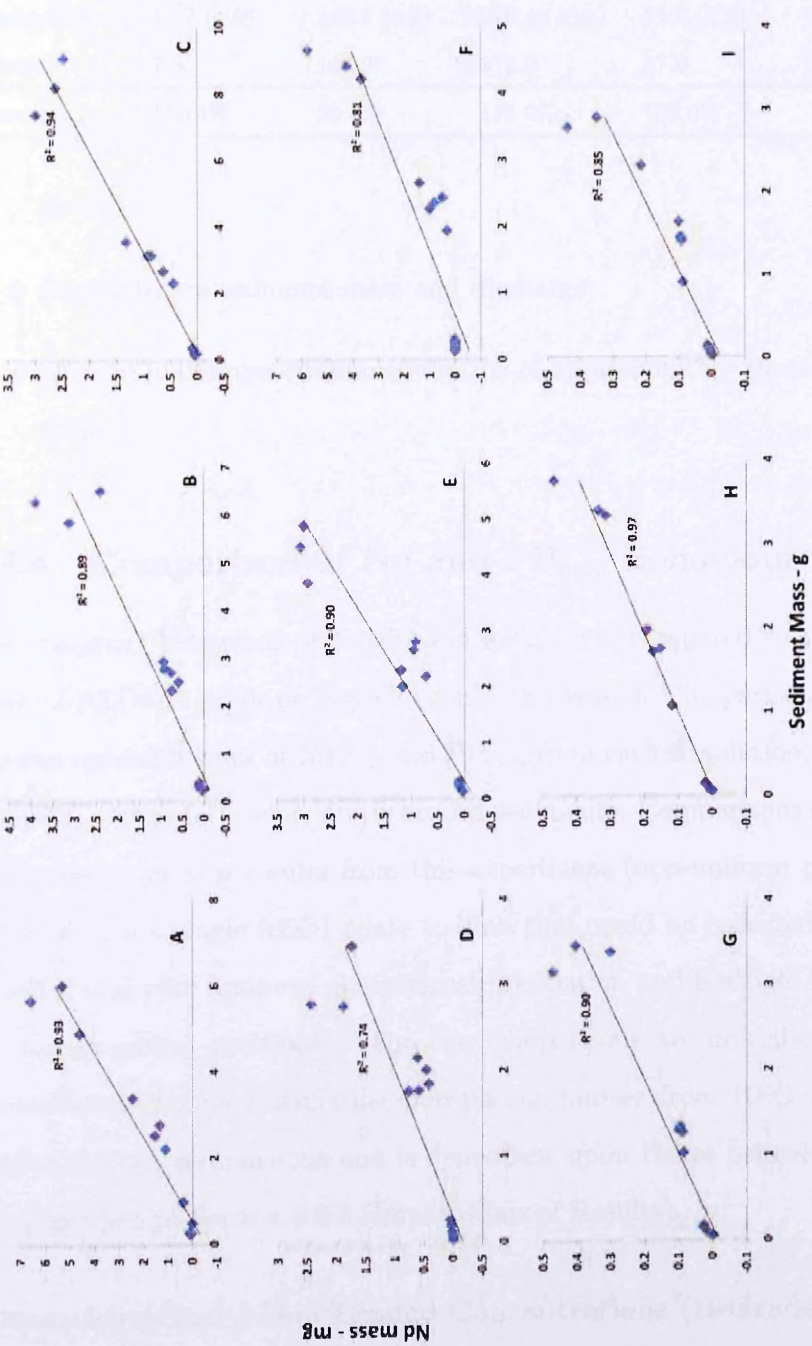

Figure 6.11: Scatter plots of total Nd mass from eroded sediment in surface runoff samples plotted against total sediment mass. Figures A-C, D-F and G-I represent triplicated simulations at slopes of 9%, 6% and 3% respectively.

Table 6.1: Extracted concentrations of lanthanoid elements from the certified reference soil. Standard deviations are shown in parentheses (n = 14 for each value).

	Gd	La	Nd	Pr	Sm
	REE Concentration ($\mu g.g^{-1}$)				
Extracted	11.7 (1.0)	148.4 (4.4)	250.4 (10.4)	61.6 (2.7)	23.4 (1.5)
Target	7.8	164.0	210.0	57.0	18.0
Percentage	150.4%	90.5%	119.2%	108.0%	130.2%

particles;

- Correlated to sediment mass and discharge;
- Showed maximum enrichment ratios of approximately three at 6% and 9% slope.

6.6.4 Comparison of Nd and PP_{map} Behaviour

The transport behaviour of Nd_2O_3 and PP_{map} was compared so that the tracing grade of REOs (A-grade or B-grade) could be assessed. Comparisons were made of: i) mean eroded masses of Nd_2O_3 and PP_{map} from each simulation, and; ii) Nd_2O_3 and PP_{map} transport behaviour in eroded sediments. Comparisons commence with a description of how results from this experiment (non-uniform phosphorus distribution and a single REO) relate to data that could be collected from a typical experimental plot (uniform phosphorus distribution and multiple REOs in different topographical positions). The two comparisons are described qualitatively. Quantitative tracing (estimating phosphorus masses from REO concentrations) applies to both comparisons and is dependent upon tracer behaviour; it is therefore described in Section 6.6.6 (Implications of Results).

Comparison One: Mean Eroded Concentrations (B-Grade)

Polyakov et al. (2004) measured the sediment loss from a 0.33 ha semi-arid watershed by applying different REOs to contrasting topographical positions and collecting runoff from the bottom of the watershed. In studies such as these it

is expected that when sediment loss from a tagged location increases, a greater mass of the corresponding REO is eroded. This allows the individual sediment loss from each tagged location to be shown from the corresponding REO concentration in eroded sediments. It would also be possible to show phosphorus loss from different tagged locations if the eroded masses of both REO and phosphorus rise as sediment loss increases. This will be demonstrated using the results of this investigation by comparison of the total loss of Nd and PP_{map} in surface runoff from different slopes.

Total eroded masses of both Nd and PP_{map} were calculated for each simulation by multiplying sediment mass by Nd and PP_{map} concentration for each sample and then summing the masses from all samples. Positive linear correlation was observed between the total eroded masses of Nd and PP_{map} (Figure 6.12). The significant correlation (p <0.05) demonstrates that REOs can be used to estimate the contribution of different tagged locations to total eroded phosphorus averaged from a runoff event. This is sufficient to state that B-grade tracing has been achieved.

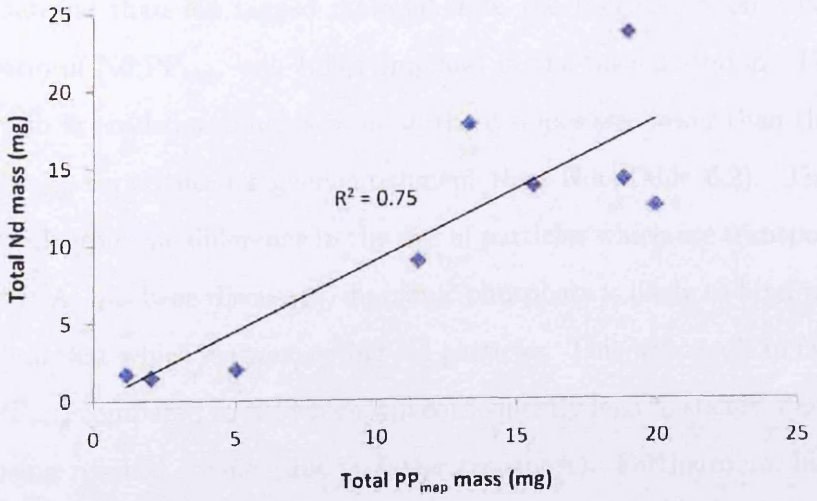

Figure 6.12: Scatter plot of applied particulate phosphorus (PP_{map}) mass plotted against Nd mass in eroded sediments. Each data point is calculated from the bulk eroded sediment sample from each replicated simulation.

Comparison Two: Transport Behaviour (A-Grade)

A further use of REOs as sediment tracers is to show the locations and origins of deposited sediments (such as the work of Michaelides et al. (2010) who investigated deposition processes of sediments using a 2.5 m × 6 m plot containing a break of slope), or to show the transport distances of sediment (such as the work of Stevens and Quinton (2008) who showed the distance over which soil material is transported into tramlines). Similar work, monitoring the transport of particulate bound phosphorus, could be performed using REOs. However, in order to provide accurate data it is important that the transport behaviour of REOs and the sediment transporting phosphorus is comparable. Preferential transport of either REOs or particulate phosphorus will cause poor replication of deposition locations and transport distances. Transport behaviour of REOs and particulate phosphorus will be examined using individual enrichment ratios of Nd and PP_{map} and the concentration ratios of Nd:PP_{map}.

The differences in mean and maximum enrichment ratios observed for Nd and PP_{map} (Table 6.2) indicate greater preferential transport of PP_{map} tagged material than Nd tagged material from the tagged section. The concentration ratio of Nd:PP_{map} was 1.69:1 (mg:mg) in the tagged section. The concentration ratio in eroded sediments from all three slopes was lower than this value because PP_{map} experienced higher enrichment than Nd (Table 6.2). This is believed to result from the difference in the size of particles which are transporting PP_{map} and Nd. As has been discussed, inorganic phosphate is likely to bind to finer sediments than that which is transporting Nd particles. This will result in faster transport of PP_{map} compared to Nd which will consequently lead to steady state concentrations being reached sooner (due to faster transport). Furthermore, higher enrichment ratios may be reached due to size selective transport causing eroded sediments to have finer particle size distributions than whole soil.

Figure 6.13, which shows the concentration ratio of Nd:PP_{map} for each sample collected, indicates that in the majority of samples the concentration ratio is below 1.69:1. The concentration ratio of the tagged section is indicated by the dashed

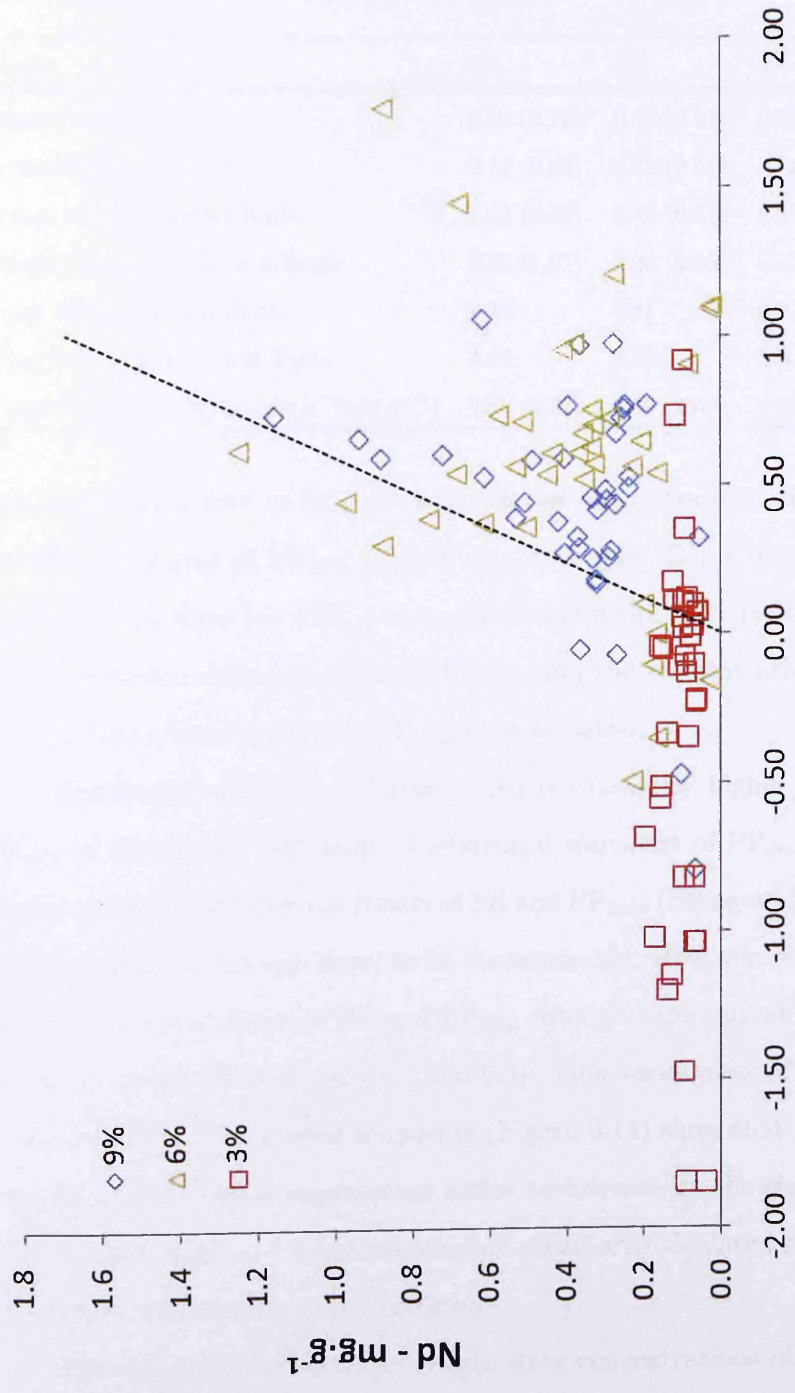

Figure 6.13: Scatter plot of Nd concentrations plotted against applied particulate phosphorus (PP_{map}) concentrations from tagged simulations at all slopes. The black hashed line represents the ratio of Nd to phosphorus concentrations in the tagged section prior to rainfall.

Table 6.2: Mean eroded concentrations, enrichment ratios and concentration ratios of Nd and applied particulate phosphorus (PP_{map}) in surface runoff from tagged simulations. Standard deviations are shown in parentheses. All values are taken from the average simulations calculated from the three replicates at each slope.

Slope	9%	6%	3%
Mean Nd ($mg.g^{-1}$)	0.39 (0.15)	0.39 (0.07)	0.09 (0.02)
Mean PP_{map} ($mg.g^{-1}$)	0.44 (0.26)	0.52 (0.41)	-0.33 (0.22)
Mean Nd Enrichment Ratio	1.42 (0.58)	1.42 (0.51)	0.34 (0.11)
Mean PP_{map} Enrichment Ratio	2.75 (1.61)	3.25 (2.55)	-1.19 (1.54)
Max Nd Enrichment Ratio	2.45	3.41	0.52
Max PP_{map} Enrichment Ratio	4.98	7.95	5.5
Mean Nd:PP_{map} Ratio ($mg.g^{-1}$:$mg.g^{-1}$)	0.80 (0.47)	0.69 (1.30)	-0.87 (4.64)

line, any data points to its right indicate low concentrations of Nd compared to the concentrations of PP_{map} in that runoff sample. Some data points collected from 3% slope show low PP_{map} concentrations for the reasons discussed in Section 6.6.2. However, data points correlated around the concentration ratio line once steady state concentrations of PP_{map} were achieved.

Enrichment of PP_{map} relative to Nd is caused by higher concentrations of PP_{map} in the eroded sediments. Preferential transport of PP_{map} tagged material does not cause concentration trends of Nd and PP_{map} (changes of concentrations in eroded sediments through time) to be incomparable. However, changes in the individual enrichment ratios of Nd and PP_{map} through time caused the concentration trends to visibly differ (Figures 6.5 and 6.8). Time series plots of the concentration ratios (Nd:PP_{map}) in eroded sediments (Figure 6.14) show that the rising concentrations of Nd cause concentration ratios to increase as the simulations proceed through time (high and low concentration ratios are calculated when either PP_{map} or Nd concentrations are close to zero).

The difference between the steady state concentrations observed for PP_{map} and the rising concentrations observed for Nd caused the Nd:PP_{map} concentration ratio to increase through time. This indicates that a proportion of the particulate material containing PP_{map} shows transport from the tagged section which is not

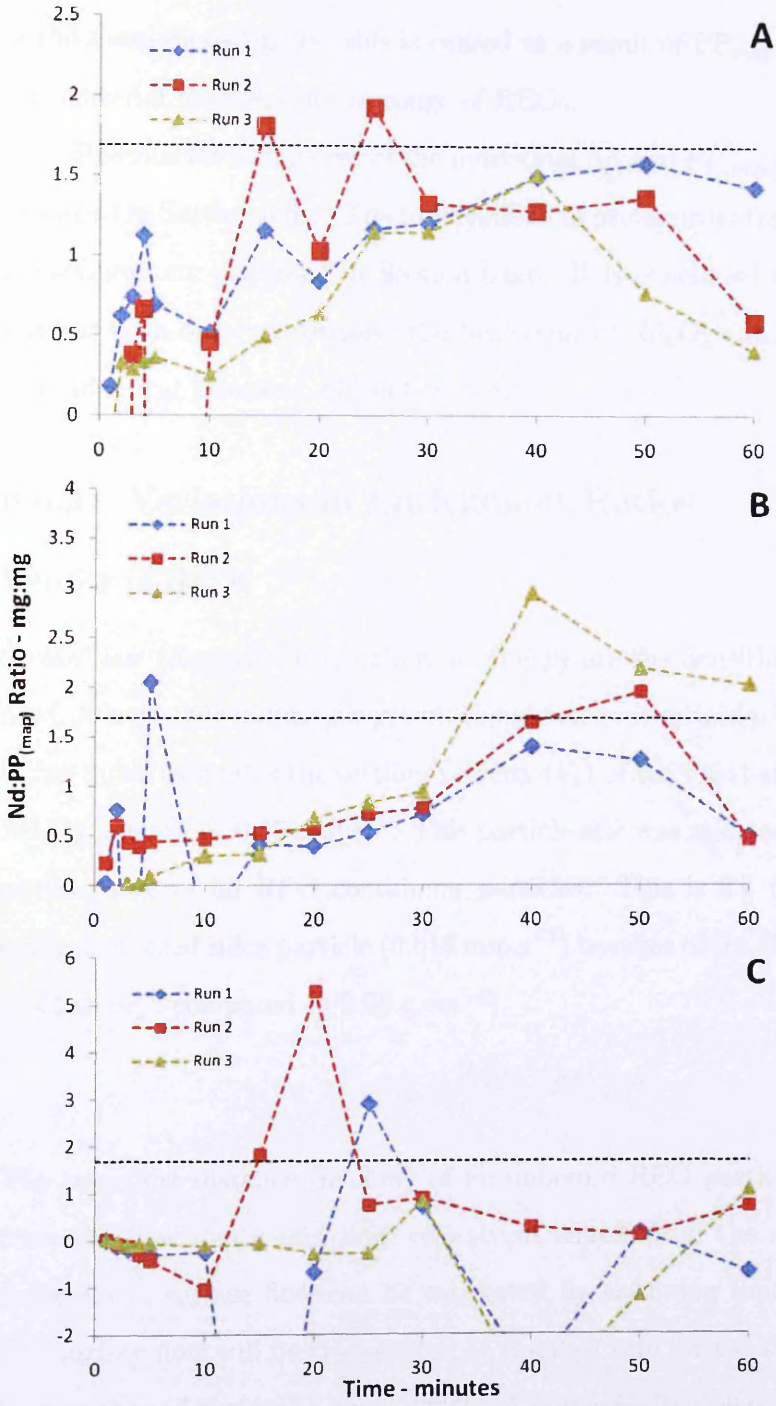

Figure 6.14: Concentration ratios of Nd to PP_{map} in tagged surface runoff samples plotted as a time series. The black hashed line represents the concentration ratio in the tagged section prior to rainfall. Data points with exceptionally high or low values (due to concentrations close to zero) have been omitted to avoid obscuring the trends. Figures A-C represent simulations at 9-3% slope respectively.

comparable to Nd tagged material. The high concentrations of PP_{map} at the start of the simulations suggest this is caused as a result of PP_{map} being transported in fine material outside the size range of REOs.

Reasons for differences of the individual Nd and PP_{map} enrichment ratios are proposed in Section 6.6.5. The implications of preferential transport of particulate phosphorus are discussed in Section 6.6.6. It is concluded that A-grade tracing has not been observed because the behaviour of Nd_2O_3 and PP_{map}, when eroded from identical locations, did not match.

6.6.5 Variations in Enrichment Ratios

Density of REOs

Stokes' law (Equation 6.1) (where p_p and p_f are the densities of the particle and fluid, R is particle radius, g is gravitational acceleration and μ is kinematic viscosity of the fluid) estimates the settling velocity (V_s) of the finest size (2 μm), unbound, Nd_2O_3 particle as 0.06 mm.s^{-1}. This particle size was selected as it has the lowest settling rate of all REO containing particles. This is 3.8 times faster than an equivalent sized silica particle (0.016 mm.s^{-1}) because of the REOs' greater density (7.42 g.cm^{-3} compared to 2.65 g.cm^{-3}).

$$V_s = \frac{2}{9}\frac{(p_p - p_f)}{\mu} g R^2 \tag{6.1}$$

The transport distance (in flow) of an unbound REO particle can be calculated from the flow depth and flow velocity of runoff from the soil box. Transport distances in surface flow can be estimated by assuming that particles mobilised into surface flow will be transported at the flow rate for the time it takes to settle back to the soil surface (Kinnell, 2002). A flow velocity of 0.67 cm.s^{-1} is calculated assuming a flow depth of 0.1 cm (flow width is 25 cm and steady state discharge was 1.67 cm^3.s^{-1}). Therefore, a 2 μm unbound REO particle will travel 10.6 cm before reaching the soil surface, while an equivalently sized silica particle will travel 41.9 cm.

The depth of flow was estimated, but transport distances do not change if

an increased depth is used. The calculated flow rate must increase when depth of flow is decreased because the discharge and flow width are constants.

The greater density of REOs will cause slower transport of a REO containing particle compared to the equivalent sized silica particle if the presence of REOs results in a higher settling velocity. This occurs because *'particles travelling by flow transport may travel at about the same velocity as the flow if they travel as suspended load, or at a lower velocity if they saltate'* (Kinnell, 2002).

Association with Fines

High concentrations of PP_{map} relative to Nd concentrations at the start of simulations may result from material transporting PP_{map} which is finer than material represented by Nd_2O_3. Zhang et al. (2001) showed uniform distribution of REOs in 11 aggregate size classes ranging from whole soil to < 0.01 mm, while Kimoto, Nearing, Zhang and Powell (2006) showed a preference for REOs to bind into 0.09 - 0.7 mm aggregates. This shows a strong affinity of REOs for silt and sand sized aggregates. Furthermore, Nd_2O_3 has a size range of approximately 2 - 38 μm. Therefore, soil material in the 0.45-2 μm size range which is not Nd_2O_3 will be transported at a higher velocity than all other Nd_2O_3 material due to lower settling velocities. A 2 μm REO particle has the same settling velocity as a 3.9 μm silica particle (see previous section); the 0.45 - 3.9 μm size fraction of sediment accounted for 15% of transported sediments collected between 5 and 10 minutes of simulations (Appendix E). Therefore, 15% of sediments (within the PP_{map} size range) are expected to travel faster than any REO containing particle.

Conversely, phosphorus shows a stronger preference to bind into fine sediment fractions (clays and silt). Syres and Walker (1969) classically demonstrated how inorganic phosphorus has concentrations orders of magnitude higher in the clay fraction of soils than the coarser fractions. Quinton et al. (2001) also showed how the phosphorus concentration in surface runoff from arable land is strongly correlated to the clay content of the runoff. Based upon these previous observations, the high concentrations of PP_{map} in runoff at the start of simulations

indicate that particulate material finer than the size range represented by REOs was transporting a fraction of the total PP_{map} eroded, and it was this that caused PP_{map} concentrations to rise faster than Nd concentrations.

6.6.6 Implications of Results

The B-grade tracing behaviour demonstrated by REOs (as a tracer of particulate phosphorus) allows qualitative assessment of phosphorus loss from locations experiencing different rates of sediment loss (Figure 6.12). This is possible because eroded masses of both REOs and particulate phosphorus have been shown to increase with slope. This tracing grade will also allow quantitative estimates of phosphorus loss from different tagged locations. If the mass of particulate phosphorus in sediment eroded from a range of tagged locations is quantified, then the mass of phosphorus eroded from individual tagged locations can be determined from the relative concentration of the corresponding REOs. Phosphorus may show enriched concentrations in eroded sediments compared to REOs. However, this would not affect quantitative estimates unless phosphorus loss from one tagged position was high and not reflected by the corresponding REO concentration. The linear correlation shown by eroded masses of Nd and PP_{map} indicates this does not occur at slopes of 3% or greater.

A-grade tracing behaviour of REOs was not observed. Particulate phosphorus showed higher enrichment ratios and different concentration trends in eroded sediments when compared to Nd_2O_3. This was explained by transport of a fraction of total particulate phosphorus in finer sediments then those represented REOs. A lack of A-grade tracing ability limits accuracy when estimating transport rates and redistribution patterns. Transport rates calculated from REOs will be inaccurate if particulate phosphorus eroded from a tagged location arrives at a sediment collection point prior to the corresponding REO. The location of particulate phosphorus deposition, following erosion from a tagged location, may not match that of the corresponding REOs if the sediment transporting the particulate phosphorus has a lower settling velocity or faster rate of transport. However, although REOs

may not reflect the transport of particulate phosphorus in very fine sediments, they will still have comparable transport to particulate phosphorus transported in the size range they do represent.

6.6.7 Applied Dissolved Phosphate (DP_{map})

Dissolved phosphate collected from blank simulations (DP_b) was consistently below instrumental detection limits (0.01 $mg.l^{-1}$) when analysed following the dilutions required to bring all other samples into the analytical concentration range (0.01 - 1 $mg.l^{-1}$). It was therefore reported as zero and not subtracted from dissolved phosphate collected from tagged simulations (DP_{map}).

All simulations showed a rising DP_{map} concentration in runoff during the first 0 - 10 minutes of the simulations, followed by a gradual decline in concentration (Figure 6.15). This can be explained from the behaviour of the DP_{map} matrix (surface water) and the two DP_{map} sources (the tagged section and sediments transported from the tagged section). Breakthrough was considered to have ceased when DP_{map} concentrations fell, followed by either: i) a further drop in concentration, or; ii) a rise in concentration less than twice the size of the initial concentration drop. Rising DP_{map} concentrations at the start of simulations are caused by the transport of DP_{map} from the tagged section to the exit point. Surface water leaving the soil box at the start of simulations originates near the exit point and therefore contains little, if any, DP_{map}. Surface water which originates from the tagged section (and upslope) reaches the exit point as runoff progresses, therefore the concentration of DP_{map} increases. Surface flow velocities increase with slope, therefore breakthrough occurs sooner at higher slope (2nd, 5th and 10th minutes (mean, closest sampling interval) for slopes of 9%, 6% and 3% respectively)(Figure 6.15). This is also shown by the rate of DP_{map} concentration increase during the first five minutes of the simulations (0.77 $mg.l^{-1}.min^{-1}$, 0.59 $mg.l^{-1}.min^{-1}$ and 0.42 $mg.l^{-1}.min^{-1}$ for slopes of 9%, 6% and 3% respectively).

Breakthrough does not occur during a single sampling interval because runoff which originates from the tagged section will have variable flow rates due to the

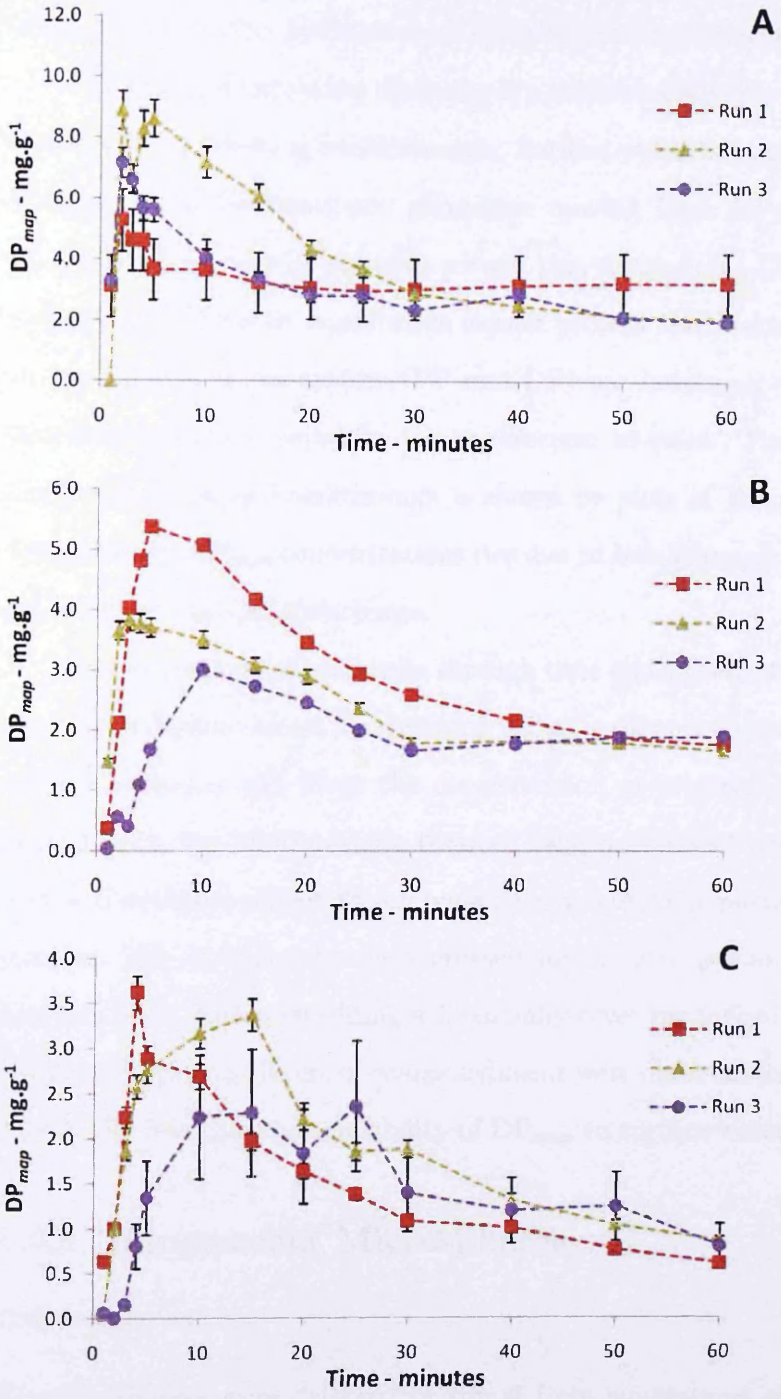

Figure 6.15: Concentrations of applied dissolved phosphorus (DP_{map}) in surface runoff samples collected from tagged simulations. Concentrations from blank simulations were not subtracted from these data as all concentrations were below detection limits and were reported as zero. Error bars are calculated from the error associated with triplicated measurements of the penultimate sample. Figures A-C represent simulations at 9-3% slope respectively.

existence of flow threads and preferential flow pathways (Dunkerly, 2004). The DP_{map} concentration peaks once all contributions have reached the exit point.

The effect of increasing discharge is a probable cause for the falling concentration of DP_{map} following breakthrough. Surface water increase will cause dilution of DP_{map}. Applied inorganic phosphate moving from the particulate phase to the dissolved phase will partially correct this dilution (Le Châtelier principle for equilibrium). However, equilibrium cannot prevent the dilution occurring because all components of the system (PP and DP) are becoming diluted, and because dilution may be too rapid for the equilibrium to react. The falling DP_{map} concentration following breakthrough is shown by plots of DP_{map} against discharge (Figure 6.16). DP_{map} concentrations rise due to breakthrough but fall once DP_{map} peaks due to the rising discharge.

The coarsening of sediments through time and the effects of surface shielding are other possible causes for declining DP_{map} concentrations. The coarsening of eroded sediments will lower the concentration of material finer than 0.45 μm. Furthermore, the interface area between tagged sediment and surface water will decline if sediment concentration remains constant while particle size distributions coarsen. This is caused by the increased surface area per mass unit as sediment becomes finer. Surface shielding will partially cover the tagged section in deposited sediment (deposited layers of coarse sediment were observed following simulations) potentially lowering the availability of DP_{map} to surface water.

6.6.8 Fluorescent Microspheres

Behaviour

No microspheres were detected in runoff from simulations at 3% and 6% slope despite basing the estimate of microsphere recovery (1%) on a comparable study. Samples were analysed for microsphere concentrations between each increase in gradient, therefore applied volumes were increased (from 0.5 ml to 2 ml to 4 ml for simulations at 3%, 6% and 9% slope respectively) and the time between microsphere addition and the start of the simulations was reduced (from 5 minutes

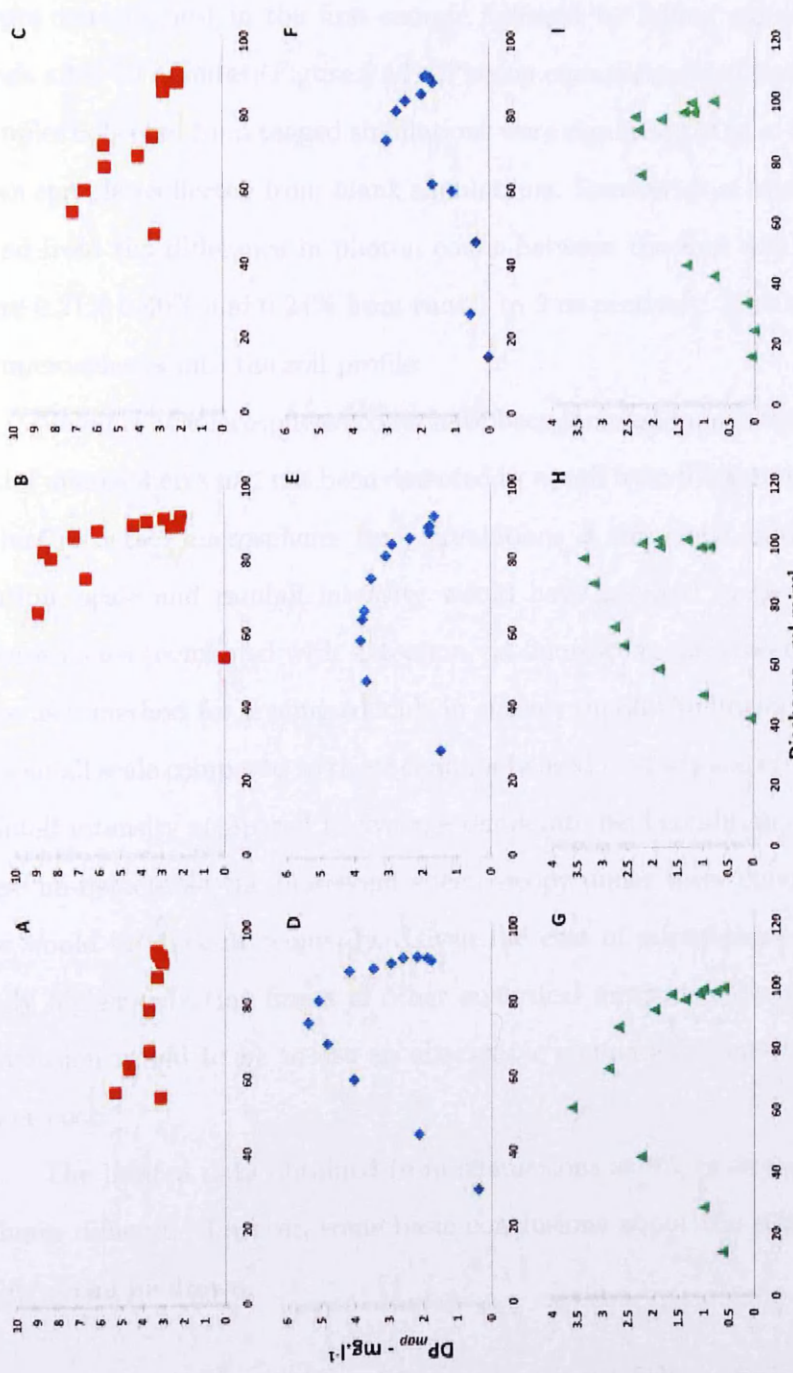

Figure 6.16: Scatter plots of dissolved phosphorus concentrations from tagged simulations (DP_{map}) plotted against discharge. Figures A-C, D-F and G-I represent triplicated simulations at slopes of 9%, 6% and 3% respectively.

to 1 minute to 30 seconds for simulations at 3%, 6% and 9% slope respectively) as the gradient was increased in order to aid detection.

Photon counts caused by the presence of microspheres in runoff from 9% slopes were highest in the first sample followed by falling values to background levels after 10 minutes (Figure 6.17). Photon counts recorded from the first runoff samples collected from tagged simulations were significantly ($p < 0.01$) higher than from samples collected from blank simulations. Recoveries of microspheres, calculated from the difference in photon count between the first and second samples, were 0.21% 0.40% and 0.24% from runs 1 to 3 respectively. This shows a high loss of microspheres into the soil profile.

Volumes of microspheres could have been increased until detection was achieved if microspheres had not been detected in runoff from 9% simulations. However, failure to detect microspheres from simulations at this slope, microsphere concentration, scale and rainfall intensity would have resulted in the conclusion that microspheres (combined with detection via fluorescent spectroscopy) were unsuitable as a method for tracing colloids in surface runoff. Microspheres were applied at a small scale compared to those commonly used to study soil erosion, with a high rainfall intensity compared to average temperate field conditions. If microspheres were un-detectable via fluorescent spectroscopy under these conditions then their use would be difficult to justify. Given the cost of microspheres and the potentially higher detection limits of other analytical methods (Chapter 4) the logical conclusion would to be to use an alternative enumeration method or a tracer of lower cost.

The limited data obtained from simulations at 9% makes grading of microspheres difficult. However, some basic conclusions about the suitability of microspheres can be drawn.

Comparison of Fluorescent Microsphere and DP_{map} Behaviour

The recovery of microspheres and concentrations of DP_{map} must show positive linear correlation for B-grade tracing to be achieved. However, this is not possible

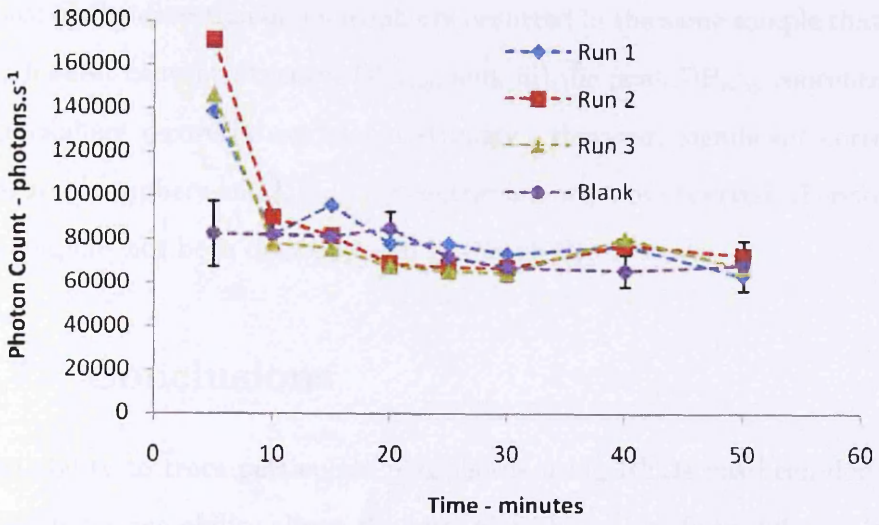

Figure 6.17: Photon counts resulting from the presence of microspheres in surface runoff from simulations at 9% slope. Error bars on blank data points represent the standard deviation of samples collected from triplicated simulations.

because microspheres were only detected at a single slope. Increasing the soil box gradient to 9% resulted in increased concentrations of DP_{map} in runoff and also resulted in microspheres being detected in runoff. However, changes were also made to the concentration of microspheres applied and the time between microsphere application and the start of the simulations. Therefore, increases in slope cannot be conclusively stated as a cause of increasing DP_{map} and microsphere concentrations because not all variables remained constant between simulations at different slopes.

It is possible to compare the peak concentrations of DP_{map} and microsphere recovery from the three simulations at 9% slope. This allows some indication of whether variations in soil box behaviour impacted DP_{map} and microspheres in a comparable way. Peak DP_{map} concentration and microsphere recovery correlated strongly ($r = 0.92$) indicating that higher recoveries of microspheres occurred when concentrations of DP_{map} were also high. However, due to the low number of data point ($n = 3$) this cannot be reported as a statistically significant correlation.

B-grade tracing is indicated due to three findings: i) the detection of microspheres occurred at the same slope that provided the highest DP_{map} concentra-

tions; ii) the detection of microspheres occurred in the same sample that contained the highest concentrations of DP_{map}, and; iii) the peak DP_{map} concentrations and microsphere recoveries correlated strongly. However, significant correlation between microsphere and DP_{map} concentrations was not observed, therefore B-grade tracing has not been demonstrated in this study.

6.7 Conclusions

The ability to trace particulate phosphorus using REOs has been demonstrated. B-grade tracing ability allows the total phosphorus loss from different locations of an experimental plot to be qualitatively and quantitatively determined. This is important as it allows the source and sink locations of particulate phosphorus to be determined. REOs have been successfully used as tracers of sediments in many studies. However, the results presented confirm that there is a strong correlation between the loss of sediments traced by REOs and the sediments transporting phosphorus. Effective tracing is a powerful tool for understanding erosion processes and development of methods which minimise sediment and nutrient loss. Therefore these findings confirm that REOs can be a useful tool for minimising nutrient loss from arable fields.

The results also highlight how the range of different sized particles which comprises soil material complicates the tracing process. The affinity of REOs to bind into silt and sand fractions of soil and their high density may prevent them from effectively tracing particulate phosphorus transported by fine clay material. However, particulate phosphorus is not solely transported by fine clay material unless only this size of material is eroded. Therefore, REOs are likely to show comparable transport behaviour to particulate phosphorus transported by coarse clays and silts.

The low recovery of microspheres prevented effective tracing of phosphorus finer than 0.45 μm, although evidence of B-grade tracing was observed. Consequently, a dual tracing method was not successfully developed. However, the results showed contrasting behaviour of phosphorus either side of the 0.45 μm size

divide. This highlights the need for multiple tracers representing different size ranges. Two things are required in order to develop the multi-phase tracing of phosphorus further; i) a more effective clay tracer; ii) a colloid tracer which exists in various sizes and with improved detection limits in surface runoff compared to microspheres.

Chapter 7

Field Experiment

7.1 Chapter Outline

A tracing experiment was conducted at a larger scale than the indoor simulations (Chapter 6) in order to test the use of REOs as tracers of phosphorus under field conditions. Fluorescent microspheres were not used to trace dissolved phosphorus (DP) due to the significantly lower recovery of microspheres expected from a field study (compared to the indoor simulations of Chapter 6) and the infeasibility of using a sufficient quantity of microspheres to allow detection.

Nd_2O_3 and mono-ammonium phosphate (MAP) were both applied to a 3 m $\times$ 6 m field plot (ploughed, bare soil) between February and June 2009. Surface runoff generated from natural rainfall was collected at four different locations at the bottom of the plot. This was followed by a surface sampling campaign to determine the redistribution of REOs and phosphorus.

7.2 Introduction

Utilising REOs for indoor and simulated sediment tracing studies has provided important data on sediment dynamics, corroborating our understanding of erosion processes (Zhang et al., 2003) and providing data suitable for model validation (Matisoff et al., 2001). However, REO tracing is also required from field studies in order to provide data from large uncontrolled systems (Polyakov et al., 2004; Kimoto, Nearing, Shipitalo and Polyakov, 2006). Therefore, it was necessary to demonstrate the comparability between the selected tracers and phosphorus (P) under field conditions, as well as under the controlled conditions applied in Chapter 6. However, tracing under field conditions also provided an opportunity to examine field tracing techniques.

Sediment tracing at larger scales and under field conditions increases experimental difficulty. This is not only an issue for REO sediment tracing, but for all sediment tracing techniques; the difficulty in applying any applied tracer to large scale plots is the reason that native tracers are preferred for tracing at the field and watershed scale (Section 3.2). The two main problems experienced during field tracing studies are that: i) we cannot ensure that precipitation of suitable intensity, energy or duration will be provided during the experimental period (tracing studies may well be limited by agricultural practice or project time constraints), and; ii) applying tracers to large scale plots (e.g. > 0.05 ha) increases in difficulty (logistical not methodological) as plot size increases.

Applications of REOs can be categorised by the proportion of the plot to which the tracers are applied and the application method used. Application sizes include point ($< 0.1\%$), partial area ($\approx 30\%$), and whole area (100%) applications (Liu et al., 2004; Kimoto, Nearing, Shipitalo and Polyakov, 2006; Yang, Song, Sui and Ding, 2008). Application methods include excavation, tagging & repacking (ETR) application (Yang, Wang, Sui and Ding, 2008) or the distribution of tagged material (TM) (Polyakov et al., 2004) which can be followed by tillage where permissible.

The size of area to which the REOs are applied is dependent upon the aims of

the experiment. Point applications have been used when precise data on the depth of erosion or transport distances of sediments has been required (Matisoff et al., 2001; Yang, Song, Sui and Ding, 2008; Yang, Wang, Sui and Ding, 2008). The depth of tracer incorporation has to be accurate, therefore ETR application was used. However, it is necessary to tag large areas of the plot (partial or whole area applications) when the aim of the experiment is to visualise sediment sources and transport pathways (Polyakov et al., 2004, 2009). The larger size of the area to be tagged excludes ETR application; instead TM must be distributed over the whole plot. This is labour intensive because the plot has to be sub-divided into smaller sections to ensure an even distribution of the TM over the whole area (Polyakov et al., 2004). Labour can be minimised by the use of mechanical distribution, i.e. fertiliser spreading equipment (Kimoto, Nearing, Shipitalo and Polyakov, 2006; Stevens and Quinton, 2008), but this is not always possible (Polyakov et al., 2009).

A primary function of TM is to provide a medium through which REOs can be applied. A higher uniformity of REO distribution on the plot may result if the formation of TM can be avoided. Spatial variability of REO concentrations caused by non-uniform TM application will be exacerbated unless the distribution of REOs in TM is perfect. Direct spraying of REOs onto experimental plots may provide a more uniform method of applying REOs. Experimental plots undergo tillage or wetting to help incorporate TM into the native soil (Polyakov et al., 2004; Kimoto, Nearing, Shipitalo and Polyakov, 2006); the differences between spraying and the use of TM should be minimal if the same processes are used following spray application.

The rationale for conducting this study was to examine the use of REOs as field tracers of phosphorus (P). A similar experiment to the one performed in Chapter 6 was therefore required, where an area of a plot is tagged with a REO and the concentration of inorganic P is increased. This experimental design allows the transport of both REOs and P out of the tagged section to be compared. It was desirable to increase the complexity of this experiment. The logical progression from the experimental design used during the indoor study, described in Section

6.3, was to increase the number of tagged locations. Each tagged location would be tagged with a different REO; this is common in sediment tracing studies where REOs are applied (Zhang et al., 2003; Stevens and Quinton, 2008). This would require that each location is tagged with a distinguishable source of inorganic P so that transport of REOs and P from each tagged location could be easily compared. This would allow the transport pathways and locations of deposition of P and REOs from different sources to be compared.

A more intricate experimental design, such as the one which has been described, would have provided a greater amount of data and have been more fitting for the culmination of the thesis. However, time constraints prevented a suitable method to distinguish different P sources from being investigated (e.g. applying P at different concentrations at different locations, distinguishable forms of P which have comparable transport behaviour to one another) prior to the start of winter 2008. Therefore, the decision was taken to use the same experimental design that was being used for indoor tracing experiments, but with spray application to investigate its suitability for field use. This provided a reliable method to collect basic data on the comparability of REO and P transport behaviour and also allowed for investigation of spraying as a field application method of REOs.

The investigation will attempt to answer three questions: i) does REO distribution following rainfall under field conditions match that of P; ii) do REO powders experience rapid, incidental loss when applied via spraying; iii) do redistribution patterns of REOs and PP match if weak REO to soil binding causes REO transport to be faster than sediments.

7.3 Materials

7.3.1 Field Site and Plot

A 134 m $\times$ 57 m area of un-grazed grassland at Hazelrigg research station (Lancashire, UK, (SD,4925,5780)) had been ploughed to investigate soil erosion processes. The field had an average gradient of 7.5%, and an aspect of 275°. A

3 m × 6 m (width × length) plot was selected for this tracing experiment, located in the south-west corner of the field 0.5 m in-field from a drainage ditch that ran the length of the field (Figures 7.1 and 7.2).

The plot was selected as it contained non-uniform surface roughness. The centre 0.6 m (Section C) of the plot contained a narrow (0.2 m) tramline. The left-hand 0.6 m (section A) and right-hand 1.2 m (Section D) sections of the plot contained no features but surface roughness comparable to Section C. The remaining 0.6 m (Section B) contained lower average surface roughness (see Figure 7.2). Four gerlach troughs (width 0.5 m) were dug into the bottom of the plot below each section (Figures 7.1 and 7.2). The gerlach troughs were connected to 30 L collection tanks located 3 m downslope and placed in a drained trench so that the connecting pipe had a constant negative gradient. The collection tanks and connecting pipes were acid washed prior to installation in the field. Drainage ditches (0.2 m wide and 0.2 m deep) were dug along the top and left-hand sides of the plot to prevent run-on from upslope entering the plot.

7.3.2 Rare Earth Oxides, Phosphorus and Soil

The same REO powder (Nd_2O_3) and phosphate source (monoammonium phosphate - MAP) used in Chapter 6 was selected (see Chapter 6 for full descriptions) in order to maintain continuity. The Hazelrigg soil was a silt loam comprising of 7.4% clay, 69.5% silt and 23.2% sand. The Nd concentration (9.5 $\mu g.g^{-1}$) was determined via the USEPA soil extraction and analysis using ICP-MS (see Chapter 6 for details). The total phosphorus (TP) concentration (569 $mg.kg^{-1}$) was determined by standard acid digestions and colourimetric analysis using a Seal AQ2+ discrete nutrient analyser.

7.3.3 Fluorescent Microspheres

The larger scale, lack of incidental runoff and presence of macropores and surface fissures would result in a higher volume of fluorescent microspheres being required to achieve detection than was used for the indoor simulations (Chapter 6). The

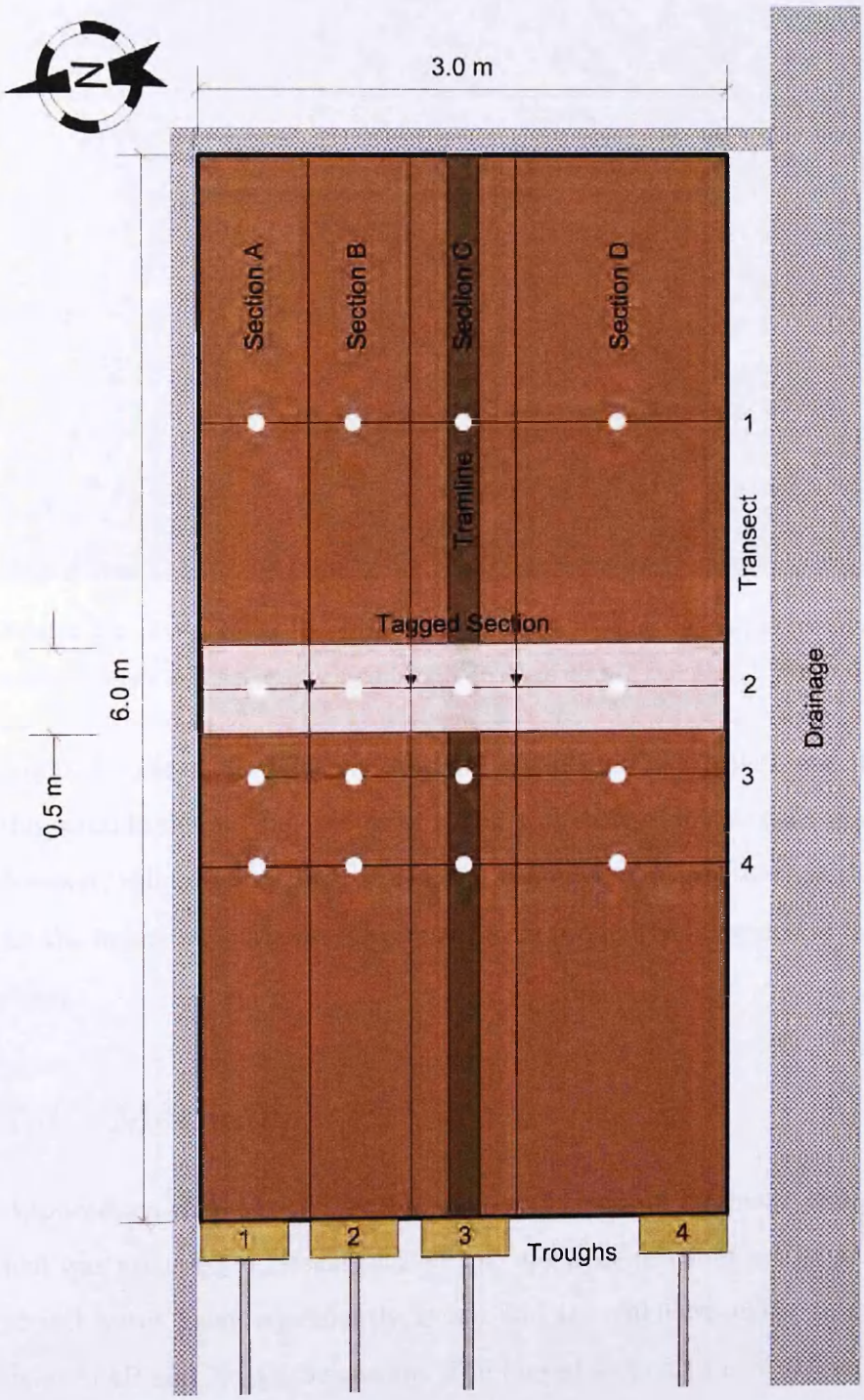

Figure 7.1: Diagramatic representation of the field plot at Hazelrigg research station. White circles mark the locations of surface sampling.

Figure 7.2: Field plot at Hazelrigg research station showing the central tram-line, the tagged section (visible as a lighter coloured band), drainage ditches and gerlach troughs.

required volume of microspheres would be difficult to calculate accurately due to the variable timing and volume of runoff and changes in soil macropore numbers; however, volumes were likely to be orders of magnitude greater than those required for the indoor simulations. This made them prohibitively expensive for use in this study.

7.4 Methods

Applications of MAP and Nd_2O_3 were performed on February 18th, 2009. The plot was prepared in December 2008 but applications could not be performed due to soil water being consistently frozen and the unknown effect this would have upon MAP and Nd_2O_3 behaviour. The tagged section (3 m $\times$ 0.5 m, Figure 7.1) was demarcated using cord suspended above plot. The mass of MAP required to increase the concentration of TP in the tagged area to ten times background concentrations to a depth of 5 cm (2.2 kg) was dissolved into the minimum volume of de-ionised water possible (7 L) to minimise the volume of water applied. The

tagged area was visually divided into three sections (1 m wide). Each section was tagged individually using one third of the MAP solution in a pressurised 5 L hand sprayer at a rate that avoided ponding of the MAP solution. Each section of the plot was passed with the sprayer a minimum of 100 times to ensure that the distribution of MAP was not affected by the variability of the spray rate.

Nd_2O_3 was applied via spraying. This method had been used by C. Deasy (Lancaster University, UK, personal communication) for field applications of REO powders to determine the contribution of different upslope positions on large (70 m $\times$ 5 m) experimental plots. The mass of Nd_2O_3 required to increase the concentration of Nd in the tagged area to 500 times background in the top 0.5 cm of the plot was dispersed in 5 L of deionised water and sprayed onto the tagged area in the same fashion as MAP solution. The concentration of REO in the tagged area was 4.8 $mg.g^{-1}$.

Two methods were used to compare REO and TP transport rates: i) concentrations in surface runoff, and; ii) redistribution on the plot. Runoff samples were removed from the collection tanks into acid washed sample bottles within 12 hours of collection. Surface samples were taken (September 18th) from transects running downslope to the gerlach trough, at 1.5 m, 3 m, 3.5 m and 4 m downslope from the top of the plot (Figure 7.1). Triplicate surface samples were taken at each sampling point (48 samples in total). A greater number of surface samples would have provided more information on REO transport. However, surface sampling was limited by the expense of REO analysis. All sediment and soil samples were digested via the USEPA digestion method (Chapter 6) and sent to the University of Plymouth (UK, Devon) for analysis via ICP-OES.

Surface cover was created when growth of annual broad-leaf weeds and grasses began during May 2009. Repeated mechanical removal of the cover to keep the plot clear was considered too likely to cause disruption or compaction of the soil and redistribution of tagged sediment. Chemical removal of vegetation presented the risk of herbicides competing for phosphate binding sites, as has been identified for glyphosphate (Gimsing and Borggaard, 2002; Gimsing et al., 2004) and car-

boxylic acid based herbicides (Lindegren and Persson, 2009, 2010). This may not have caused leaching of MAP derived phosphate from the tagged section, but may have resulted in lower MAP absorption downslope. Rainfall predictions for the preceding months were low, therefore the vegetation was left for the remainder of the growing season causing minimal disturbance to the plot and preventing runoff through surface cover. A single mechanical removal of vegetation was performed in early September 2009 allowing surface samples to be taken to determine REO and TP redistribution. This also gave the possibility of continuing the experiment through the following winter. No surface runoff was observed in runoff collection tanks during the months when vegetation was present on the surface of the plot.

7.5 Results and Discussion

7.5.1 Events and Runoff

Meteorological data (Figure 7.3) shows the daily rainfall and temperature during the experimental period (February 18th - May 30th 2009) with the events which resulted in runoff indicated. The figure also indicates the low temperatures prior to February 15th which delayed the commencement of the experiment. Total rainfall (230.9 mm) was lower than the long term averages (1966 - 1998) for this period (276.6 mm). Total hours of sunshine (724 h) and average minimum and maximum temperatures (6.9°C - 13.9 °C) were higher than the seasonal averages (614.1 h, 5.8°C, and 12.4°C respectively). The runoff volumes and sediment concentrations of samples collected from the events indicated in Figure 7.3 are shown in Table 7.1.

Runoff volumes were highest from Section C (apart from the March 10th event), demonstrating the channelisation and decreased infiltration rates caused by tramline features. Sediment concentrations showed little correlation with surface roughness or runoff volumes. Sediment concentrations declined during the experimental period, including the May 20th event which had the highest total rainfall and highest maximum rainfall intensity, while infiltration rates increased.

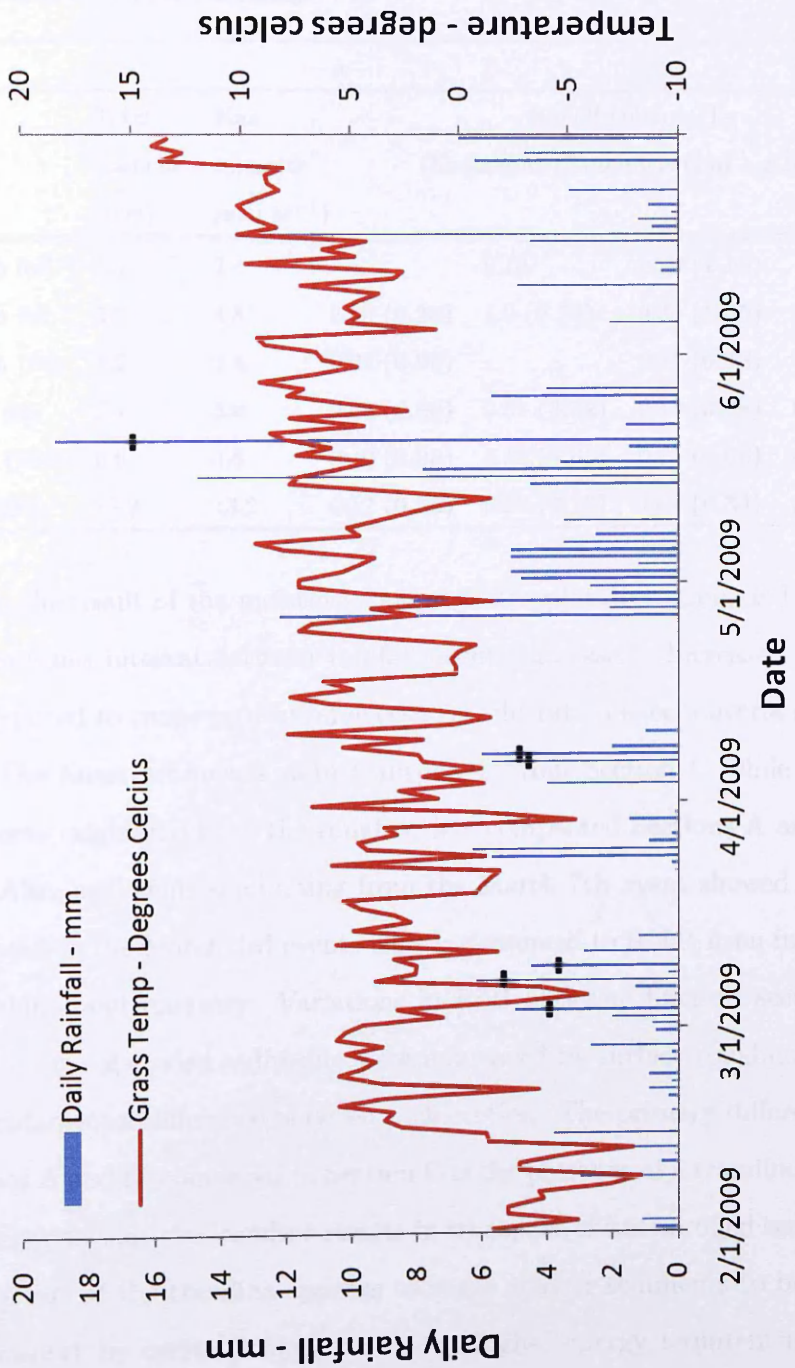

Figure 7.3: Daily rainfall and temperature data from Hazelrigg research station. Events from which runoff was collected are indicated.

Table 7.1: Runoff volumes and sediment concentrations from the Hazelrigg field site collected between March and June 2009. Rainfall intensities are taken from rainfall measurements collected at 10 minute intervals. Samples collected on March 7th were measured in-situ using volumetric apparatus so have a lower accuracy.

Tank			A	B	C	D
Date	Total Rainfall (mm)	Max Intensity ($mm.hr^{-1}$)	Runoff volume - l **(Sediment Concentration - $g.l^{-1}$)**			
March 3rd	4.4	2.4		0.10	0.39 **(1.19)**	
March 7th	5.8	4.8	2.60 **(0.28)**	4.0 **(0.74)**	9.30 **(1.05)**	2.70 **(2.32)**
March 10th	4.2	2.4	0.22 **(0.09)**		0.17 **(0.58)**	
April 6th	5.4	3.6	0.09 **(0.86)**	0.01 **(3.52)**	0.15 **(0.48)**	0.12 **(1.29)**
April 7/8th	6.6	4.8	0.10 **(0.00)**	0.10 **(0.00)**	0.25 **(0.08)**	0.13 **(0.00)**
May 20th	15.2	13.2	0.12 **(0.52)**	0.32 **(0.13)**	1.04 **(0.34)**	0.22 **(0.22)**

This is the result of the moisture content of the plot decreasing as both the temperature and interval between rainfall events increased. Increased precipitation was required to cause saturation excess, or infiltration excess overland flow.

The finest sediments were transported from Section C while the coarsest sediments originated from the rougher, less compacted Sections A and D (Figure 7.4). Also, sediments originating from the March 7th event showed a coarsening compared to the March 3rd event. This is presumed to result from increased rainfall volume and intensity. Variations in PSD between different sections suggest that the size of eroded sediments were influenced by surface roughness which was the fundamental difference between each section. The primary difference between Sections A and D, compared to Section C is the presence of a tramline. This therefore suggests that the tramline results in transport of finer eroded sediments. The compaction of the tramline appears to cause coarser sediments to be unavailable to transport by overland flow due to the higher energy requirements to detach soil from the compacted area. This occurred even though the tramline provided higher runoff volumes from this section (see Table 7.1). PSDs were only determined for samples from the first two events because subsequent events did not

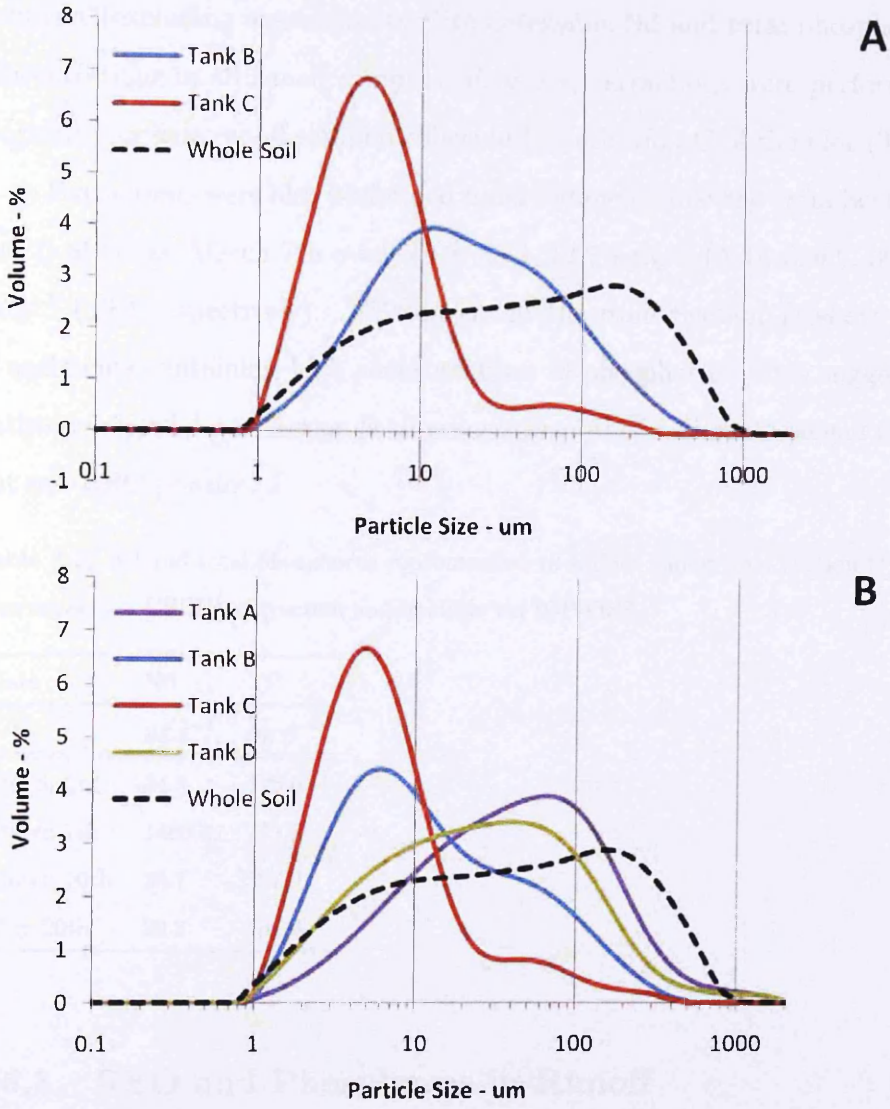

Figure 7.4: Particle size distribution data of surface runoff samples collected on a) March 3rd 2009 and b) March 7th 2009. Whole soil PSD was collected by A. Armstrong, using the same instrumental methods as all other samples, by dispersing whole soil in water and with no further dispersion method.

provide sufficient masses of sediment for PSD and REO analysis.

7.5.2 REO Transport

All samples analysed for Nd concentration were digested and analysed in the same sample batch as the surface runoff samples detailed in Chapter 6; therefore, all values have been corrected for instrumental interference. There was insufficient

sediment (excluding organic matter) to determine Nd and total phosphorus (TP) concentrations in all runoff samples. However, extractions were performed upon four dried surface runoff samples collected from Section C of the plot (Table 7.2).

Extractions were also performed upon sediment collected from Sections A, B and D after the March 7th event (9.9, 35.3, 12.7 $\mu g.g^{-1}$ (Nd), 329.9, 393.9, 1341 $\mu g.g^{-1}$ (TP) respectively). TP concentrations from Section D show transport of sediments containing high concentrations of phosphorus. This suggests a flow pathway existed down Section D allowing transport of sediments tagged with MAP, but not REO powder.

Table 7.2: Nd and total phosphorus concentration in surface runoff from Section C (tramline), determined via USEPA extraction and analysis via ICP-OES.

Date	Nd	TP
	$\mu g.g^{-1}$	$\mu g.g^{-1}$
March 3rd	34.3	316.0
March 7th	1465.3	781.2
March 10th	28.7	587.9
May 20th	29.3	494.8

7.5.3 REO and Phosphorus in Runoff

Both Nd and TP concentrations of sediments from Section C spiked during the March 7th event (Table 7.2). This indicates that a source of Nd_2O_3 powder was available for immediate transport from the tagged section, but that this source was discrete in nature, removed from the tagged area in a single event and not succeeded by similar concentrations of unbound Nd powder. The total mass of Nd powder collected only constituted 0.2% of the applied REO powder into the tramline. The coinciding of Nd and TP spikes shows good comparability between REO and TP transport behaviour. No concentration increases of the same magnitude were observed from any of the other three sections suggesting that particle transport was attenuated by surface roughness.

The particle size range which transported Nd powder and P could not be

identified because of the labile movement of inorganic P between different particles and into solution, and also the sediment disaggregation processes which occur when tagged sediments were stored in collection tanks. However, the PSDs from Section C (Figure 7.4) showed finer particle size distribution than sediments in runoff from the other three sections. The removal of weakly bound REO powders is reported in the majority of REO tracing studies, including field experiments (Kimoto, Nearing, Shipitalo and Polyakov, 2006; Polyakov et al., 2009) and the studies reported in Chapter 6. This suggests that the transport behaviour of Nd powder, either removed from aggregates or bound to silt sized aggregates, is comparable to inorganic phosphate transported in clay and silt fractions. However, as has been stated, this cannot be definitively proven.

7.5.4 REO and Phosphorus Redistribution

The surface samples showed little movement of Nd or phosphorus downslope from the tagged section (Table 7.3). The lack of Nd powder in the tramline at 0.5 m and 1 m downslope from the tagged section again indicates that the spike in Nd concentration on March 7th was not the beginning of a wave of unbound Nd powder, but a single removal of unbound REOs. The concentration of Nd in the tramline of the tagged section was not depleted to background concentrations, showing that the spike in Nd in eroded sediment was not caused by complete removal of all applied Nd to the tramline. Therefore, some binding strength between Nd powder and soil aggregates when REOs are applied by spraying is indicated by the short transport distance (≤ 0.25 m) of the Nd powder.

One sample taken from Section D in transect three showed increased levels of both Nd (70.8 $\mu g.g^{-1}$) and TP (280.6 $\mu g.g^{-1}$) which were significantly higher than the average concentration of Nd (28.35 $\pm$ 9.11 $\mu g.g^{-1}$) and TP (192.4 $\pm$ 22.3 $\mu g.g^{-1}$) for that transect (Table 7.3). This again indicates some comparable transport behaviour between Nd and P.

Table 7.3: Concentrations and co-efficients of variation (CVs) of Nd and total phosphorus taken from the surface of the Hazelrigg plot (n = 3 for all values). Sampling locations are shown in Figure 7.1

Section	A	B	C	D	A	B	C	D
Distance from head of slope	Nd concentration - $\mu g.g^{-1}$				TP concentration - $\mu g.g^{-1}$			
1	18.3	17.0	14.6	13.2	193.9	207.3	197.7	161.9
2	368	780.8	1757.7	1762.7	853.47	822.2	920.3	889.4
3	28.9	18.7	18.4	35.0	188.2	170.9	186.5	223.7
4	20.0	17.3	13.8	14.5	172.1	180.5	162.0	192.5
Distance from head of slope	Nd concentration - CV				TP concentration - CV			
1	31.1	12.8	8.5	4.3	5.0	2.4	3.2	10.6
2	57.8	85.1	32.5	63.5	14.6	3.2	4.0	3.6
3	10.5	18.8	6.8	69.7	1.0	5.7	4.4	22.1
4	29.2	7.3	8.6	5.5	2.9	3.4	2.9	6.2

7.5.5 Spray Application

The application of solutions (MAP) via spraying appeared to provide a suitably uniform method with low co-efficients of variation (CVs) for applied concentrations in the tagged section (6.35% average in the tagged section, see Table 7.3), showing the spraying method was reproducible. However, the average CV of Nd_2O_3 in the tagged section was far higher (59.7% average). This may result from non-uniform transport of REOs out of the tagged section or the settling of REO powders into depressions during rainfall. A visible feature of spray application was the settling of applied suspensions into surface depressions where it became concentrated (Figure 7.5). Concentration of powder in such depressions is the likely source of the poorly bound REO powder detected at the base of the plot after the March 7th event. This may also contribute to the higher variation of REO distributions in the tagged section. This process is less likely to occur with phosphorus as it chemically binds to soil.

The co-efficients of variation reported by Kimoto, Nearing, Shipitalo and

Figure 7.5: The tagged section of the Hazelrigg experimental plot following REO application showing the movement of applied REO suspensions into surface depressions.

Polyakov (2006) ranged between 21% and 43% for TMs applied using a seed spreader and following disking. Comparisons are hard to make as uniformity measurements are dependent upon the size of sub-samples taken. Furthermore, no disking was applied to this plot which should increase REO uniformity. Disking will improve REO uniformity by increasing soil surface homogeneity, therefore REO application via spraying may provide comparable uniformity to the use of TM. However, the percentage improvement in uniformity provided by disking is unknown.

The variability of REO distribution following application via spraying may preclude its use as a standalone application method for REO field studies. However, some evidence of REO to soil binding was shown by the limited transport distance of REOs (Table 7.3), despite the removal of a small proportion of applied REOs from the plot (Table 7.2). Therefore spray application may be a possible method for field scale tagging if followed by tillage. Differences in the REO to soil binding strength and REO uniformity should be minimal following tillage, regardless of whether spraying or TM is used for REO application. Therefore, spraying may be preferable as there is no requirement to form the TMs (a potential source of non-uniformity).

7.5.6 Influence of Rainfall Variability

Total rainfall during the available experimental period was lower than the seasonal average. Rainfall events which resulted in significant redistribution of sediments upon the experimental plot were lacking. This highlights the impact of unpredictable rainfall upon the success of field experiments. Despite the lack of tracer and phosphorus movement on the plot, useful data was collected on the transport of weakly bound REOs. However, extensive redistribution of both REOs and phosphorus would have been desirable.

7.6 Conclusions

Three questions were to be answered by this experiment: i) does REO distribution following rainfall under field conditions match that of P; ii) do REO powders experience rapid, incidental loss when applied via spraying; iii) do redistribution patterns of REOs and PP match if weak REO to soil binding causes REO transport to be faster than sediments.

The patterns of REOs and P redistribution showed some comparability, but the usefulness of this data was limited by the minimal erosion caused by low rainfall. It has been shown that a proportion of REOs experience rapid incidental loss when applied via spraying, where poorly bound REOs are washed away from the tagged area. However, this only constitutes a small percentage of applied REOs, and the lack of tillage following the application may have caused increased incidental loss. Furthermore, poorly bound REO powder was transported down the same pathways as phosphorus, at comparable rates. Despite the lack of REO movement on the plot, some preferential flow pathways of phosphorus were replicated by REO transport.

The lack of movement of REOs from the tagged section following 231 mm of rainfall shows that the majority of REOs did not experience rapid transport. However, if greater erosive force was applied to the plot a large variation in the transport of REOs and P may have been observed. The limited data collected prevents firm conclusions from being drawn. The rapid transport of unincorporated REO powder provides an opportunity to gain qualitative data on sediment and phosphorus transport pathways. The methods (spraying and use of tagged material) should be comparable in regards to uniformity of REO distribution and REO to soil binding strength if tillage is used to incorporate applied tracers. It may also be possible to incorporate REOs via tillage, and then subsequently apply an unincorporated layer of a different REO to provide data from rainfall events of lower intensity. This may further increase the usability of REOs as sediment/phosphorus tracers and overcome difficulties related to variable rainfall rates.

Chapter 8

Summary and Conclusions

8.1 Main Findings (Description and Implications)

The main findings of this thesis will be described. This also allows the originality of the thesis and the contributions to existing knowledge, which result from the main findings, to be identified. It is highlighted when the findings relate to specific aims or objectives of the project. The first three objectives were completed in Chapters 2 and 3 and are not referred to in the description of the main findings.

8.1.1 B-Grade Tracing of Particulate Phosphorus

The transport of REOs and particulate phosphorus was compared for the first time in this thesis (Objective 5). The results reported in Chapter 6 demonstrated a strong correlation between the total eroded masses of a REO powder and phosphorus bound to sediments larger than 0.45 μm. Higher masses of both REO powder and phosphorus were transported from the soil boxes as the gradient was increased. This demonstrated that increased masses of both REOs and particulate phosphorus are eroded when the energy of surface runoff is increased, and resulted in REOs being classed as a B-grade tracer for particulate phosphorus. The comparison of a particulate tracer to particulate phosphorus was a component of the fifth objective of this project.

Although REOs are proven tracers for sediments, and sediments are the main carrier of phosphorus, a direct link between REO and particulate phosphorus transport had not previously been demonstrated. This study has proven that there is comparability between REOs and the sediments which transport phosphorus. As a result, REOs can now be used to qualitatively and quantitatively identify the predominant sources of phosphorus from arable land in the same fashion as they have been used to investigate sediment sources (Stevens and Quinton, 2008). This is useful for the development and assessment of mitigation techniques for soil erosion and nutrient transport such as minimal tillage, contour ploughing and boundary strips. This thesis has therefore helped develop a method which can aid in minimising the occurrence of eutrophication caused by diffuse pollution from

arable land.

8.1.2 A-Grade Tracing of Particulate Phosphorus

This thesis also provided the first detailed comparison of REOs and particulate phosphorus behaviour (Chapter 6), comparing individual enrichment ratios and concentration trends in eroded sediments for both Nd_2O_3 and particulate phosphorus (Objective 5). This comparison identified that particulate phosphorus was initially transported at higher concentrations than REOs, but that these concentrations maintained steady state. This contrasted with Nd_2O_3 which experienced breakthrough at lower concentrations but showed constant rising concentrations. This was explained by the ability of phosphorus to bind to sediments outside the size range of Nd_2O_3, and by the density of REOs which may slow their transport in surface runoff when compared to equivalent sized silica particles. This novel finding will be important when using REO particles to investigate the transport of particulate phosphorus. The transport of particulate phosphorus in finer sediments may lead to differences in locations of deposition and transport rates when compared to REOs. It is important to be aware of this difference in transport behaviour to avoid drawing inaccurate conclusions regarding particulate phosphorus transport. However, although a fraction of the sediment responsible for the transport of particulate phosphorus is not traced by REOs, a large range of particle sizes are. Therefore, the transport of REOs will reflect the transport of particulate phosphorus in the REO size range.

8.1.3 Spray Tagging of REOs for Field Use

The application of REOs to field plots via spraying has not been published and, to our knowledge, has only been performed by C. Deasy (Lancaster University, UK, personal communication). The spray application of REOs outlined in Chapter 7 (which completed Objective 6) was therefore only the second field application of REOs via spraying and the first time REOs have been compared to the transport of phosphorus on a field plot.

Only one sample from the soil surface downslope from the tagged section contained REOs or phosphorus at concentrations higher than background concentrations despite the plot receiving 230.9 mm of rainfall during the experimental period. Concentrations of Nd and phosphorus peaked in surface runoff collected from the same event suggesting comparability between transport rates of rapidly transported REOs and phosphorus. Both of these observations demonstrated sufficiently strong binding of REOs to soil when applied via spraying and also comparability between the physical pathways via which REOs and phosphorus were transported. The mass of REO recovered comprised only 0.2% of applied REO powder, showing loss of a small percentage of applied REO from the tagged area as has been detailed in other studies.

Providing evidence of sufficient REO to soil binding following spray application has important implications for the future use of REOs as a field scale tracer of sediments and phosphorus. The use of spray applications circumvents the need to form tagged material which is subsequently distributed upon the experimental plot. Furthermore, it is possible to use tillage to incorporate REOs into the soil profile so that the duration of experiments can be increased compared to surface only applications of REOs. This mixing process may also improve REO to soil binding. Applications of liquids to arable land can be performed using agricultural spraying equipment which can easily be calibrated to achieve the required application rates. Spray application using agricultural equipment increases the range of scales over which REOs can be applied and therefore increases the potential uses of the tracer. Increased scales of application could result in REOs being an alternative to the fingerprinting techniques described in Chapter 3.

8.1.4 Microsphere Use in Surface Runoff

At the date of writing it is believed that there are no published studies where fluorescent microspheres have been used as a colloid tracer in surface runoff from arable fields. Furthermore, there are also believed to be no publications to date where fluorescent spectroscopy has been used to enumerate fluorescent microspheres from

surface runoff samples. The development of methods to separate microspheres from both particulate and dissolved material (Chapter 5, Objective 4) and the use of microspheres to trace the greater than 0.45 μm fraction of phosphorus (Chapter 6, Objective 5) identified that microspheres are unsuitable as a tracer for colloids in surface runoff when paired with enumeration via fluorescent spectroscopy. This resulted from the low recovery ($< 1\%$) of microspheres, even at a small scale where microspheres were applied immediately prior to runoff commencing, and the high fluorescent background of surface runoff due to the presence of dissolved and particulate organic matter.

Although the development of the tracing method was not successful, it has provided an important development step for the tracing of colloids in surface runoff. Microspheres are known to make good tracers for infiltration studies of colloids into soils (see Chapters 2 and 3). These studies typically use epi-fluorescent microscopy to enumerate microspheres. The use of fluorescent spectroscopy has been applied to many studies using microspheres in 'clean' silica or artificial porous systems due to its fast and sensitive detection of fluorophores. However, it is now known that it is an unsuitable method for enumeration of microspheres in surface runoff samples. This will allow future development of colloid tracers for surface runoff to focus on either alternative enumeration methods for microspheres, or an alternative tracer.

8.1.5 Development of a Dual Tracing Method

The second and third aims of this thesis were to develop a combination of tracers which would allow tracing of sediments larger and smaller than the arbitrary 0.45 μm threshold and to identify the usefulness of the developed methodology for tracing phosphorus. This combination of two different tracers for sediments in surface runoff was novel. The development was not successful due to the problems of detecting microspheres in surface runoff using fluorescent spectroscopy. However, the differing behaviour of phosphorus larger and smaller than 0.45 μm shown in Chapter 6 is further evidence of the need to combine tracers which represent different size ranges. Furthermore, the findings of the thesis which have been de-

scribed in Section 8.1 will aid the future development of multiple tracer techniques for sediments in surface runoff (Section 8.2).

8.1.6 Classification of Tracer Grade

Not all publications using tracers have been examined for the presence of a classification system for tracers due to the high number of scientific disciplines which use tracing methodologies. However, the development of a grading system for different tracers based upon their performance appears to be either novel or uncommon. Tracers were divided into A-grade and B-grade dependent upon their ability to represent the characteristics of their chosen analyte. Classification of tracers in this manner allows easier selection of a tracer based upon the requirements of the experiment. Although the grading has only been used to show two types of behaviour, the system could easily be developed to represent a greater range of behavioural characteristics.

8.2 Continuation of Tracer Development

This project has highlighted the requirement for tracers which can represent a large range of particle sizes. REOs are known to represent a range of particle sizes by binding with differently sized aggregates (Zhang et al., 2001; Kimoto, Nearing, Shipitalo and Polyakov, 2006). However, when compared to the transport of particulate phosphorus (which was expected to be transported in the clay and fine silt fraction) it was shown that they could not physically represent the transport of very fine sediments. This resulted in REOs being deemed a B-grade tracer of particulate phosphorus only. It has to therefore be assumed that the majority of other tracers reviewed (Chapter 3) would have given a poorer representation of the transport of particulate phosphorus.

The conclusion from Chapter 6 was that a third size of sediment tracer is required, smaller than the silt and sand range represented by REOs, but larger than the colloid size range represented by fluorescent microspheres. This gives two

options for the continuation of particulate phosphorus tracing:

- Develop a third size of sediment tracer which bridges the gap between REOs and fluorescent microspheres
- Develop a new tracer which can effectively represent all particle sizes from 0.45 to 2000 μm.

It may be possible to continue the use of rare earth compounds to bridge the gap between REOs and colloid tracers. Matisoff et al. (2001) demonstrate the binding of soluble rare earth salts to sediments. This method could be used to tag just the clay fraction of sediments in order to provide a unique rare earth tracer. The number of rare earth elements available would allow different REEs to be placed in different topographical positions and bound to different sizes of sediments. A second option would be the grinding of REO powders into the desired size range and using them without mixing them into soils. Other alternatives are the use of magnetic iron oxides ground to the desired size range or the modification of the magnetic properties of clay particles, both of which are methods presently being researched (A. Armstrong, Lancaster University, UK, personal communication) (G. Guzman, Instituto de Agricultura Sostenible, Spain, personal communication). Either of these methods could be used as a direct replacement or complimentary method for REO tracing if they could be used to trace sediments below the REO size range.

A second conclusion from Chapter 6 was a need for a successful colloid tracer. Similarly to REOs, this could either be achieved by modification of the methods developed in this thesis or by use of a different tracer. Epi-fluorescent microscopy has been used to enumerate microspheres from soil samples and may therefore provide a more effective method of overcoming the high background fluorescence of surface runoff. However, the majority of the studies using microspheres have investigated the infiltration of microspheres, not transport in surface flow. The low recovery of microspheres in surface runoff from soil boxes ($< 1\%$) suggests that an alternative tracer which can be applied in much higher quantities would

be required for field use. A number of colloid tracers were reviewed in Chapter 3. However, the majority of reviewed tracers were either manufactured or modified. This increases the difficulty of applying large numbers of tracers. The option with the most potential as a field scale surface runoff colloid tracer is the application of a large mass of material which is not present on the experimental plots, such as organic macromolecules or bacteria.

Furthermore, greater success in field scale tracing may be achieved by timing the application of colloid tracers to coincide with rainfall which will generate runoff. This would minimise the loss of tracers into the soil profile during both the initial application and subsequent rainfall events which do not transport the tracers from the tagged location.

The time spent on ensuring that the rainfall simulator, experimental design and experimental setup would produce reliable data (Chapter 6) left time to only conduct the indoor simulations upon one soil. Soil texture, specifically the clay and silt content of soils, will be an important influence upon the transport behaviour of phosphorus. Therefore, it is desirable to compare the behaviour of REOs and particulate phosphorus upon soils of different textures. However, the results of Chapter 6 showed a distinct difference in the transport behaviour of REOs and phosphorus. This result is unlikely to be reversed by a change in soil texture.

The field experiment (Chapter 7) was limited by the lack of rainfall which caused limited movement of both REOs and phosphorus on the plot. Also, it was not possible to use fluorescent microspheres at the field scale to trace dissolved phosphorus. Therefore it is also desirable to conduct further comparisons of REOs and phosphorus at the field scale with the use of a suitable colloid tracer.

8.3 Closing Remarks

The tracing of sediments and phosphorus results in an improved understanding of transport processes. This aids in minimising the impacts of diffuse pollution described in Chapter 2. This project has improved the knowledge relating to two separate tracing methodologies and demonstrated how the methodologies could

be used in tandem to trace multiple size fractions of phosphorus. Therefore, it is hoped that this thesis, and publications resulting from it, can aid in the future development of effective tracers for sediments and phosphorus, and that this research can play a small part in reducing the impacts of diffuse pollution.

Appendix A

Rainfall Simulator Setup

A.1 Initial Investigation

Images and a description of the simulator are presented in Section 6.4.6. There was no detailed, documented information available for the operation of the rainfall simulation when the work of Chapter 6 was started. Initial investigation of the rainfall simulator resulted in some basic improvements. Both the simulator and the mesh screen were levelled. A quick release, adjustable fastening system was used to allow quick removal and adjustment of the mesh screen. The footprint of the rainfall simulator was marked on the floor. The water inlet tubing was fixed to the base of the simulator trough to minimise turbulence from inflowing water. Bent or damaged needles were replaced.

A standard operating procedure was developed:

1. The water flow is turned on and used to rinse the base of the simulator to remove any deposited material.

2. The simulator is locked into the upright position with the overflow set in the higher position, and filled until water reaches the overflow.

3. Air-locked needles are freed by drawing water through the needles using a syringe.

4. The overflow gate is removed if the lower overflow position is required.

5. Needles which are air-locked when under the lower head of water are freed (see point three).

6. Following completion of rainfall the simulator is emptied and stored with the trough in the down position to prevent build up of dust or debris.

Water was supplied to the simulator through either the water mains or from a RIOS 100 millipore de-ioniser. Water from either source was fed into the simulator via output pressure, with no addition pumping mechanism.

A.2 Uniformity

The uniformity of rainfall distribution was calculated using the Christiansen Uniformity Co-efficient (CUC):

$$CUC = 100 \times (1 - \frac{A}{B}) \tag{A.1}$$

where A is the average absolute deviation from the mean and B is the mean value for each container. A series of containers (diameter = 6.5 cm) were placed in a 3 x 7 grid under the rainfall footprint of the simulator. The cups were distributed over the same footprint area a soil box used for simulations (25 x 50 cm). The rainfall collected for 30 minutes and the volume calculated. Uniformity co-efficients were initially calculated when 30%, 50% and 75% of needles were blocked. Uniformity co-efficients were also calculated when the mesh screen was removed to identify the influence of the screen on uniformity (Table A.1).

The uniformities were high, all equal to or larger than 80% indicating that spatial uniformity of rainfall was more than sufficient (Bliesner and Keller, 2001)(Table A.1). The presence of the screen resulted in a significant improvement in spatial uniformity of rainfall. This indicated that rainfall intensity from individual needles was variable, but the presence of the mesh caused this variability to be minimised.

Table A.1: Christiansen uniformity co-efficients (CUCs) for the gravity fed rainfall simulator at a range of needle blocking levels.

Setup	CUC	Mean	Max	Min
		Rainfall Intensity - $mm.hr^{-1}$		
30%	94.3	65.6	73.6	57.1
30% (No Screen)	80.0	66.4	91.4	27.9
50%	93.7	56.7	68.0	50.1
75%	90.9	25.3	30.6	19.5

A.3 Intensity

Rainfall intensities resulting from different needle blocking patterns were initially measured by placing an empty soil box under the simulator for one hour and measuring the volume of rainfall collected. Intensities were measured with a range of blocking patterns. The main finding was that rainfall intensities measured over one hour were lower than intensities measured over 30 minutes (when measuring rainfall uniformity), showing a declining intensity through time (Table A.2).

Table A.2: Rainfall intensities measured using a soil box placed directly under the rainfall simulator compared to intensities calculated from uniformity investigations. Intensities were measured with different percentages of the needles blocked and also with a high and low head of water.

Blocking	Head	Measured Intensity	Intensity from Table A.1
		$mm.hr^{-1}$	
25%	High	168	N/A
25%	Low	65	N/A
30%	Low	55	65.6
30% (no screen)	Low	54	66.4
50%	Low	46.5	56.7
75%	Low	21.7	25.3

The resulted showed that there was a constant drop in rainfall intensity. This was less significant when a high head was applied to the needles (Figure A.1) and was not affected by the water source used (Figures A.3 and A.4). The duration of rainfall simulations required for the research in Chapter 6 had not been decided; therefore, the decline in rainfall intensity limited the duration of experiments available. Furthermore, desired rainfall intensities were approximately 50 $mm.hr^{-1}$ or lower. The higher head and a high percentage of needle blocking would be required to achieve this rainfall intensity consistently through time. This would result in a lower CUC than the simulator was capable of providing. It was for these reasons that the temporal variation in rainfall intensity was investigated further.

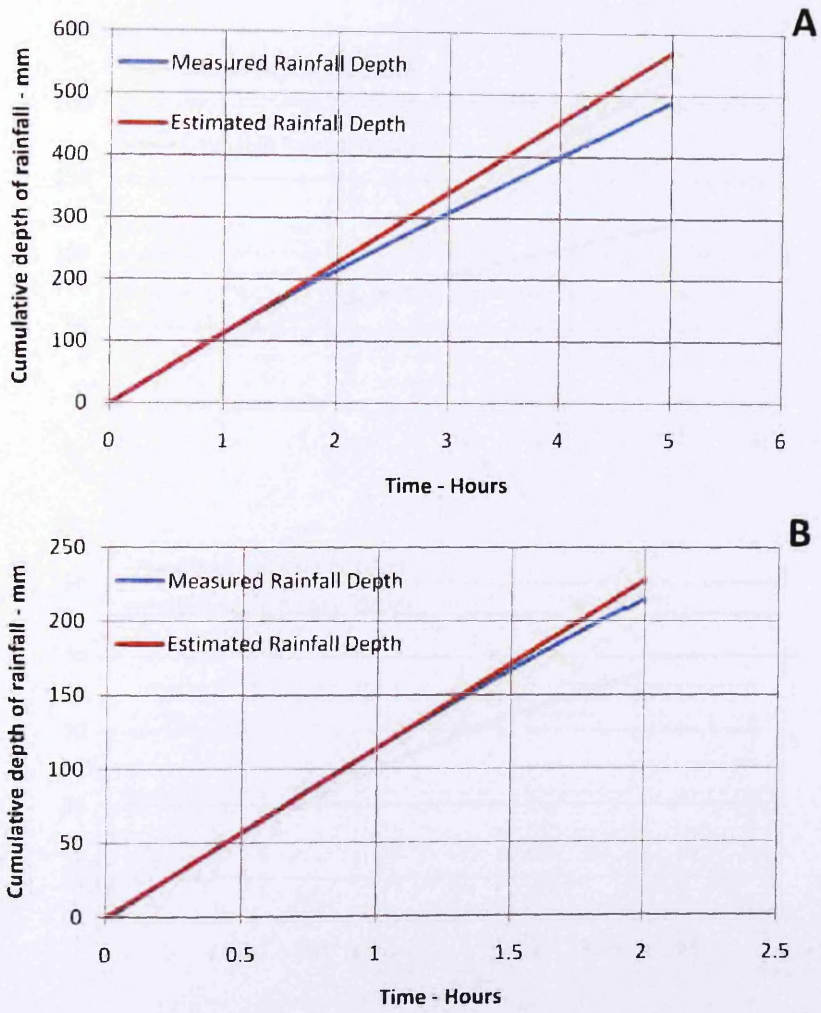

Figure A.1: Cumulative depth of rainfall through time calculated from the total mass of rainfall collected into metal soil boxes measured by electronic scales at one minute intervals. Water was supplied from the mains source. 50% of needles were blocked. A high head of water was used. Figures A and B show the same rainfall event but at different time scales. Estimated rainfall depths represent the extrapolation of the rainfall intensity measured during the first 15 minutes.

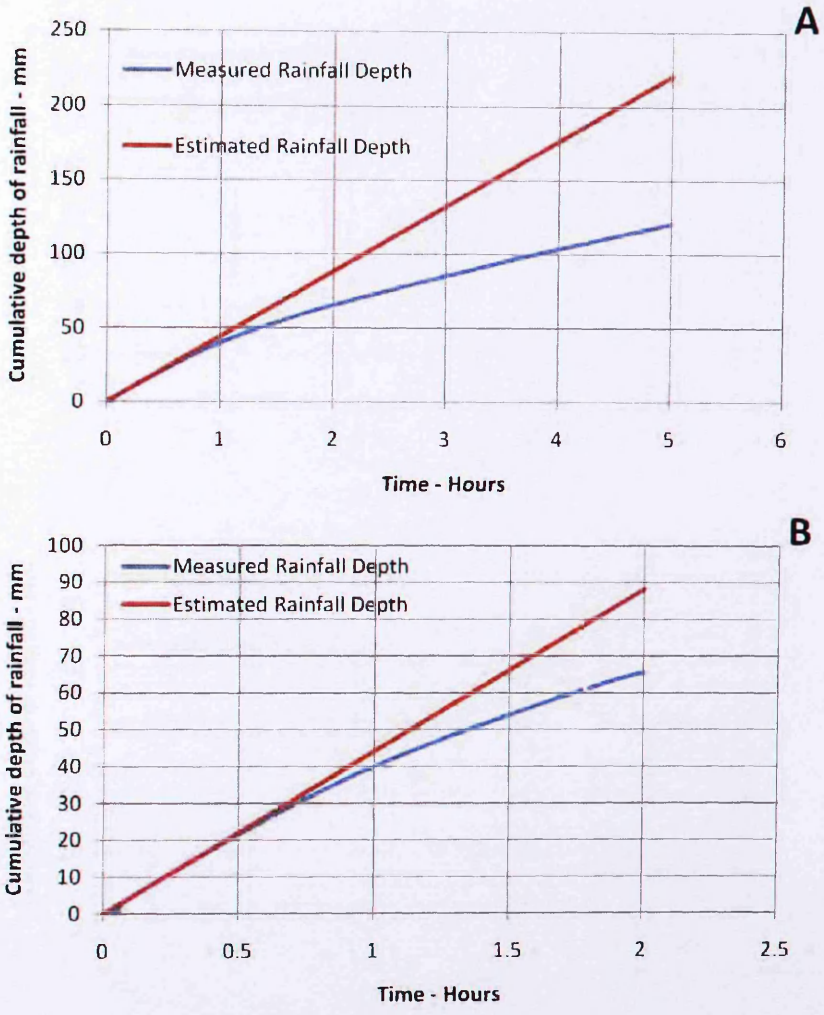

Figure A.2: Cumulative depth of rainfall through time calculated from the total mass of rainfall collected into metal soil boxes measured by electronic scales at one minute intervals. Water was supplied from the mains source. 50% of needles were blocked. A low head of water was used. Figures A and B show the same rainfall event but at different time scales. Estimated rainfall depths represent the extrapolation of the rainfall intensity measured during the first 15 minutes.

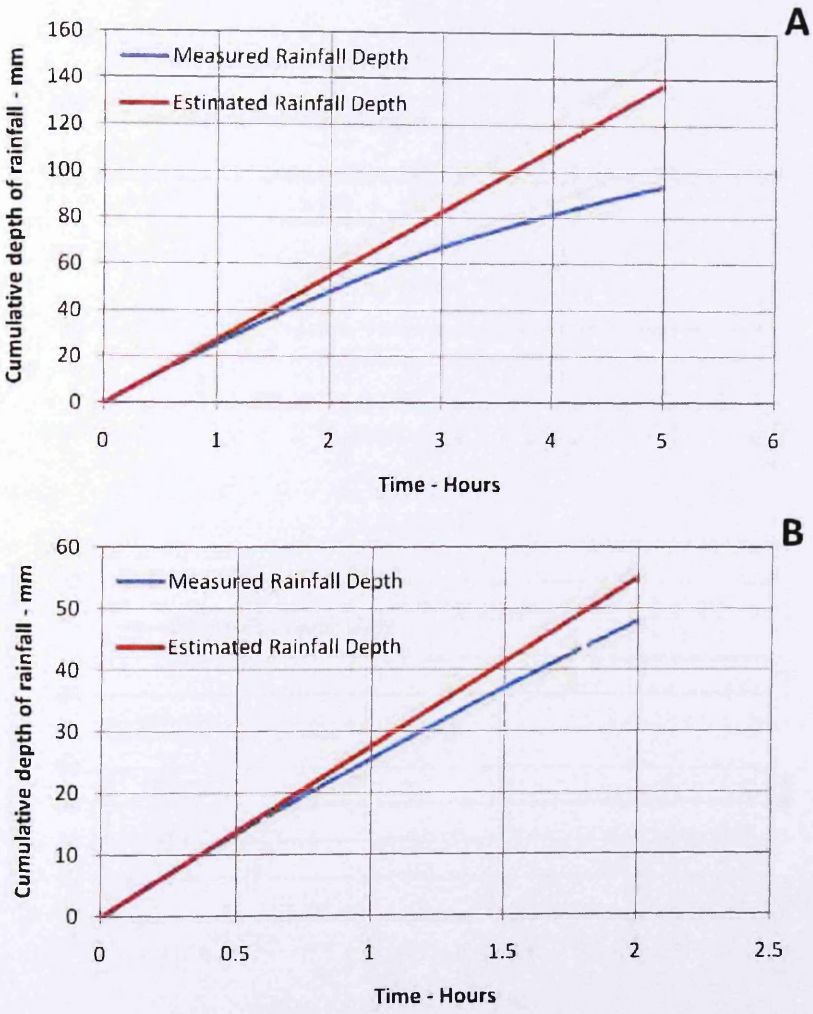

Figure A.3: Cumulative depth of rainfall through time calculated from the total mass of rainfall collected into metal soil boxes measured by electronic scales at one minute intervals. Water was supplied from the mains source. 75% of needles were blocked. A low head of water was used. Figures A and B show the same rainfall event but at different time scales. Estimated rainfall depths represent the extrapolation of the rainfall intensity measured during the first 15 minutes.

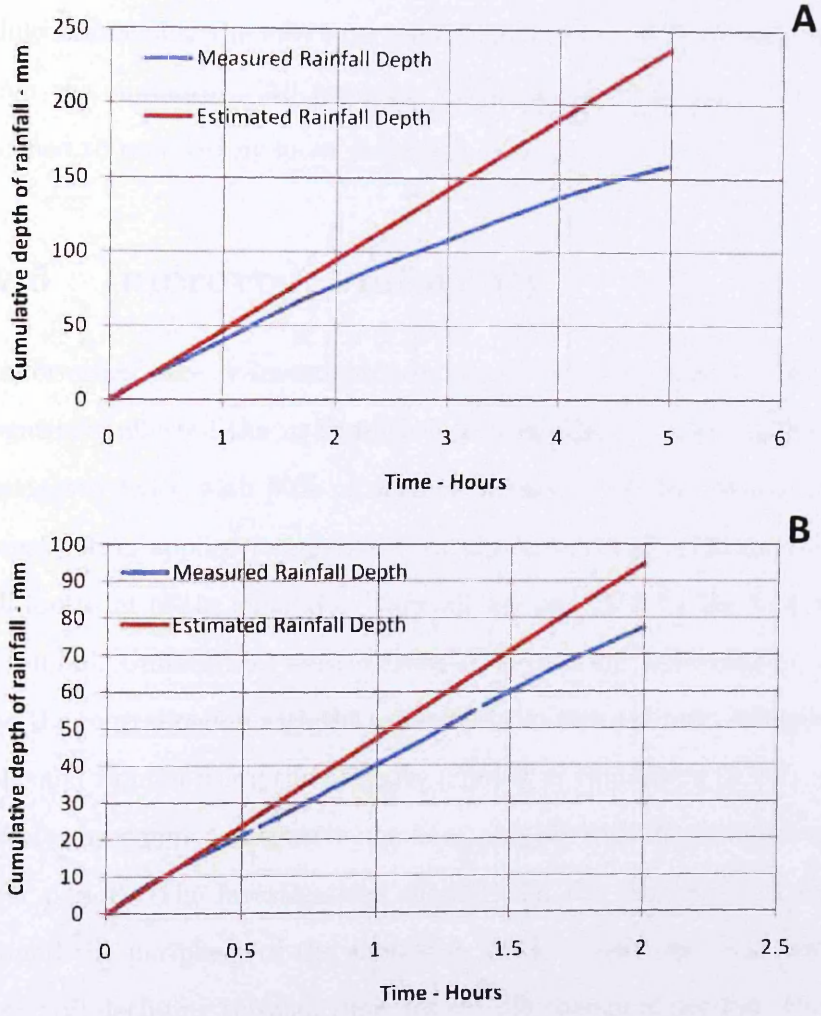

Figure A.4: Cumulative depth of rainfall through time calculated from the total mass of rainfall collected into metal soil boxes measured by electronic scales at one minute intervals. Water was supplied from RIOS water de-ioniser. 50% of needles were blocked. A low head of water was used. Figures A and B show the same rainfall event but at different time scales. Estimated rainfall depths represent the extrapolation of the rainfall intensity measured during the first 15 minutes.

A.4 Change of Needles

Replacement of the needles allowed a change to a lower gauge (0.6 mm to 0.5 mm diameter) which resulted in lower rainfall intensities with the same level of needle blocking. This would allow intensities closer to the target range to be achieved while minimising the effect on rainfall uniformity. All old needles were removed from the simulator. All retaining rubber bungs were remove concurrently and cleaned to remove any loose material.

A.5 Improved Uniformity

Uniformities were re-investigated to ensure that the changing of needles had not negatively affected the uniformity co-efficient (Table A.3). Uniformities were investigated twice with 50% of needles blocked for both investigations. The first investigation applied a larger number of containers (7 x 12) to cover the full rainfall footprint of the simulator. Rainfall was collected for the first and third hours of rainfall. Uniformities were calculated for both the full footprint of the simulator and the central region with the same footprint as a soil box. A second investigation collected rainfall using the previous number of containers (3 x 7), measuring uniformity over four consecutive one hour periods with 30 minute between each one hour period. The investigations showed that the uniformity of rainfall intensity around the periphery of the simulator was low, and also that rainfall intensities were still declining through time despite the change of needles. Uniformities were still above 90% for the first hour of each investigation. Rainfall rate in the third hour of simulation was 11.5 $mm.hr^{-1}$ lower for the second investigation suggesting that the processes affecting rainfall intensity was not consistent.

A.6 Improved Intensity

Further measurement was made of the rainfall intensity at high temporal resolution. The results are shown in Figure A.5. The decline in intensities was less severe

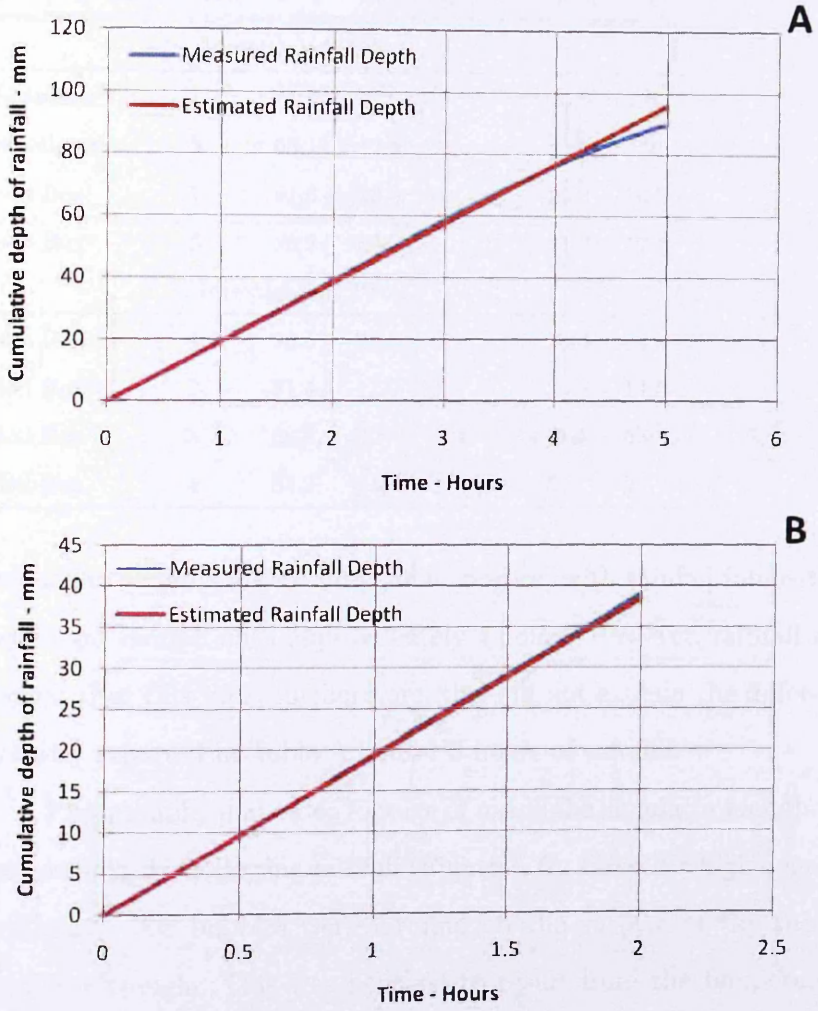

Figure A.5: Cumulative depth of rainfall through time calculated from the total mass of rainfall collected into metal soil boxes measured by electronic scales at one minute intervals. Water was supplied from RIOS water de-ioniser. 50% of needles were blocked. A low head of water was used. Estimated rainfall depths represent the extrapolation of the rainfall intensity measured during the first 15 minutes.

Table A.3: Christiansen uniformity co-efficients (CUCs) and mean, maximum and minimum rainfall intensities for the gravity fed rainfall simulator following a change of needles. Measurement were either made using the footprint of the whole simulator (simulator) or just the footprint of a 25 × 50 cm soil box (soil box).

Footprint Area	Hour	CUC	Mean Intensity	Max	Min
		Investigation One			
Simulator	1	67.8	17.9	26.3	4.5
Simulator	3	63.1	12.8	21.2	2.2
Soil Box	1	91.3	22.8	26.3	16.3
Soil Box	3	96.2	19.0	21.2	17.5
		Investigation Two			
Soil Box	1	95.5	22.4	24.3	19.8
Soil Box	2	91.4	17.9	20.8	14.5
Soil Box	3	86.9	8.5	11.1	6.0
Soil Box	4	84.2	4.0	5.8	2.5

that with the previous 0.6 mm gauge needles, with rainfall intensities maintaining a constant rainfall until approximately 4 hours. However, rainfall was still seen to decline after this time; furthermore, this did not explain the differences in rainfall intensity reported in Table A.3 after 3 hours of rainfall.

Photography and video footage of inside the simulator trough, and also inside the needle heads following rainfall (Figure A.6), showed a high degree of air bubble formation. Air bubbles were forming on the surface of the rubber bungs and simulator trough. This was believed to result from the temperature increase of the water between the exit of water de-ioniser and when stored in the simulator trough. This would result in dissolved gases coming out of solution and forming air bubbles. Prevention of the formation of air bubbles may have been possible by collecting and de-gasing a large volume of de-ionised water prior to simulations. However, this would require a pumping mechanism to transport the water into the simulator; furthermore, development of the experimental setup (Appendix B) suggested that one hour simulation time would be sufficient for experimentation. Therefore, it was decided to cease improvements to rainfall simulation and proceed

(A)

(B)

Figure A.6: Air bubbles inside the trough of the rainfall simulator forming around the heads of the 0.5 mm gauge hypodermic needles (50% blocking pattern) during simulated rainfall(A), and air bubbles inside the head of a 0.5 mm gauge hypodermic needle in the trough of the gravity rainfall simulator following the simulation of rainfall (B).

with the experimental simulations.

Appendix B

Trial Simulations

A large number of development simulations were conducted prior to the final 18 simulations reported in Chapter 6. These were conducted to perfect the methods used to pack the soils boxes, apply the tracers and analyse samples. The details of these development runs are summarized in Table B.1. The key points of the simulations are noted, but all simulations were used to build experience and familiarity with methods to be used in the final simulations from which data was collected. Final simulations had to be performed as reproducibly as possible due to the expense of REO analysis and the time delay between sample digestion and the receipt of the analytical results. Soil box packing methods and tagging methods were also tested without the use of rainfall simulation and are not detailed in the Table. Images of soil box wetting, tagging via ponding water using soil separation and REO addition by drop-wise addition of REO suspension are shown in Figures B.1, B.2 and B.3 respectively. Soil boxes used for triplicated simulations were packed and tagged simultaneously to increase the accuracy of replication, and rained upon on the same day. If one soil box showed anomalous behaviour, for example depressions in the soil surface caused by movement in the sand and gravel base, all three simulations would be repeated.

Table B.1: Details of trial simulations performed prior to the simulations reported in Chapter 6.

Simulation Number	Rainfall Intensity	Slope	Duration	Notes
1	45 mm.hr^{-1}	3°	1.5 hr	Soil was saturated (via rainfall with a mesh cover) and drained for 5 hours. Depressions in soil surface observed due to compression of sand and gravel base.
2	45 mm.hr^{-1}	3°	1 hr	Soil was wetted for 1 hour (via rainfall with a mesh cover) and drained for 2. Improved packing of sand and gravel to prevent vertical movement of the soil surface during rainfall. Soil level was below exit lip and affected sediment transport.
3	45 mm.hr^{-1}	9°	5 hr	Increased slope. Soil depth increased. Longer but slower pre-wetting (7 days). Runoff sampled to determine discharge through time.
4	45 mm.hr^{-1}	9°	1.5 hr	Soil excavated and repacked prior to rainfall. No visual difference was observed between the tagged area and the rest of the soil surface once rainfall had commenced.
5	45 mm.hr^{-1}	9°	1.5 hr	Soil was wetted for 20 minutes (via rainfall with a mesh cover). Soil was packed 0.25 cm above the height of the exit lip to ensure consistent runoff, which was observed.
6	20 mm.hr^{-1}	9°	1.5 hr	Runoff volumes and sampling intervals investigated to check that all sample analysis could be performed, and to practice the procedures used for phosphorus dilution and filtration during the simulations. Sample volumes were insufficient for all analyses to be performed.

Simulation Number	Rainfall Intensity	Slope	Duration	Notes
7	20 mm.hr^{-1}	9°	1.5 hr	Operation of moisture probe was investigated. Packed soil was sieved to 5 mm instead of 10 mm to improve surface uniformity.
8-10	50 mm.hr^{-1}	9°	1 hr	First full trial runs. All samples analysed for phosphorus.
11-13	50 mm.hr^{-1}	9%	1 hr	Slope reduced, phosphorus concentrations reduced, sampling frequency increased at the start of simulations, run time reduced.
14-16	50 mm.hr^{-1}	9%, 6% and 3%	1 hr	Blank Simulations. To be repeated due to an error with one or more of the triplicates. The number of blanks will be increased to three per slope to allow accurate background determination.
17-25	50 mm.hr^{-1}	9%, 6% and 3%	1 hr	Tagged simulations. To be repeated due to an error with one or more of the triplicates.

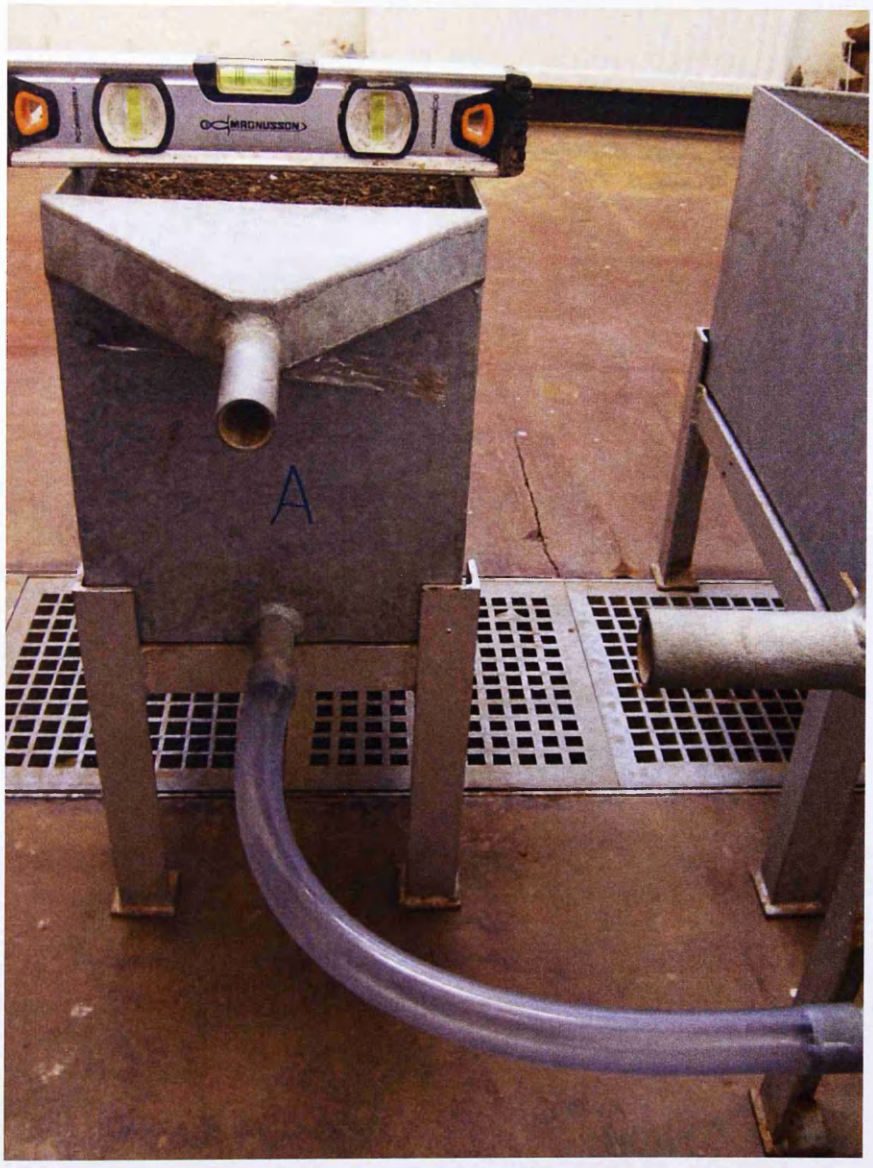

Figure B.1: Image showing the connection of a filled soil box and an empty soil box containing water via the bottom exit points to allow wetting of the soil.

Figure B.2: Image showing separation of the soil surface using a fabricated aluminium box. REO suspensions were ponded above the soil surface by pouring the suspension into the box.

Figure B.3: Image showing REOs applied to the surface of a soil box by careful drip-wise addition of a REO suspension.

Appendix C

Phosphorus Analysis

C.1 Procedure

The standard samples digestion and instrumental operational procedures used by the CSWM nutrient analysis laboratory was followed for all phosphorus analysis. Following digestion the samples are analysed using a Seal AQ2+ discrete nutrient analyser.

1. Add 8.2 ml of diluted runoff sample to a digestion bottle, with flushing of the pipette between additions.
2. Add 1.6 ml of potassium persulfate.
3. Add 0.2 ml of 11N H_2SO_4.
4. Partially tighten lid and autoclave for 1 hour at 124°C and 18 PSI.

C.2 Quality Control

Three different reference samples are digested with all runoff samples. All three standards have a known phosphorus concentration. Two of the standards (Water Reference 1 and 2) are used to confirm that the digestion procedure was effective. These references are analysed at the start and end of each set of samples analysed on the instrument. The third reference (control) is used to ensure instrumental stability while a set of samples is analysed. Samples of the third reference are analysed between every eighth runoff sample to check for machine drift. A series of seven standards, with phosphorus concentrations between 1 $mg.l^{-1}$ and 0 $mg.l^{-1}$ are digested along with the reference samples and are used to calibrate the instrument each time it instrument is used.

Appendix D

Fluorescent Microsphere Analysis

A method was required to determine the contribution of microspheres to fluorescent intensity, as the fluorescent signature of dissolved organic matter (DOM) and microsphere overlap. Determination of microsphere concentrations in samples from tagged simulations which had photon counts comparable to blank simulations would be difficult due to the variability of background fluorescence. This would only be an issue is photon counts from tagged simulations were not significantly higher than blank simulations.

A reference position was selected on the water Raman line (constant intensity) where only DOM fluorescence occurred, so that any increase in fluorescent intensity was caused by DOM. The relationship between DOM fluorescence at the reference point and the position of microsphere fluorescence could be determined for a range of DOM concentrations using blank samples. This relationship could then be used to estimate the fluorescent intensity from DOM in tagged samples, based upon DOM intensity at the reference point (no interference from microsphere samples). This method relies on the assumption that relationships between DOM intensity at the reference point and microsphere detection point are similar for blank and tagged samples. This should hold true, as the soil for all simulation was homogeneous, and the relationship calculated for each slope.

An alternative method for microsphere detection was the use of excitation-emission matrix (EEM) scanning with PARAFAC statistical analysis. This method has been used in the analysis of DOM in surface water and ground water to determine the contribution of different fluorphores. However, analysis is limited to separating a limited number (2 or 3) fluorophores, which are of similar intensity. The method is used for natural systems where the intensity of different fluorophores is of interest. Enumeration of microspheres could be achieved by simply using a concentration of microspheres detectable above background interference, as the experiment allowed for the varying of the concentration of the fluorophore of interest.

Appendix E

Soil Box Behaviour

Varying the slope of a soil system will cause its response to rainfall to change. Erosion processes occurring at a single slope gradient are unique because slope affects sediment splash distance, flow depth, stream power, ponding, and flow turbulence. It is known, and accepted, that increasing slope will cause runoff volumes and erosion rates to rise. However, there are publications which report that this behaviour is not observed at very low slope ($< 3\%$) (Cochrane and Flanagan, 2006; Asadi et al., 2007). This erroneous behaviour is reported as being the result of high ponding depths at very low slopes ($< 3\%$) which alters aggregate stability, surface connectivity and depth of flow, so that sediment detachment and transport becomes more favourable.

Work by Armstrong et al. (2010) showed complex relationships between slope, discharge and sediment concentrations for identical slope gradients and soil class as this study, applying comparable rainfall intensities but at a larger scale (5 m $\times$ 2 m). Therefore, describing sediment behaviour is important as these counter-intuitive effects of slope gradient may occur during this study. However, unlike Armstrong et al. (2010) this experiment was not designed to investigate the effects of slope, therefore explanations of behaviour will be brief, as they are of less importance than the description of behaviour and are based upon limited data.

Surface discharge from the soil boxes fitted the classical behaviour of a soil system receiving precipitation (Figure E.1), increasing during the first 20 minutes of the simulations as a result of increasing infiltration excess overland flow occurring as the infiltration rate declined. Discharge reached steady state once infiltration rates became constant. The work by Armstrong et al. (2010) showed no correlation between slope and steady state discharge rate. Similarly, steady state discharge volumes did not increase with slope in this study.

Discharge from 9% simulations was higher than 6% and 3% simulations (which were indistinct) during the first four minutes of the simulations. Higher discharge from 6% simulations occurred after 20 minutes, when discharge from 9% and 3% became indistinct. The reasons for variability in runoff records suggested by Armstrong et al. (2010) were variable rainfall intensity and infiltration rates,

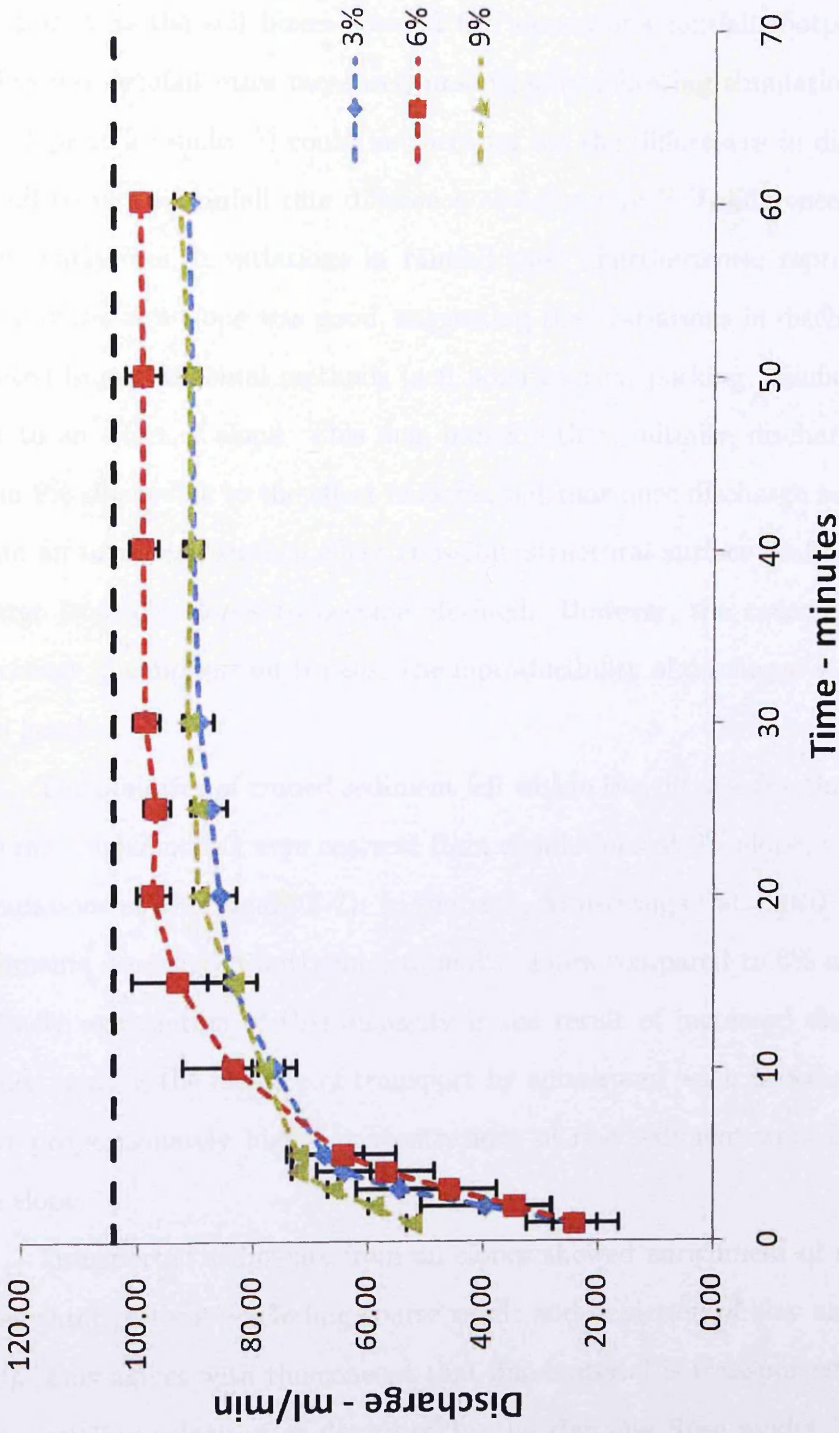

Figure E.1: Average discharges from tagged simulations. Maximum discharge, resulting from zero infiltration, is indicated by the horizontal black hashed line. Error bars are $\pm$ one standard deviation calculated from the triplicate replications of each slope.

and development of surface sealing. Variable rainfall intensity was disregarded by Armstrong et al. (2010) due to the low CV of rainfall intensity (5.3%). Rainfall intensity could not be accurately monitored during the simulations reported in Chapter 6 as the soil boxes covered the simulator's rainfall footprint; however, differences rainfall rates measured immediately following simulations at 6% and 9% slope (2.2 $mm.hr^{-1}$) could not account for the differences in discharge which would require a rainfall rate difference of 4.8 $mm.hr^{-1}$ if differences in discharge were solely due to variations in rainfall rate. Furthermore, reproducibility for simulations at a slope was good, suggesting that variations in discharge were not related to experimental methods (soil homogeneity, packing, rainfall variability), but to an effect of slope. This may indicate that, initially, discharge was higher from 9% slopes due to the effect of slope, but that once discharge achieved steady state an undefined surface effect (possibly structural surface sealing) caused discharge from 6% slopes to become elevated. However, the cause of the variable discharge is unimportant because the reproducibility of discharge at a single slope was good.

The majority of eroded sediment fell within the silt size fraction (Table E.1). Average distributions were coarsest from simulations at 9% slope, and finest from simulations at 6% (Figure E.2). In contrast, Armstrong et al. (2010) reported that sediments were significantly finer from 3% slopes compared to 6% and 9% slopes. A likely explanation of this disparity is the result of increased discharge at 6% slopes causing the balance of transport by splash and wash processes to vary, so that proportionately higher concentrations of fine sediment were transported at 6% slope.

Transported sediments from all slopes showed enrichment of the sand fractions through time (excluding coarse sand) and depletion of clay and silt (Figure E.3). This agrees with the concept that fine material is transported faster due to lower settling velocities as described by the Hairsine Rose model (Sander et al., 1996), and demonstrated by Armstrong et al. (2010).

Table E.1: Volumes (as percentages of total volumes) of particle size classes of surface runoff samples collected from tagged simulations using laser diffraction particle size analysis. Standard deviations calculated from triplicate replications are shown in parentheses.

Gradient	Time	Clay	Silt	V.Fine Sand	Fine Sand	Medium Sand	Coarse Sand
	minutes	Percentage volume - %					
9%	5-10	4.7 (0.20)	82.7 (1.40)	5.1 (0.28)	5.2 (0.68)	1.7 (0.52)	0.5 (0.49)
	20-25	4.3 (0.13)	80.5 (1.40)	6.7 (1.14)	6.6 (1.14)	1.7 (0.59)	0.1 (0.18)
	40-50	3.9 (0.46)	76.8 (5.42)	8.7 (1.92)	8.2 (3.50)	2.1 (0.96)	0.2 (0.31)
6%	5-10	4.7 (0.30)	88.2 (2.12)	3.8 (0.55)	2.5 (1.18)	0.5 (0.45)	0.2 (0.32)
	20-25	3.9 (0.78)	86.8 (6.32)	4.7 (2.49)	3.7 (2.81)	0.8 (0.84)	0.1 (0.08)
	40-50	3.8 (0.07)	86.7 (3.03)	5.5 (1.45)	3.3 (1.50)	0.7 (0.35)	0.1 (0.05)
3%	5-10	4.6 (0.10)	87.3 (0.86)	4.0 (0.68)	3.1 (0.67)	0.8 (0.35)	0.2 (0.14)
	20-25	4.2 (0.24)	85.6 (3.27)	5.0 (1.16)	3.9 (1.44)	1.1 (0.79)	0.1 (0.13)
	40-50	3.9 (0.25)	83.3 (2.13)	7.0 (1.40)	4.7 (0.98)	1.2 (0.38)	0.0 (0.04)

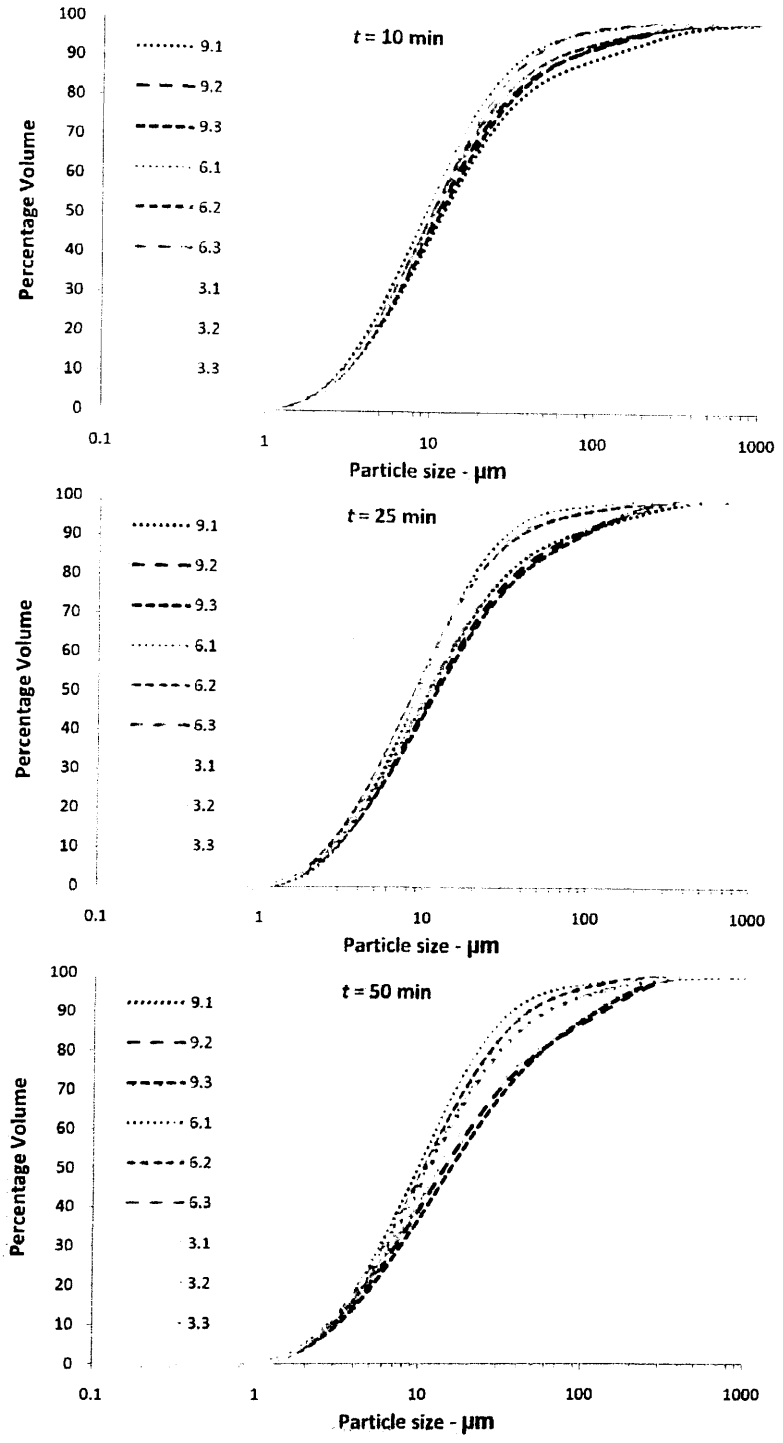

Figure E.2: Cumulative particle size distributions for tagged simulations. Values in the key represent the slope gradient, with the replicate number following the decimal.

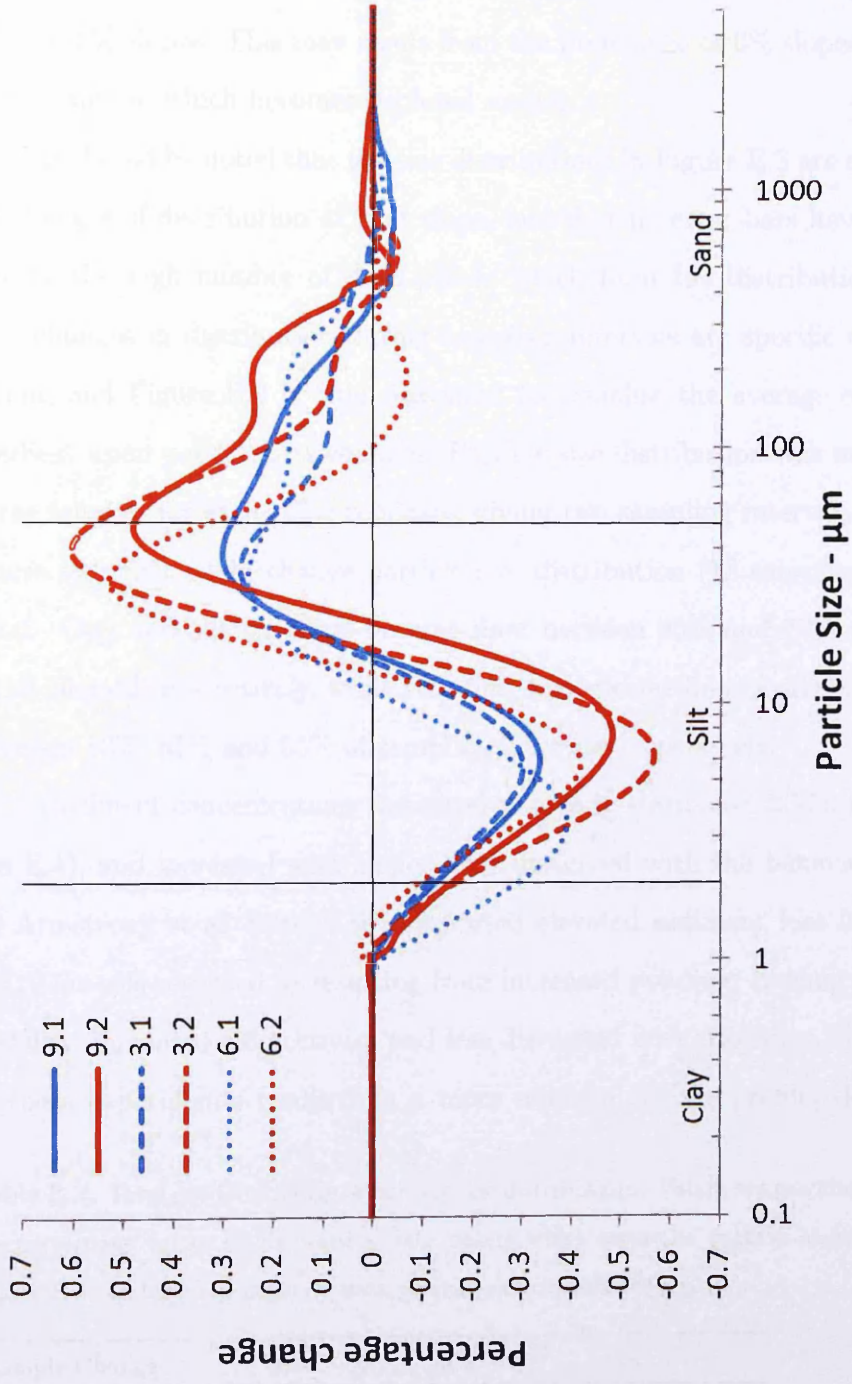

Figure E.3: Changes in the volumes of the particle size distributions of eroded sediments between the measurements presented in Figure E.2. Values in the key represent the slope gradient, with either the first or second change in particle size shown after the decimal.

Sediments from 9% and 3% slopes showed greater coarsening between the second and third samples measured for particle size, while at 6% slope the shifts between sampling intervals were more comparable (Figure E.3 and Table E.2). This shows a more rapid coarsening of eroded sediments from 6% slopes than from 3% and 9% slopes. This may result from the preference of 6% slopes to transport finer material, which becomes depleted sooner.

It should be noted that the size distributions in Figure E.3 are averaged from all changes of distribution at that slope, and that no error bars have been added due to the high number of data points which form the distributions (n = 75). The changes in distribution during sampling intervals are specific to each simulation, and Figure E.3 is only presented to visualise the average effect of slope gradient upon particle size changes. Particle size distribution was measured from three samples for each slope replicate, giving two sampling intervals per replicate where sediment could change particle size distribution (18 sampling intervals in total. Clay and silt fractions became finer between 83% and 72% of these sampling intervals respectively, while very fine, fine and medium sands became coarser between 83%, 61% and 55% of sampling intervals respectively.

Sediment concentrations increased to steady state after 20-30 minutes (Figure E.4), and increased with slope. This disagreed with the behaviour described by Armstrong et al. (2010), who reported elevated sediment loss from slopes of 3%. This was reported as resulting from increased ponding, causing aggregate instability, increased connectivity and less disrupted flow. However, the small scale of these experiments resulted in a more uniform surface profile, decreasing the

Table E.2: Total positive change in particle size distributions. Values are calculated by summing the percentage values of all positive data points which form the particle size distributions in Figure E.3. Inclusion of negative data would result in zero values.

Sample Change	9%	6%	3%
	Percentage volume change - %		
Sample 1 - 2	4.2	4.4	3.3
Sample 2 - 3	6.2	4.4	6.3

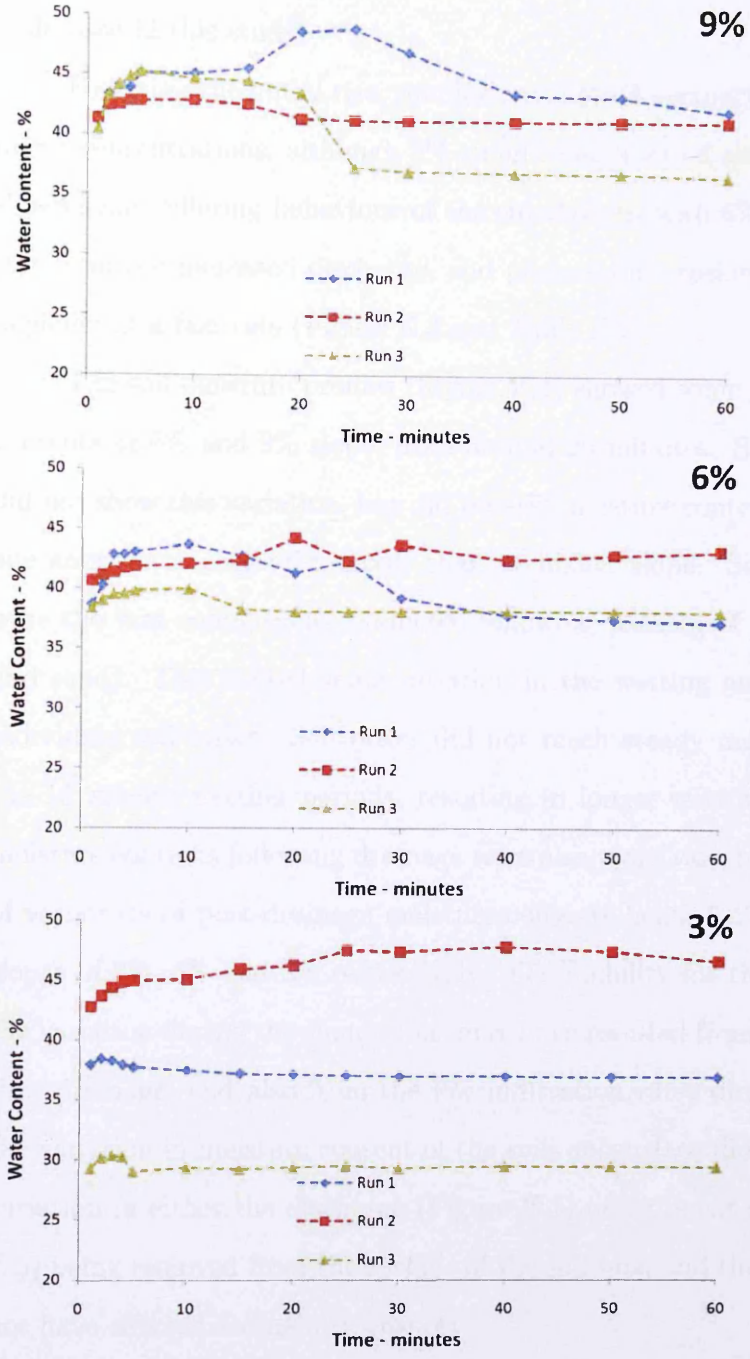

Figure E.4: Subsurface soil moisture profiles from tagged simulations collected at the rear of the soil box from 0-6 cm depth. Average soil moisture profiles are not displayed as the decreases in moisture content occur at different times causing the average moisture profile to indicate a more gradual sealing over a longer period of time. Replicated simulations are noted by S1-3.

proportion of surface area which is ponded through a lack of surface depressions. A lower slope may be required to show increases in sediment concentration at the scale used in this study.

Following the initial rise, simulations showed comparatively steady state sediment concentrations, although 6% simulations showed some decline. Again, this shows some differing behaviour of the simulations with 6% slopes, which may result from the increased discharge, and preferential erosion of fine material which depleted at a fast rate (Figure E.3 and Table E.2)

The soil moisture profiles (Figure E.4) showed some decline in soil moisture contents at 6% and 9% slope, from around 20 minutes. Simulations at 3% slope did not show this variation, but did possess moisture contents which differed from one another to a greater extent than at higher slope. Simulations at 3% slope were the first simulations conducted following packing of the base layers (gravel and sand). This caused some variation in the wetting and drainage rate of the individual soil boxes. Soil boxes did not reach steady moisture contents during the 15 minute wetting periods, resulting in longer wetting times. Steady state moisture contents following drainage were also more variable, with the co-efficient of variations of post-drainage moisture contents being 6.4%, 3.1% and 18.3% for slopes of 9%, 6% and 3% respectively. The inability for the soil boxes to correct the variation during the simulations may have resulted from the low slope, causing slow drainage, and also from the low infiltration rates during rainfall. However, the variation in moisture content of the soils subsurface did not cause comparable variation in either the discharge (Figure E.1) or sediment concentrations (Figure E.5) being removed from the surface of the soil box, and therefore is considered to not have effected sediment transport.

If subsurface moisture content declines the removal of soil water by subsurface flow must be greater than the rate of infiltration. This may be further evidence suggesting that surface sealing was occurring, as was reported by Armstrong et al. (2010) as an explanation for variable discharge. Structural surface sealing occurs when fine material is washed into the soil profile, combined with compaction

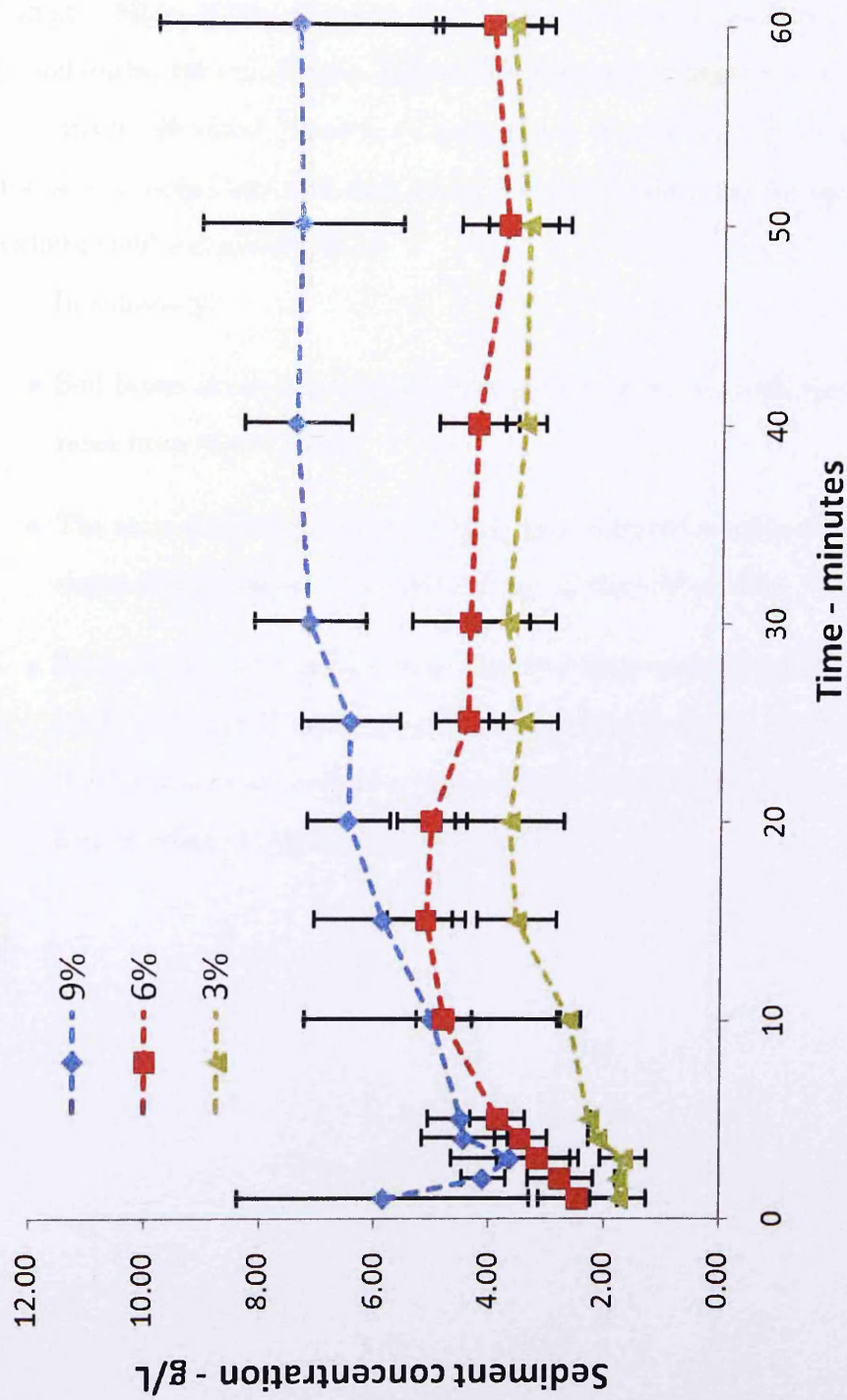

Figure E.5: Average sediment concentrations collected from tagged simulations. Error bars represent one standard deviation calculated from triplicated replicates.

through raindrop impact, causing reduced hydraulic conductivity (Neave and Rayburg, 2007) due to the formation of two discrete layers, an approximately 0.1 mm thick skin overlying an approximately 2.0 mm thick washed-in layer (McIntyre, 1958a,b). Many of the influences upon seal formation (Table E.3) were applied to the soil during the experiment. Further description of surface sealing does not need to be made. However, there is an assumption that some form of surface sealing process was occurring, and that his may be an explanation for the variations in discharge and associated effects.

In summary:

- Soil boxes showed the classical behaviour expected, with increased erosion rates from higher slopes.
- The aims of the experimental design were achieved as simulations at different slopes showed reproducible behaviour, distinct from other slope gradients.
- Some anomalous behaviour was observed from simulations at 6% slope (high discharge) and 3% slope (variable subsurface moisture contents). However, this behaviour either has no impact upon the assessment of tracers (6%), or had no effect on surface processes (3%).

Table E.3: Major influences upon surface sealing reported in published literature.

Cause	Effect	References
Wetting Rate	Slaking causes increased aggregate breakdown due to swelling, heat release, the action of moving water and the release (explosion) of trapped air.	Knapen et al. (2005)
Antecedent Moisture Content	Soils which low moisture content at the start of a rainfall event are more likely to seal as the effects of slaking are increased.	Knapen et al. (2005)
Electrical Conductivity	Low electrical conductivity results in a destabilizing effect upon colloids.	Shainberg et al. (1992); Levy et al. (1994)
Surface Cover	Plots with no cover, including stone and litter cover, are shown to suffer worse from sealing.	Ela et al. (1992); Neave and Rayburg (2007)
Rainfall Intensity and Energy	Increased rainfall intensity with similar rainfall energy (per mm of rainfall), and increased rainfall energy with similar rainfall intensity result in more rapid seal development. However, high rainfall intensity also causes seal erosion.	Baumhard et al. (1991)
Clay Content	Soils with very high ($\geq$ 300 g.kg^{-1}), or low ($\leq$ 100 g.kg^{-1}) clay percentages are less prone to sealing as a high clay content results in soils with high aggregate stability, while low clay content results in a diminished effect of the washed-in layer (the clay contents stated are dependent upon all other seal affecting factors, and are specific to that experimental setup).	Ben-Hur et al. (1985); Lado et al. (2004); Lado and Ben-Hur (2004)
Gradient	Seals of lower hydraulic conductivity form at lower slopes due to increased wash-in of fines.	Assouline and Ben-Hur (2006)

Bibliography

Albrecht, A. (1999), 'Radiocesium and 210-Pb in sediments, soils and surface waters of a high alpine catchment: A mass balance approach relevant to radionuclide migration and storage', Aquatic Sciences **61**, 1–22.

Armstrong, A., Quinton, J., Heng, B. C. and Chandler, J. (2010), 'Dominant controls over interrill erosion at low slopes', Earth Surface Processes and Landforms **In Press**.

Asadi, H., Ghadiri, H., Rose, C., Yu, B. and Hussein, J. (2007), 'An investigation of flow-driven soil erosion processes at low streampowers', Journal of Hydrology **342**, 134 – 142.

Assouline, S. and Ben-Hur, M. (2006), 'Effects of rainfall intensity and slope gradient on the dynamics of interrill erosion during soil surface sealing', Catena **66**, 211 – 220.

Baker, D. B. (1985), 'Regional water-quality impacts of intensive row-crop agriculture - a Lake Erie basin case-study', Journal of Soil and Water Conservation **40**, 125 – 132.

Bakker, M. M., Covers, G., Kosmas, C., Vanacker, V., van Oost, K. and Rounsevell, M. (2005), 'Soil erosion as a driver of land-use change', Agriculture, Ecosystems and Environment **105**, 467 – 481.

Bales, R., Hinkle, S., Kroeger, T., Stocking, K. and Gerba, C. (1991), 'Bacteriophage adsorption during transport through-porous media - chemical pertur-

bations and reversibility.', Environmental Science and Technology. **25**, 2088 – 2095.

Ball, B. C., Campbell, D. J., Douglas, J. T., Henshall, J. K. and O'Sullivan, M. F. (1997), 'Soil structural quality, compaction and land management', European Journal of Soil Science **48**, 593 – 601.

Barth, F. and Fawell, J. (2001), 'The Water Framework Directive and European Water Policy', Ecotoxicological and Environmental Safety **50**, 103 – 105.

Baumann, T. and Werth, C. (2004), 'Visualization and modeling of polystyrol colloid transport in a silicon micromodel', Vadose Zone Journal **3**, 434 – 443.

Baumann, T. and Werth, C. (2005), 'Visualization of colloid transport through heterogeneous porous media using magnetic resonance imaging', Colloids and Surfaces **265**, 2 – 10.

Baumhard, R., Romkens, M., Parlange, J. and Whisler, F. (1991), 'Predicting soil-surface seal conductance from incipient ponding and infiltration data', Journal of Hydrology **128**, 277 – 291.

Becker, M., Reimus, P. and Vilks, P. (1998), 'Transport and attenuation of carboxylate-modified latex microspheres in fractured rock laboratory and field tracer tests', Groundwater **37**, 387 – 395.

Ben-Hur, M., Shainger, I., Bakker, D. and Keren, R. (1985), 'Effect of soil texture and and $CaCo_2$ content on water infiltration in crusted soils as related to water salinity', Irrigation Science **6**, 281 – 284.

Benn, H. (2010), 'Speech by Rt. Hon. Hilary Benn MP at the Oxford Farming Conference, 5 January 2010', www.defra.gov.uk.

Bennett, E. M., Carpenter, S. R. and Caraco, N. F. (2001), 'Human impact on erodable phosphorus and eutrophication: A global perspective', Bioscience **51**, 227–234.

Blake, W., Walling, D. and He, Q. (2002), 'Using cosmogenic beryllium-7 as a tracer in sediment budget investigations', Geografiska Annaler **84**, 89 – 102.

Blanford, W., Brusseau, M., Yeh, T. J., Gerba, C. and Harvey, R. (2005), 'Influence of water chemistry and travel distance on bacteriophage PRD-1 transport in a sandy aquifer', Water Research **39**, 2345 – 2357.

Bliesner, R. and Keller, J. (2001), Sprinkle and Trickle Irrigation, The Blackburn Press, New York, New York, USA. 652p.

Bradford, S., Bettahar, M., Simunek, J. and Genuchten, M. (2004), 'Straining and attachment of colloids in physically heterogeneous porous media', Vadose Zone Journal **3**, 384 – 394.

Bradford, S., Torkzaban, S. and Walker, S. (2007), 'Coupling of physical and chemical mechanisms of colloid straining in saturated porous media', Water Research **41**, 3012 – 3024.

Bridge, J., Banwart, A. and Heathwaite, L. (2007), 'High-resolution measurement of pore saturated and colloid removal efficiency in quartz sand using fluorescence imaging', Environmental Science and Technology **41**, 8288 – 8294.

Brink, J. W. (1978), World Resources of Phosphorus, first edn, Elsevier, pp. 23 – 49.

Bryan, R. (2000), 'Soil erodibility and processes of water erosion on hillslope', Geomorphology **32**, 385 – 415.

Burkhardt, M., Kasteel, R., Vanderborght, J. and Vereecken, H. (2008), 'Field study on colloid transport using fluorescent microspheres', European Journal of Soil Science **59**, 82 – 93.

Caitcheon, G. (1998), 'The significance of various sediment magnetic mineral fractions for tracing sediment sources in Killimicat Creek', Catena **32**, 131 – 142.

Campbell, N., D'Arcy, B., Frost, A., Novotny, V. and Sansom, A. (2004), Diffuse Pollution - An introduction to the problems and solutions, IWA Publishing, London, UK. 322p.

Carpenter, S., Caraco, N., Correll, D., Howarth, R., Sharpley, N. and Smith, V. (1998), 'Nonpoint pollution of surface waters with phosphorus and nitrogen', Ecological Applications **8**, 559 – 568.

Carter, J., Owens, P., Walling, D. and Leeks, G. (2003), 'Fingerprinting suspended sediment sources in a large urban river system', The Science of the Total Environment **314**, 513 – 534.

Catt, J., Howse, K., Farina, R., Brockie, D., Todd, A., Chambers, B., Hodgkinson, R., Harris, G. and Quinton, J. (1998), 'Phosphorus losses from arable land in England', Soil Use and Management **14**, 168 – 174.

Cerdan, O., Govers, G., Bissonnais, Y. L., Oost, K. V., Poesen, J., Saby, N., Gobin, A., Vacca, A., Quinton, J., Auerrswald, K., Klik, A., Kwaad, F. J. P. M., Raclot, D., Ionita, I., Rejman, J., Rousseva, S., Muxart, T., Roxo, M. J. and Dostal, T. (2010), 'Rates and spatial variations of soil erosion in Europe: A study based on erosion plot data', Geomorphology **122**, 167 – 177.

Cey, E., Rudolph, D. and Passmore, J. (2009), 'Influence of macroporosity on preferential solute and colloid transport in unsaturated field soils', Journal of Contaminant Hydrology **107**, 45 – 57.

Chen, G. and Flury, M. (2005), 'Retention of mineral colloids in unsaturated porous media as related to their surface properties', Colloids and Surfaces **256**, 207 – 216.

Close, M., Pang, L., Flintoft, M. and Sinton, L. (2006), 'Distance and flow effects on microsphere transport in a large gravel column', Journal of Environmental Quality **35**, 1204 – 1212.

Cochrane, T. and Flanagan, D. (2006), 'Sediment deposition in a simulated rill under shallow flow conditions', Transactions of ASABE **49**, 893 – 903.

Collins, A. and McGonigle, D. (2008), 'Monitoring and modeling diffuse pollution from agriculture for policy support: UK and European experience', Environmental Science and Policy **11**, 97 – 101.

Collins, A. and Walling, D. (2002), 'Selected fingerprint properties for discriminating potential suspended sediment sources in river basins', Journal of Hydrology **261**, 218 – 244.

Collins, A., Walling, D. and Leeks, D. (1997), 'Source type ascription for fluvial suspended sediment based on a quantitative composite fingerprinting technique', Catena **29**, 1–27.

Collins, A., Walling, D. and Leeks, G. (1998), 'Use of composite fingerprints to determine the provenance of the contemporary suspended sediment load transported by rivers', Earth Surface Processes and Landforms **23**, 31 – 52.

Commission of the European Communities (2006a), 'Directive 2006/7/ec of the European Parliament and of the Council', Official Journal of the European Union **64**, 37 – 51.

Commission of the European Communities (2006b), 'Impact assessment of the thematic strategy on soil protection'.

Commission of the European Communities (2006c), Proposal for a directive of the European Parliament and of the Council establishing a framework for the protection of soil and amending Directive 2004/35/ec, Technical report, Commission of the European Communities.

Commission of the European Communities (2006d), 'Thematic strategy for soil protection'.

Commission of the European Communities (2006e), 'Thematic strategy for soil protection - summary of the impact assessment'.

Compere, F., Porel, G. and Delay, F. (2001), 'Transport and retention of clay particles in saturated porous media. influence of ionic strength and pore velocity', Journal of contaminant Hydrology **49**, 1 – 21.

Crane, M. (2003), 'Proposed development of sediment quality guidelines under the European Water Framework Directive: a critique', Toxicological Letters **142**, 195 – 206.

Csatho, P., Sisak, I., Radimszky, L., Lushaj, S., Spiegel, H., Nikolova, M. T., Nikolov, N., Cermak, P., Klir, J., Astover, A., Karklins, A., Lazauskas, S., Kopinski, J., Hera, C., Dumitru, E., Manojlovic, M., Bogdanovic, D., Torma, S., Leskosek, M. and Khristenko, A. (2007), 'Agriculture as a source of phosphorus causing eutrophication in Central and Eastern europe', Soil Use and Management **23**, 36 – 56.

D'Arcy, B., Ellis, J., Ferrier, R., Jenkins, A. and Dils, R. (2000), Diffuse Pollution Impacts: The Environmental and Economic Impacts of Diffuse Pollution in the UK, Terrance Dalton Publishers, Laverham, UK. 180p.

Deasy, C., Heathwaite, A. and Brazier, R. (2008), 'A field methodology for quantifying phosphorus transfer and delivery to streams in first order agricultural catchments', Journal of Hydrology **350**, 329 – 338.

Deasy, C., Quinton, J., Silgram, M., Bailey, A., Jackson, B. and Stevens, C. (2009), 'Mitigation options for sediment and phosphorus loss from winter-sown arable crops', Journal of Environmental Quality **38**, 2121 – 2130.

DeJonge, L., Kjaergaard, C. and Moldrup, P. (2004), 'Colloids and colloid-facilitated transport of contaminants in soils: An introduction', Vadose Zone Journal **3**, 321 – 325.

Denovio, N., Saiers, J. and Ryan, J. (2004), 'Colloid movement in unsaturated porous media: Recent advances and future directions', Vadose Zone Journal **3**, 338 – 351.

Department of the Environment, Food and Rural Affairs (2009a), Safeguarding our soils - a strategy for England, Technical report, Department of the Environment, Food and Rural Affairs.

Department of the Environment, Food and Rural Affairs (2009b), Soil strategy for England - supporting evidence pape, Technical report, Department of the Environment, Food and Rural Affairs.

Doody, D., Moles, R., Tunney, H., Kurz, I., Bourke, D., Daly, K. and O'Regan, B. (2006), 'Impact of flow path length and flow rate on phosphorus loss in simulated overland flow from a humic gleysol grassland soil', Science of the Total Environment **372**, 247 – 255.

Dougherty, W., Fleming, N., Cox, J. and Chittleborough, D. (2004), 'Phosphorus transfer in surface runoff from intensive pasture systems at various scales: A review', Journal of Environmental Quality **33**, 1973 – 1988.

Duke, M., Plante, A. and McGill, W. (2000), 'Application of INAA in the characterisation and quantification of Dy-labeled ceramic spheres and their use as inert tracers in soil studies', Journal of Radioanalytical and Nuclear Chemistry **244**, 165 – 171.

Dunkerly, D. (2004), 'Flow threads in surface run-off: Implications for the assessment of flow properties and friction coefficients in soil erosion and hydraulics investigations', Earth Surface Processes and Landforms **29**, 1011 – 1026.

Edmeads, D. C. (2003), 'The long-term effects of manure and fertilisers on soil productivity and quality: A review', Nutrient Cycling in Agroecosystems **66**, 165 – 180.

Edwards, A. and Withers, P. (1998), 'Soil phosphorus management and water quality: A UK perspective', Soil Use and Management **14**, 124 – 130.

Edwards, A. and Withers, P. (2008), 'Transport and delivery of suspended solids, nitrogen and phosphorus from various sources to freshwaters in the UK', Journal of Hydrology **350**, 144 – 153.

Eggermont, H. and Verschuren, D. (2003), 'Impact of soil erosion in disturbed tributary drainages on the benthic invertebrate fauna of Lake Tanganyika, East Africa', Biological Conservation **113**, 99 – 109.

El-Farhan, Y., Denovio, N., Herman, J. and Hornberger, G. (2000), 'Mobilization and transport of soil particles during infiltration experiments in an agricultural field, Senandoah Valley, Virginia', Environmental Science and Technology **34**, 3555 – 3559.

Ela, S., Gupta, S. and Rawls, W. (1992), 'Macropore and surface seal interactions affecting water infiltration', Soil Science Society of America Journal **56**, 714 – 721.

Elimelech, M., Nagai, M., Ko, C. and Ryan, J. (2000), 'Relative insignificance of mineral grain zeta potential to colloid transport in geochemically heterogeneous porous media', Environmental Science and Technology **34**, 2143 – 2148.

Emsley, J. and Hall, D. (1976), The Chemistry of Phosphorus, Harper and Row, London, UK. 563p.

Environment Agency (1998), Aquatic eutrophication in england and wales: A proposed management strategy, Technical report, Environment Agency.

Erpul, G., Norton, L. and Gabriels, D. (2002), 'Raindrop-induced and wind-driven soil particle transport', Catena **47**, 227 – 243.

Everett, D. (1992), Basic Principles of Colloid Science, third edn, Royal Society of Chemistry, UK. 150p.

Fitzgerald, S. (2001), 'Beryllium-7 as a tracer of short-term sediment deposition and resuspension in the Fox River, Wisconsin', Environmental Science and Technology **35**, 300 – 305.

Follett, R., Murphy, L. and Donahue, R. (1981), Fertilizers and Soil Amendments, Prentice-Hall, Inc., New Jersey, USA. 557p.

Fortune, S., Lu, J., Addiscott, T. and Brookes, P. (2005), 'Assessment of phosphorus leaching losses from arable land', Plant and Soil **269**, 99 – 108.

Foth, H. (1990), Fundamentals of Soil Science, John Wiley and Sons, New York, USA. 360p.

Fox, J. and Papanicolaou, A. (2008), 'An un-mixing model to study watershed erosion processes', Advances in Water Resources **31**, 96 – 108.

Gimbert, L., Haygarth, P. and Worsfold, P. (2008), 'Application of flow field-flow fractionation and laser sizing to characterize soil colloids in drained and undrained lysimeters', Journal of Environmental Quality **37**, 1656 – 1660.

Gimsing, A. L. and Borggaard, O. K. (2002), 'Effect of phosphate on the adsorption of glyphosphate on soils, clay minerals and oxides', International Journal of Environmental Analytical Chemistry **82**, 545 – 552.

Gimsing, A. L., Borggaard, O. K. and Bang, M. (2004), 'Influence of soil composition on adsorption of glyphosphate by contrasting Danish surface soils', European Journal of Soil Science **55**, 183 – 191.

Gitis, V., Adin, A., Nasser, A., Gun, J. and Lev, O. (2002), 'Fluorescent dye labelled bacteriophages - a new tracer for the investigation of viral transport in porous media: 1. Introduction and characterization', Water Research **36**, 4227 – 4234.

Goldscheider, N., Hotzl, H., Klass, W. and Ufrecht, W. (2003), 'Combined tracer tests in the karst aquifer of the artesian mineral springs of Stuttgart, Germany', Environmental Geology **43**, 922 – 929.

Goldwhite, H. (1981), Introduction to Phosphorus Chemistry, Cambridge University Press, Cambridge, UK. 113p.

Goppert, N. and Goldscheider, N. (2008), 'Solute and colloid transport in karst conduits under low and high-flow conditions', Ground Water **46**, 61 – 68.

Gosling, P. and Shepherd, M. (2005), 'Long-term changes in soil fertility in organic arable farming systems in England, with particular reference to phosphorus and potassium', Agriculture, Ecosystems and Environment **105**, 425 – 432.

Gouzie, D., Dodd, R. and White, D. (2010), 'Dye-tracing studies in Southwestern Missouri, USA: Indication of stratigraphic flow control in the Burlington Limestone', Hydrogeology Journal **18**, 1043 – 1052.

Govers, G., Vandaele, K., Desmet, P., Poeson, J. and Bunte, K. (1994), 'The role of tillage in soil redistribution on hillslopes', Journal of European Soil Science **45**, 469 – 478.

Grolimund, D., Borkovec, M., Barmettler, K. and Sticher, H. (1996), 'Colloid-facilitated transport of strongly sorbing contaminants in natural porous meida: A laboratory column study', Environmental Science and Technology **30**, 3118 – 3123.

Guggenberger, G., Christensen, B. and Zech, W. (1994), 'Land-use effects on the composition of organic matter in particle-size separates of soils: I. lignin and carbohydrate signature', European Journal of Soil Science **45**, 449 – 458.

Harmata, A. (2002), 'Vernal migration of bald egles from a South Colorado wintering area', Journal of Raptor Research **36**, 256–264.

Harvey, R., Kinner, N., Bunn, A., MacDonald, D. and Metge, D. (1995), 'Transport behaviour of groundwater protozoa and protozoan-sized microspheres in sandy aquifer sediments', Applied and Environmental Microbiology **61**, 209 – 207.

Haygarth, P., Bilotta, G., Bol, R., Brazier, R., Butler, P., Freer, J., Gimbert, L., Granger, S., Krueger, T., Macleod, C., Naden, P., Old, G., Quinton, J. and Worsfold, B. S. P. (2006), 'Processes affecting transfer of sediment and colloids, with associated phosphorus, from intensively farmed grasslands: An overview of key issues', Hydrological Processes **20**, 4407 – 4413.

Haygarth, P., Condron, L., Heathwaite, A., Turner, B. and Harris, G. (2005), 'The phosphorus transfer continuum: Linking source to impact with an interdisciplinary and multi-scaled approach', Science of the Total Environment **344**, 5 – 14.

Haygarth, P. and Jarvis, S. (1997), 'Soil derived phosphorus in surface runoff from grazed grasslands lysimeters', Water Research **31**, 140 – 148.

Haygarth, P., Wood, F., Heathwaite, A. and Butler, P. (2005), 'Phosphorus dynamics observed through increasing scales in a nested headwater-to-river channel study', Science of the Total Environment **344**, 83 – 106.

He, Q. and Walling, D. (1997), 'The distribution of fallout Cs-137 and Pb-210 in undisturbed and cultivated soils', Applied Radioactive Isotopes **48**, 677 – 690.

Heathwaite, A. and Dils, R. (2000), 'Characterising phosphorus loss in surface and subsurface hydrological pathways', The Science of the Total Environment **251**, 523 – 538.

Heathwaite, A., Dils, R., Liu, S., Carvalho, L., Brazier, R., Pope, L., Hughes, M., Phillips, G. and May, L. (2005), 'A tired risk-based approach for predicting diffuse and point source phosphorus losses in agricultural areas', Science of the Total Environment **344**, 225 – 239.

Heathwaite, L., Haygarth, P., Matthews, R., Preedy, N. and Butler, P. (2005), 'Evaluating colloidal phosphorus delivery to surface waters from diffuse agricultural sources', Journal of Environmental Quality **34**, 287 – 298.

Huber, N., Baumann, T. and Niessner, R. (2000), 'Assessment of colloid filtration in natural porous media by filtration theory', Environmental Science and Technology **34**, 3774 – 3779.

Huh, C. and Su, C. (2004), 'Distribution of fallout radionuclides (Be-7, Cs-137, Pb-210 and Pu-239,240) in soils of Taiwan', Journal of Environmental Radioactivity **77**, 87 – 100.

Hutchins, M., Fezzi, C., Bateman, I., Posen, P. and Deflandre-Vlandas, A. (2009), 'Cost-effective mitigation of diffuse pollution: Setting criteria for river basin management at multiple locations', Environmental Management **44**, 256 – 267.

Ilg, K., Dominik, P., Kaupenjohann, M. and Siemens, J. (2008), 'Phosphorus-induced mobilization of colloids: Model systems and soils', European Journal of Soil Science **59**, 233 – 246.

Issa, O., Bissonnais, Y., Planchon, O., Favis-Mortlock, D., Silvera, N. and Wainwright, J. (2006), 'Soil detachment and transport on field- and laboratory-scale interrill areas: Erosion processes and the size-selectivity of eroded sediment', Earth Surface Processes **31**, 929 – 939.

Jamieson, R., Joy, D., Lee, H., Kostaschuk, R. and Gordon, R. (2005), 'Resuspension of sediment-associated escherichia coli in a natural stream', Journal of Environmental Quality **34**, 581 – 589.

Jonge, L. D., Moldrup, P., Rubaek, G., Shelde, K. and Djurhuus, J. (2004), 'Particle leaching and particle-facilitated transport of phosphorus at field scale', Vadose Zone Journal **3**, 462 – 470.

Kaika, M. (2003), 'The Water Framework Directive: A new directive for a changing social, political and economic European framework', European Planning Studies **11**, 299 – 316.

Kay, D., Aitken, M., Crowther, J., Dickson, I., Edwards, A., Francis, C., Hopkins, M., Jeffrey, W., Kay, C., McDonald, A., McDonald, D., Stapleton, C. and Watkins, J. (2007), 'Reducing fluxes and faecal indicator compliance parameters to bathing waters from diffuse agricultural sources: The Brighouse Bay study, Scotland', Environmental Pollution **147**, 138 – 149.

Keay-Bright, J. and Boardman, J. (2002), 'The influence of land management on soil erosion in the Sneeuberg Mountains, Central Karoo, South Africa', Land Degradation and Development **18**, 423 – 439.

Keller, A. and Sirivithayapakorn, S. (2004), 'Early breakthrough of colloids and bacteriophage MS2 in a water-saturated sand column', Water Resources Research **40**, 2676 – 2687.

Kimoto, A., Nearing, M., Shipitalo, M. and Polyakov, V. (2006), 'Multi-year tracking of sediment sources in a small agricultural watershed using rare earth elements', Earth Surface Processes and Landforms **31**, 1763 – 1774.

Kimoto, A., Nearing, M., Zhang, X. and Powell, D. (2006), 'Applicability of rare earth element oxides as a sediment tracer for coarse-textured soils', Catena **56**, 214–221.

Kinnell, P. (2000), 'The effect of slope length on sediment concentrations associated with side-slope erosion', Soil Science Society of America Journal **64**, 1004 – 1008.

Kinnell, P. (2002), 'Raindrop-impact-induced erosion processes and prediction: A review', Hydrological Processes **57**, 375 – 380.

Kleinman, P., Sharpley, A., Veith, T., Maguire, R. and Vadas, P. (2004), 'Evaluation of phosphorus transport in surface runoff from packed soil boxes', Journal of Environmental Quality **33**, 1413 – 1423.

Kleinman, P., Srinivasan, M., Dell, C., Schmidt, J., Sharpley, A. and Bryant, R. (2006), 'Role of rainfall intensity and hydrology in nutrient transport via surface runoff', Journal of Environmental Quality **35**, 1248 – 1259.

Knapen, A., Posen, J. and Baets, A. D. (2005), 'Rainfall-induced consolidation and sealing effects on soil erodibility during concentrated runoff for loess-derived topsoils', Earth Surface Processes and Landforms **19**, 2815 – 2844.

Knaus, R. and Gent, D. (1989), 'Accretion and canal impacts in a rapidly subsiding wetland. iii. a new soil horizon marker method for measuring recent accretion', Estuaries **12**, 269 – 283.

Kosenius, A. K. (2010), 'Heterogenius preferences for water quality attributes:

The case of eutrophication in the Gulf of Finland, the Baltic Sea', Ecological Economics **69**, 528–538.

Kretzschmar, R., Borkovec, M., Grolimund, D. and Elimelech, M. (1999), 'Mobile subsurface colloids and their role in contaminant transport', Advances in Agronomy **66**, 121 – 193.

Lado, M. and Ben-Hur, M. (2004), 'Soil mineralogy effects on seal formation, runoff and soil loss', Applied Clay Science **24**, 209 – 224.

Lado, M., Ben-Hur, M. and Shainberg, I. (2004), 'Soil wetting and texture effects on aggregate stability, seal formation, and erosion', Soil Science Society of America Journal **68**, 1992 – 1999.

Laedgsmand, M., Moldrup, P. and Jonge, L. D. (2007), 'Modeling of colloid leaching from unsaturated, aggregated soil', European Journal of Soil Science **58**, 692 – 703.

Lakowicz, J. R. (1983), Principles of Fluorescent Spectroscopy, Plenum Press, New York, USA. 496p.

Lal, R. (2003), 'Soil erosion and the global carbon budget', Environment International **29**, 437 – 450.

Lauth, P., Bauer, R., Ralfs, C., Ustohal, P., Vanderborght, J., Vereecken, H. and Klumpp, E. (2007), 'Fluorescent macrophotogrpahy as a tool to visualise and quantify spatial distribution of deposited colloid tracers in porous media', Colloids and Surfaces **306**, 118 – 125.

Lazouskaya, V., Jin, Y. and Or, D. (2006), 'Interfacial interactions and colloid retention under steady flows in a capillary channel', Journal of Colloid and Interface Sciences **303**, 171 – 184.

Lei, T., Zhang, Q., Zhao, J. and Nearing, M. (2006), 'Tracing sediment dynamics and sources in eroding rills with rare earth elements', European Journal of Soil Science **57**, 287 – 294.

Levy, G., Levin, J. and Shainberg, I. (1994), 'Seal formation and interrill soil erosion', Soil Science Society of America Journal. **58**, 203 – 209.

Li, M., Li, Z., Ding, W., Liu, P. and Yao., W. (2002), 'Using rare earth element tracers and neutron activation analysis to study rill erosion process', Applied Radiation and Isotopes **64**, 402–408.

Li, X., Lin, C., Miller, I. and Johnson, W. (2006), 'Pore-scale observation of microsphere deposition at grain-grain contacts over assemblage-scale porous media domains using X-ray microtomography', Environmental Science and Technology **40**, 3762 – 3768.

Lindegren, M. and Persson, P. (2009), 'Competitive adsorption between phosphate and carboxylic acids: Quantitative effects and molecular mechanisms', European Journal of Soil Science **60**, 982 – 993.

Lindegren, M. and Persson, P. (2010), 'Competitive adsorption involving phosphate and benzenecarboxylic acids on geothiite - effects on molecular structures', Journal of Colloid and Interface Science **343**, 263 – 270.

Lindstrom, M., Nelson, W. and Schumacher, T. (1992), 'Quantifying tillage erosion rates due to moldboard plowing', Soil Tillage Research **24**, 243 – 255.

Liu, P., Tian, J., Zhou, P., Yang, M. and Shi, H. (2004), 'Stable rare earth element tracers to evaluate soil erosion', Soil and Tillage Research **76**, 147 – 155.

Liu, Y., Villalba, G., Ayres, R. and Schroder, H. (2008), 'Global phosphorus flows and environmental impacts from a consumption perspective', Journal of Industrial Ecology **12**, 557 – 569.

Lopez-Bermudez, F., Romero-Diaz, A., Martinez-Fernandez, J. and Martinez-Fernandez, J. (1998), 'Vegetation and soil erosion under a semi-arid Mediterranean climate: A case study from Murcia (Spain)', Geomorphology **24**, 51 – 58.

Loveland, J., Bhattacharjee, S., Ryan, J. and Elimelech, M. (2003), 'Colloid transport in a geochemically heterogeneous porous medium: Aquifer tank experiment and modeling', Journal of Contaminant Hydrology **35**, 161 – 182.

Maguire, R., Edwards, A., Sims, J., Kleinman, P. and Sharpley, A. (2002), 'Effect of mixing soil aggregates on the phosphorus concentration in surface waters', Journal of Environmental Quality **31**, 1294 – 1299.

Mahler, B., Winkler, M., Bennett, P. and Hillis, D. (1998), 'DNA-labeled clay: A sensitive new method for tracing particle transport', Geology **26**, 831 – 834.

Mainstone, C., Dils, R. and Withers, P. (2008), 'Controlling sediment and phosphorus transfer to receiving waters - a strategic management perspective for England and Wales', Journal of Hydrology **350**, 131 – 143.

Makris, K. C., Grove, J. H. and Matocha, C. J. (2006), 'Colloid-mediated vertical phosphorus transport in a waste-amended soil', Geoderma **136**, 174 – 183.

Mamedov, A., Huang, C. and Levy, G. (2006), 'Antecedent moisture content and aging duration effects on seal formation and erosion in smectitic soils', Soil Science Society of America Journal **70**, 832 – 843.

Massoudieh, A. and Ginn, T. (2007), 'Modeling colloid-facilitated transport of multi-species contaminants in unsaturated porous media', Journal of Contaminant Hydrology **92**, 162 – 183.

Matisoff, G., Bonniwell, E. and Whiting, P. (2002), 'Soil erosion and sediment sources in an Ohio watershed using beryllium-7, cesium-137 and lead-210', Journal of Environmental Quality **31**, 54 – 61.

Matisoff, G., Ketterer, M., Wilson, C., Layman, R. and Whiting, P. (2001), 'Transport of rare earth element-tagged soil particles in response to thunderstorm runoff', Environmental Science and Technology **35**, 3356 – 3362.

McCarthy, J. and McKay, L. (2004), 'Colloid transport in the subsurface: Past, present, and future challenges', Vadose Zone Journal **3**, 326 – 337.

McCarthy, J. and Zachara, J. (1989), 'Subsurface transport of contaminants', Environmental Science and Technology **23**, 496 – 502.

McDowell, R. and Sharpley, A. (2001), 'Soil phosphorus fractions in solution: Influence of fertiliser and manure, filtration and methods of determination', Chemosphere **45**, 737 – 748.

McDowell, R. and Sharpley, A. (2002), 'Effect of plot scale and an upslope phosphorus source on phosphorus loss in overland flow', Soil Use and Management **18**, 112 – 119.

McDowell, R., Sharpley, A., Condron, L., Haygarth, P. and Brookes, P. (2001), 'Processes controlling soil phosphorus release to runoff and implications for agricultural management', Nutrient Cycling and Agroecosystems **59**, 269 – 284.

McDowell, R., Sharpley, A. and Folmar, G. (2001), 'Phosphorus export from an agricultural watershed: Linking source and transport mechanisms', Journal of Environmental Quality **30**, 1587 – 1595.

McGechan, M. (2002), 'Transport of particulate and colloid-sorbed contaminants through soil, Part 2: Trapping processes and soil pore geometry', Biosystems Engineering **83**, 387 – 395.

McGechan, M. and Lewis, D. (2002), 'Sorption of phosphorus by soil, Part 1: Principles, equations and models', Biosystems Engineering **82**, 1–24.

McIntyre, D. (1958a), 'Permeability measurements of soil crusts formed by raindrop impact', Soil Science **85**, 261 – 266.

McIntyre, D. (1958b), 'Soil splash and the formation of surface crusts by raindrop impact', Soil Science **85**, 185 – 189.

McKay, L., Harton, A. and Wilson, G. (2002), 'Influence of flow rate on transport of bacteriophage in shale saprolite', J. Environ. Qual. **31**, 1095 – 1105.

Mermut, A. R., Luk, S. H., Romkens, M. J. M. and Poesen, J. W. A. (1997), 'Soil loss by splash and wash during rainfall from two loess soils', Geoderma **75**, 203 – 214.

Met Office (2008), 'Weather extremes'.
URL: *http://www.metoffice.gov.uk/climate/uk/extremes/*

Mibus, J., Sachs, S., Pfingsten, W., Nebelung, C. and Bernhard, G. (2007), 'Migration of uranium(iv)/(vi) in the presence of humic acids in quartz sand: A laboratory column study', Journal of Contaminant Hydrology **89**, 199 – 217.

Michaelides, K., Ibraim, I., Nord, G. and Esteves, M. (2010), 'Tracing sediment redistribution across a break in slope using rare earth elements', Earth surface processes and landforms **35**, 575 – 587.

Mie, G. (1908), 'Beitrge zur optik trber medien, speziell kolloidaler metallsungen', Annals of Physics **330**, 377 – 445.

Montgomery, D. R. (2007z'), Dirt - The Erosion of Civilisations, University of California Press, Berkley, USA. 285p.

Morgan, M. (1997), Phosphorus Loss from Soil to Water, first edn, CAB International, Wallingford, UK, pp. 137 – 150. 467p.

Morgan, R. (2005), Soil Erosion and Conservation, third edn, Blackwell Publishing, Oxford, UK. 304p.

Mortensen, A., Jensen, K., Nilsson, B. and Juhler, R. (2004), 'Multiple tracing experiments in unsaturated fractured clayey till', Vadose Zone Journal **3**, 634 – 644.

Motha, J., Wallbrink, P., Harsine, P. and Grayson, R. (2002), 'Tracer properties of eroded sediment and source material', Hydrological Processes **16**, 1983 – 2000.

Muxika, I., Borja, A. and Bald, J. (2007), 'Using historical data, expert judgement and multivariate analysis in assessing reference conditions and benthic ecolog-

ical status, according to the European Water Framework Directive', Marine Pollution Bulletin **55**, 16 – 29.

Nearing, M., Norton, L., Bulgakov, D., Larionov, G., West, L. and Dontsova, K. (1997), 'Hydraulics and erosion in eroding rills', Water Resources Research **33**, 865 – 876.

Neave, M. and Rayburg, S. (2007), 'A field investigation into the effects of progressive rainfall-induced soil seal and crust development on runoff and erosion rates: The impact of surface cover', Geomorphology **87**, 378 – 390.

Office for National Statistics (2001), 'Agricultural statistics, 2001: Regional trends 38'.

URL: *http://www.statistics.gov.uk/STATBASE/ssdataset.asp?vlnk=7649*

Oost, K. V., Quine, T., Govers, G., Gryze, S. D., Six, J., Harden, J., Ritchie, J., McCarthy, G., Heckrath, G., Kosmas, C., Giraldez, J., de Silva, J. M. and Merckx, R. (2007), 'The impact of agricultural soil erosion on the global carbon cycle', Science **318**, 626–629.

Owens, P. and Collins, A. (2006), Soil Erosion and Sediment Redistribution in River Catchments, CABI, Wallingford, UK. 328p.

Owens, P., Walling, D. and He, Q. (1996), 'The behaviour of bomb-derived caesium-137 fallout in catchment soils', Journal of Environmental Radioactivity **32**, 169 – 191.

Perk, M., Slavik, O. and Fulajtar, E. (2002), 'Assessment of spatial variation of caesium-137 in small catchments', Journal of Environmental Quality **31**, 1930 – 1939.

Pimentel, D., Harvey, C., Resosudarmo, P., Sinclair, K., Kurz, D., McNair, M., Crist, S., Shpritz, L., Fitton, L., Saffouri, R. and Blair, R. (1995), 'Environmental and economic costs of soil erosion and conservation benefits', Science **267**, 1117 – 1123.

Plante, A., Duke, M. and Mcgill, W. (1999), 'A tracer sphere detectable by neutron activation for soil aggregation and translocation studies', Soil Science Society of America Journal **63**, 1284 – 1290.

Polyakov, V., Kimoto, A., Nearing, M. and Nichols, M. (2009), 'Tracing sediment movement on a semiarid watershed using rare earth elements', Soil Science Society of America Journal **73**, 1559 – 1565.

Polyakov, V. and Nearing, M. (2004), 'Rare earth element oxides for tracing sediment movement', Catena **55**, 255 – 276.

Polyakov, V., Nearing, M. and Shipitalo, M. (2004), 'Tracking sediment redistributions in a small watershed: Implications for agro-landscape evolution', Earth Surface Processes and Landforms **29**, 1275 – 1291.

Poreba, G. (2006), 'Caesium-137 as a soil erosion tracer: A review', Geochronometria **25**, 37 – 46.

Preedy, N., McTiernan, K., Mathews, R., Heathwaite, L. and Haygarth, P. (2001), 'Rapid incidental phosphorus transfers from grasslands', Journal of Environmental Quality **30**, 2105 – 2112.

Quine, T. (1999), 'Use of caesium-137 data for validation of spatially distributed erosion models: the implications of tillage erosion', Catena **37**, 415 – 430.

Quine, T., Govers, G., Walling, D., Zhang, X., Desmet, P., Zhang, Y. and Vandaele, K. (1997), 'Erosion processes and landform evolution on agricultural land - new perspectives from caesium-137 measurements and topographic-based erosion modeling', Earth Surface and Processes and Landforms **22**, 799 – 816.

Quinton, J. and Catt, J. (2004), 'The effects of minimal tillage and control cultivation on surface runoff, soil loss and crop yields in the long-term Woburn Erosion Reference Experiment on sandy soil at Woburn, England', Soil Use and Management **20**, 343 – 349.

Quinton, J. and Catt, J. (2007), 'Enrichment of heavy metals in sediment resulting from soil erosion on agricultural fields', Environmental Science and Technology **41**, 3495 – 3500.

Quinton, J., Catt, J. and Hess, T. (2001), 'The selective removal of phosphorus from soil. is event size important?', Journal of Environmental Quality **30**, 538 – 545.

Ripa, M., Leone, N., Garnier, M. and Porto, A. (2006), 'Agricultural land use and best management practises to control nonpoint water pollution', Environmental Management **38**, 253 – 266.

Robinson, P. A. and Sutherland, W. J. (2002), 'Post-war changes in arable farming and biodiversity in Great Britain', Journal of Applied Ecology **39**, 157 – 176.

Rompaey, A. J. V., Govers, G., Hecke, E. V. and Jacobs, K. (2001), 'The impacts of land use policy on the soil erosion risk: A case study in central Belgium', Agriculture, Ecosystems and Environment **83**, 83 – 94.

Rose, C. (2004), An Introduction to the Environmental Physics of Soil, Water and Watersheds, Cambridge University Press, Cambridge, UK. 441p.

Rosen, T., Cortis, A. and Berkowitz, B. (2005), 'Magnetic resonance imaging and quantitative analysis of particle deposition in porous media', Environmental Science and Technology **39**, 7208 – 7216.

Royall, D. (2001), 'Use of mineral magnetic measurements to investigate soil erosion and sediment delivery in a small agricultural catchment in limestone terrain', Catena **46**, 15 – 34.

Russel, E. W. (1973), Soil Conditioning and Plant Growth, Longman, New York, USA. 849p.

Ryan, J. and Elimelech, M. (1996), 'Colloid mobilization and transport in groundwater', Colloids and Surfaces **107**, 1–56.

Sac, M., Ugar, A., Yener, G. and Ozden, B. (2008), 'Estimates of soil erosion using ceasium-137 tracer models', Environmental Monitoring and Assessment **136**, 461 – 467.

Salles, C. and Poesen, J. (2000), 'Rain properties controlling soil splash detachment', Hydrological Processes **14**, 271 – 282.

Sander, G. C., Hairsine, P. B., Rose, C. W., Dassisy, D., Parlange, J. Y., Hogath, W. L. and Lisle, I. G. (1996), 'Unsteady soil erosion model, analytical solutions and comparison with experimental results', Journal of Hydrology **178**, 351 – 367.

Sanderson, I. (2002), Cranfield University. BSc. Thesis.

Scottish Environment Protection Agency (n.d.), 'Significant water management issues in the Scotland river basin district', pp. 1–158.

Sen, T. and Khilar, K. (2009), 'Review on subsurface colloids and colloid-associated contaminant transport in saturated porous media', Advances in Colloid and Interface Science **119**, 71 – 96.

Shainberg, L., Levy, G., Rengasamy, P. and Frenkel, H. (1992), 'Aggregate stability and seal formation as affected by drops' impact energy and soil amendments', Soil Science **154**, 113 – 119.

Sharma, P., Flury, M. and Zhou, J. (2008), 'Detachment of colloids from a solid surface by a moving air-water interface', Journal of Colloid and Interface Science **326**, 143 – 150.

Shriver, D. and Atkins, P. (2002), Inorganic Chemistry, Oxford University Press, Oxford, UK. 763p.

Siemens, J., Ilg, K., Lang, F. and Kaupenjohann, M. (2004), 'Adsorption controls mobilization of colloids and leaching of dissolved phosphorus', European Journal of Soil Science **55**, 253 – 263.

Sirivithapakorn, S. and Keller, A. (2003), 'Transport of colloids in saturated porous media: A pore-scale observation of the size effect and colloid acceleration', Water Resource Research **39**, 1109 – 1120.

Slattery, M. and Bryan, R. (1992), 'Hydraulic conditions for rill incision under simulated rainfall - a laboratory experiment', Earth surface processes and landforms **17**, 127 – 146.

Smith, V. H., Tilman, G. D. and Nekola, J. C. (1999), 'Eutrophication: Impacts of excess nutrient inputs on freshwater, marine and terrestrial ecosystems', Environmental Pollution **100**, 179–196.

Stevens, C. and Quinton, J. (2008), 'Investigating source areas of eroded sediments transported in concentrated overland flow using rare earth elements tracers', Catena **73**, 31 – 36.

Sutherland, R., Wan, Y., Ziegler, A., Lee, C. and el Swaify, A. (1996), 'Splash and wash dynamics: An investigation using an oxisol', Geoderma **69**, 85 – 103.

Syres, J. K. and Walker, T. W. (1969), 'Fractionation of phosphorus in two cultivated soils and particle size separates', Soil Science **108**, 283 – 289.

Syversen, N., Oygarden, L. and Salbu, B. (2001), 'Ceasium-134 as a tracer to study particle transport processes within a small catchment with buffer zone', Journal of Environmental Quality **30**, 1771 – 1783.

Tang, X. and Weisbrod, N. (2009), 'Colloid-facilitated transport of lead in natural discrete fractures', Environmental Pollution **157**, 2266 – 2274.

Tian, J., Zhou, P. and Liu, P. (1994), 'Ree tracer method for studies on soil erosion', International Journal of Sediment Research **9**, 39 – 46.

Topp, N. (1965), The Chemistry of the Rare Earth Elements, Elsevier Publishing Company, Amsterdam, Netherlands. 164p.

Toy, T. J., Foster, G. R. and Renard, K. G. (2002), Soil Erosion - Processes, Prediction, Measurement, and Control, John Wiley and Sons, New York, USA. 338p.

Turner, B., Mahieu, N. and Condron, L. (2003), 'Phosphorus-31 nuclear magnetic resonance spectral assignments of phosphorus compounds in soil NaOH-EDTA extracts', Soil Science Society of America Journal **67**, 497 – 510.

Tyan, J. and Gschwend, P. (1994), 'Effect of solution chemistry on clay colloid release from an iron oxide-coated aquifer sand', Environmental Science and Technology **28**, 1717 – 1726.

Tyrrel, S. and Quinton, J. (2003), 'Overland flow transport of pathogens from agricultural land receiving faecal wastes', Journal of Applied Microbiology **94**, 87 – 93.

Ulen, B., Bechmann, M., Folster, J., Jarvie, H. and Tunney, H. (2007), 'Agriculture as a phosphorus source for eutrophication in the north-west European countries, Norway, Sweden, United Kingdom and Ireland: A review', Soil Use and Management **23**, 5–15.

United Nations Statistics Division (2010), 'Population, rate of increase, birth and death rates, surface area and density for the world, major areas and regions: selected years'. Spreadsheet.
URL: *http://unstats.un.org/unsd/demographic/products/dyb/dyb2006/Table01.pdf*

United States Department of Agriculture (2007), Food availability, Technical report. Spreadsheets: File names MTPCC and GRAINS.
URL: *http://www.ers.usda.gov/data/FoodConsumption/FoodAvailSpreadsheets.htm*

Vadas, P., Gburek, W., Sharpley, A., Kleinman, P., Moore, P., Cabrera, M. and Harmel, R. (2007), 'A model for phosphorus transformation and runoff loss from surface-applied manures', Journal of Environmental Quality **36**, 324 – 332.

Vadas, P., Kleinman, P., Sharpley, A. and Turner, B. (2005), 'Relating soil phosphorus to dissolved phosphorus in runoff: A single extraction coefficient for water quality modeling', Journal of Environmental Quality **34**, 572 – 580.

Ventura, E., Nearing, M., Amore, E. and Norton, L. (2002), 'The study of detachment and deposition on a hillslope using a magnetic tracer', Catena **48**, 149 – 161.

Ventura, E., Nearing, M. and Norton, L. (2001), 'Developing a magnetic tracer to study soil erosion', Catena **43**, 277 – 291.

Vilks, P., Frost, L. and Bachinski, D. (1997), 'Field-scale colloid migration experiments in a granite fracture', Journal of Contaminant Hydrology **26**, 203 – 214.

Walling, D. (2005), 'Tracing suspended sediment sources in catchments and river systems', Science of the Total Environment **344**, 159 – 184.

Walling, D., Collins, A. and Stroud, R. (2008), 'Tracing suspended sediment and particulate phosphorus sources in catchments', Journal of Hydrology **350**, 274 – 289.

Walling, D. and He, Q. (1999), 'Using fallout lead-210 measurements to estimate soil erosion on cultivated land', Soil Science Society of America Journal **63**, 1404 – 1412.

Walling, D., Owens, P. and Leeks, G. (1999), 'Fingerprinting suspended sediment sources in the catchment of the River Ouse, Yorksire, UK', Hydrological Processes **13**, 955 – 975.

Walling, D., Schuler, P., Zhang, Y. and Iroume, A. (2009), 'Extending the timescale for using beryllium 7 measurements to document soil redistribution by erosion', Water Resources Research **45**, 1029 – 1042.

Wan, Y., El-Swaify, S. A. and Sutherland, R. A. (1996), 'Partitioning interrill

plash and wash dynamics: A novel laboratory approach', Soil Technology **9**, 55 – 69.

Ward, R., Harrison, L., Leader, R. and Williams, A. (1997), 'Fluorescent polystyrene microspheres as tracers of colloidal and particulate materials: Examples of their use and developments in analytical technique', Tracer Hydrology **97**, 99 – 104.

Wei, S., Puling, L., Mingyi, Y. and Yazhou, X. (2003), 'Using REE tracers to measure sheet erosion changing to rill erosion', Journal of Rare Earths **21**, 587 – 590.

Weisbrod, N., Niemet, M. and Selker, J. (2003), 'Light transmission technique for the evaluation of colloidal transport and dynamics in porous media', Environmental Science and Technology **37**, 3694 – 3700.

Wild, A. (2003), Soil, Land and Food - Managing the land during the twenty-first century, Cambridge University Press, Cambridge, UK. 246p.

Withers, P., Davidson, I. and Foy, R. (2000), 'Prospects for controlling phosphorus loss to water: A UK perspective', Journal of Environmental Quality **29**, 167 – 175.

Withers, P. and Haygarth, P. (2007), 'Agriculture, phosphorus and eutrophication: A European perspective', Soil Use and Management **23**, 1–4.

Withers, P., Hodgkinson, R., Bates, A. and Withers, C. (2007), 'Soil cultivation effects on sediment and phosphorus mobilization in surface runoff from three contrasting soil types in England', Soil and Tillage Research **93**, 438–451.

Wood, P. J. and Armitage, P. D. (1997), 'Biological effects of fine sediment in the lotic environment', Environmental Management **21**, 203 – 317.

Wright, C., Amrani, M., Akbar, A., Heaney, D. and Vanderwel, D. (2006), 'Determining phosphorus release rates to runoff from selected Alberta soils using laboratory rainfall simulation', Journal of Environmental Quality **35**, 806 – 814.

Yang, D., kanae, S., Oki, T., Koike, T. and Musiake, K. (2003), 'Global potential soil erosion with reference to land use and climate changes', Hydrological Processes **17**, 2913 – 2928.

Yang, J., Jones, C., Kim, H. and Jacobsen, J. (2002), 'Soil inorganic phosphorus fractions and olsen-p in phosphorus-responsive calcareous soils: Effects of fertilizer amount and incubation time', Communications in Soil Science and Plant Analysis **33**, 855 – 871.

Yang, W., Song, X., Sui, G. and Ding, G. (2008), 'A europium tracer method for investigating vertical distribution of loess slopeland soil erosion', Communications in Soil Science and Plant Analysis **39**, 824 – 832.

Yang, W., Wang, Z., Sui, G. and Ding, G. (2008), 'Quantitative determination of red-soil erosion by an Eu tracer method', Soil and Tillage Research **101**, 52 – 56.

Yin, H. and Li, C. (2001), 'Human impact on floods and flood disasters on the Yangtze River', Geomorphology **41**, 105–109.

Zhang, P. and Wang, Y. (2006), 'Epi-fluorescent imaging of colloid transport in porous media at decimeter scales', Environmental Science and Technology **40**, 6064 – 6069.

Zhang, Q., Lei, T. and Zhao, J. (2008), 'Estimation of the detachment rate in eroding rills in flume experiments using aREE tracing method', Geoderma **147**, 8 – 15.

Zhang, X., Friedrich, J., Nearing, M. and Norton, L. (2001), 'Potential use of rare earth oxides as tracers for soil erosion and aggregation studies', Soil Science Society of America Journal **65**, 1508 –1515.

Zhang, X., Nearing, M., Polyakov, V. and Friedrich, J. (2003), 'Using rare-earth oxide tracers for studying soil erosion dynamics', Soil Science Society of America Journal **67**, 279 – 288.

Zhang, X., Quine, T., Walling, D. and Li, Z. (1994), 'Application of the caesium-137 technique in a study of soil erosion on gully slopes in a Yuan Area of the Loess Plateau near Xifeng, Gansu Province, China', Geografiska Annaler **76**, 103 – 120.

Zhuang, J., Jin, Y. and Flury, M. (2004), 'Comparison of hanford colloids and kaolinite transport in porous media', Vadose Zone Journal **3**, 395 – 402.

Zvikelsky, O., Weisbrod, N. and Dody, A. (2008), 'A comparison of clay colloid and artificial microsphere transport in natural discrete fractures', Journal of Colloid and Interface Science **323**, 286 – 292.